

2009

# Effect of permeate suction on the performance of spiral wound nanofiltration module

Awad El-Shamy  
*University of South Florida*

Follow this and additional works at: <http://scholarcommons.usf.edu/etd>

 Part of the [American Studies Commons](#)

---

## Scholar Commons Citation

El-Shamy, Awad, "Effect of permeate suction on the performance of spiral wound nanofiltration module" (2009). *Graduate Theses and Dissertations*.  
<http://scholarcommons.usf.edu/etd/1949>

This Dissertation is brought to you for free and open access by the Graduate School at Scholar Commons. It has been accepted for inclusion in Graduate Theses and Dissertations by an authorized administrator of Scholar Commons. For more information, please contact [scholarcommons@usf.edu](mailto:scholarcommons@usf.edu).

Effect of Permeate Suction on the Performance of Spiral Wound  
Nanofiltration Module

by

Awad Abdel Monem El-Shamy

A dissertation submitted in partial fulfillment  
of the requirements for the degree of  
Doctor of Philosophy  
Department of Civil and Environmental Engineering  
College of Engineering  
University of South Florida

Co-Major Professor: Mahmoud Nachabe, Ph.D.  
Co-Major Professor: Robert Carnahan, Ph.D.  
Aydin Sunol, Ph. D.  
Mark Ross, Ph.D.  
Ahmed Said, Ph.D.

Date of Approval:  
March 12, 2009

Keywords: reverse osmosis, concentration polarization, desalination, diffusion, Peclet  
number

© Copyright 2009 , A. El-Shamy

## **DEDICATION**

To my country Egypt, the origin of the secrets of life.

To the souls of my parents, whom under their wings I learned how to be fascinated with knowledge and science.

To my wife and my sister in law, who have always inspired me to pursue my graduate studies.

To my four brother and sisters, with whom I share my love and concerns.

To my four children, may God lighten their lives with the love of knowledge.

To all of the above, I present this work.

## **ACKNOWLEDGMENTS**

This work would not have been completed without the endless contributions of two persons; my advisor Dr. Robert Carnahan, and my wife Azzah El-Menshawi. Despite his retirement from the University of South Florida (USF) a couple of years ago, Dr. Carnahan has always been supportive for years, armed with the real spirit of the great giving scientist, especially at the frequent critical times of my uncertainty. Azzah has been very patient with me, and has sacrificed long sleepless nights helping me finish this work. She encompassed me with her passion and kindness.

I owe a lot to every professor in my committee. Dr. Nachabe helped me learn how to validate the hypothesis during a time when I was about to lose my way. My friend Dr. Ahmed Said taught me how to professionally present my work. Dr. Sunol was the first professor to give me guidance from the first day I entered USF with a dream of pursuing my graduate studies. Dr. Ross has challenged and inspired me with his deep scientific knowledge.

I also want to thank the senior management of my company Crane Environmental, especially Don Borden and Dennis Greco, who took upon themselves the financial burden of this work.

There are many persons that I feel grateful to because they supported this work. Some of them are Colin Leonard, Eugene Tally, Mario Van Sevren, Dr. Harold Fravel, Dr. Maya Trotz, and my colleague Dr. Mayssom Sallam.

**NOTE TO READER**

The original of this document contains color that is necessary for understanding the  
data.

The original dissertation is on file with the USF library in Tampa, Florida.

## TABLE OF CONTENTS

LIST OF TABLES	iv
LIST OF FIGURES	vii
LIST OF SYMBOLS	x
ABSTRACT	xv
CHAPTER 1 INTRODUCTION TO THE RESEARCH	1
1.1 Importance of the Research Topic	1
1.2 Problem Definition	2
1.3 Research Objective	6
1.4 Research Approach	7
1.5 Dissertation Outline	9
CHAPTER 2 CONCENTRATION POLARIZATION IN RO AND NF MODLUE: LITERATURE REVIEW	11
2.1 Background	11
2.2 Preface	12
2.3 Historical Background	12
2.4 Definition of Reverse Osmosis	14
2.5 Water Treatment by Pressure Driven Membranes	15
2.6 Reverse Osmosis Membrane Properties	16
2.7 Reverse Osmosis Membrane and Module Configuration	18
2.8 Concentration Polarization	22
2.9 Previous Studies to Reduce Concentration Polarization	23
2.10 Limiting Factors for Membrane Fouling	25
2.11 The Promise of Nanofiltration Membrane	28
2.11.1 Nanofiltration for Contaminated Drinking Water	28
2.11.2 Nanofiltration for Wastewater	30
2.11.3 Nanofiltration in Hybrid Seawater Distillation	31
2.11.4 Nanofiltration in Replacing Standard Seawater RO Membrane	32
2.12 New Generation of Nanofiltration Membrane	33
2.13 History of Using Permeate Suction in Pressure Driven Membrane	36

2.14 Effect of Increasing Suction Pressure on the Boundary Layer	38
2.15 Reverse Osmosis Models	41
2.15.1 Irreversible Thermodynamics Models	43
2.15.2 Porous Models	43
2.15.3 Charged Membrane Models	44
2.15.4 Solution-Diffusion Models	45
2.15.4.1 Solution-Diffusion-Imperfection Model	46
2.15.4.2 Assumptions when using Solution-Diffusion Model	48
2.16 Determining Membrane Surface Concentration	49
2.17 Determining Mass Transfer Coefficient and Thickness of Concentration Polarization Layer	51
2.18 Using Sherwood Number to Determine Mass Transfer Coefficient	51
2.19 Overcoming the Disadvantages of using Sherwood Number to Determine Mass Transfer with Permeate Suction	53
2.19.1 Film Theory	53
2.19.2 Peclet Number	55
2.20 Determining Diffusion Coefficient of Strong Electrolytes	57
2.20.1 1-1 Strong Electrolyte	58
2.20.2 Non 1-1 Strong Electrolyte	59
 CHAPTER 3 EXPERIMENTAL METHODOLOGY	 60
3.1 Dilute Solutions Preparation	60
3.2 Reasons behind Choosing the Chemicals	61
3.3 Experimental Setup	62
3.4 Assumptions of the Experiments	70
 CHAPTER 4 RESULTS AND DISCUSSION	 72
4.1 Effect of Permeate Suction on the Concentration Polarization Layer Thickness	72
4.1.1 Statistically Testing the Experimental Design for Concentration Polarization Layer Thickness	80
4.1.1.1 ANOVA for $MgCl_2$ Solutions	80
4.1.1.2 ANOVA for $MgSO_4$ Solutions	81
4.1.1.3 ANOVA for $NaCl$ Solutions	82
4.2 Effect of Permeate Suction on Mass Transfer Coefficient	83
4.3 Effect of Permeate Suction on Permeate Flow	87
4.4 Effect of Permeate Suction on Permeate Concentration	91
4.5 Effect of Permeate Suction on Concentrate Concentration	95
4.6 Effect of Permeate Suction on Membrane Wall Concentration	99
4.7 Effect of Permeate Suction on Peclet Number	104

CHAPTER 5 CONCLUSION AND RECOMMENDATIONS	109
5.1 Conclusion	109
5.2 Recommendations	112
5.3 Future Researches	113
LIST OF REFERENCES	114
APPENDICES	118
Appendix A: Tables of Test Results for <i>NaCl</i> Solutions	119
Appendix B: Tables of Test Results for <i>MgSO<sub>4</sub></i> Solutions	130
Appendix C: Tables of Test Results for <i>MgCl<sub>2</sub></i> Solutions	141
ABOUT THE AUTHOR	End Page



## LIST OF TABLES

Table 2-1	Comparison of new generation of NF membrane performance at standard operating conditions	34
Table 2-2	Several values of Sherwood number factors found in literature	52
Table 2-3	Ionic diffusion coefficients in water at 25 degree C dilution in $10^{-10} \text{ cm}^2 / \text{s}$	58
Table 3-1	Dilute solutions concentration and operating pressures for the experiments	61
Table 3-2	Instrumentation and specifications	64
Table 3-3	Geometrical parameters for the tested FilmTec membrane Model NF270-2540	68
Table 4-1	ANOVA Table for $MgCl_2$ Solutions	81
Table 4-2	ANOVA Table for $MgSO_4$ Solutions	82
Table 4-3	ANOVA Table for $NaCl$ Solutions	83
Table A-1	Readings for distilled water before running $NaCl$ solutions experiments	120
Table A-2	Readings for $NaCl$ solution at 730 mg/l and 80 psi feed pressure	121
Table A-3	Readings for $NaCl$ solution at 730 mg/l and 110 psi feed pressure	122
Table A-4	Readings for $NaCl$ solution at 830 mg/l and 160 psi feed pressure	123
Table A-5	Readings for $NaCl$ solution at 1,200 mg/l and 80 psi feed pressure	124
Table A-6	Readings for $NaCl$ solution at 1,200 mg/l and 110 psi feed pressure	125

Table A-7	Readings for <i>NaCl</i> solution at 1,200 mg/l and 160 psi feed pressure	126
Table A-8	Readings for <i>NaCl</i> solution at 1,750 mg/l and 80 psi feed pressure	127
Table A-9	Readings for <i>NaCl</i> solution at 1,750 mg/l and 110 psi feed pressure	128
Table A-10	Readings for <i>NaCl</i> solution at 1,750 mg/l and 160 psi feed pressure	129
Table B-1	Readings for distilled water before running <i>MgSO<sub>4</sub></i> solutions experiments	131
Table B-2	Readings for <i>MgSO<sub>4</sub></i> solution at 800 mg/l and 80 psi feed pressure	132
Table B-3	Readings for <i>MgSO<sub>4</sub></i> solution at 800 mg/l and 100 psi feed pressure	133
Table B-4	Readings for <i>MgSO<sub>4</sub></i> solution at 800 mg/l and 130 psi feed pressure	134
Table B-5	Readings for <i>MgSO<sub>4</sub></i> solution at 1,250 mg/l and 80 psi feed pressure	135
Table B-6	Readings for <i>MgSO<sub>4</sub></i> solution at 1,250 mg/l and 100 psi feed pressure	136
Table B-7	Readings for <i>MgSO<sub>4</sub></i> solution at 1,250 mg/l and 130 psi feed pressure	137
Table B-8	Readings for <i>MgSO<sub>4</sub></i> solution at 1,750 mg/l and 80 psi feed pressure	138
Table B-9	Readings for <i>MgSO<sub>4</sub></i> solution at 1,750 mg/l and 100 psi feed pressure	139
Table B-10	Readings for <i>MgSO<sub>4</sub></i> solution at 1,750 mg/l and 130 psi feed pressure	140
Table C-1	Readings for distilled water before running <i>MgCl<sub>2</sub></i> solutions experiment	142
Table C-2	Readings for <i>MgCl<sub>2</sub></i> solution at 800 mg/l and 80 psi feed pressure	143
Table C-3	Readings for <i>MgCl<sub>2</sub></i> solution at 800 mg/l and 100 psi feed pressure	144
Table C-4	Readings for <i>MgCl<sub>2</sub></i> solution at 800 mg/l and 130 psi feed pressure	145
Table C-5	Readings for <i>MgCl<sub>2</sub></i> solution at 1,250 mg/l and 80 psi feed pressure	146
Table C-6	Readings for <i>MgCl<sub>2</sub></i> solution at 1,250 mg/l and 100 psi feed pressure	147

Table C-7	Reading for $MgCl_2$ solution at 1,250 mg/l and 130 psi feed pressure	148
Table C-8	Readings for $MgCl_2$ solution at 1,750 mg/l and 80 psi feed pressure	149
Table C-9	Readings for $MgCl_2$ solution at 1,750 mg/l and 100 psi feed pressure	150
Table C-10	Readings for $MgCl_2$ solution at 1,750 mg/l and 130 psi feed pressure	151

## LIST OF FIGURES

Figure 1-1	Concentration polarization layer near membrane surface	4
Figure 2-1	Schematic drawing of water and salt fluxes in direct osmosis and reverse osmosis	14
Figure 2-2	Kinds of rejected species by different pressure driven membrane types	15
Figure 2-3	Thin Film Composite (TFC) cross section view	18
Figure 2-4	Structure of thin film barrier layer of RO aromatic polyamide membrane	19
Figure 2-5	Structure of thin film barrier layer of the aromatic/aliphatic nanofiltration membrane	20
Figure 2-6	A cross section in the thin film composite (TFC) spiral wound reverse osmosis membrane showing feed channel spacer	21
Figure 2-7	Configuration of permeate spacer (top) and feed spacer (bottom) in spiral wound RO/NF element	22
Figure 2-8	Limiting factors for RO and NF membrane fouling	27
Figure 2-9	Inorganic scaling stages	27
Figure 2-10	Comparison of energy consumption for seawater desalination with seawater membrane; brackish water- seawater membrane & NF-NF membrane	33
Figure 2-11	Image of the surface of the new generation NF ESNA1-LF membrane compared to the low pressure RO ESPA3 membrane showing relative surface smoothening	35

Figure 2-12	Comparison of surface charge of new generation NF ESNA1-LF membrane, typical NF LFC1 membrane, and low pressure fouling RO LFC1 membrane	36
Figure 2-13	Membrane bio-reactor using permeate suction to treat wastewater by immersed UF membrane	37
Figure 2-14	Application of suction to the membrane to prevent boundary layer separation	39
Figure 2-15	Feed side concentration polarization layer	51
Figure 3-1	Experimental equipment skid showing pressure gauges, TDS meter, and NF membrane pressure vessel	62
Figure 3-2	Variable frequency drives for the high pressure pump, and the permeate pump	63
Figure 3-3	The assembled high pressure pump (top), and permeate pump (bottom)	63
Figure 3-4	First setup by running the high pressure pump only	66
Figure 3-5	Second setup by running the high pressure pump and the permeate pump	67
Figure 4-1	Concentration polarization layer thickness versus feed concentration - $MgCl_2$	74
Figure 4-2	Concentration polarization layer thickness versus feed concentration - $MgSO_4$	75
Figure 4-3	Concentration polarization layer thickness versus feed concentration - $NaCl$	77
Figure 4-4	Concentration polarization layer thickness versus feed concentration at 100-110 psi for the three $MgCl_2$ , $MgSO_4$ , and $NaCl$ solutions	78
Figure 4-5	Concentration polarization layer thickness versus net operating Pressure - $MgCl_2$	79
Figure 4-6	Mass transfer coefficient versus feed concentration - $MgCl_2$	84

Figure 4-7	Mass transfer coefficient versus feed concentration - $MgSO_4$	85
Figure 4-8	Mass transfer coefficient versus feed concentration - $NaCl$	86
Figure 4-9	Permeate flow versus feed concentration - $MgCl_2$	88
Figure 4-10	Permeate flow versus feed concentration - $MgSO_4$	89
Figure 4-11	Permeate flow versus feed concentration - $NaCl$	90
Figure 4-12	Permeate concentration versus feed concentration - $MgCl_2$	92
Figure 4-13	Permeate concentration versus feed concentration - $MgSO_4$	93
Figure 4-14	Permeate concentration versus feed concentration - $NaCl$	94
Figure 4-15	Concentrate concentration versus feed concentration - $MgCl_2$	96
Figure 4-16	Concentrate concentration versus feed concentration - $MgSO_4$	97
Figure 4-17	Concentrate concentration versus feed concentration - $NaCl$	98
Figure 4-18	Membrane wall concentration versus feed concentration - $MgCl_2$	100
Figure 4-19	Membrane wall concentration versus feed concentration - $MgSO_4$	101
Figure 4-20	Membrane wall concentration versus feed concentration - $NaCl$	102
Figure 4-21	Fully developed velocity profiles and concentration profiles in the boundary layer without and with permeate suction	103
Figure 4-22	Peclet number versus feed concentration - $MgCl_2$	106
Figure 4-23	Peclet number versus feed concentration - $MgSO_4$	107
Figure 4-24	Peclet number versus feed concentration - $NaCl$	108

## LIST OF SYMBOLS

A	Pure water permeability coefficient
$\text{\AA}$	Angstrom
$A_1$	Wetted membrane surface area
$a_1, b_1, c_1$	Coefficients in Peclet number model equations
B	Solute permeability coefficient in I.T. model
BW	Brackish water
b	Membrane length
$C_F$	Bulk feed concentration
$c_i$	Total dissolved salts
$C_i$	Molar concentration of the solute
$(C_m)_{avg}$	Logarithmic mean solute concentration in the membrane
$C_{mem}$	Membrane wall concentration
$C_R$	Reject concentration
$C_P$	Product concentration
$c_Q$	Dimensionless volume coefficient
$c_w$	Concentration of water in the membrane
D	Diffusivity coefficient for solute transport through solvent

DBNPA	Dibromo nitrilo propionamide
$D_{1-2}$	Diffusivity coefficient in the ionized electrolyte
DI	Deionized water
$D_w$	Diffusivity coefficient of water in the membrane
$d_f$	Filament diameter of the feed spacer
$\delta$	Boundary layer thickness
$\delta_F$	Concentration polarization layer feed side
$\delta_p$	Concentration polarization layer feed side
$\delta_M$	Active membrane thickness
$\delta_s$	Porous support membrane thickness
DOF	Degrees of freedom
$D_w$	Diffusion coefficient of the solute in the membrane
$\Delta P$	Hydraulic pressure difference across the membrane
$\Delta\pi$	Osmotic pressure difference across the membrane
I. T.	Irreversible thermodynamic
EPA	Environmental protection agency
$\varepsilon$	Porosity of the feed – concentrate spacer
$J_w$	Permeate flux
$h_d$	Hydraulic diameter of the membrane
HDPE	High density polyethylene
HP	Horse power



Hz	Hertz
K	Mass transfer coefficient
$k_2$	Solute permeability coefficient due to diffusion in solution diffusion model
$k_3$	Coupling coefficient in solution diffusion-imperfection model
$k_s$	Distribution coefficient of the solute from the feed into the pore of the membrane
$\frac{k_s D_w}{\delta_F}$	Solute transport parameter
MED	Multi effect distillation
MF	Microfiltration
MSF	Multi stage flash
MWCO	Molecular weight cut-off
$MW_i$	Molecular weight of species
N	Number of ions formed when the solute dissociates
NF	Nanofiltration
NPSH	Net positive suction head
$N_s$	Total solute flux
$N_w$	Total water flux
PA	Synthetic polyamide aromatic
$P_e$	Diffusive Peclet number
$\rho$	Density
$\pi(X_F)$	Osmotic pressure of the feed side

$\pi(X_p)$	Osmotic pressure of the permeate side
Ph	Phase
pH	Negative power of hydrogen
Q	Quantity of fluid removed during suction
L	Membrane width
$L_p$	Hydrodynamic permeability coefficient
R	Gas constant
Re	Reynold's number
$R_L$	Reynold's number related to the length of the membrane
RO	Reverse Osmosis
rpm	Revolution per minute
$R^2$	Proportion of variability in data
Sc	Schmidt number
Sh	Sherwood number
SW	Seawater
T	Absolute temperature
$\tau$	Frictional shearing stress
TDS	Total dissolved solids
TFC	Thin film composite
THM	Trihalomethane
TOC	Total organic carbon
u	Average free stream bulk velocity at the x direction
UF	Ultrafiltration

$\mu$	Absolute viscosity
$\mu m$	Micro meter
$\mu s$	Micro siemens
V	Volt
$v_0$	Velocity due to suction
$V_w$	Permeate velocity
VC	Vapor compression
VFD	Variable frequency drive
w	With suction
w/o	Without suction
WHO	World health organization
$W_F$	Concentration gradient feed side
$W_p$	Concentration gradient permeate side
$\nu$	Dynamics viscosity of the solution
$\sigma$	Coefficient of coupling between salt and water in I.T. model
$\omega$	Salt permeability coefficient
X,a,b,c	Coefficients in Sherwood number
$X_F$	Solute mole fraction feed side
$X_p$	Solute mole fraction permeate side
$Z_i$	Valent number of anion or cation

## Effect of Permeate Suction on the Performance of Spiral Wound Nanofiltration Module

Awad Abdel Monem El-Shamy

### **ABSTRACT**

Fouling in a nanofiltration membrane module is usually a result of concentration polarization. The effect of permeate suction on the slightly negatively charged spiral wound nanofiltration membrane is investigated. According to the film theory, the mass transfer coefficient is inversely proportional to concentration polarization. The effect of permeate suction destabilizes the boundary layer. This will decrease the concentration polarization layer, and consequently will increase mass transfer through the membrane's surface.

To validate the hypothesis, experiments were carried out on a NF membrane that can be described by the solution-diffusion model. This model has coefficients that can be measured experimentally. Using the membrane wall concentration in this model instead of the bulk feed concentration can help estimating the mass transfer coefficient more appropriately.

Two experimental studies were carried out, one with a standard high pressure pump, and another one with the added effect of suction pressure applied to the permeate collector tube.

Three different concentrations of binary dilute solutions of  $NaCl$ ,  $MgSO_4$ , and  $MgCl_2$ , at three different pressures (low, medium, and high) were tested.

For all tested solutions, permeate suction increased the diffusive Peclet number as a function of the feed concentration ( $x$ ) according to the equation  $P_e = a_1x^2 + b_1x + c_1$ , with  $R^2 > 0.99$ , where  $x$  is the feed concentration in Mol/l, and  $a_1$ ,  $b_1$ , and  $c_1$  are coefficients dependent on feed pressure for every salt solution. With the increase of the Peclet number, it was observed that the concentration polarization decreased, and both the product flow and the product quality were improved. Suction had the greatest impact at the range of 100 to 110 psi feed pressure, where the concentration polarization reduced approximately 14 to 20 %.

ANOVA for the concentration polarization showed that suction was significant in reducing the calculated concentration polarization layer for all tested solutions.

It was concluded that permeate suction reduced concentration polarization, increased product flow rate, and improved product quality. Thus, adding permeate suction has beneficial consequences because it reduces membrane fouling and extends its useful service life.

## **CHAPTER 1**

### **INTRODUCTION TO THE RESEARCH**

#### 1.1 Importance of the Research Topic

The rapid growth of the new generation of nanofiltration as an attractive membrane separation process suggests renewed investigations of the current design methods for developing an improved design configuration to reduce membrane fouling. Fouling in reverse osmosis (RO)/nanofiltration (NF) membrane modules is usually a result of concentration polarization. Membrane fouling has a serious economical implications on the water treatment plant because it causes permeate flux decline, reduces product quality, and shortens the life of the membrane. Spiral wound configuration, which is the most dominant module used in the application of pressure driven membrane for drinking water treatment, was rarely investigated by researchers as far as the permeate suction is concerned.

Nanofiltration membrane, which is sometimes called loose reverse osmosis membrane, is more manageable than RO membrane for permeate suction because its permeability coefficient is substantially higher than RO membrane. This is despite that NF membrane systems are typically designed like RO but with much lower driving pressures. Currently NF membranes are traditionally used to treat low salinity water, waste water, or in the process industry like extracting chemicals or protein from dilute water.

The state of the art in NF membrane researches is taking advantages of using it in seawater desalination, either for pretreatment for existing thermal distillation plants; pretreatment of seawater RO plants; or to replace the traditional seawater RO membranes so that it improves production rate, or saves energy (Leon Awerbuch, 2007; Hassan, 2004; Yann Gouellec et al., 2006).

This is an indication of the inspiring future that awaits the NF membrane in the pressure driven membrane technology.

Despite the numerous studies that have addressed the NF membrane fouling, few researchers have addressed using permeate suction as a means of reducing fouling in the widely used spiral wound thin film composite membrane configuration.

## 1.2 Problem Definition

Membrane fouling and scaling can significantly increase the cost of a membrane system as well as reduce its reliability. This limitation is behind the great deal of research that has made significant developments in membrane science.

Fouling is a term generally used to describe the undesirable formation of deposits on the surface of the membrane. Membrane fouling is a complicated phenomenon because it results from a group of physical, chemical, and biological effects that can lead to an irreversible loss of membrane permeability (Salbani et al., 2001). Attempts to analyze the fouling phenomena have shown that its primary characteristics are adsorption of feed components, and deposition of solids on the membrane surface, accompanied by crystallization and compaction of the membrane structure. However, the occurrence of fouling is almost always a result of concentration polarization (Jamal et al., 2004).

Concentration polarization (Figure 1-1), may be defined as the presence of a higher concentration of rejected species at the surface of a membrane than in the bulk solution, due to the convective transport of both solute and solvent. It is generally considered a totally reversible effect (Jamal et al, 2004). The reduction of concentration polarization layer ( $\delta_F$ ) is important for the improvement of the performance of osmotic type membranes, as it will inevitably lead to reduction in the fouling of the membrane (Jamal et. al, 2004).

Depending on molecular weight, which will determine diffusive back-transport from the membrane, concentration polarization is more or less distinct.

Although concentration polarization can also be found on the permeate side as indicated in Figure 1-1, it is usually neglected in pressure driven membrane since it is much less pronounced than feed side polarization (Fritzmann et al., 2007).

Concentration polarization has several negative effects on membrane performance: (1) rejection decreases due to higher salt flux because of increased salt concentrations at the membrane surface; (2), solubility limits can be exceeded, especially for divalent ions, leading to a precipitation layer on the membrane surface, which negatively influences mass transfer, that dramatically reduce permeate flux; (3) water flux is reduced due to higher osmotic pressure associated with higher salt concentration at the feed side membrane surface; (4) and particles are accumulated at the membrane which can lead to cake formation on the surface.



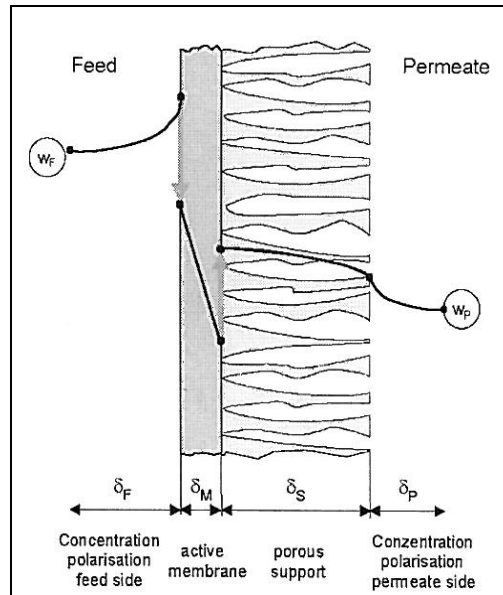


Figure 1-1. Concentration polarization layer near membrane surface (adopted from Fritzmann et al., 2007)

Several approaches have been used to try to minimize the effects of fouling. In thin film composite spiral wound module, the hydraulic flow is laminar due to channels between the membrane layers. The mass transfer coefficient is the most widely used parameter in the design of pressure-driven membrane separation systems such as reverse osmosis and nanofiltration. The role of suction in mass transfer through porous membranes is very important. It was identified by several researchers (e. g. Van den Berg et al., 1989; Gekas et al., 1987) that the effect of permeate suction enhances the mass transfer from the bulk to the membrane surface. By applying suction at the end of the collector tube of the membrane module, an increased rate of pressure along the stream will present. This increase in pressure rate will destabilize the boundary layer at steady state conditions (Schlichting, 1979).

The conventional way to estimate the mass transfer coefficient is to use Sherwood number relationships obtained from heat and mass transfer analogy.

Numerous Sherwood number relationships have been proposed and extensively reviewed (C. Van de Liskdonk et al., 2000). The Graetz-Leveque correlation of Sherwood number, which is used for laminar flow when the velocity field is fully developed and the concentration boundary layer is not fully developed, is typically used to estimate mass transfer coefficient as:

$$\text{Sh} = X(\text{Re})^a (\text{Sc})^b \left(\frac{d_h}{L}\right)^c \quad (1-1)$$

where  $\text{Re} = \text{Reynold's number} = \frac{V_w d_h}{\nu}$ ;  $\text{Schmidt number} = \text{Sc} = \frac{\nu}{D}$ ;  $\nu = \text{kinematics viscosity}$ ;  $V_w = \text{average cross-flow permeate velocity}$ ;  $d_h = \text{hydraulic diameter of the membrane element}$ ;  $D = \text{the diffusion coefficient for solute transport through solvent}$ , and  $L = \text{the spiral wound membrane width}$  (Taylor et al., 1999).  $D$  in this relationship is equal to  $K \delta_F$ , where  $K$  is the mass transfer coefficient, and  $\delta_F$  is the concentration polarization layer thickness. The terms  $X$ ,  $a$ ,  $b$ , and  $c$  are coefficients that have taken extremely different values by different researchers (e.g. Isaacson, 1979; Schocket Miquel, 1979; Taylor, 1991). Further discussions about these terms will be included in Chapter 2.

There are several limitations upon using the above-mentioned equation:

(1) the above mentioned Sherwood number relationship is derived for flow through non-porous conduit; hence, the effect of suction can not be considered using these relationships; (2) the axial change in osmotic pressure at membrane surface due to the concentration polarization change is not considered in the above mentioned Sherwood number correlations; (3) and suction will change the species concentration at the

membrane surface that will change the solution's physical properties like viscosity, density, and diffusivity, which are functions of the concentration. Consequently, the above-mentioned Reynold's number, and Schmidt number, will be variable along the membrane length. Those changes are not considered with this form of Sherwood number relationship.

The diffusive Peclet number is expressed as  $P_e = \frac{V_w h_d}{D}$  (1-2)

where  $V_w$  is the cross flow permeate velocity;  $D$  is the diffusivity coefficient of the species; and  $h_d$  is the hydraulic diameter of the spiral wound membrane.

The diffusive Peclet number measures the dimensionless ratio of convective mass transfer to the membrane to the diffusive mass transfer towards the bulk solution at the opposite direction. The Peclet number is also called the dimensionless flux. If the diffusive Peclet number is increased due to suction, while the associated concentration polarization is being reduced, this means that the suction has increased membrane production with more favorable conditions to the membrane, as far as inorganic fouling is concerned. Therefore, the Sherwood number can be avoided in the calculations due to the above-mentioned limitations.

### 1.3 Research Objective

The objective of this research is to investigate the effect of permeate suction on the mass transfer coefficient, concentration polarization layer, product quality, production flow rate, and membrane diffusive Peclet number for spiral wound NF module.

The goal is to increase system permeate flow without subjecting the membrane to an increasing tendency for inorganic precipitation. This was carried out by comparing the data collected from running two tests on the membrane: the first test will be run using the standard high pressure feed pump only, and second will be done by running the test after adding the effect of the permeate suction pump to the original setup.

### 1.3 Research Approach

For high rejection membranes of the type used in reverse osmosis and nanofiltration membrane applications, the water flux can be presented by the solution diffusion model (Lonsdale et al.1965; Soltanieh and Gill, 1981), which states that the solvent flux is proportional to the effective pressure difference ( $\Delta P - \Delta \pi$ ). The solvent flux is caused by the gradient of chemical potential which includes a concentration diffusion term, and a pressure diffusion term. For real membranes that have some imperfections like holes or microspores, the measured flux is not purely diffusive, but it contains a term contributed by convection. Recent researches did not find pores in neither RO nor NF membranes, such that the transport of solvent is accomplished through the free volume between the segments of the polymers of which the membrane is constituted (William, 2003). In diffusion controlled hyperfiltration (RO and NF) membrane process, the solution-diffusion imperfection based model is widely used, because most of the coefficients used in this model are actual operating conditions that can be directly measured, as opposed to theoretical models that have parameters difficult to be measured in reality (Williams, 2003). Furthermore, for dilute solutions, which is the typical solution

fed to NF membrane, this convection term is so small such that it can be neglected (Soltanieh and Gill, 1981) to further simplify the real model.

Mass transfer models typically assume that the bulk feed solution concentration is equal to the membrane wall solution concentration, which is not always true.

This has to be related to the concentration polarization expressions (Williams, 2003).

Concentration polarization complicates the modeling of membrane systems because it is very difficult to experimentally determine the membrane wall concentration ( $c_{mem}$ ).

Membrane wall concentration is necessary to be determined since it and not the bulk feed concentration ( $c_F$ ) should be used in RO and NF transport models.

In the limited feed flow rate that is typically used for hyperfiltration (RO and NF) membrane processes, the flow in the membrane channels is laminar, and the difference between the wall and bulk concentrations can be substantial, so calculations of the concentration at the membrane wall must be appropriately estimated.

Bhattacharya et al. (1996) have developed a generalized mass-transfer relationship from first principals to obtain a theoretically modified form for the Sherwood number using the wall Peclet number to estimate the mass-transfer coefficient using permeate suction.

This correlation is debated due to the above-mentioned items that were discussed earlier.

The permeate suction was tested, and was experimentally validated for NF spiral wound TFC module in this research. An experimental setup for the membrane system was tested with the conventional operating setup in order for it to be compared with the permeate suction setup results. The research was conducted for three different dilute

strong electrolyte binary solutions, namely:  $NaCl$ ,  $MgCl_2$ ,  $MgSO_4$ , which are 1-1, 2-1, and 2-2 electrolytes, respectively, at three different pressures and three different dilute concentrations. The experiment was set at a constant temperature of 25 degrees Celsius in order to keep the diffusion coefficient constant for the different dilute solutions.

### 1.5 Dissertation Outline

Chapter 2 of this dissertation is divided into five parts. The first part presents general information related to RO and NF membrane properties and module configurations. It also includes literature review of the previous researches accomplished to reduce concentration polarization in RO and NF. The second part emphasizes the properties of NF membranes, and their benefits in recent developments in either brackish water desalination or seawater desalination. It also explores the distinguished importance of the new generation of NF membranes. The third part demonstrates the history of using permeate suction in pressure-driven membranes; and discusses the effect of gradually increasing suction on the boundary layer in fluid dynamics. The fourth part illustrates various mass transport models, describing the advantages and disadvantages of each model. Emphasis was placed on the solution-diffusion model which is the mass transport model used in this research.

The fifth part in Chapter 2 discusses the theories related to different equations that will be utilized to avoid using the Sherwood number relationship for mass transfer estimations.

Chapter 3 presents the experimental setup that is being used to validate the hypothesis. A detailed description of the assumptions, equipment, solutions of salts, and chemicals used in the experiments are presented.

Chapter 4 of this dissertation explores the results obtained from the above-mentioned experiments; along with detailed discussions for the results.

Chapter 5 exhibits the conclusion from the experimental results and the discussions. Recommendations were presented in this chapter, along with the suggested future permeate suction researches that can be conducted on higher concentrations of brackish water and seawater membranes to reduce concentration polarization in order to elongate the membrane life.

**CHAPTER 2**  
**CONCENTRATION POLARIZATION IN RO AND NF MODULE:**  
**LITERATURE REVIEW**

This chapter is divided into five main parts. The first part presents general information related to RO and NF membrane properties and module configurations.

The second part explores the distinguished importance of the new generation of NF membranes, and the promising future of this important type of membrane. The third part demonstrates the history of using permeate suction in pressure-driven membranes; and discusses the effect of gradually increasing suction on the boundary layer in fluid dynamics. The fourth part demonstrates various mass transport models, describing the advantages and disadvantages of each model. This includes the solution diffusion model for mass transport in the NF membrane, and the advantage of using it in the application to the new generation of NF membrane. The fifth part demonstrates the theories used to prove the hypothesis related to the chosen mass transport model in dilute solutions, which are used as a feed for NF membrane.

### 2.1 Background

Information similar to that presented in this section can be found in numerous publications describing hyperfiltration membranes and processes. References are made only occasionally and mainly when information is specific to a source.



## 2.2 Preface

Water shortages and lack of access to safe drinking water will continue to be major global problems. At present, more than one billion people lack access to safe drinking water, and 2.4 billion people lack access to proper sanitation, nearly all of them in developing countries. At present a third of the world's population live in water-stressed countries, and by 2025, the number is expected to rise to two-thirds.

Scarcity of fresh water has serious implications on human beings. It can slow down economic expansion, reduce agricultural output, hamper food independence, and degrade public health and quality of life. Since it was first introduced in the 1950's, hyperfiltration membranes (reverse osmosis and nanofiltration) have most commonly been used for desalting seawater, and brackish water by removing salts and other impurities in order to improve the color, taste or properties of the water for drinking and irrigation. Hyperfiltration is finding increasing uses in industrial applications for highly pure water because of its reliability and cost-effectiveness. Membrane separation has gained considerable importance because they offer superior treatments at relatively modest capital and operating cost (Madireddi et al., 1999). However, membrane fouling will continue to be the major obstacle for the efficient operation of RO membrane systems (Jamal et al., 2004).

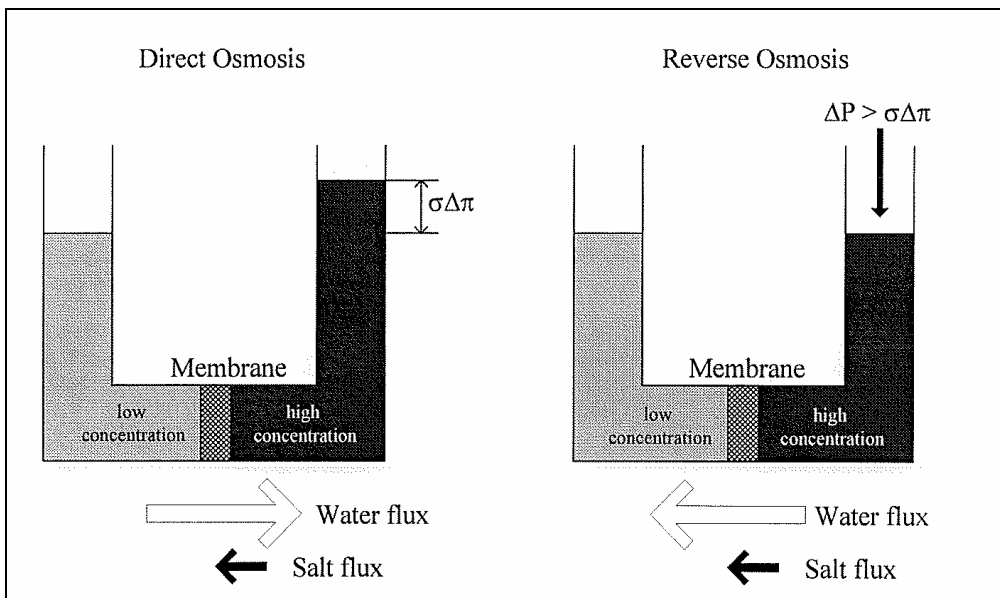
## 2.3 Historical Background

The ancient Egyptians treated water by siphoning water out of the huge jars after allowing the muddy Nile River to settle and separate; the first United States water plant with filters was built in 1872 in Poughkeepsie, New York. Membrane filtration represents

the advanced ring in that historical development of water treatment, and RO is the finest level of filtration available. The concepts of "direct osmosis" and "reverse osmosis" have been known for many years. In fact, studies on osmosis were carried out as early as 1748 by the French scientist Nollet, and many researchers investigated these phenomena over the next two centuries (Reid, 1966; Mason, 1991; Williams, 2003). However, the use of reverse osmosis (RO) as a feasible separation process is a relatively young technology. In fact, only in the late 1950's did the work of Reid show that cellulose acetate RO membranes were capable of separating salt from water, even though the water fluxes obtained were too small to be practical (Reid and Breton, 1959; Ferguson, 1980; Lonsdale, 1982; Applegate, 1984). Then, in the early 1960's, Loeb and Sourirajan developed a method for making asymmetric cellulose acetate membranes with relatively high water fluxes and separations, thus making RO separation both possible and practical (Loeb and Sourirajan, 1962; Loeb, 1981; Sourirajan and Matsuura, 1985). Since then, the development of newer generation membranes such as the thin-film composite membrane that can tolerate a wider pH range, higher temperatures, and harsh chemical environments, and that have highly improved water flux and solute separation characteristics has resulted in many RO applications. In addition to the traditional seawater and brackish water desalination processes, RO and NF membranes have found uses in wastewater treatment, production of ultrapure water, water softening, and food processing, as well as many other applications (Bhattacharyya, 1992).

## 2.4 Definition of Reverse Osmosis

Osmosis is a natural phenomenon that occurs in all living cells in which a solvent passes through a semi-permeable barrier from the side with lower solute concentration to the higher solute concentration. Reverse osmosis is based on a property of certain polymers called semi-permeability. While they are very permeable for water, their permeability for dissolved substances is low. By applying a pressure difference across the membrane the water contained in the feed is forced to permeate through the membrane. In order to overcome the feed side osmotic pressure, fairly high feed pressure is required.



2-1a

2-1b

Figure 2-1. Schematic drawing of water and salt fluxes in direct osmosis and reverse osmosis  
(Adopted from Ghu et Carnahan, 2003)

As shown in Figure 2-1a, solvent flow continues until the chemical potential equilibrium of the solvent is established. At equilibrium, the pressure difference between the two sides of the membrane is equal to the osmotic pressure of the solution. To reverse the flow of water (solvent) a pressure difference greater than the osmotic pressure difference is applied as illustrated in Figure 2-2b. As a result, separation of water from

the solution occurs as pure water flows from the high concentration side to the low concentration side. This phenomenon is termed reverse osmosis or hyperfiltration.

The RO process is attractive because it is relatively simple in design. It consists of a feed water source, feed pretreatment, high pressure pump, RO membrane modules, and in some cases post-treatment steps.

## 2.5 Water Treatment by Pressure-Driven Membranes

The membrane processes that has the greatest immediate application to potable water treatment are reverse osmosis (RO), nanofiltration (NF), ultrafiltration (UF), and microfiltration (MF). Figure 2-2 shows the kind of rejected species by different types of pressure-driven membranes.

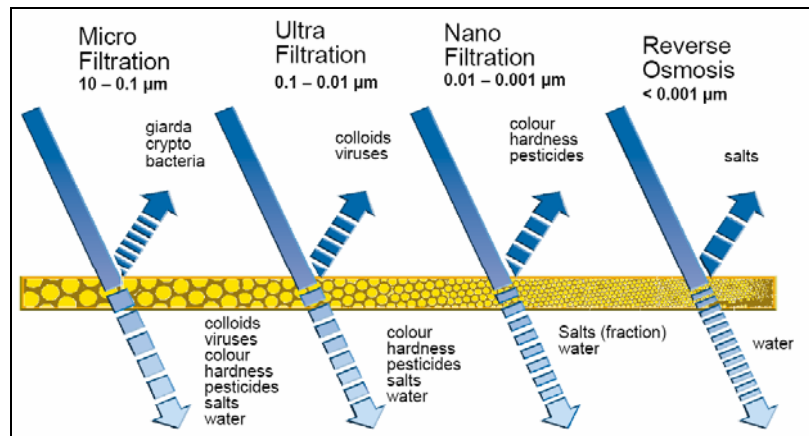


Figure 2-2. Kinds of rejected species by different pressure-driven membrane types (Adapted from Koch membrane manufacturer, 2009)

Reverse osmosis is primarily used to remove salts from brackish water or seawater, and it is also capable of very high rejection of synthetic organic compounds (SOCs). Nanofiltration is used to soften fresh water, and remove disinfection by-product (DBP) precursors. Ultrafiltration, and microfiltration are used to remove turbidity, pathogens, and particles from fresh water. A membrane, the common element of all these

processes, could be defined as any barrier to the flow of suspended, colloidal, or dissolved species in any solvent. Contaminants larger than the maximum pore size of the membrane are removed by sieving in a diffusion-controlled process.

MF and UF membranes have pores in the filtration layer of the membrane, while the active layer in RO and NF membranes is nonporous. The transport of solvent in RO and NF is accomplished through the free volume between the segments of the polymers of which the membrane is constituted (William, 2003).

Contaminants rejection by diffusion-controlled membrane processes increases as species charge and molecular weight increases. Consequently, satisfactory removal of metals, total dissolved solids (TDS), radionuclides, and disinfection by-products precursors can be attained.

Membranes are classified by molecular weight cutoffs, solute and solvent solubility in the membrane film, active membrane material, active film thickness, surface charge, and smoothness of the active film surface.

## 2.6 Reverse Osmosis Membrane Properties

Reverse osmosis membrane separation is governed by the properties of the membrane used in the process. These properties depend on the chemical nature of the membrane material as well as its physical structure. Most currently available RO membranes fall into two types of membranes: asymmetric membranes, and thin film composite (TFC). Asymmetric membrane containing one polymer, and thin film composite membranes consist of two or more polymer layers. Asymmetric RO membranes have a very thin, perm selective skin layer supported on a more porous sub-

layer of the same polymer. This membrane is used to produce the hollow fine fiber (HFF) configuration. The hollow fiber element consists of large number of fine hollow fiber membranes (with an outer diameter up to 200  $\mu\text{m}$ ) placed in a pressure vessel; the feed flows outside the fibers and permeates through them (Allegrezza, 1988; Baker, 1990; Bhattacharyya et al., 1992). These elements have an extremely high packing density, and so can have high permeate production rates per module. However, these modules are highly prone to fouling, and thus are not feasible for many of the applications.

Thin film composite membrane is the one used in spiral wound membrane configuration. The dominant form of the synthetic materials is TFC aromatic polyamide membrane. The development of the cross-linked fully aromatic polyamide thin film composite membrane in the 1970's represented a major advance in membrane technology. TFC membrane provides very thin active film that requires much less energy to induce fluid passage than other materials, making them more economical to use on a large scale. Figure 2-3 shows the composition of both the hydrophilic, and the hydrophobic TFC membrane. Both hydrophilic and hydrophobic films are laid in a composite film by cross-linking different polymers. The thickness of the nonporous layer is typically less than 1  $\mu\text{m}$ . The widely used aromatic polyamide membranes are unfortunately susceptible to oxidation, and are often impacted by the side chain reaction between the disinfectant oxidizing agent like chlorine, and the polyamide groups. This reaction disrupts their stable linkages, and conformational structure. Consequently, this renders them ineffective for their intended function. There have been several attempts to create chlorine-resistance membranes for more than 25 years, but without success (Mukiibi, 2008).

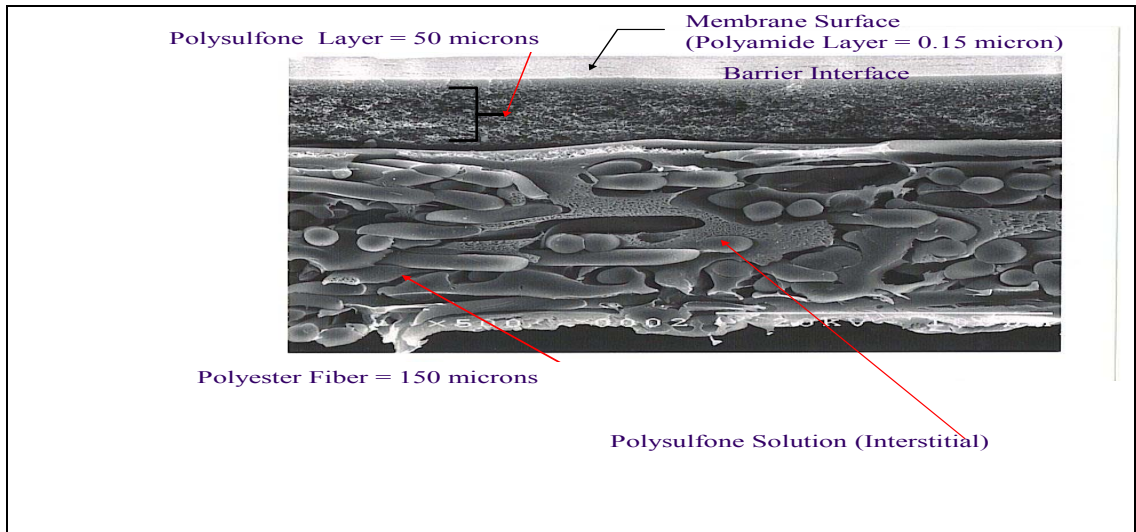


*Figure 2-3. Thin film composite (TFC) cross section view*

*(Adopted from Hydranautics Membrane Manufacturer, 2009)*

## 2.7 Reverse Osmosis Membrane and Module Configuration

The available membrane modules using asymmetric type include plate-and-frame, tubular, and spiral-wound configuration. Plate-and-frame modules consist of stacks of flat sheet membrane placed on supports; each membrane and support are separated by spacers which direct the feed across each membrane and channel permeate out of the module (Allegrezza, 1988; Baker, 1990; Strathmann, 1990; Bhattacharyya et al., 1992).

Tubular membrane elements consist of membrane tubes supported within perforated stainless steel tubes; as feed flows through the tubes, the permeate passes through the membrane and the support. While the plate-and-frame module, and the tubular module are resistant to fouling, they have low membrane surface area per element. This makes them expensive and can limit their use in areas with space restrictions.

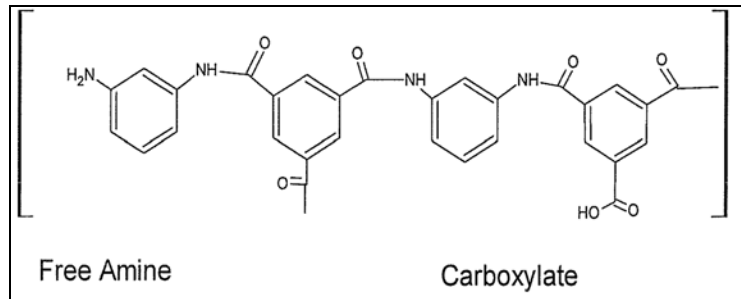


Figure 2-4. Structure of thin film barrier layer of RO aromatic polyamide membrane  
(Adopted from FilmTec Membrane Manufacturer, 2009)

While these elements are also fouling resistant, and are easy to clean, the modules have a low packing density, and can be expensive to operate because of the necessary high feed flow rates. Because of the plate-and-frame, and tubular element disadvantages, these modules are used primarily for highly fouling feeds, or in laboratory researches. Figure 2-4, and Figure 2-5 illustrate the chemical structure of the RO and NF thin film composite polyamide, respectively. The spiral wound membrane configuration is the most common membrane for production of drinking, and industrial process water (Allegrezza, 1988; Bhattacharyya, 1992). This type of element has a high packing density, moderate fouling resistance, and lower capital and operating costs compared to plate-and-frame or tubular modules. The typical configuration of the spiral wound element leaves the membrane easily accessible to cleaning agents. Due to that, the spiral wound membrane can be cleaned more thoroughly, and it is less subject to fouling compared to HFF membranes (Williams et al., 1992). Spiral wound elements are manufactured using flat sheet membranes.

A typical spiral wound element, as shown in Figure 2-6, consists of envelopes (leaves) attached to a center tube that collects the permeate stream.



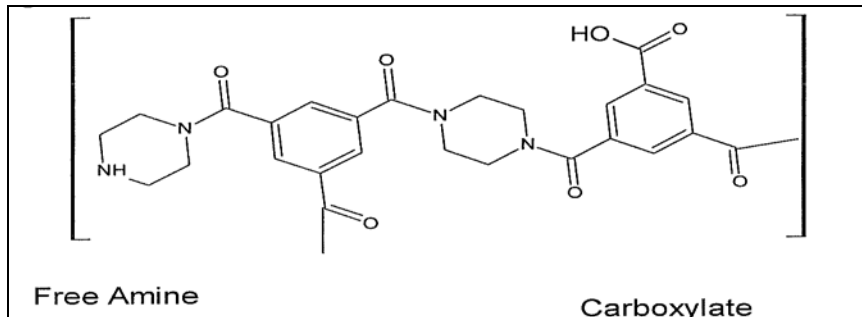


Figure 2-5. Structure of thin film barrier layer of the aromatic /aliphatic polyamide nanofiltration membrane (Adopted from FilmTec Membrane Manufacturer, 2009)

The sheet itself consists of two layers forming a folded envelope. The envelope is glued along three open sides and near the fold, completely enclosing the permeate spacer. The glue line on the fold end is a short distance away from the fold, because the fold end is attached to the center collection tube. The glue line at the fold end stops the flow of the feed stream, and allows the remaining pressure in the permeate stream to drive it through the membrane into the center collection tube. An envelope is formed by folding one flat sheet over a permeate stream spacer. Feed spacer and permeate spacer, shown in Figure 2-7, are attached to each envelope prior to establishing the fold end glue line.

Several envelopes, including feed spacers, and permeate spacers are attached to the center collection tube, and wrapped in a spiral around it. An epoxy shell or tape wraps are applied around the envelope, completing the spiral wound element. The feed stream enters the end of the spiral wound element in the channel created by the feed stream spacer. The feed stream can flow either in a path parallel to the center collection tube or through the active membrane film and membrane supports into a channel created by the permeate stream spacers.

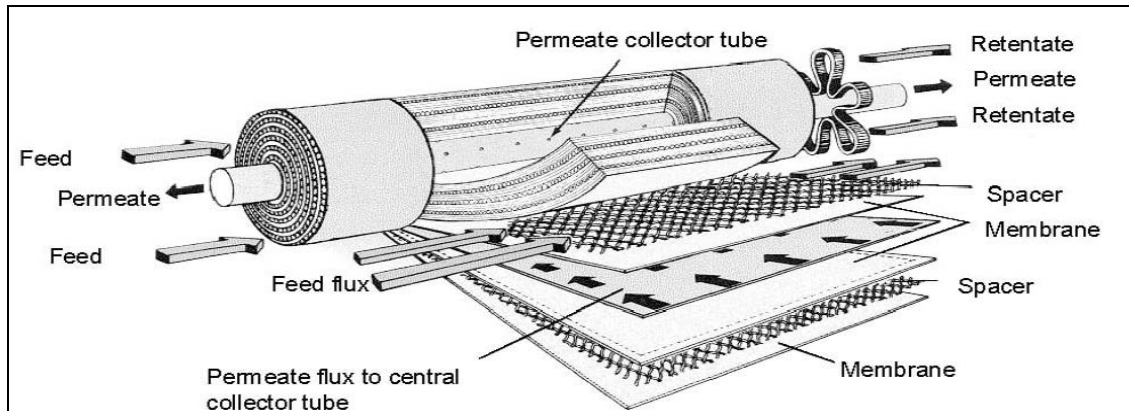
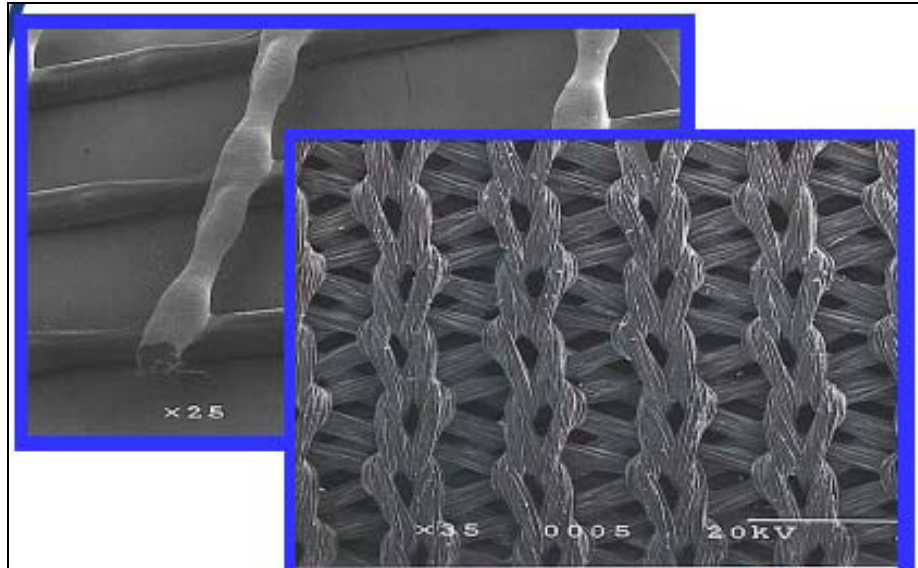


Figure 2-6. A cross section in the thin film composite (TFC) spiral wound reverse osmosis membrane showing feed channel spacer (adopted from Fritzmann et al., 2007)

The permeate stream follows a spiral path into the center collection tube, and is taken away as product for point of use. The recovery in a spiral wound element varies from approximately 5 to 20 percent. The Reynold's number typically ranges from 100 to 1,000. The feed stream spacer creates additional turbulence and increases the Reynold's number (J. S. Taylor, 1999). The highest and lowest feed stream velocities occur at the entrance, and the exit of the element, respectively. The feed flow is in the laminar region, and the last element in series is the one which is most likely subjected to chemical fouling, if the species in the feed water are subjected to super saturation. Fouling from particle deposition could occur mainly in the first element in series.

Because of the importance of the membrane module used in the RO process, much research has been performed to optimize the design of each element type. As a result, many models describing the various modules are available, such that allowing determination of different module hydrodynamics, or optimizing the membrane spacer placement and height.



*Figure 2-7. Configuration of permeate spacer (top) and feed spacer (bottom) in spiral wound RO/NF element (adopted from Hydranautics membrane manufacturer, 2009)*

Reverse osmosis membrane modules can be arranged in several configurations in the RO process (Williams et al., 1992). For a single-pass arrangement, a single high rejection membrane sufficiently removes the solute from the feed. In a double-pass configuration, the permeate of one set of membranes is used as the feed to another set of membranes in order to provide adequate overall removal of the solute. The modules can also be placed in stages in order to increase water recoveries. In this configuration, the concentrate from one set of membranes is used as the feed for another set, and consequently high overall water recoveries are possible.

## 2.8 Concentration Polarization

Concentration polarization, which is illustrated in Figure 1-1 in Chapter 1, is the term used to describe the accumulation of rejected solute at the surface of a membrane so that the solute concentration at the membrane wall is higher than that of the bulk feed

solution. As water passes through the membrane, the convective flow of solute to the membrane surface is much larger than the diffusion of the solute back to the bulk feed solution. As a result, the concentration of the solute at the membrane wall increases. Reviews of concentration polarization are given by Matthiasson and Sivik (1980), Gekas and Hallstrom (1987), Rautenbach and Albrecht (1989), and Bhattacharyya and Williams (1992). Possible negative effects of concentration polarization include: (1) decrease in water flux due to increased osmotic pressure at the membrane wall; (2) increase in solute flux through the membrane because of increased concentration gradient across the membrane; (3) precipitation of the solute if the surface concentration exceeds its solubility limit, leading to scaling or particle fouling of the membrane, and reduced water flux; (4) changes in membrane separation properties; (5) enhancement of fouling by particulate or colloidal materials in the feed which block the membrane surface and reduce water flux. The extent of concentration polarization can be reduced by promoting good mixing of the bulk feed solution with the solution near the membrane wall. Mixing can be enhanced through membrane module optimization of turbulence promoters, or feed spacer geometrical configuration and height, or by increasing axial velocity to promote turbulent flow.

## 2.9 Previous Studies to Reduce Concentration Polarization

Several techniques that have the potential to reduce the concentration polarization to control the fouling have been proposed and adopted. One method is to adjust the operating parameters, e.g. using an intermittent mode of operation, or employing variable means to reduce concentration polarization. Both of these phenomena are

impacting flux (Mahlab, 1978). Other techniques include increasing the flow rate; assembling an intensifier for turbulent flow; the use of impulse methods and agitating methods; the periodic depressurization of the membrane tube, flow reversal, pre-coating of the membrane surfaces; enzyme immobilization; modification of the membrane's polymeric structure; and the mechanical and ultrasonic vibration of the membranes (e.g., Mahlab, 1978; Cruver, 1973). The turbulence promoter acts to reduce concentration polarization and therefore fouling is decreased by increasing the friction factor and bulk velocity. A model has been developed by Chiolle for reverse osmosis with turbulence promoting nets for the parallel wall channels module (Chiolle et al, 1978). The model developed by Drioli and Bellucci shows the effect of the interaction between concentration polarization and solute-membrane on the pressure driven membranes, when a multi-component solution is involved (Drioli and Bellucci, 1978).

The modification of the membrane's polymeric structure plays an important role in the reduction of concentration polarization through the fluidized bed that was developed by Van der Waal (Van der Waal, 1977). Bhattacharyya developed a finite elements program to compute the concentration profile throughout a reverse osmosis membrane module to predict the performance of the module. The finite element method allowed rapid evaluation of various membrane module configurations, such as tapered cell geometry and channels containing spaces (Bhattacharyya et. al, 1990; Gupta, 2005).

The model developed by Van der Meer has shown that an increase of 20% in the permeate productivity of the spiral wound RO process is achievable by lowering the number of membrane modules from six per vessel to two in a pressure vessel (Van der Meer et al., 1988).

## 2.10 Limiting Factors for Membrane Fouling

Membrane processes are not only limited by increasing osmotic pressure due to concentration polarization and rising overall concentrations along the membrane, but by other factors leading to reduced performance and they can be differentiated by their mechanism. Various chemicals can harm the active layer of the membrane, leading to irreversible damage associated with reduced rejection capability and even destruction of the membrane. Oxidants used in pre-treatment of the reverse osmosis feed water, or as cleaning chemicals are the most important group of chemicals responsible for membrane deterioration. In addition, polymeric membranes are more or less susceptible to very low or high pH values. Therefore pH adjustment and control is necessary to ensure stable operation. During operation of a reverse osmosis plant, care has to be taken that no dissolved, colloidal or biologic matter accumulate at the membrane surface, building a continuous layer that reduces or inhibits mass transfer across the membrane.

Precipitation on the membrane is caused by super-saturation of inorganic compounds concentrated on the feed side. Super-saturated salts can precipitate on the membrane surface building a thin layer, which hinders mass transfer through the membrane. Scaling always occurs at the membrane surface because of the increased salt concentration near the membrane caused by concentration polarization. Some of the most important scaling substances are  $CaCO_3$ ,  $CaSO_4$ ,  $BaSO_4$ ,  $SrSO_4$ ,  $CaF_2$ ,  $Mg(OH)_2$ , and  $SiO_2$ . Scaling can drastically reduce permeate flux, and has to be avoided by all means. Figure 2-8 illustrates the species that can foul or scale the membrane that leads to deteriorated performance. Most susceptible to scaling is the downstream part of the RO stage where concentration in the feed solution is the highest. Therefore, pre-treatment is

used for stabilization of substances that could cause scaling. By pH adjustment, and the use of antiscalants, precipitation can be inhibited. Crystal growth is usually divided into three stages as shown in Figure 2-9. Antiscalants inhibit one or more of these building stages (Fritzmann et al., 2007). Membrane fouling is caused either by convective and diffusive transport of suspended or colloidal matter, or by bio-fouling. An existing fouling layer adds to the overall resistance to mass transfer of the membrane and overall performance decreases significantly. In addition, membrane fouling also increases pressure loss along the membrane, while rejection is decreased. In RO operations, fouling can never fully be prevented even with optimized pre-treatment. Therefore, periodical membrane cleaning has to be performed. Complete removal is not possible and fouling has to be tolerated up to a decrease of mass flux down to 75% of original flux (Fritzmann et al., 2007). Good operating practice calls for chemical cleaning of the membranes, either normalized permeate flow decreases by 10%, feed channel pressure loss increases by 15%, or normalized salt rejection decreases by 10% from initial conditions during the first 48 hours of plant operation.

A key phase in the membrane separation processes is the transition from concentration polarization to fouling. This occurs at a critical flux.

Song (1998) developed a mechanistic model, based on first principles, for predicting the limiting flux. He showed that for a given suspension there is a critical pressure below which a concentration polarization layer will exist at the membrane surface.

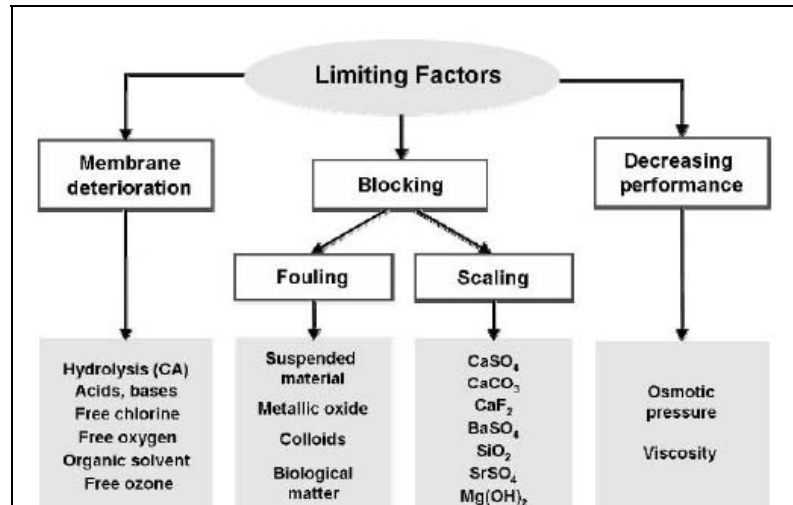


Figure 2-8. Limiting factors for RO and NF membrane fouling

(adopted from Fritzmann et al., 2007)

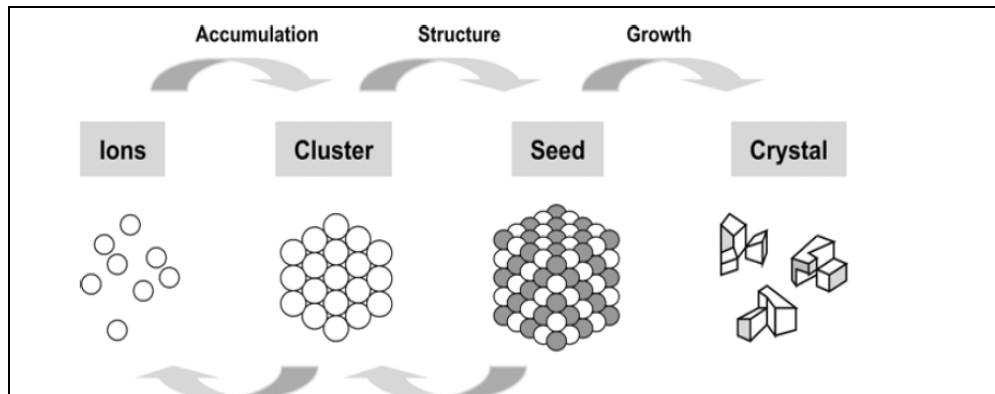


Figure 2-9. Inorganic scaling stages (Adopted from Fritzmann et al., 2007)

However, a cake layer will form between the polarization layer, and the membrane surface when the applied pressure exceeds a critical pressure. The limiting or critical flux values predicted by the mechanistic model compared well with the integral model for a low concentration feed. However, it deviated at high solute feed concentrations (Salbani et al., 2001).



## 2.11 The Promise of Nanofiltration Membrane

NF membrane is sometimes called a loose RO pressure-driven membrane process because of its relatively much higher permeability coefficient. NF processes operate at pressures between 50 psi, and 150 psi - much lower than reverse osmosis (200 to 1,000 psi), but higher than ultrafiltration, and micorfiltration (10 to 70 psi). The molecular weight cut-off (MWCO) is generally between 300 and 1,000 Dalton.

In treating brackish water, NF has been widely used due to more stringent drinking water regulations. Brackish water desalination is assumed to grow at higher rates than seawater desalination in the near future (Fritzmman et al., 2007). Delivery of fresh water from seawater desalination plants demands piping and pumping systems to transport product water from coastal regions to residential areas, which increase cost. High availability of most brackish water in residential areas makes expensive delivery piping and pumping unnecessary.

### 2.11.1 Nanofiltration for Contaminated Drinking Water

Nanofiltration membrane, although a relatively recent development, has attracted a great deal of attention for use in water softening, and removal of various contaminants from drinking water sources (Williams, 2003). NF membranes are usually negatively-charged, and, as a result, ion repulsion is the major factor in determining salt rejection. For example, more highly charged ions such as  $SO_4^{--}$ ,  $Ca^{++}$ , and  $Mg^{++}$  are rejected by nanofiltration membranes to a greater extent than monovalent ions such as  $Cl^-$ , or  $Na^-$ . NF processes can reduce or remove TDS, hardness, color, agricultural chemicals, and high molecular weight humic and fulvic materials, which can form trihalomethanes when

chlorinated. Dykes and Conlon (1989), Conlon and McClellan (1989), Watson and Hornburg (1989), and Conlon et al. (1990) have identified NF as an emerging technology for compliance with THM regulations and for control of TDS, TOC, color, and THM precursors. Clifford et al. (1988) discussed the use of NF70 membranes of FilmTec for contaminated groundwater treatment. Removals included 91% for radium-226 and 87% for TDS. Taylor et al. (1989) reported that NF70 membranes could allow control of THM formation, TOC, TDS, and produce high quality product water from an organic contaminated groundwater. They indicated that the cost of a NF process would be competitive with conventional treatment processes which do not control THM formation.

Amy et al. (1990) used NF70 membranes to remove dissolved organic matter from both groundwater, and surface water in order to reduce THM precursors; they found that the process was effective in reducing the organics as well as conductivity in both water sources. NF membranes also reject organic compounds with molecular weights above 200 to 500. These properties have made possible some interesting new applications in wastewater treatment, such as selective separation, and recovery of pollutants that have charge differences, separation of hazardous organics from monovalent salt solutions, and membrane softening to reduce hardness, and THM precursors in drinking water sources (Eriksson, 1988; Cadotte et al., 1988; Williams et al., 1992). Arsenic, which is the most extensive environmental poisonous chemical element throughout the world, can be removed by NF to meet World Health Organization (WHO) standards (Larry Henke, 2008).

### 2.11.2 Nanofiltration for Wastewater

Nanofiltration has also been used to remove both organics and inorganics in various wastewaters. Bindoff et al. (1987) reported the use of NF membranes to remove color-causing compounds from effluent containing lignin, and high salt concentrations in a wood pulping process. Color removals were >98% at water recoveries up to 95% while the inorganic was poorly rejected, allowing the use of low operating pressures, since the osmotic pressure of organic matters is small. Ikeda et al. (1988) indicated NF could give high separations of color-causing compounds such as lignin sulphonates in paper pulping wastewaters. Afonso et al. (1992) found NF removal (>95%) of chlorinated organic compounds from alkaline pulp and paper bleaching effluents with high water fluxes. Simpson et al. (1987) reported the use of NF membranes to remove hardness and organics in textile mill effluents. Gaeta and Fedele (1991) also indicated that high water recoveries (up to 90%) from textile dye house effluent could be achieved with NF membranes. Ikeda et al. (1988) and Cadotte et al. (1988) reported the use of NF membranes in the treatment of food processing wastewaters. Some specific uses included the desalting of whey and the reduction of high BOD and nitrate levels in potato processing waters (Anonymous, 1988). Bhattacharyya et al. (1989) used NF membranes to selectively separate mixtures of cadmium and nickel. Chu et al. (1990) detailed the use of NF in a process for treating uranium wastewater; uranium rejections were 97% to 99.9%. Dyke and Bartels (1990) discussed the use of NF membranes to replace activated carbon filters for the removal of organics from offshore produced water containing residual oils. The produced waters contained ~1,000 mg/l soluble organics (mostly carboxylic acids) and high inorganic concentrations (~15,000 mg/l  $Na^+$  and ~25,000

mg/l  $Cl^-$  as well as other dissolved ions). Organic rejections were suitable to meet discharge standards, while inorganics rejections were low (<20%), allowing operation at low pressures.

### 2.11.3 Nanofiltration for Hybrid Seawater Distillation

The use of NF membrane is the state of the art in sea water distillation industry (Anwerbuch, 2007). The process comprises the operation of the NF selective membrane to soften the feed to distillation units. NF membrane substantially increases the water production from the mature technology of multi stage flash (MSF), multi effect distillation (MED), and vapor compression (VP) distillation techniques.

The scaling in sea water distillation systems occurs due to inverse solubility of calcium sulfate at higher temperature. In order to increase the water production of the existing distillation units, it is required to increase operation temperatures, so that higher recovery or higher concentration factor are obtained. NF selective membranes were used to reject the high content of sulfate, and hardness in the sea water before it is fed to the distillation units. This allows the operators to optimize the operation of the units to run at higher temperatures than that it was designed for because of the reduction of sulfate and hardness in the re-circulated seawater after being pretreated with NF membrane.

Experiments show that the water temperature was increased from design of 105 degree C to a maximum of 117.9 degree C, which helped to achieve a product capacity increase of 40%, and a decrease in operating cost by 40% for the operation of MSF plants (Anwerbuch, 2007). Hassan (2004) from Saline Water Conversion Corporation (SWEC) of Saudi Arabia has successfully introduced a new concept to seawater desalination by

combining the NF membrane process with one or more of the conventional seawater desalination processes in one fully integrated process system to form: a NF-SWRO, a NF-MSF, and a NF-SWRO reject -MSF, which were successfully evaluated at the pilot, and demonstration plant level. The NF-SWRO hybrid has increased the productivity by 42%, and raised SWRO unit water recovery ratio to 56% from 28%. After four years in operation, no SWRO membrane replacement, or cleaning were needed.

#### 2.11.4 Nanofiltration Membrane in Replacing Standard Seawater RO Membrane

The Long Beach Water Department of California (LBWD) has recently patented a two-pass NF membrane for seawater desalination (Le Gouellec et al., 2006).

NF membranes have a significantly higher permeability than seawater RO membrane, but with higher salt passage, especially for monovalent ions. In a two pass NF-NF system, the seawater is treated by a first pass NF system. Because of the lower salt rejection ability of the NF membrane, permeate from the first pass is further treated by a second pass NF system to produce a permeate water of acceptable quality.

According to the results, the overall recovery of the system is approximately 40% to 43%. The two staged NF system is as much as 20% more energy efficient than the typical seawater desalination RO membrane for Pacific Ocean seawater with salinity of 35,000 mg/l. The typical energy saving possible with the two configurations discussed above is illustrated in Figure (2-10). A standard RO configuration is also shown for comparison. As indicated in the figure, higher recovery with lower energy consumption is possible with brackish and seawater element. The NF-NF configuration results in the lowest energy consumption at a slightly lower recovery than standard RO seawater system.

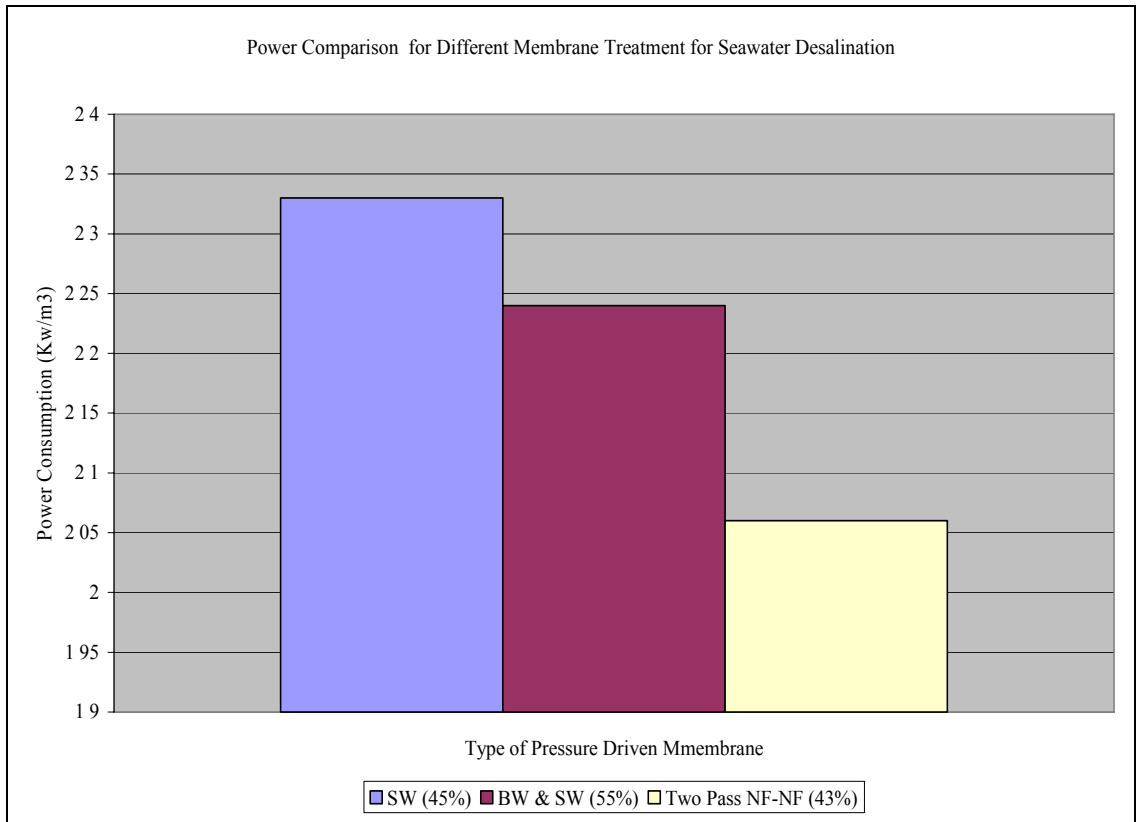


Figure 2-10. Comparison of energy consumption for seawater desalination with SW membrane; BW-SW membrane & NF-NF membrane. Recoveries are shown in parentheses (Le Gouellec et al., 2006)

## 2.12 New Generation of Nanofiltration Membrane

New NF membranes have been recently developed which can be tailored to have a range of hardness rejection. These membranes are the composite polyamide type, similar to the existing standard RO membranes, but are chemically treated to adjust the hardness rejection. This treatment also imparts fouling resistance (Wilf et al., 2007).

Among the makers of the new generation of NF membranes are Hydranautics, and FilmTec membrane manufacturers. Table 2-1 illustrates the performance comparison for various types of the new generation of NF membranes. For example, the rejection characteristics of Hydranautics membrane manufacturer new NF can be tailored to meet a variety of hardness rejection values ranging between 83% to 93 % at standard operating

pressure of a feed of 500 mg/l of  $CaCl_2$  and 75 psi feed pressure at 25 degree C, as shown in table 2-1.

*Table 2-1 Comparison of new generation of NF membranes performance at standard operating conditions (Adopted from FilmTec, and Hydranautics Membrane Manufacturer, 2009)*

Manufacturer	Product	Element Area		Nominal Flow		Rejection %
		( $ft^2$ )	( $m^2$ )	(gpd)	(m3/d)	
Hydranautics	ESNA1-LF	400	37.2	8,200	31.1	89 (1)
Hydranautics	ESNA1-LF2	400	37.2	10,500	39.8	86 (1)
Hydranautics	ESNA-LF3	400	37.2	7,200	27.3	90 (1)
FilmTec	NF-270-400	400	37.2	14,700	55.6	40-60 (2) 97 (3)
FilmTec	NF-200-400	400	37.2	8,000	30.3	50-65 (2) 97 (3)

*Test Conditions*

- (1) 500 mg/l of  $CaCl_2$ , 75 psi, 25 C, 15% recovery
- (2) 500 mg/l of  $CaCl_2$ , 70 psi, 25 C, 15% recovery
- (3) 2,000 mg/l of  $MgSO_4$ , 70 psi, 25 C, 15% recovery

FilmTec has introduced a similar new type of NF membrane model NF270, and model NF200. These membranes have a salt rejection of 97% at standard operating conditions of 2,000 mg/l of  $MgSO_4$  at 70 psi, and 25 degree C., and a salt rejection of 40-60% at 500 mg/l of  $CaCl_2$ . (FilmTec, 2007).

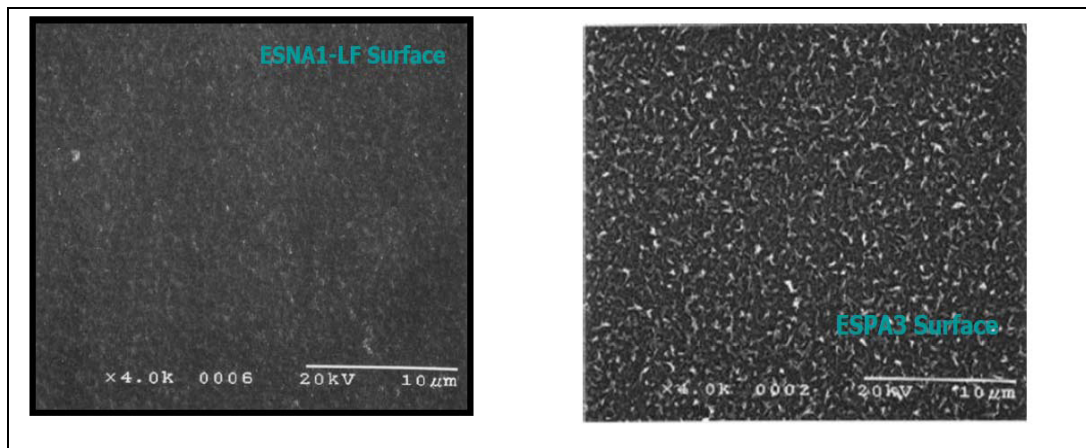
The other feature of those types of membranes is the low fouling nature due to the smoothness of the membrane surface and the near neutral surface charge (Wilf, 2007).

Figure 2-11 indicates the relative surface smoothness of the new NF membrane model ESNA1-LF compared to the standard low pressure RO membrane model ESPA3. Both products are manufactured by Hydranautics.

The lower negative charge of the new generation NF ESNA1-LF membrane from Hydranautics can be seen in Figure 2-12. The figure shows the Zeta potential of the

membrane surface measured as a function of the feed pH. It can be seen that the traditional NF membrane ESNA-1 has a very strong negative charge at neutral pH.

In contrast, the low pressure low fouling RO membrane, LFC1, has a slight negative charge at these pH values. Similarly, the ESNA1-LF membrane has a slight charge, or near neutral surface charge. This minimal surface charge minimizes the interaction with some organic compounds. It is interesting to mention that due to the slight negative surface charge of the new generation of this type of NF membranes, the membrane mass transport can be modeled using the typical Solution-Diffusion Model which is normally used for RO membrane rather than the more sophisticated models like Donnan exclusion, and extended Nernst- Planck models, that include electrostatic effects. These charged membrane models are discussed in more details later in item 2.15.3.



*Figure 2-11. Image of the surface of the New Generation NF ESNA1-LF membrane compared to the Low Pressure RO ESPA3 membrane Showing Relative Surface Smoothing  
(Adopted from Hydranautics membrane manufacturer, 2007)*



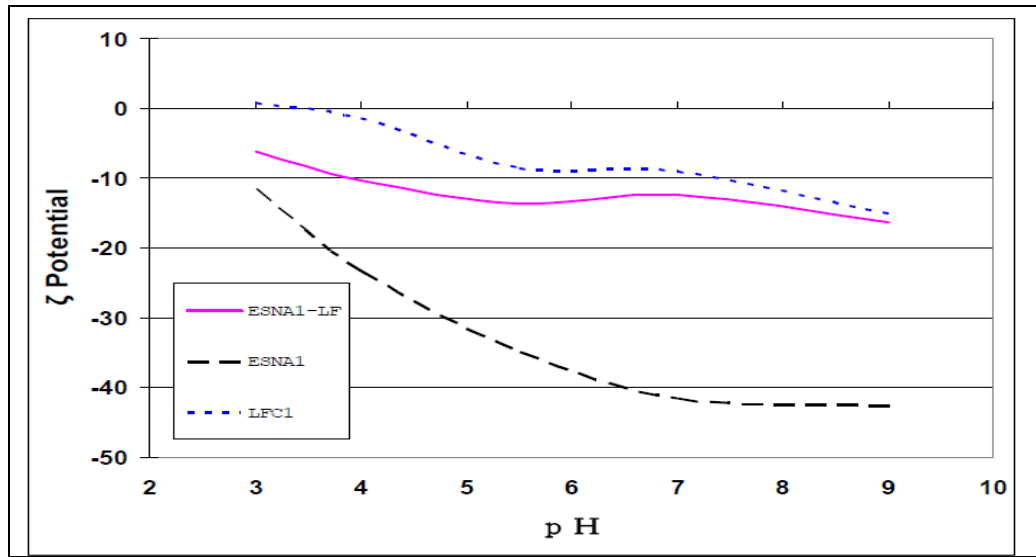


Figure 2-12. Comparison of surface charge of new generation NF ESNA1-LF membrane, typical NF LFC1 membrane, and low pressure low fouling RO LFC1 membrane (Adopted from Hydranautics membrane manufacturer, 2007)

### 2.13 History of Using Permeate Suction in Pressure-Driven Membrane

Permeate suction has not been commercially used before in RO or NF.

However, permeate suction was theoretically investigated by several researchers.

Bhattacharya, et al. (1996) have developed a generalized mass-transfer relation from first principals to obtain a theoretically modified form for Sherwood number using the wall Peclet number to estimate the mass-transfer coefficient using permeate suction in rectangular channel cell, tubular module, and cross flow cell. He concluded that suction through the porous membrane had a significant effect on the mass transfer coefficient, and, in turn, the permeate flux for both RO and UF. He mentioned that this should be of immense help to the process and design engineer to improve the module design.

The role of suction in mass transfer through porous membranes is very important. It was identified by several researchers (Van den Berg et al., 1989; Gekas et al., 1987) that the effect of permeate suction enhances the mass transfer from the bulk to the

membrane surface. Gekas and Hallstrom (1987) found that suction at the membrane surface increased the mass transfer coefficient from the surface to the bulk. Sirshendu and Bhattacharya (1988) have proposed a modified Sherwood number relationship including the effect of property variations due to permeate suction for laminar flow in a rectangular channel cross flow ultrafiltration for bovine serum and dextran (Sirshendu and Bhattacharya, 1999).

Immersed UF membrane (Figure 2-13) is used to treat wastewater that has virtually no osmotic pressure, so only small suction pressure is enough to create water flow from the permeate side to penetrate through the membrane (about 4-9 psi).

In this case, suction pressure can not theoretically exceed the atmospheric pressure which is about 14.7 psi (1 atm), in order to avoid cavitation in the permeate suction pump.

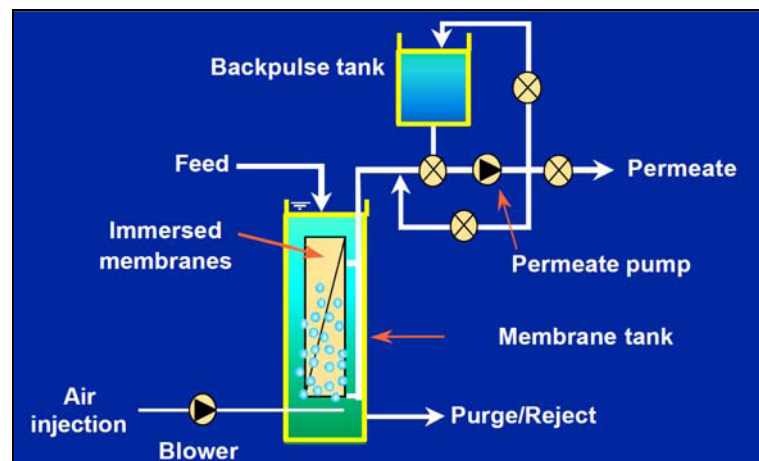


Figure 2-13. Membrane bio-reactor using permeate suction to treat wastewater by immersed UF membrane (Adopted from Zenon Environmental membrane manufacturer, 2006)

## 2.14 Effect of Increasing Suction Pressure on the Boundary Layer:

In a two dimensional laminar flow, the thickness of the boundary layer which has not separated can be estimated as follows: the inertia force per unit volume is equal to

$\rho u \frac{\partial u}{\partial x}$ . And for a membrane envelop of width L, the gradient of  $\frac{\partial u}{\partial x}$  is proportional to  $\frac{u}{L}$ , where u denotes the velocity outside the boundary layer. Hence the inertia force is of the order  $\rho \frac{u^2}{L}$ . On the other hand the friction force per unit volume is equal to  $\frac{\partial \tau}{\partial y}$ , which is in the assumption of the laminar flow is equal to  $\mu \frac{\partial^2 u}{\partial y^2}$ . The velocity gradient  $\frac{\partial u}{\partial y}$  in the direction perpendicular to the membrane is of the order  $\frac{u}{\delta}$ , so that the friction force per unit volume is (Schlichtings, 1979)  $\frac{\partial \tau}{\partial y} \approx \mu \frac{u}{\delta^2}$  (2-1)

From the condition of equality of the friction and inertia forces, assuming a constant viscosity, we obtain:

$$\mu \frac{u}{\delta^2} \approx \frac{\rho U^2}{L} \quad (2-2)$$

Solving for the boundary layer thickness  $\delta$  at any point of the membrane length, it is found at laminar flow that:

$$\delta \approx \sqrt{\frac{\mu L}{\rho u}} = \sqrt{\frac{\nu L}{u}} \quad (2-3)$$

Hence for laminar flow region, the boundary layer thickness is:

$$\delta = 5 \sqrt{\frac{\nu L}{u}}, \text{ where L is the membrane width. (Schlichting, 1979)} \quad (2-4)$$

In NF spiral wound membrane, the flow is laminar, and the local Reynold's

number ranges between 100-1,000 ( Taylor et al., 1999). By applying suction at the end of the collector tube of the membrane module, an increase of pressure gradient along the stream at x direction will present. This increase in pressure will de-stabilize the boundary layer (Schlichting, 1979). This is oppisite to the case of a decrease in the pressure gradient along x direction. In the latter case, the bounary layer will be stabilized, and will not create a suitable condition for the reduction of the concnetration polarization.

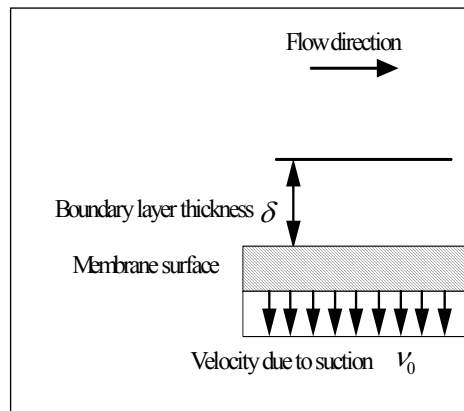


Figure 2-14. Application of suction to the membrane to prevent the boundary layer separation

The de-stabilization of the boundary layer will have two effects: first, it will reduce the boundary layer thickness and a thinner boundary layer is less prone to become turbulent. Secondly, since in the dilute solutions the concentration polarization layer is impeded in the boundary layer (Probstein, 1994), suction will consequently reduce concentration polarization.

In a flat surface membrane, it is assumed that the quantities of fluid particles in the immediate neighborhood of the membrane surface are sucked away.

This is equivalent to that the ratio of suction velocity  $v_0(x)$  to free stream velocity  $u$  is very small, say  $\frac{v_0}{u} = 0.0001$  to  $0.01$  (Schlichting, 1979). When the suction velocity is of such a small order of magnitude, it is possible to neglect the loss of mass or “sink-effect” on the external potential flow. On the flat surface membrane, the quantity of fluid removed  $Q$ , will be expressed through a dimensionless volume coefficient by

$$\text{putting } Q = c_Q A_1 u \quad (2-5)$$

where  $A_1 =$  wetted membrane surface area ( $b \times L$ )

And for the flat membrane

$$Q = b \int_0^L [-v_0(x)] dx \quad (2-6)$$

Since equation (2-5) equals to equation (2-6), consequently

$$c_Q A_1 u = b \int_0^L [-v_0(x)] dx$$

$$\text{or } c_Q = \frac{1}{Lu} \int_0^L [-v_0(x)] dx \quad \text{where } A_1 = bL \quad (2-7)$$

where  $Q =$  quantity of fluid removed during suction,  $c_Q =$  Dimensionless volume coefficient,  $u =$  Average bulk velocity at the  $x$  direction, and for the case of increasing suction pressure:

$v_0$  increases over the  $x$  axis, i.e.  $v_0(x)$ .

$$\text{The suction pressure is necessary to be dependent on } x \text{ and } y, \text{ i.e. } P(x,y) \quad (2-8)$$

and the continuity and Navier–Stokes equations that govern the laminar two dimensions flow at steady state condition when there is a mass transfer through

porous membrane surface are, and using the mean flow is (Schlichting, 1979):

$$\frac{\partial u'}{\partial x} + \frac{\partial v'}{\partial y} = 0 \quad (2-9)$$

$$\text{and } u \frac{\partial u'}{\partial x} + v' \frac{\partial u'}{\partial y} = - \frac{1}{\rho} \frac{\partial P'}{\partial x} + \nu \nabla^2 u' \quad (2-10)$$

$$\text{and } u \frac{\partial v'}{\partial x} = - \frac{1}{\rho} \frac{\partial P'}{\partial y} + \nu \nabla^2 v' \quad (2-11)$$

where  $\nabla^2$  denotes the Laplacian operator  $\frac{\partial^2}{\partial x^2} + \frac{\partial^2}{\partial y^2}$

From equations 2-9, 2-10, and 2-11 the velocity gradient due to permeate suction can be Calculated, and the boundary conditions are:

at  $y=0$  :  $u = 0$ , and  $v = v_0 < 0$  at  $x = 0$ ,

and at  $y = \infty$  :  $u = U(x)$

## 2.15 Reverse Osmosis Models

Many mathematical models have been proposed to describe reverse osmosis membranes. Some of these descriptions rely on relatively simple concepts while others are far more complex and require sophisticated solution techniques.

Models that adequately describe the performance of RO membranes are essential, since These are needed in the design of RO processes. Reverse osmosis models can be divided Into four types: irreversible thermodynamics (I. T.) models; nonporous homogeneous models; pore models; and charged membranes models. A fundamental difference exists between the assumptions of the homogeneous and porous membrane models.

The homogeneous models assume that the membrane is nonporous, that is transport takes place between the interstitial spaces of the polymer nodules, usually by diffusion. The porous models assume that transport takes place through pores that run the length of the membrane barrier layer; as a result transport can occur by both diffusion and convection through the pores. While both concepts have had some success in predicting RO separation, the question of whether a RO membrane is nonporous or porous is still a point of debate (Williams, 2003).

### 2.15.1 Irreversible Thermodynamics Models

Irreversible thermodynamics (I.T.) models, such as the Spiegler-Kedem model, assume that the membrane is in mechanical equilibrium, no external force acting on the system, and flux can be described by the phenomenological equations relationships.

The water flux according to the Spiegler-Kedem model is given by

$$J_w = L_p (\Delta p - \sigma \Delta \pi) \quad (2-12)$$

while the solute flux is expressed as

$$J_s = \omega \Delta \pi + (1 - \sigma) (C_m)_{avg} J_w \quad (2-13)$$

where  $L_p$  is the hydrodynamic permeability coefficient;  $\sigma$  is the coefficient of coupling between salt and water;  $\Delta \pi$  is the difference in the osmotic pressure across the membrane;  $\Delta p$  is the operating pressure;  $\omega$  is the salt permeation coefficient; and  $(C_m)_{avg}$  is the logarithmic mean solute concentration in the membrane (Soltanieh and Gill, 1984).

The Spiegler-Kedem model has found a wide use for the description and analysis of RO membrane separation. However a major disadvantage of the model is the treatment of the membrane as a black box. It does not provide insight into the transport mechanisms

of the membrane. I. T. models also do not include any convection effects, and considers transport of the solvent and solute take place only by the effect of the chemical potential gradient, which includes concentration, and pressure diffusion. These models assume that Onsager reciprocal relations are valid (Soltanieh et Gill, 1981). This assumption is controversial in processes far from equilibrium (Rosenbaum and Skiens, 1968). As a result, I. T. models are not very useful in optimizing separation based on membrane structure and properties. These models also do not adequately describe water flux for some solute systems, in particular some dilute organics that have no osmotic pressure (Williams, 2003).

#### 2.15.2 Porous Models

The porous models assume that transport takes place through pores that run the length of the membrane barrier layer; as a result, transport can occur by both diffusion and convection through the pores. The preferential sorption-capillary flow model (PSCP) proposed by Sourirajan (1970); Sourirajan and Matsuura (1985) states that the membrane is assumed to be microporous and the barrier layer has chemical properties such that it has a preferential sorption for the solvent or preferential repulsion for the solutes of the feed solution. As a result, a layer of almost pure solvent is preferentially sorbed on the surface and in the pores of the capillary pores under pressure.

The total water flux is given by  $N_w = A [\Delta p - (\pi(X_F) - \pi(X_P))]$  (2-14)

The total solute flux is expressed as  $N_s = \frac{ck_s D_w}{\delta_M} (X_F - X_P)$  (2-15)

where A is the pure water permeability constant of the membrane;  $\Delta p$  is the applied pressure difference;  $\pi(X)$  represents the osmotic pressure of the feed or permeate side



with solute mole fraction  $X$ ;  $C$  is the molar concentration of salt;  $k_s$  is the distribution coefficient of the solute from the feed into the pore of the membrane;  $D_w$  is the diffusion coefficient of the solute in the membrane; and  $\delta_M$  is the active membrane thickness. The term  $\frac{k_s D_w}{\delta_F}$ , which is treated as a single parameter, is called “solute transport parameter”. In their experiments, Alegranti et al. (1975), suggested that the fixed pore diameter equivalent of free volume of the hollow fiber skin layer of 0.4 micron is  $10 \text{ \AA}$  or less. The limit of the electron microscope used in their work was  $15 \text{ \AA}$ . This suggests that possible microspores in the skin layer could not be detected (Soltanieh et Gill, 1981). Sourirajan and Matsuura (1985) have utilized the above equations to analyze transport for a large number of solutes and membranes; however the above equations failed to describe the water flux drop, and rejection for some organics, and solutes.

### 2.15.3 Charged Membrane Models

Charged membrane models, like the one used for standard NF, account for electrostatic effects as well as for diffusive and/or convective flow in order to describe the solute separation. Many charged membrane transport theories have been proposed. Donnan equilibrium models assume that a dynamic equilibrium is established when a charged membrane is placed in a salt solution (Bhattacharyya and Cheng, 1986; Bhattacharyya and Williams, 1992). The counter-ion of the solution, opposite in charge to the fixed membrane charge, typically carboxylic or sulfonic groups, is present in the membrane at a higher concentration than that of the co-ion (same charge as the fixed membrane charge) because of electrostatic attraction and repulsion effects. This creates a

Donnan potential which prevents the diffusive exchange of the counter-ion, and co-ion between the solution, and membrane phase. When a pressure driving force is applied to force water through the charged membrane, the effect of the Donnan potential is to repel the co-ion from the membrane; since electroneutrality must be maintained in the solution phase. The counter-ion is also rejected, resulting in ionic solute separation. The model correctly predicted that the solute rejection was a function of membrane charge capacity, ion feed concentration, and ion charge. However, this model does not take into account solute diffusive and convective fluxes which are also important in charged membrane separations. Lakshminarayanaiah (1965, 1969), Dresner (1972), and Dresner and Johnson (1980) have described the use of extended Nernst-Planck equations for the prediction of solute ion fluxes. The model represents the solute flux due to diffusion, convection and Donnan potential. Dresner (1972) has shown that the extended Nernst-Planck model correctly predicts the trends expected for ionic solute rejection, including conditions under which a negative rejection is obtained. However, the difficulty of experimentally measuring the model parameters limits its use for solute flux, and flux prediction.

#### 2.15.4 Solution-Diffusion Models

The solution diffusion model assumes that the water transport across the membrane is only by diffusion, and so can be expressed by Fick's law (Soltanieh et Gill, 1981) as:

$$J_w = - D_w \frac{dc_w}{dy} \quad (2-16)$$

where  $c_w$  and  $D_w$  are the concentration, and the diffusivity coefficient of water in the membrane, respectively.

$$\text{The water flux is given by } J_w = A (\Delta P - \Delta \pi) \quad (2-17)$$

where A is the membrane solvent permeability coefficient and it is the property of the membrane;  $\Delta p$  is the operating pressure;  $\Delta \pi$  is the difference in the osmotic pressure across the membrane.

$$\text{And the solute flux is expressed as } J_s = k_2 (C_R - C_P) \quad (2-18)$$

where  $k_2$  is the membrane solute permeability coefficient; and  $C_R$  and  $C_P$  are the reject and product concentration, respectively.

#### 2.15.4.1 Solution-Diffusion-Imperfection Model

Sherwood et al. (1967) have extended the solution-diffusion model by including additional terms due to pore flow in addition to diffusion of solvent and solute through the membrane as the mechanism of transportation. This modified model recognizes that there may be small imperfections or defects (pores) on the surface of the membrane through which transport can occur.

The total water flux,  $N_w$ , and the total salt flux,  $N_s$ , are given by:

$$N_w = J_w + k_3 \Delta P C_{mem} = A (\Delta P - \Delta \pi) + k_3 \Delta P C_{mem} \quad (2-19)$$

$$N_s = J_s + k_3 \Delta P C_R = k_2 (C_P - C_R) + k_3 \Delta P C_R \quad (2-20)$$

where  $C_{mem}$  is the water concentration on the upstream side of the membrane.

The coefficient  $k_3$  can be viewed as a coupling coefficient.

If we divide both sides of equation (2-19) by  $C_{mem}$ , the left hand side will be equal to the water permeation velocity expressed as  $V_w = \frac{N_w}{C_{mem}}$ , which is very close to the total permeation velocity.

For real membranes, which have some imperfections, the measured flux ( $N_w$ ) is not purely diffusive ( $J_w$ ), but it contains a term contributed by convection. It is necessary to distinguish between the two, although in the literature, they are usually used interchangeably (Soltanieh et Gill, 1981).

The solute flux is equal to the permeation velocity multiplied by the product concentration, i.e.  $N_s = V_w C_P$

Equations (2-21) & (2-22) then can be written in terms of the permeation velocity:

$$V_w = k_1(\Delta P - \Delta\pi) + k_3\Delta P \quad (2-21)$$

$$V_w = k_2(C_P - C_R) + k_3\Delta PC_R \quad (2-22)$$

where  $k_1 = \frac{A}{C_{mem}}$

It is interesting to compare the relative contribution of diffusive and pore flow Fluxes based on the calculated values of  $k_1$  &  $k_2$  and  $k_3$  from Applegate, and Antoson (1972). Applegate, and Antoson used the above equations to analyze the rejection pressure drop data for asymmetric aromatic polyamide membranes, and cellulose acetate membrane. The values of  $k_3$  from all membranes, and concentrations were at least two orders of magnitude smaller than those of  $k_1$ .

Since in the solvent flux equation (2-21),  $\Delta P$  and  $(\Delta P - \Delta\pi)$ , are of the same order of magnitude, the second term  $k_3\Delta P$  (the pore flow) is negligible as compared to

the first term  $k_1(\Delta P - \Delta\pi)$  (the diffusive flow). This is true for dilute solutions.

In the solute flux equation (2-22), we have to compare  $k_3\Delta P$  with  $k_2$  since  $C_R$  is of the same order as  $(C_R - C_p)$ . Calculations of Soltanieh and Gill (1981) illustrated that the calculations of Applegate and Antonson experiments for dilute solutions ( $< 0.05$  M), showed that the contribution of the pore flow to the solute flux is very small (about 2% of total flux). At higher concentrations, say about 0.1 M, the contribution of pore flow is about 8%, and for a 0.5 M feed, the pore flow contributes to about 25-40% of the solute flux for polyamide membrane. The standard NF membrane used to be described by the Donnan equilibrium model (Battacharyya and Cheng, 1986; Battacharyya and Williams, 1992), or by the extended Nernst-Planck model (Lakshminaraiah, 1969; Dresner and Jonson, 1980) to predict the solvent and solute flux, because it is negatively charged. The new generation of NF membranes has a slight negative charge at the membrane surface, and this charge is approximately close to neutral as shown in Figure 2-12 (Wilf et al, 2006), so these sophisticated models are not required any more to describe the solvent, and solute flux in this type of membranes. Instead, the above-mentioned simpler solution-diffusion model can describe the membrane, when the pore flow terms are neglected.

#### 2.15.4.2 Assumptions when using Solution-Diffusion Model

Based on the above equations for the solution diffusion-imperfection model, the following assumptions are going to be considered (Fritzmann et al, 2006):

(1) the active membrane layer is a dense membrane without pores. Permeating components dissolve in the membrane phase; (2) at all times there is chemical equilibrium at the phase interface between membrane and feed/permeate side; (3) salt and water flux are independent of each other. Salt flux results solely from concentration

gradient, but not from pressure; (4) due to membrane swelling, water concentration and water diffusion coefficient across the membrane are constant; (5) the driving force for permeation of each component can be split into two terms, the concentration or activity difference, and the pressure difference between the feed and the permeate sides; (6) at relatively low salt concentrations, the pressure driving force for permeating salt components is negligible; (7) due to the assumption of constant water concentration in the membrane, solely the applied pressure difference  $\Delta p$  causes water flux across the membrane; (8) the measured flux  $N_w$ , and the purely diffusive flux  $J_w$  are assumed to be equal.

#### 2.16 Determining Membrane Surface Concentration

RO membrane transport models typically assume that the bulk feed solution concentration is equal to the membrane wall solution concentration, which is not always true. This has to be related to the concentration polarization expressions (Williams, 2003). Concentration polarization complicates the modeling of membrane systems because it is very difficult to experimentally determine the solute membrane wall concentration ( $C_{mem}$ ). The membrane wall concentration is necessary to be determined since it is not equal to the bulk feed concentration ( $C_F$ ). In the limited feed flow rate that is typically used for hyperfiltration (RO and NF) membrane processes, the flow in the membrane channels is laminar, and the difference between the membrane wall concentration and bulk concentrations can be substantial. So, calculating the membrane wall concentration must be appropriately estimated.

For dilute solutions, and from equation (2-21) above, the water flux will be equal to

$$J_w = A (\Delta P - \Delta \pi) \quad (2-23)$$

where A is the permeability coefficient of the membrane, and it is a function of the membrane construction. The membrane permeability coefficient A can be determined from distilled water where  $\Delta \pi$  in equation (2-23) in this case will be approximately equal to zero. The term  $\Delta P$  is the hydraulic pressure difference across the membrane, and is equal to the applied membrane pressure minus the permeate pressure, while  $J_w$  is the permeate flux and equal to the permeate flow rate divided by the membrane cross flow area. The term  $\Delta \pi$  is equal to the difference between the osmotic pressure at the membrane surface minus the permeate osmotic pressure. Osmotic pressure is a property of the solution and does not in any way depend on the membrane properties (Probstein, 1994). For dilute solutions the osmotic pressure is independent of the solute species, and is given by Van't Hoff equation:

$$\pi_i = n_i RT \sum_{i=1}^n C_i \quad (2-24)$$

Where  $n_i$  = number of ions formed when the solute dissociates.

And  $C_i$  = molar concentration of the solute =  $c_i / 1000 MW_i$

and  $c_i$  = total dissolved solids as mg/l ;  $MW_i$  = molecular weight of the dilute solution;

R= gas constant; and T= absolute temperature.

From equations (2-23) and (2-24) above, membrane wall concentration  $C_{mem}$  can be calculated.

## 2.17 Determining Mass Transfer Coefficient and Thicknesses of the Concentration Polarization Layer

Under the condition of mass transfer-limited permeate flux shown in Figure 2-15, the accumulation of materials near the membrane can be envisioned as a balance between advection of materials towards the membrane due to permeation, and back diffusion that occurs as a concentration gradient builds up near the membrane (Letterman and Taylor, et al. 1999). Figure 2-15 illustrates the flow directions of solvent and solute near the membrane surface.

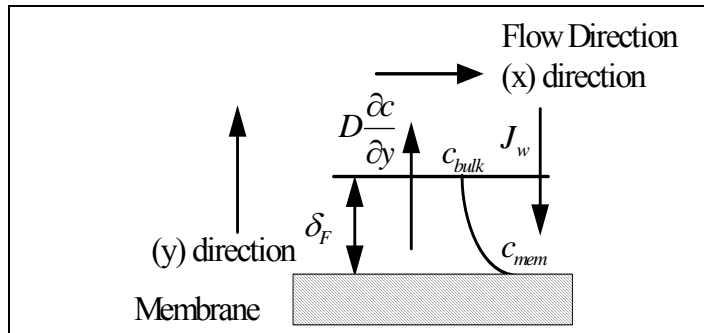


Figure 2-15. Feed side concentration polarization layer

## 2.18 Using Sherwood Number to Determine Mass Transfer Coefficient

The conventional way to estimate the mass transfer coefficient is to use Sherwood number relationships obtained from the heat and mass transfer analogy. Numerous Sherwood number relationships have been proposed and extensively reviewed.

The Graetz-Leveque correlation of Sherwood number, which is used for laminar flow when the velocity field is fully developed and the concentration boundary layer is not fully developed, is typically used to estimate mass transfer coefficient as:

$$\text{Sh} = X(\text{Re})^a (\text{Sc})^b \left(\frac{d_h}{L}\right)^c \quad (2-25)$$



where  $Re = \text{Reynold's number} = \frac{V_w d_h}{\nu}$ ; Schmidt number =  $Sc = \frac{\nu}{D}$ ;  $\nu$  = kinematics viscosity;  $V_w$  = average cross-flow permeate velocity;  $d_h$  = hydraulic diameter of the membrane element;  $D$  the diffusion coefficient for solute transport through solvent, and  $L$  is the spiral wound membrane width. (Taylor et al.,1999).  $D$  in this relationship is equal to  $K \delta_F$ , where  $K$  is the mass transfer coefficient, and  $\delta_F$  is the concentration polarization layer thickness. The terms  $X$ ,  $a$ ,  $b$ , and  $c$  are coefficients that have taken extremely different values by different researchers (Isaacson, 1976; Schock & Miquel, 1987; Xuesong, 1987; Taylor, 1991; Van de Lisdonk et.al, 2001). Table 2-2 demonstrates the different values of coefficients found in the literature by some of those researchers to calculate Sherwood number at different operating conditions. It is clear from the table that the different coefficients vary considerably.

*Table 2-2. Several values of Sherwood number coefficients found in literature*

Literature	Year	X	a	b	c
Isaacson	1976	0.2-0.27	0.5	0.33	0
Schock & Miquel	1987	0.065	0.875	0.25	0
Wang Xuesong	1987	1.66	0.36	0.34	0.42
Taylor	1991	1.86	0.33	0.33	0.33
Van de Lisdonk	2001	0.265	0.33	0.52	0

There are several limitations in using the above-mentioned equation: (1) the above mentioned Sherwood number relationship is derived for flow through non-porous conduit; hence, the effect of suction can not be considered using these relationships; (2) the axial change in osmotic pressure at membrane surface due to the concentration polarization change is not considered in the above mentioned Sherwood number correlations; (3) suction will alter the velocity gradient in the bulk stream through the

boundary layer (Schlichting, 1979) that will impact Reynolds number, which is not considered in calculating the Graetz-Leveque Sherwood number; (4) and suction will change the species concentration at the membrane surface that will change the solution physical properties like viscosity, density, and diffusivity, which are function of the concentration. Consequently, the above mentioned Reynold's number, and Schmidt number, will be variable along the membrane length. These changes are not considered with this form of Sherwood number relationships. It is concluded that in the case of suction, calculating the concentration polarization layer using the traditional way of using Sherwood number correlations will lead to erroneous results due to the change in the solution properties that are not considered in the above mentioned relationship.

## 2.19 Overcoming the Disadvantages of using Sherwood Number to Determine Mass Transfer Coefficient with Permeate Suction

Of great interest is the case of dilute solution where  $Sc \gg 1$ . In this case the diffusion concentration polarization layer is imbedded in the viscous boundary layer, and the velocity it sees is that close to the wall (Probstein, 1994).

### 2.19.1 Film Theory

According to the film theory, mass transfer coefficient is inversely proportional to the concentration polarization layer (Taylor et al., 1999; Williams, 2003), so if the concentration polarization layer decreases, the mass transfer coefficient will increase, and the permeate flow and quality will improve; and consequently membrane fouling can be reduced. Referring to Figure 2-15 at item 2.17 above, the Navier-Stokes diffusion-

convection equation for flow over a flat sheet membrane, gives the concentration profile by (Bhattacharyya and Williams, 1992)

$$u \frac{\partial C}{\partial x} + V_w \frac{\partial C}{\partial y} - D \left( \frac{\partial^2 C}{\partial x^2} + \frac{\partial^2 C}{\partial y^2} \right) = 0 \quad (2-26)$$

With boundary conditions:

For x direction  $C(0,y) = C_F$

And for y direction  $\frac{\partial C(x,0)}{\partial y} = 0$

Assuming a constant permeation rate, and a concentration polarization layer with axial distance (Figure 2-14), mass balance on the concentration polarization layer yields

$$J_w C = -D \frac{\partial c}{\partial y} \quad (2-27)$$

where  $J_w$  is the permeate water flux;  $C$  is the concentration of the species subject to concentration-polarization,  $D$  is the diffusivity coefficient for solute transport through solvent (calculated from Cussler, 1984), and  $y$  is the distance with the boundary layer such that  $C = C_{mem}$  at  $y = 0$ ; and  $C = C_F$  at  $y = \delta_F$

If the boundary layer is assumed to be stagnant over the channel length, the equation will be:

$$J_w \frac{\partial C}{\partial y} = D \frac{\partial^2 C}{\partial y^2} \quad (2-28)$$

Integrating this expression over the thickness of the stagnant concentration-polarization layer  $\delta_F$ , results in the following expression:

$$\frac{C_{mem} - C_P}{C_F - C_P} = \exp \frac{J_w \delta_F}{D} \quad (2-29)$$

This is the widely applied film theory developed by Brian (Brian 1966; Bhattacharyya and Williams, 1992). The ratio of the diffusion coefficient for solute transport through solvent to the concentration polarization layer thickness in this film theory model defines a mass transfer coefficient K:

$$K = \frac{D}{\delta_F} \quad (2-30)$$

where K is the mass transfer coefficient.

Using equation (2-30), the concentration polarization layer  $\delta_F$  can be calculated, if the diffusivity coefficient of the species D, and the mass transfer coefficient K are determined, without having to use Sherwood number correlations.

### 2.19.2 Peclet Number

Peclet number is defined as the dimensionless ratio of the rate of mass transported by convection to the membrane, and the rate of mass transported by diffusion back to the bulk solution; in other words the diffusive membrane Peclet number is expressed as:

$$P_e = \frac{V_w h_d}{D_{1-2}} \quad (2-31)$$

where  $V_w$  is the permeate velocity which is equal to the permeate flux per one sheet of membranes;  $D_{1-2}$  is the diffusivity coefficient of the ionized electrolyte; and  $h_d$  is the hydraulic diameter of the spiral wound membrane. The diffusive Peclet number is a measure of how permeate goes through the membrane, so if  $P_e$  is less than unity, this is an indication of no concentration polarization, while a large Peclet number means that there is a concentration polarization at the membrane surface. Peclet number is called the

dimensionless flux. If the diffusive Peclet number is increased due to suction, while the associated concentration polarization is being reduced, this means that suction has increased membrane production with more favorable conditions to the membrane, as far as inorganic fouling is concerned. Therefore, we using Sherwood number can be avoid in the calculations due to the above-mentioned limitations. For the 2.5 inch diameter membrane, which is composed of two envelopes (leaves) of membranes, where every envelope is composed of two sheets, the hydraulic diameter is the ratio of the cross section of the flow channel to the wetted circumference and can be calculated with the dimensions of the feed-concentrate spacer according to (Schock and Miquel, 1987):

$$h_d = \frac{4\varepsilon}{\frac{1}{d_f} + (1 - \varepsilon) \cdot \frac{4}{d_f}} \quad (2-32)$$

where  $\varepsilon$  is the porosity of the feed-concentrate spacer; and  $d_f$  is the filament diameter of the feed spacer, which is equal to half the feed spacer height. As in the case of NF membrane, it is observed that for dilute solutions the Schmidt number is very large, as a consequence of which the diffusive membrane Peclet number is generally large. This is true even at a moderate Reynold's number (Probstein, 1994).

Probstein (1994) also showed that at typical condition of operting the mebrane system without permeate suction, as  $P_e$  number increases, the concentration polarization boundary layer increases, and consequelty the mass transfer along with the product permeate decreases. If permeate suction increases the  $P_e$ , and the concentration polarization layer is decreased, this will indicate that permeate suction will help in reducing the membrane fouling, while product flow is increased.

## 2.20 Determining Diffusion Coefficient for Strong Electrolytes

A transport of mass or “diffusion” of mass will take place in a fluid mixture of two or more species whenever there is a spatial gradient in the properties of the mixture, that is, a concentration gradient (Probstein, 1994). Diffusion causes convection.

Convection flow can have many causes. For example, it can occur because of pressure gradient or through differences in temperature. However, even in isothermal and isobaric systems, diffusion will always produce convection (Cussler, 1984). This combination of diffusion and convection could complicate our analysis.

Multi-ions salt solutions calculations of diffusion coefficient are more complicated because more than one cation can be accompanied by one anion or vice versa, depending on the ion valence. For example, for a ternary system, there would be two concentration gradients, and the diffusive flux of each species could be affected by both concentration gradients. One instance where this is not so is the infinitely dilute solutions for which each component is unaffected by the presence of the other (Probstein, 1994). The diffusivity for dilute liquid solutions, like the case of the feed to NF membrane, may be estimated theoretically from simple hydrodynamic consideration (Probstein, 1994). In solute-solute interaction dilute solutions, like the case of NF membrane, the convection caused by diffusion is vanishingly small, and dependent on the solute concentration, and thus on temperature. This is the framework of this research. It is worthy to mention that estimates of diffusion for concentrated solutions are far more difficult (Probstein, 1994).

Salts are ionized when they are dissolved in water. For example, a Sodium Chloride solution in water diffuses as a single ion, and not as a single molecule; instead sodium ions and chloride ions move freely through the solution (Cussler, 1984).

Table 2-3 shows values of ionic diffusion coefficients in water at 25 degree C at infinite dilution.

### 2.20.1 1-1 Strong Electrolyte

Referring to the below mentioned Table 2-3, and in the above example of Sodium Chloride solution, the diffusion of  $Na^+$  is slower than that of  $Cl^-$ , and the diffusion of both ions in a dilute solution of  $NaCl$  is going to be dominated by the larger ion because the two ions are tied together electrostatically.

Table 2-3. Ionic diffusion coefficients in water at 25 degree C at infinite dilution in  $10^{-5} \text{ cm}^2 / \text{s}$ . (Calculated from data of Robinson and Stocks (adopted from Cussler, 1984))

Cation <sub>i</sub>	$D_i$	Anion <sub>i</sub>	$D_i$
H <sup>+</sup>	9.31	OH <sup>-</sup>	5.28
Li <sup>+</sup>	1.03	F <sup>-</sup>	1.47
Na <sup>+</sup>	1.33	Cl <sup>-</sup>	2.03
K <sup>+</sup>	1.96	Br <sup>-</sup>	2.08
Rb <sup>+</sup>	2.07	I <sup>-</sup>	2.05
Cs <sup>+</sup>	2.06	NO <sub>3</sub> <sup>-</sup>	1.90
Ag <sup>+</sup>	1.65	CH <sub>3</sub> COO <sup>-</sup>	1.09
NH <sub>4</sub> <sup>+</sup>	1.96	CH <sub>3</sub> CH <sub>2</sub> COO <sup>-</sup>	0.95
N(C <sub>4</sub> H <sub>9</sub> ) <sub>4</sub> <sup>+</sup>	0.52	B(C <sub>6</sub> H <sub>5</sub> ) <sub>4</sub> <sup>-</sup>	0.53
Ca <sup>2+</sup>	0.79	SO <sub>4</sub> <sup>2-</sup>	1.06
Mg <sup>2+</sup>	0.71	CO <sub>3</sub> <sup>2-</sup>	0.92
La <sup>3+</sup>	0.62	Fe(CN) <sub>6</sub> <sup>3-</sup>	0.98

When describing the ion fluxes of a single strong 1-1 electrolyte, such an electrolyte ionizes completely, and it will be producing equal numbers of cations and anions. Although the concentration of anions and cations may vary through the solution, the concentration gradient of these species are equal everywhere because of the

electroneutrality (Cussler,1984).

$$\text{and } D_{1-2} = \frac{2}{\frac{1}{D_1} + \frac{1}{D_2}} \quad (2-33)$$

Where  $D_{1-2}$ ,  $D_1$  and  $D_2$  are the diffusivity coefficient of the ionized electrolyte, the anion, and cation respectively.

### 2.19.2 Non 1-1 Strong Electrolyte

The non 1-1 electrolytes like  $MgSO_4$ , and  $MgCl_2$  are parallel to the above mentioned 1-1 electrolyte, but more complicated algebraically (Cussler,1984).

The diffusivity coefficient of the ionized electrolyte in this case is going to be expressed as:

$$D_{1-2} = \frac{\frac{|Z_1| + |Z_2|}{\frac{|Z_1|}{D_2} + \frac{|Z_2|}{D_1}}}{\frac{|Z_1|}{D_2} + \frac{|Z_2|}{D_1}} \quad (2-34)$$

where  $D_{1-2}$ ,  $D_1$ , and  $D_2$  are the diffusivity coefficient of the ionized electrolyte, the anion, and cation respectively, while  $Z_1$  and  $Z_2$  are the absolute valent numbers of the the anion, and the cation respectively.



## CHAPTER 3

### EXPERIMENTAL METHODOLOGY

This chapter describes the technical procedure utilized in performing the experimental part of this research. The dilute solutions preparation, and the instrumentation used in the experiments are described first, followed by the experimental procedures. For the two types of experiments, a diagram of the equipment set-up is shown with each component briefly described. The description of each type of experiment contains a summary table of the salts solutions used as feed water, their concentration and the system operating parameters. The sampling and the measurement protocols, as well as the procedure for the replicate runs are presented for each type of experiment.

#### 3.1 Dilute Solutions Preparation

The feed water for all the experiments is prepared using de-ionized (DI) water and analytical grade salts. DI water is produced from a feed of tap water using RO unit. The conductivity of the product is  $16 \pm 1 \mu\text{s}$ . Only simple binary solutions of  $\text{NaCl}$ ,  $\text{MgCl}_2$ , and  $\text{MgSO}_4$  - which are 1-1, 2-1, and 2-2, respectively, strong electrolyte dilute solutions - are considered in this research. The diffusion coefficients for the binary solutions were calculated using the equations from Cussler (1984). Salt concentration was prepared to have concentration of the three different binary

solutions according to Table 3-1. The experiments were run at three concentrations for low, medium, and high values of the applied feed pressures.

### 3.2 Reasons behind Choosing the Chemicals

It is required to study the effect of both monovalent and divalent ions on the performance of the new generation of NF membrane.  $Na^-$ , and  $Cl^-$  ions are monovalent ions. The solubility of chloride salts and sodium salts are high and do not create a RO scaling problems, that may allow running the experiments at a relatively high recovery. Sodium and Chloride, in brackish and seawater, are the prevalent ions. Magnesium ( $Mg^{++}$ ) is a divalent cation, and accounts for about a third of the hardness in brackish water, leaving about the two third to Calcium ( $C^{++}$ ) cations.

*Table 3-1. Dilute solutions concentration and operating pressures for the experiments*

Dilute Solution	Feed Concentration (mg/l)	Feed Concentration (Mol/l)	Feed Pressure (psi)
Sodium Chloride	750	0.0249	80, 110,160
	1200	0.0411	80, 110,160
	1750	0.0599	80, 110,160
Magnesium Sulfate	820	0.0136	80, 100,130
	1235	0.0205	80, 100,130
	1770	0.0606	80, 100,130
Magnesium Chloride	840	0.0176	80, 100,130
	1260	0.0265	80, 100,130
	1750	0.0368	80, 100,130

The solubility of magnesium salts is high, and they typically do not cause a scaling problem in membrane systems. Sulfate ( $SO_4^{--}$ ) is a divalent anion, and  $MgSO_4$  does not cause scaling on membranes. This is unlike calcium, barium, and strontium sulfate,

which have low solubility limits, and can cause scaling problem in the back-end of the system.

### 3.3 Experimental Setup

The apparatus used in the experiment are assembled on the equipment skid shown in the pictures of figures (3-1, 3-2 and 3-3).



*Figure 3-1. Experimental equipment skid showing pressure gauges, TDS meters, flowmeters, and NF membrane pressure vessel*

The instruments used are presented in Table 3-2 together with calibration requirements, manufacturer, readings range, and accuracy. The sensors are connected to the control panel of the equipment skid for data collection and analysis. Samples were taken during the runs to test the feed water pH and the biocide content. Samples were also taken for feed flow, product flow, and concentrate flow to test the conductivity panel readings against manually held TDS meter. Whenever samples were taken for test, they were poured back to the feed water tank to keep feed water conductivity constant.



*Figure 3-2. Variable frequency drives for the high pressure pump, and the permeate pump*



*Figure 3-3. The assembled high pressure pump (top), and the permeate pump (bottom)*

Table 3-2. Instrumentation and specifications

No.	Instrument	Manuf.	Model	Calib. Req.	Range	Accuracy
1	Electrical Top loading Balance	Ohaus	Adventure	No	0 -3,100 g	± 0.1 mg
2	Conductivity Meter & Probe	Hanna	BL983318	Yes	0 -10,000 mg/l	± 1 mg/l
3	Control Box	R&D Specialties	CE2-IPC	Yes	0 – 999 mg/l	± 1 mg/l
4	Permeate Conductivity Cell	R&D Specialties	80TDS150R1	Yes	0 – 999 mg/l	± 1 mg/l
5	Flowmeter	Blue-White	F440	No	0 - 1 gpm	± 0.05 gpm
6	Flowmeter	Blue-White	F44375	No	0 - 5 gpm	± 0.05 gpm
7	2.5" Pressure Gauge	Wika	316SS tube & Connection	Yes	0 - 30 psi	± 0.1 psi
8	2.5" Pressure Gauge	Wika	316SS tube & Connection	Yes	0 - 60 psi	± 0.1 psi
9	2.5 " Pressure Gauge	Wika	316SS tube & Connection	Yes	0 - 300 psi	± 0.5 psi
10	0.5" NC Solenoid Valve	GC-Valves	H211YF02J7DG4	No	On/Off	N/A
11	Volumetric Flask	Kimax	20024	No	250 ml	± 1.4%
12	Volumetric Flask	Pyrex	3024	No	100 ml	± 1.0%
13	Hand Held Conductivity Meter	Hanna	TDS-3	Yes	0-19,999	± 10 mg/l
14	Hand Held pH Meter	Hanna	HI 98107	Yes	0-14	± 0.1
15	Volumetric Pipette	Pyrex	7101	No	0 - 50 ml	± 0.2%
16	Beaker	Kimax	14000	No	0 - 600 ml	± 5.0%
17	Beaker	Pyrex	1000	No	0 - 1,000 ml	± 5.0%
18	Low Pressure Switch	Barksdale	E1H-H90	No	0- 40 psi	± 1 psi

As shown on the schematic flow diagram Figures 3-4 and 3-5, solutions were pumped from a HDPE 35 gallons feed tank by a booster pump to the high pressure pump through 5  $\mu$  m cartridge filter to protect the pump, and the membrane from any suspended solids that may be available in the solution tank. The booster pump is a

centrifugal type; model number 594-154; manufactured by Surflow Company, USA, and rated at 3.3 gpm at 45 psi. The membrane was pre-compacted at 120 psi using re-circulated DI water, and the re-circulated solution is kept disinfected using 0.2 – 0.3 mg/l of biocide. The used biocide is Model number RoCide DB-20 manufactured by Avista Company, USA, is formulated to keep the membrane sanitized and non-oxidized. RoCide DB-20 is approved by the EPA to be used in RO systems as a fast acting; non-oxidizing biocide based on a 20% solution of the active ingredient DBNPA (Dibromo nitrilo propionamide), (Avista Company, 2008). The same concentration of biocide was kept for all the solutions during the entire experiment runs. The biocide content was periodically checked using oxidant reagent test kit. At the beginning of the experiments, the pure water permeability coefficient ( $A$ ) was calculated using equation (2-23), where  $J_w = A(\Delta P - \Delta\pi)$ , since  $A$  is the permeability coefficient of the membrane, and it is a function of the membrane chemical structure.

The membrane permeability coefficient  $A$  was determined from distilled water where  $\Delta\pi$  in equation (2-23) in this case is approximately equal to zero.

The term  $\Delta P$  is the hydraulic pressure difference across the membrane, and is equal to the applied membrane pressure minus the permeate pressure, while  $J_w$  is the permeate flux, and is equal to the permeate flow rate divided by the membrane cross flow area. The capacity of the high pressure pump was determined according to the membrane software program of the manufacturer following the design guide lines at the laboratory temperature. The pump is a rotary vane type manufactured by Procon company, USA; constructed from 304 SS, and rated at 207 gph at 200 psi and 1725 rpm.

The pump Model number is 105E265F31BA215. The motor is 1 HP at 1725 rpm; inverted duty non washdown manufactured by Baldor with electrical specifications of 230/460 V/60 Hz/ 3 Ph; and Model number IDNM3581T bolt on. The variable frequency drive (VFD) on the high pressure pump along with the concentrate control valve allows unlimited control of the membrane feed pressure according to the feed water concentration.

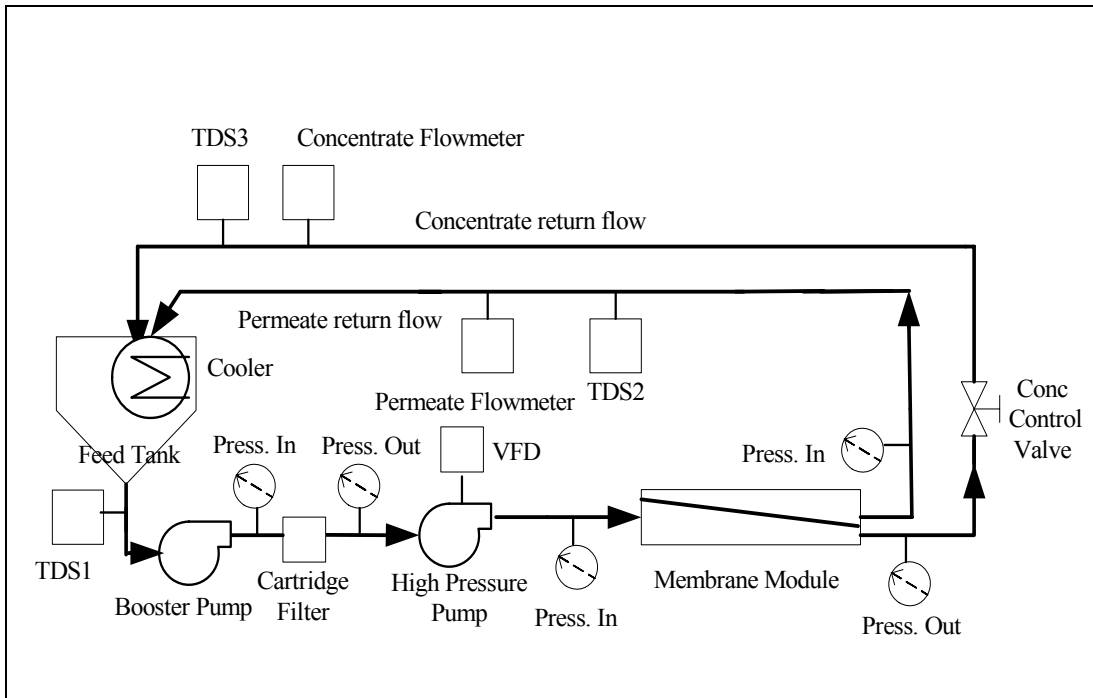


Figure 3-4. First setup by running the high pressure pump only

The setup shows the spiral wound NF TFC membrane used in the experiment. Table (3-3) demonstrates the geometrical dimensions of the tested new generation NF membrane, which is a standard size commercial 2.5 inch nominal diameter, and a 40 inch long spiral wound aromatic polyamide thin-film composite membrane Model NF270-2540, manufactured by Dow-FilmTec Inc., Minneapolis, MN.

The effective surface area is 28  $ft^2$  ( $2.6 m^2$ ). This membrane was chosen for this research

as a representative of a class of the new generation membranes, which is used increasingly in water treatment applications. The  $CaCl_2$  rejection is about 40-60%, and the magnesium sulfate rejection is 93%, as reported by the manufacturer (test conditions: feed TDS is 500 mg/l for  $CaCl_2$ , and 2,000 mg/l for  $MgSO_4$ , 70 psi, 10% recovery, and 25 °C. The feed spacer height is 28 mil (0.711 mm) with a porosity ( $\epsilon$ ) of 0.89, computed as described by Schock and Miquel (1987).

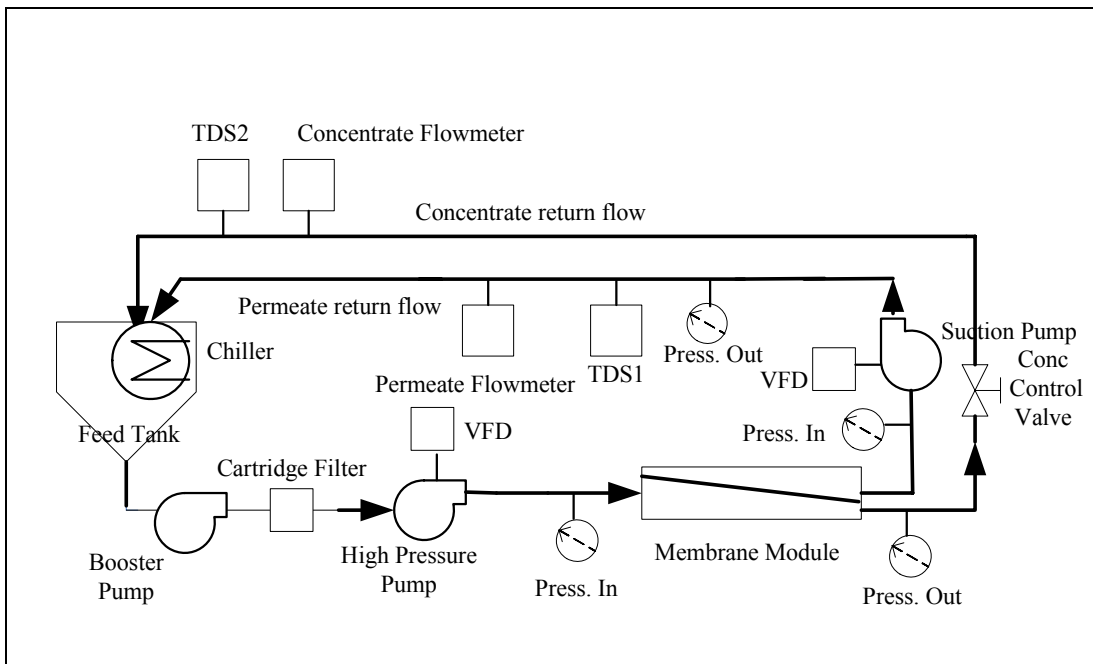


Figure 3-5. Second setup by running the high pressure pump and the permeate suction pump

The membrane zeta potential is close to neutral, so the membrane charge was assumed to be zero, to eliminate the charge effect. The membrane pressure vessel is made of reinforced fiberglass and has a rated maximum operating pressure of 300 psi.

The pressure vessel is produced by Crane Environmental.

The experiments were divided into two setups: the first setup was conducted by running the experiment using the high pressure pump only.



Table3-3. Geometrical Parameters for the tested FilmTec Membrane Model NF270-2540

Parameter	Specifications
Membrane Model No.	270NF-2540
Active Area	28 $ft^2$ (2.6 $m^2$ )
Active Length	35.4 in.(90.4 mm)
Feed Spacer Thickness	28 mil (0.71 mm)
No. of envelops (leaves)	2
Feed Spacer Porosity	0.89
Hydraulic Diameter	28 mil (0.877 mm)
Filament Diameter	14 mil (0.355 mm)

In the second setup of the experiments, the permeate suction pump was run along with the high pressure pump, to apply suction on the membrane permeate side. The capacity of the permeate suction pump was determined according to the projected permeate flow rate given by using the manufacturer software program. The pump is a positive displacement rotary vane type manufactured from bronze by Procon Company, USA, and rated at 37 gph at pressure of 50 psi and 1725 rpm. The Model number is 102E125F31BA250. The motor is 0.5 HP at 1725 rpm; inverted duty non washdown. It is manufactured by Baldor company with electrical specifications of 230/460 V/60 Hz / 3 Ph, and Model number IDNM3538. The VFD which is used to control the suction pressure is rated at 0.5 HP manufactrerd by Woods company with electrical specifications of 115 V/ 1 Phase/ 60 Hz, and Model number SE1C1S005D01.

It is worthy to mention that the suction pressure of the permeate suction pump can not be lower than the pump net positive suction head (NPSH), in order to avoid cavitations in the pump. All the interconnecting piping was made of anti-corrosion Stainless Steel tubes, or flexible braided Stainless Steel. Permeate tubing was made of polypropylene tubing. The permeate flow, concentrate flow, pressures, and total dissolved solids for the feed, permeate, and concentrate side were measured on the

control panel. The permeate flow, and concentrate flow were returned to the feed tank where the temperature was kept constant at  $25 \pm 1$  degree C by a cooler.

The cooler is a drop in chiller manufactured by Current company, USA, rated at 3,926 BTU, and model No. CD-22308- ¼ HP. Keeping the re-circulated flow at a constant temperature eliminates the effect of the change of the diffusivity coefficient of the species due to temperature change, since diffusivity coefficient is a function of the solvent temperature and solute concentration.

The salt diffusivity coefficient for the 1-1 strong ionized solution is calculated from equation (2-33), and (2-34) in Chapter 2 by:

$$D_{1-2} = \frac{2}{\frac{1}{D_1} + \frac{1}{D_2}}$$

where  $D_{1-2}$ ,  $D_1$  and  $D_2$  are the diffusivity coefficient of the ionized electrolyte, the anion, and cation respectively, and for non 1-1 strong ionized solution is calculated from:

$$D_{1-2} = \frac{\frac{|Z_1| + |Z_2|}{|Z_1|} + \frac{|Z_1| + |Z_2|}{|Z_2|}}{\frac{|Z_1| + |Z_2|}{D_2} + \frac{|Z_1| + |Z_2|}{D_1}}$$

where  $D_{1-2}$ ,  $D_1$ , and  $D_2$  are the diffusivity coefficient of the ionized electrolyte, the anion, and cation respectively, while  $Z_1$  and  $Z_2$  are the absolute valent numbers of the anion and cation respectively. The run for each salt solution is finished when the permeate water conductivity and flow rate are at equilibrium. At the end of the runs for every salt solution, the pure water permeability coefficient (A) is re-calculated using DI water. The value of the new permeability coefficient was used for the calculations of the

next salt solution. This value is typically reduced due the membrane compaction with aging. After the completion of each solution run, the system is flushed with DI water before running the next solution experiment. When applying pressure on the dilute solutions, the term  $\Delta\pi$  is equal to the difference between the osmotic pressure at the membrane surface minus the permeate osmotic pressure, as indicated in Chapter 2 above from equation number (2-24):

$$\text{where } \pi_i = n_i RT \sum_{i=1}^n C_i$$

where  $n_i$  = number of ions formed when the solute dissociates.

And  $C_i$  = molar concentration of the solute =  $c_i/1000 MW_i$ ; and  $c_i$  = Total Dissolved Solids as mg/l;  $MW_i$  = Molecular Weight of the dilute solution; R = gas constant; and T = absolute temperature.

From the equations (2-23), and (2-24) in Chapter 2 above, membrane wall concentration  $C_{mem}$  was calculated.

From equations (2-29), and (2-30) in Chapter 2, the mass transfer coefficient K, and the concentration polarization layer  $\delta_F$  were calculated.

Peclet number was calculated as per equations (2-31), and (2-32) in Chapter 2.

### 3.4 Assumptions of the Experiments

Based on the above discussion, the following assumptions in the experimental setup were made: (1) the membrane is neutral because the zeta potential is close to zero; (2) the diffusion coefficient of the binary solution species is only a function of temperature and solution concentration, hence the diffusivity is constant because the experiments are carried out at a constant temperature and constant feed concentration;

(3) the mass transfer coefficient of the whole membrane is constant, and is not a function of the permeate flux or concentrate flow velocity; (4) the concentrate flow is equally distributed on the membrane envelope and the feed and permeate spacers; (5) the type of membrane material and chemical structure does not influence concentration polarization; (6) there are no dead zones where salt can accumulate on the membrane; (7) the binary solutions used in the experiments are completely ionized in the water, and the concentrate solutions have not reached the saturation limits so that there is no species precipitations on the membrane; (8) the concentration polarization layer is stagnant and constant along the run of the membrane surface.

## CHAPTER 4

### RESULTS AND DISCUSSION

This chapter presents the results obtained from the two setups of experiments described in Chapter 3. It also discusses the results in details. The results are presented in tables and graphs. The graphs are arranged such that they can be compared with each others for each dilute solution, at different pressures.

The details of the replicate runs are shown in the tables of Appendices A, B, and C. Pressures were identified as low, medium, and high; while solute dilutions were also determined as low, medium, and high, as per table 3-2 presented previously in Chapter 3. For an easier illustration, the medium pressure 100 to 110 psi is indicated on the graphs by the solid line for both operating setups, i.e without permeate suction, and with permeate suction, while the other two pressures, i.e. low, and high pressures, are indicated by different dotted lines.

#### 4.1 Effect of Permeate Suction on the Concentration Polarization Layer Thickness

According to the equations (2-33), and (2-34) in Chapter 2, the diffusion coefficient for the dilute solutions of  $MgSO_4$ , and  $MgCl_2$ , and  $NaCl$  are  $0.85 \times 10^{-9}$ ,  $1.243 \times 10^{-9}$ , and  $1.612 \times 10^{-9} \text{ m}^2 / \text{s}$ , respectively. The molecular weights of the three binary salt solutions are 120.3, 95.3, and 58.5, respectively. This indicates that the diffusion coefficient is a function of the molecular weight; and at constant temperature,

the back diffusion of the salt is proportional to the diffusion coefficient and solute concentration. Hence, the diffusivity is assumed to be constant for all the experiments, since a cooler was used to keep the temperature at 25 degrees C. Figures 4-1, and 4-2 illustrate that the concentration polarization layer thickness, in general, is decreased with permeate suction at all the tested pressures and feed concentrations. According to the film theory, the concentration polarization layer is inversely proportional to the mass transfer coefficient. This suggests that the effect of permeate suction enhances the mass transfer from the bulk to the membrane surface, and it de-stabilizes the laminar flow condition in the conduit due to the gradual increase in the positive pressure on the bulk solution due to the permeate suction at the permeate collector tube.

The above mentioned two figures also show that the concentration polarization layer thickness increases with the increase of the TDS of the feed. A more detailed study of Figure 4-1 and 4-2 shows that the greatest impact on the concentration polarization layer was achieved at the medium feed pressure, which is 100 psi.

Also, the above two figures along with Figure 4-3 show that the thickness of the concentration polarization layer is proportional to the rejected ions in the binary dilute solution, since the solute flux in the membrane is propositional to concentration difference across the membrane.

Concentration Polarization Layer Thickness Versus Feed Concentration - MgCl<sub>2</sub>

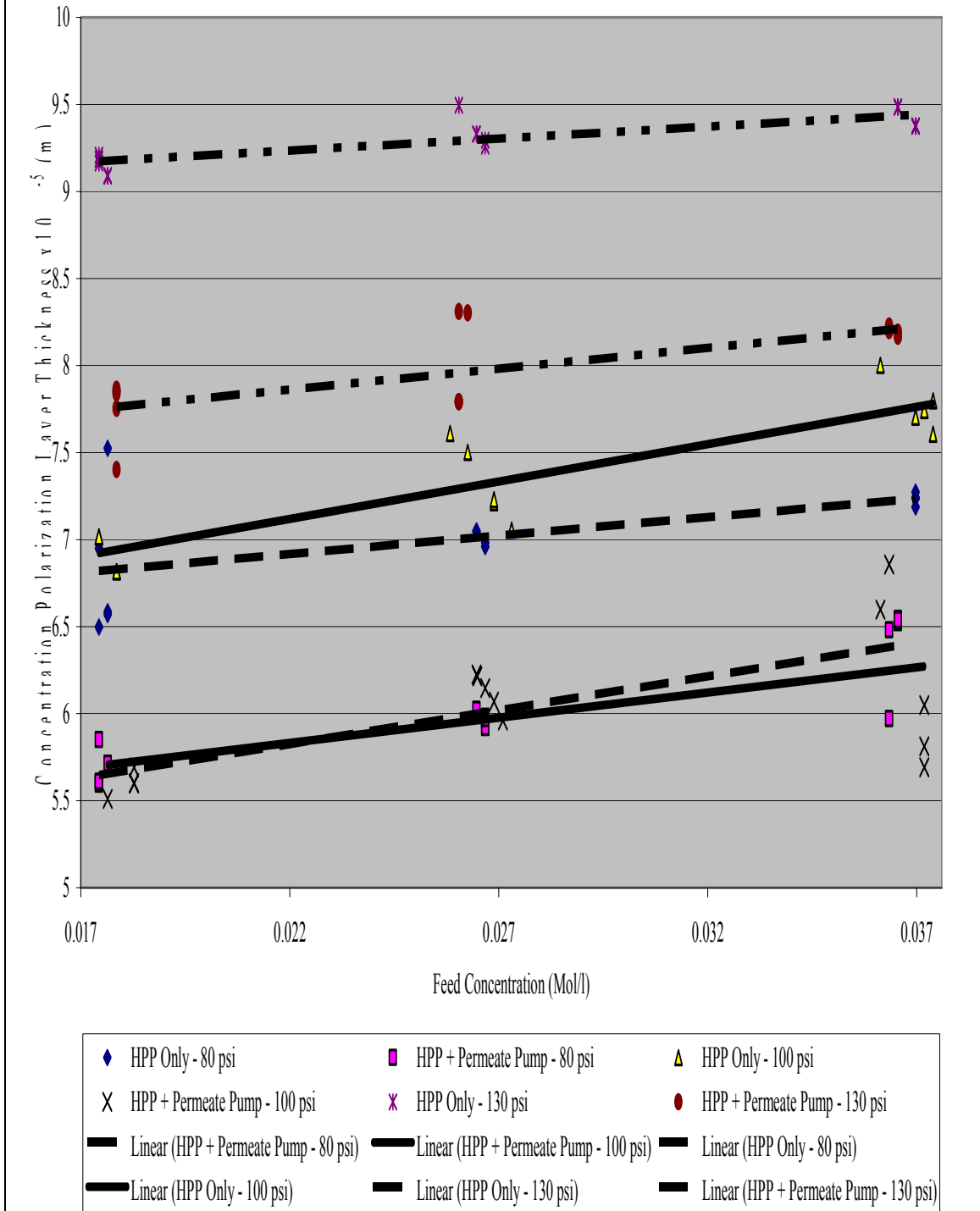


Figure 4-1 Concentration polarization layer thickness versus feed concentration - MgCl<sub>2</sub>

Concentration Polarization Layer Thickness Versus Feed Concentration - MgSO<sub>4</sub>

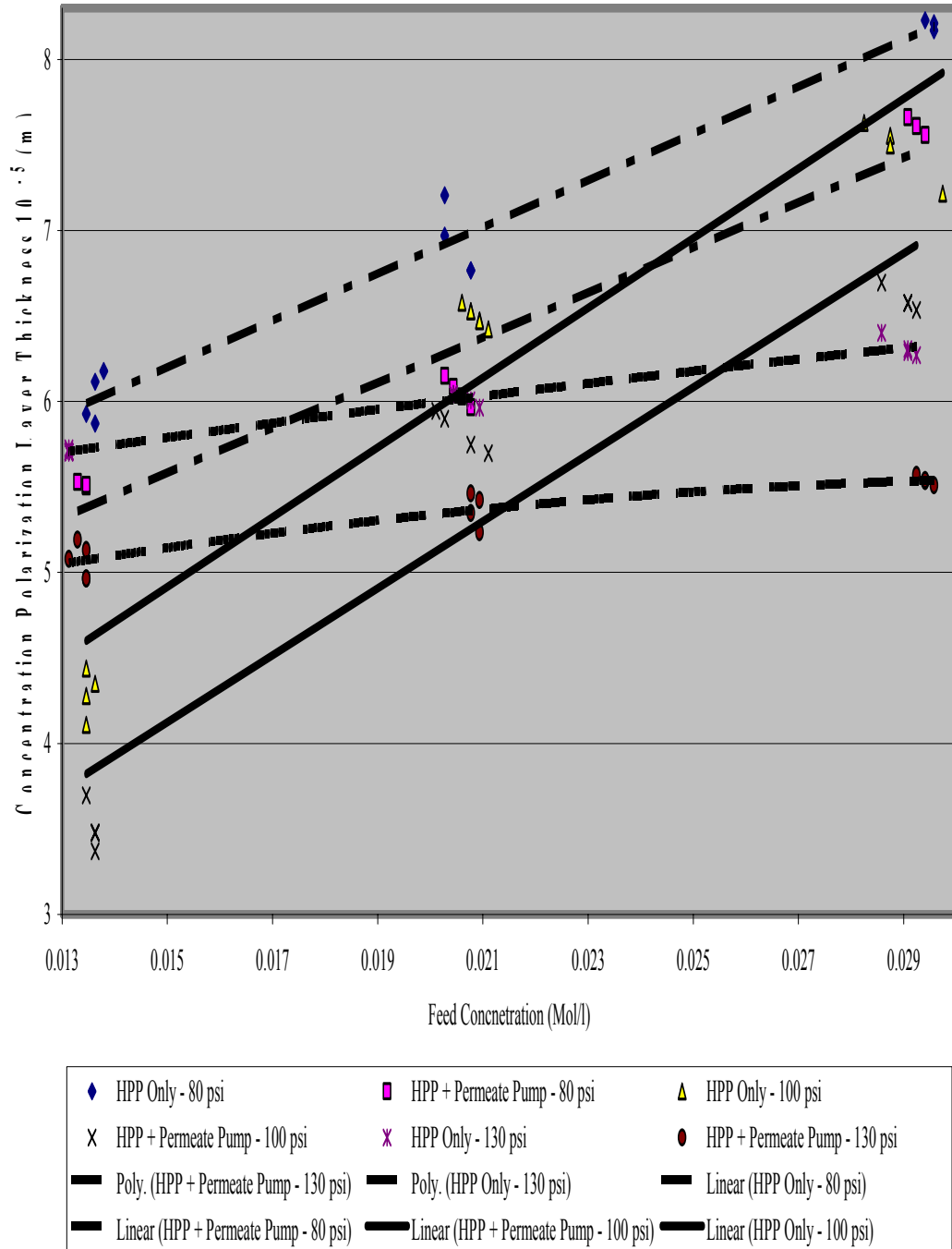


Figure 4-2. Concentration polarization layer thickness versus feed concentration - MgSO<sub>4</sub>



It is also illustrated from Figure 4-3 that *NaCl* solutions are showing the same trend as *MgCl<sub>2</sub>*, and *MgSO<sub>4</sub>* solutions, but with one higher order of magnitude.

This is due to the much lower rejection of the NF membrane for both monovalent ions in the *NaCl* solutions. According to the solution-diffusion transport model, the solute transport in the membrane is a function in the difference between the membrane wall concentration, and the permeate concentration, regardless of the operating pressure.

Since the permeate concentration is relatively high, the concentration polarization layer thickness was relatively high. Figure 4-3 also shows that the greatest reduction in concentration polarization layer thickness in the *NaCl* solution is achievable at the medium pressure which is 110 psi. As it was mentioned above, in the case of *NaCl* solutions the concentration polarization layer thickness is of one order of magnitude higher than that of the case of *MgCl<sub>2</sub>*, and *MgSO<sub>4</sub>* solutions. Part of this higher magnitude is due to the higher tested pressure for *NaCl* solutions (110 psi), as compared to the other two solutions of *MgCl<sub>2</sub>* and *MgSO<sub>4</sub>* (100 psi).

Figure 4-4 summarizes the conclusion from the above three figures. It shows the relative effect of the permeate suction on the three binary solutions at the medium range of pressure (100 to 110 psi) in which the permeate suction had the greatest impact.

It clearly shows that the concentration polarization layer thickness is reduced with suction for all the tested solutions. Detailed study of the above-mentioned figure also shows that the concentration polarization layer thickness is a function of the diffusion coefficient of the solute. As the diffusion coefficient increases from *MgSO<sub>4</sub>* to

$MgCl_2$  to  $NaCl$ , the concentration polarization layer increases if the feed solution concentration and the temperature are kept constant.

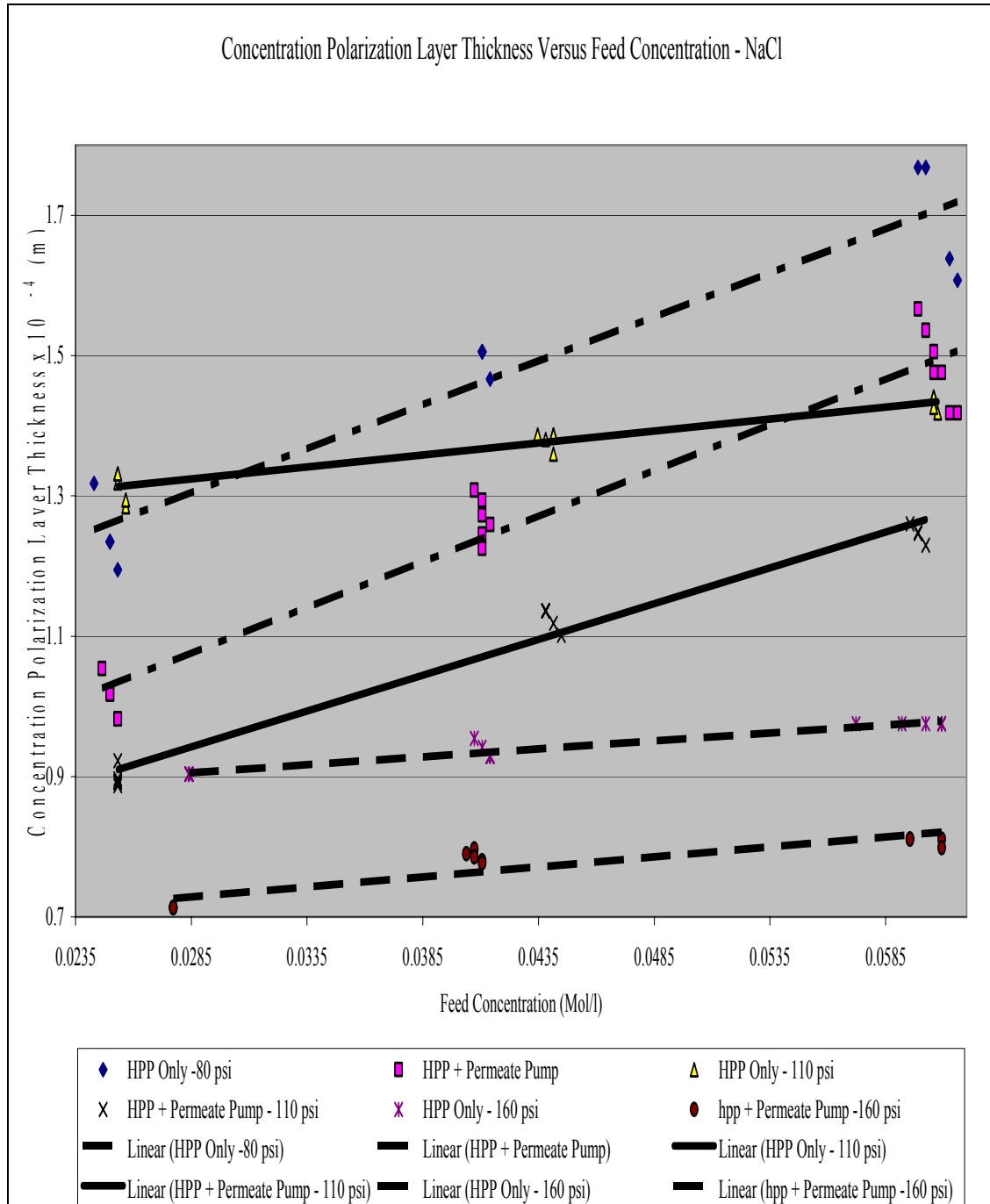


Figure 4-3. Concentration polarization layer thickness versus feed concentration – NaCl

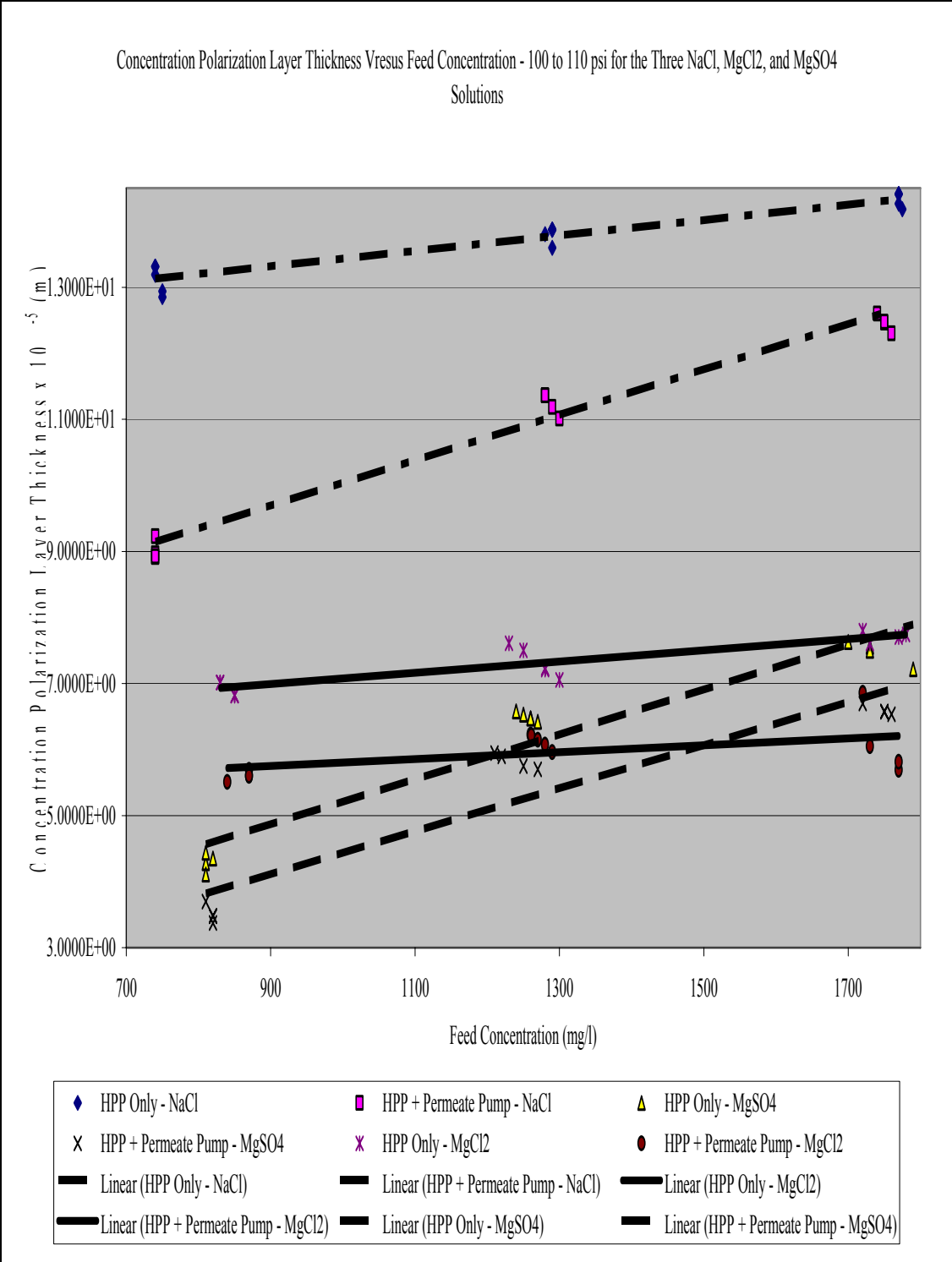


Figure 4-4. Concentration polarization layer thickness versus feed concentration at 100 to 110 psi for the three NaCl, MgCl<sub>2</sub>, and MgSO<sub>4</sub> solutions

Figure 4-5 is plotting the trend in concentration polarization layer thickness against the net operating pressure ( $\Delta P - \Delta \pi$ ) for  $MgCl_2$  solutions. The solid line is showing the trend with permeate suction, while the dotted line is presenting the trend without permeate suction. For example, at a net operating pressure of 5.45 atm, the average concentration polarization layer thickness without permeate suction was  $7.9 \times 10^{-5}$  m. This was reduced to about  $6.7 \times 10^{-5}$  m with permeate suction, resulting in a reduction of about 15%.

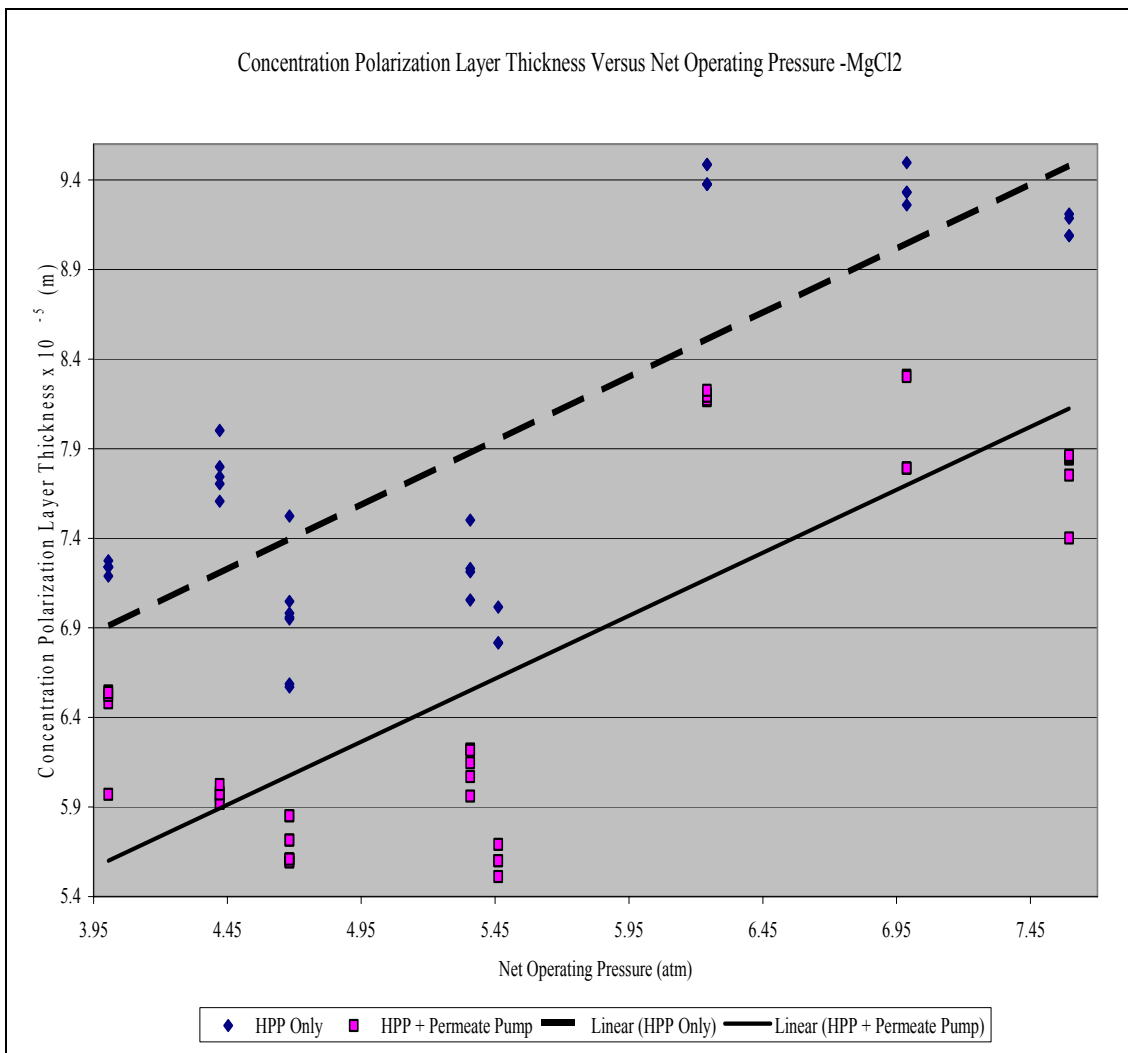


Figure 4-5. Concentration polarization layer thickness versus net operating pressure -  $MgCl_2$

#### 4.1.1 Statistically Testing the Experimental Design for Concentration Polarization Layer Thickness

The measured concentration polarization layer thicknesses were in the order of magnitude of  $10^{-5}$  to  $10^{-4}$  m. To validate the experiments, and to eliminate experimental errors, the Analysis of Variance (ANOVA) was tested.

ANOVA were carried out on the two different treatments (without permeate suction, and with permeate suction) to compare the mean value of the two tests, and to check if the permeate suction has made a significant change from the case of not having permeate suction. Two statistical hypotheses were tested:

$$H_0: \mu_1 = \mu_2$$

$$\text{and } H_1: \mu_1 \neq \mu_2$$

where  $\mu_1$  is the mean concentration layer thickness in the case of running the test without using permeate suction in m multiplied by  $10^5$ , and  $\mu_2$  is the mean concentration layer thickness in the case of using permeate suction in m multiplied by  $10^5$ .

The following ANOVA tables for three tested salts are showing the results of the experiment analysis.

##### 4.1.1.1 ANOVA for $MgCl_2$ Solutions

Referring to Table 4-1 below, and from Table IV of Design and Analysis of Experiments book (Montgomery D., 2001):

$$\text{Critical value of } F_{0.05, (a-1), (a-1)(b-1)} = F_{0.05, 1, 8} = 5.32$$

$$\text{Since } F_o = 288.552 > F_{0.05, 1, 8} = 5.32$$

so  $H_0: \mu_1 = \mu_2$  is rejected, and  $H_1: \mu_1 \neq \mu_2$

It was concluded that there was a difference between the two treatments.

Hence, the permeate suction was significantly different from the case of no suction.

Table 4-1. ANOVA Table for  $MgCl_2$  solutions

Source of Variation	Sum of Square	DOF	Mean Square	$F_o$
Treatment (w/o & w suction)	6.8672	1	6.8672	288.5552
Blocks	17.9010	8	2.2376	
Error	0.1903	8	0.0238	
Total	26.1177	17		

#### 4.1.1.2 ANOVA for $MgSO_4$ Solutions

Referring to Table 4-2 below, and from table IV of Design and Analysis of Experiments text book (Montgomery D., 2001):

Critical value of  $F_{0.05,(a-1),(a-1)(b-1)} = F_{0.05,1,8} = 5.32$

Since  $F_o = 267.2989 > F_{0.05,1,8} = 5.32$

so  $H_0: \mu_1 = \mu_2$  is rejected, and  $H_1: \mu_1 \neq \mu_2$

It was concluded that there was a difference between the two treatments.

Hence, the permeate suction was significantly different from the case of no suction.

Table 4-2. ANOVA Table for  $MgSO_4$  solutions

Source of Variation	Sum of Square	DOF	Mean Square	Fo
Treatment (w/o & w suction)	2.2493	1	2.2493	267.2989
Blocks	19.9345	8	2.4918	
Error	0.0673	8	0.0084	
Total	22.2512	17		

#### 4.1.1.3 ANOVA for $NaCl$ Solutions

Referring to Table 4-3 below, and from table IV of Design and Analysis of Experiments text book (Montgomery D., 2001):

Critical value of  $F_{0.05,(a-1),(a-1)(b-1)} = F_{0.05,1,8} = 5.32$

Since  $F_o = 10.36771 > F_{0.05,1,8} = 5.32$

so  $H_0: \mu_1 = \mu_2$  is rejected

and  $H_1: \mu_1 \neq \mu_2$

Table 4-3. ANOVA Table for  $NaCl$  solutions

Source of Variation	Sum of Square	DOF	Mean Square	Fo
Treatment (w/o & w suction)	0.5894	1	0.5894	10.3677
Blocks	104.1044	8	13.0130	
Error	0.4548	8	0.0568	
Total	105.1486	17		

#### 4.2 Effect of Permeate Suction on Mass Transfer Coefficient

As was mentioned above, the mass transfer coefficient is inversely proportional to the concentration polarization layer thickness. Figures 4-6, 4-7, and 4-8 show that the mass transfer coefficient for all dilute solutions increased with permeate suction, if compared with the case of no permeate suction.

Again, it is deduced that the permeate suction destabilizes the boundary layer in the laminar flow condition that reduces concentration polarization and enhances the mass transfer coefficient. The above-mentioned figures show that the greatest mass transfer coefficients were achievable when the operating conditions were in the range of 100 to 110 psi. However, the mass transfer coefficient rates for  $MgSO_4$  solutions were reduced faster at the higher feed concentration greater than 0.0225 Mol/l, due to the higher rate of the increase of concentration polarization layer at the higher concentrations.



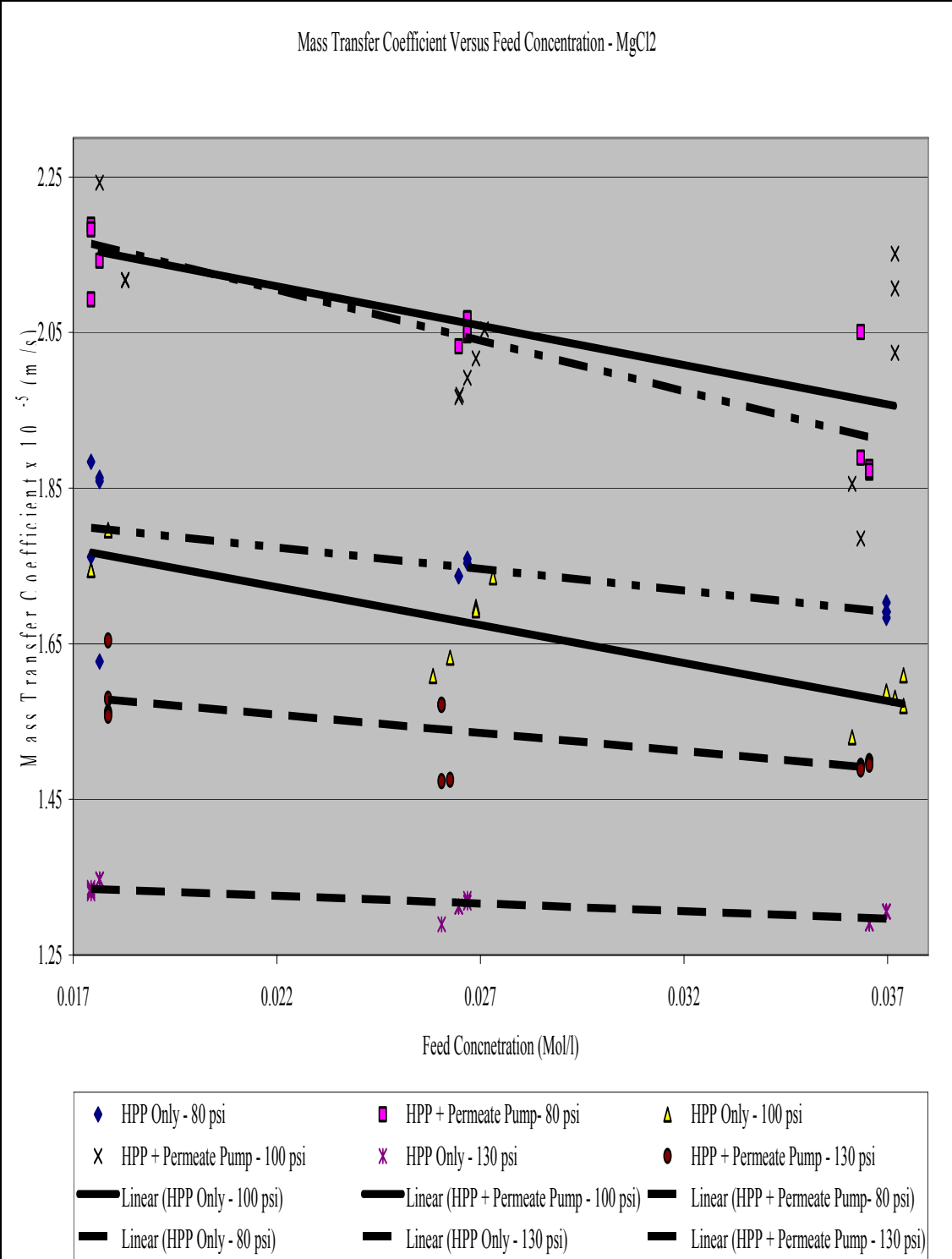


Figure 4-6. Mass transfer coefficient versus feed concentration -  $MgCl_2$

Mass Transfer Coefficient Versus Feed Concentration -MgSO<sub>4</sub>

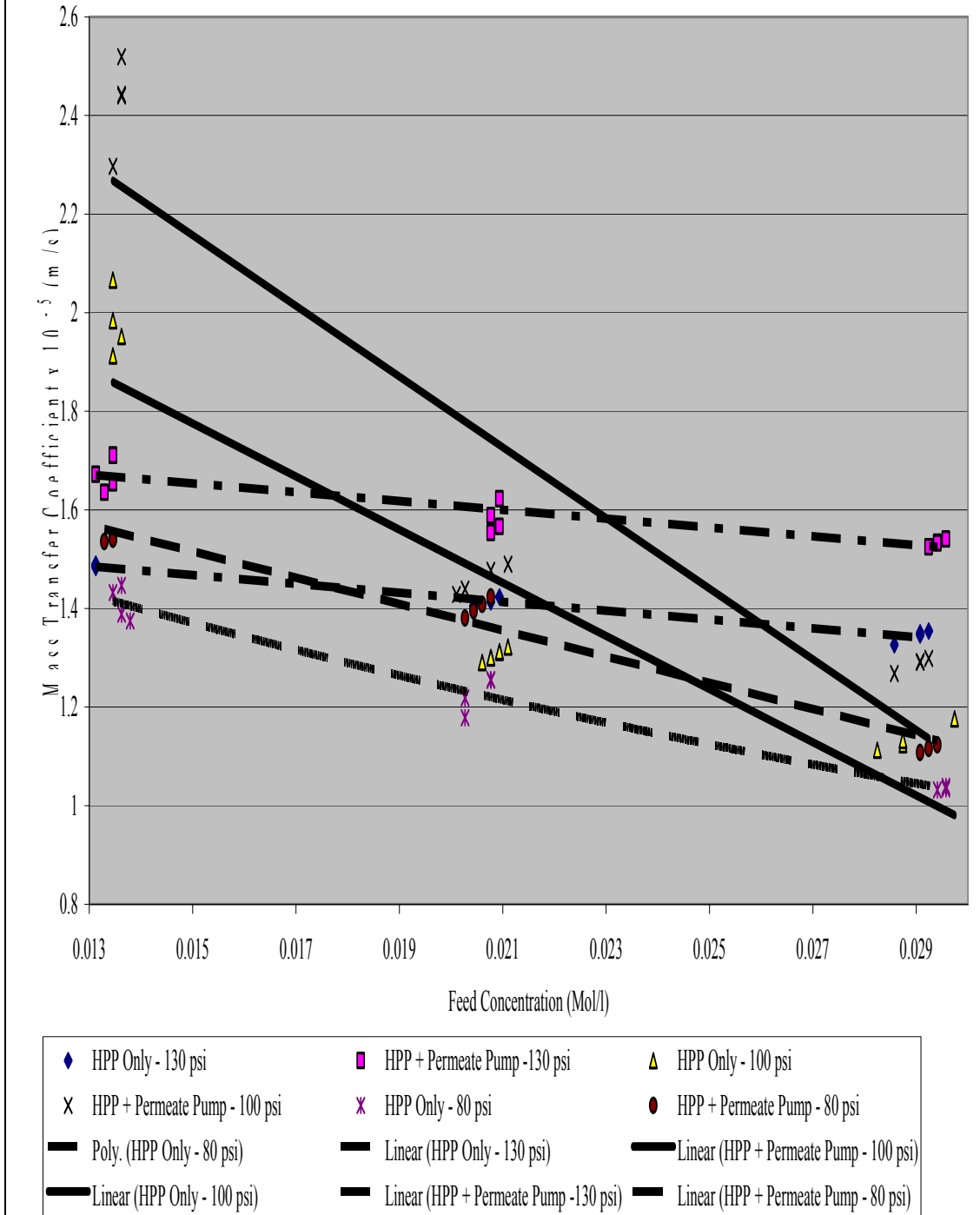


Figure 4-7. Mass transfer coefficient versus feed concentration – MgSO<sub>4</sub>

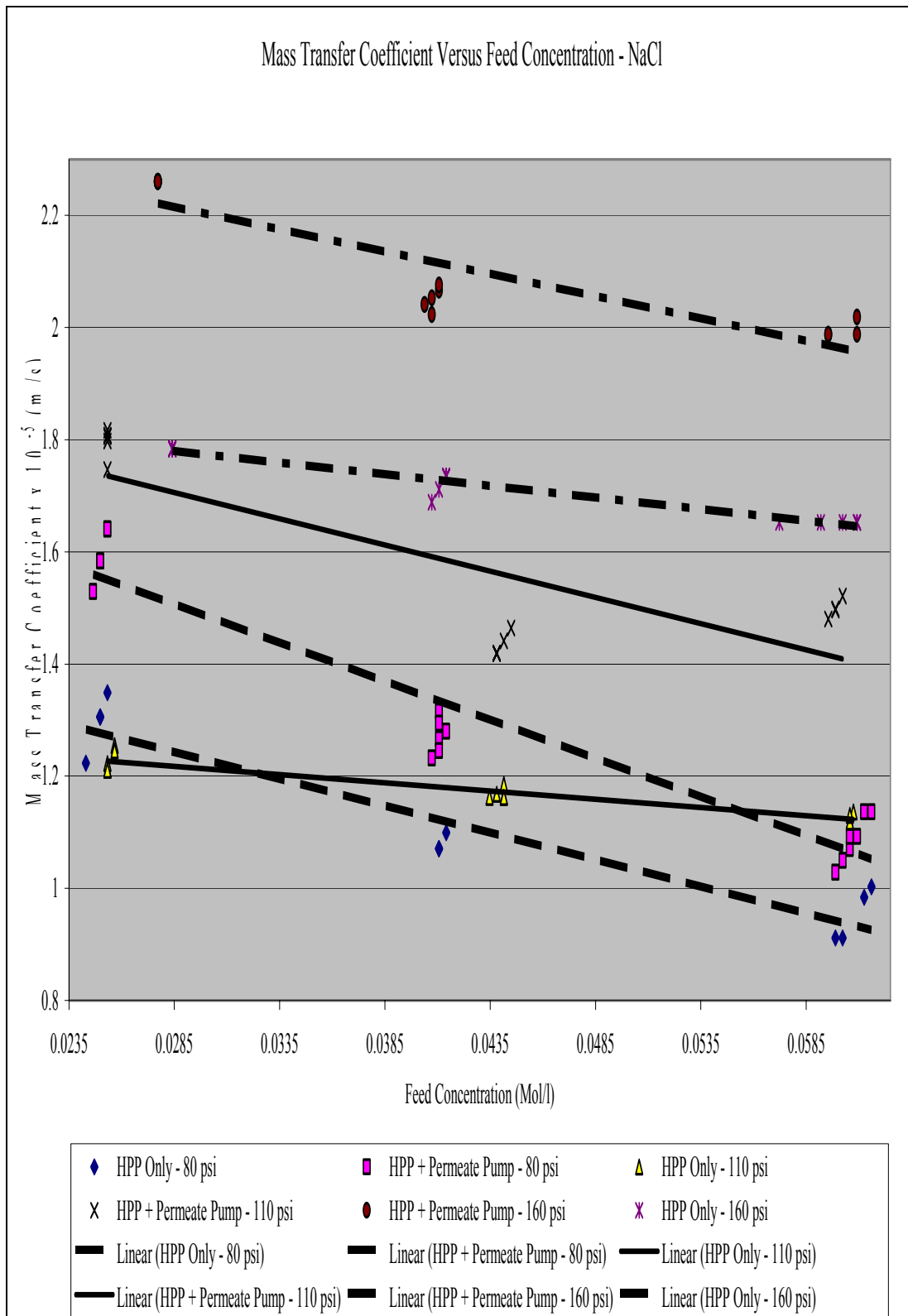


Figure 4-8. Mass transfer coefficient versus feed concentration - NaCl

#### 4.3 Effect of Permeate Suction on Permeate Flow

Figures number 4-9, 4-10, and 4-11 show the relationship between the feed concentration, and the product flow for the different dilute solutions at the three pressures. It is evident from the figures that the product flow has increased due to permeate suction for all salt solutions, and under the three tested pressures. As it was expected, the permeate flow rate, and consequently the permeate flux was increased with the higher feed pressure. In general, the product flow rate was reduced as the feed concentration increased. However, for  $MgSO_4$  and  $NaCl$  solutions the greatest rate of increase due to permeate suction was achieved at the medium operating feed pressure range (100 to 110 psi).

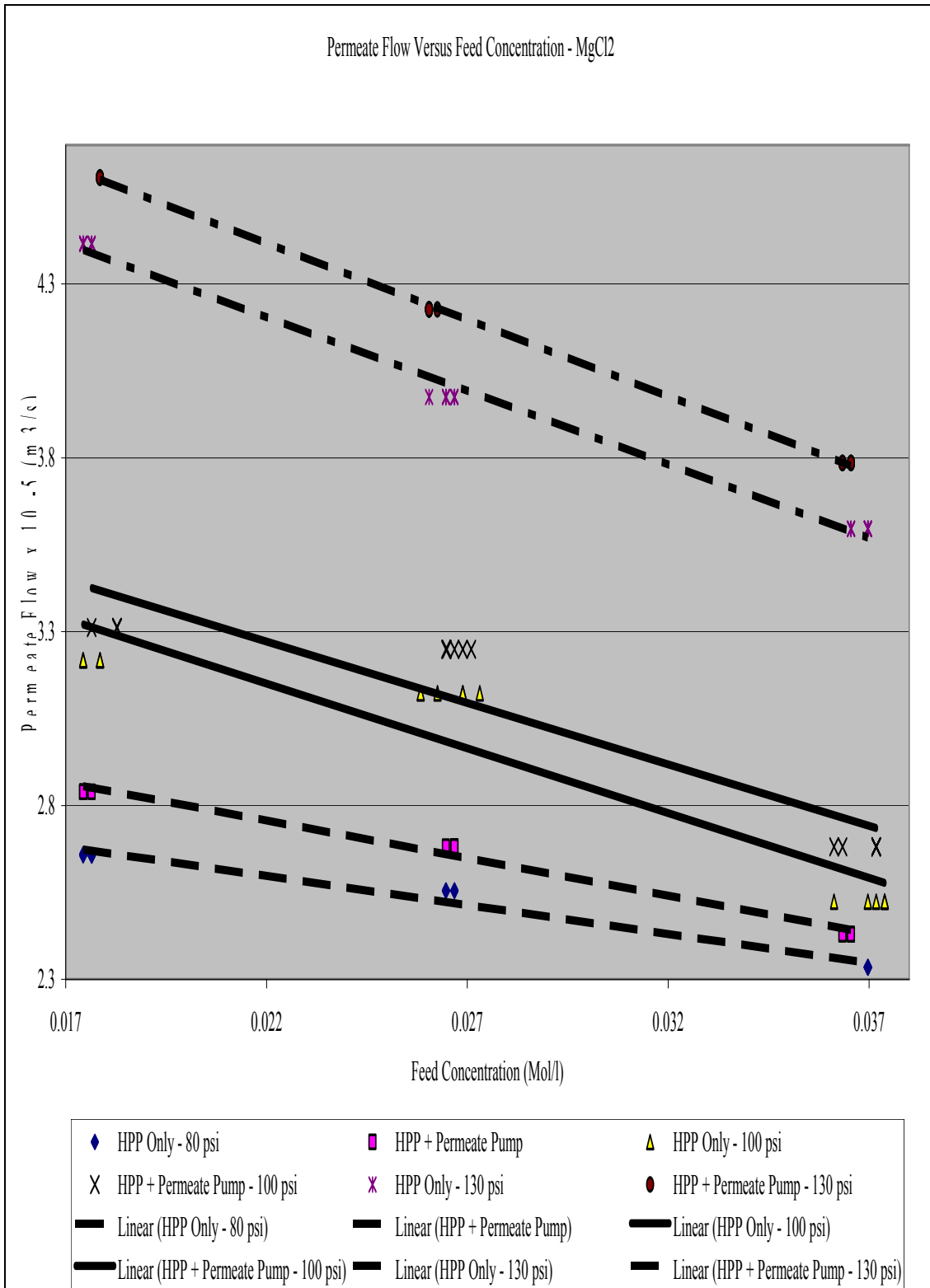


Figure 4-9. Permeate flow versus feed concentration – MgCl<sub>2</sub>

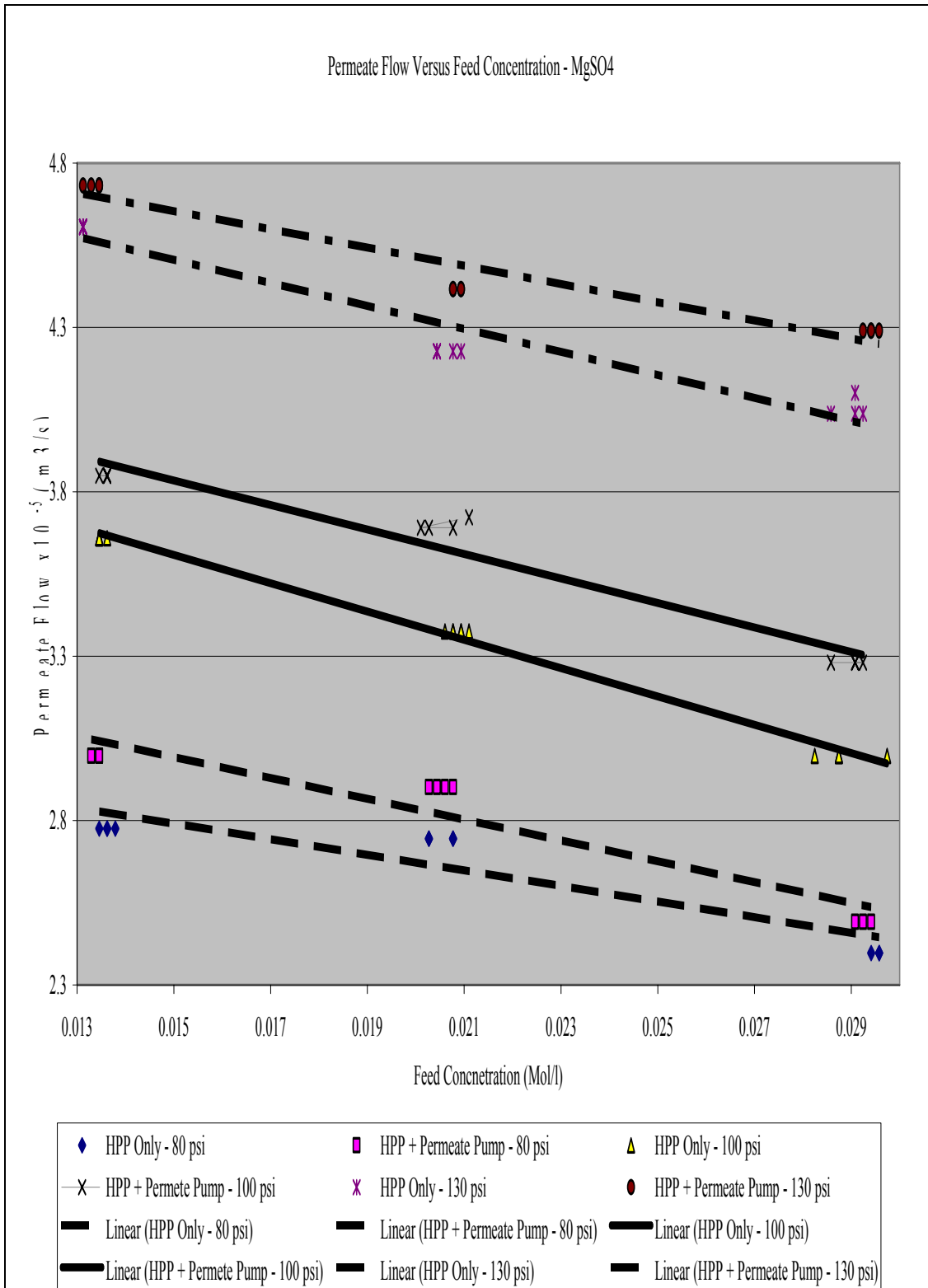


Figure 4-10. Permeate flow versus feed concentration – MgSO<sub>4</sub>

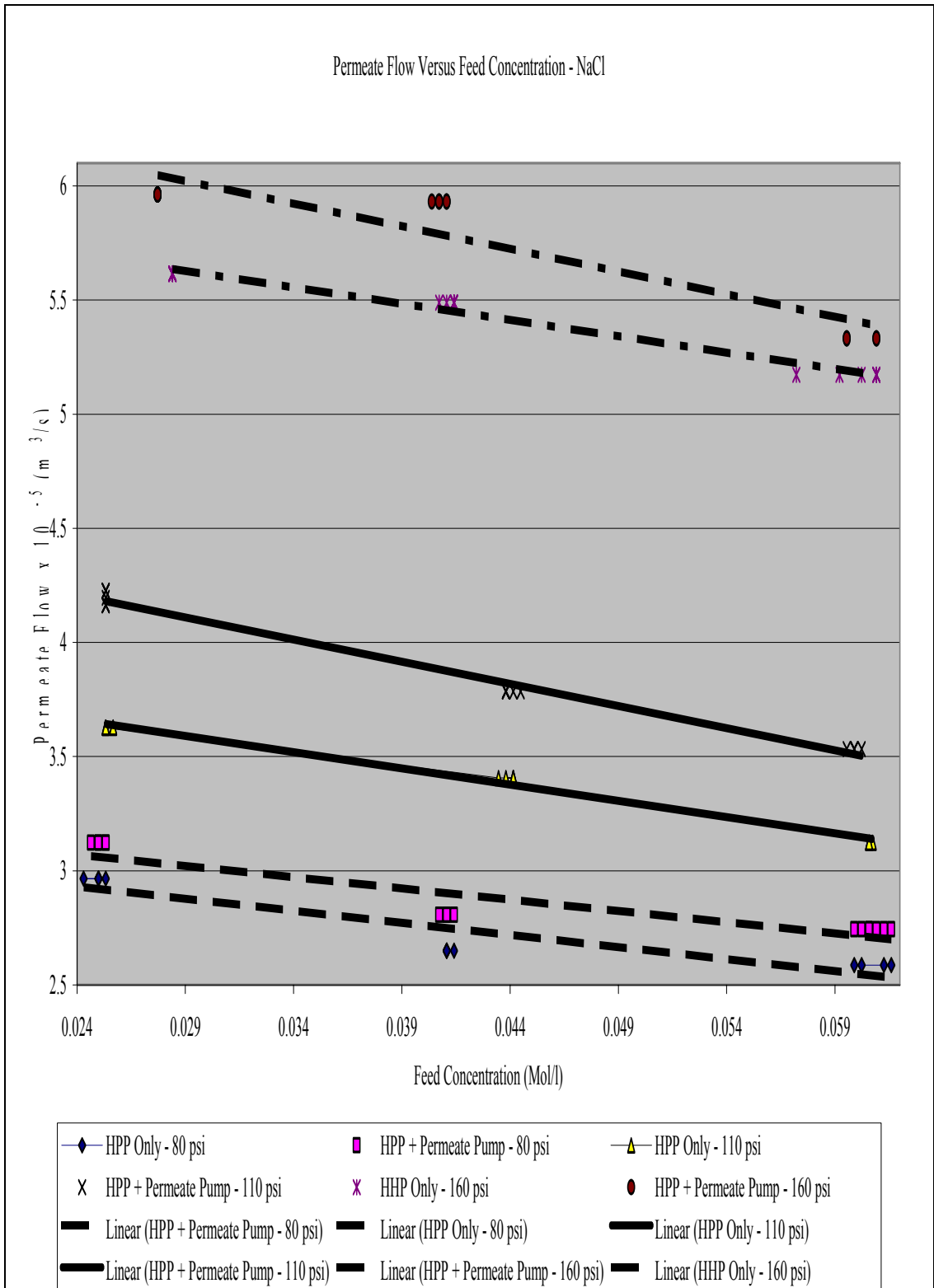


Figure 4-11. Permeate flow versus feed concentration – NaCl

#### 4.4 Effect of Permeate Suction on Permeate Concentration

Figures 4-12, 4-13, and 4-14 illustrate the change in permeate concentration versus feed concentration with permeate suction at various pressures. It is clear from the three figures that permeate suction has improved the quality of the permeate concentration at all pressures. It is interesting to notice on the first two figures that the greatest improvement was achieved at the medium feed pressure (100 psi).

It is worthy to mention that the permeate concentration of  $MgCl_2$  solutions was much higher than the permeate concentration of  $MgSO_4$  solutions under the same operating conditions. This as indicated in item 4.1 above, is due to the low rejection of the  $Cl^-$  monovalent anion by the NF membrane, while the rest of ions in the two solutions, namely,  $Mg^{++}$ , and  $SO_4^{--}$  are highly rejected because they are divalent ions.

The ionic mobility of ions has also contributed to the rate of their rejection.

Robinson and Stockes (1965) have indicated that the radius of chloride ion is  $1.81 \text{ \AA}$ , versus a greater radius for sulfate compound ion. The fact that the sulfate compound anion has a radius greater than that of the chloride element anion has helped the latter in its greater passage rate through the membrane. In all cases, the use of permeate suction has resulted in a better permeate quality. This was more pronounced in the solutions of the divalent ions than the monovalent ion solutions.



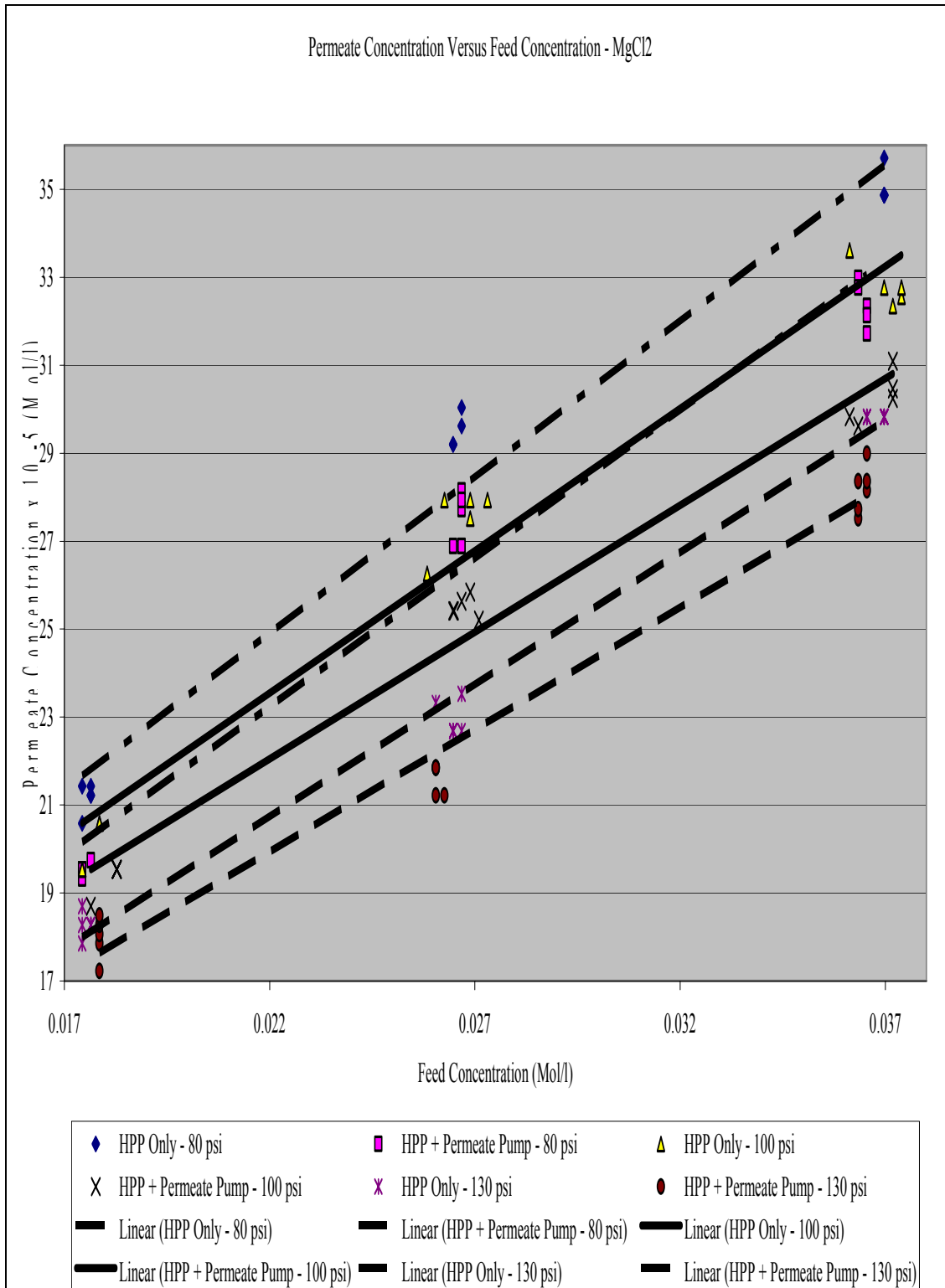


Figure 4-12. Permeate concentration versus feed concentration – MgCl<sub>2</sub>

Permeate Concentration Versus Feed Concentration - MgSO<sub>4</sub>

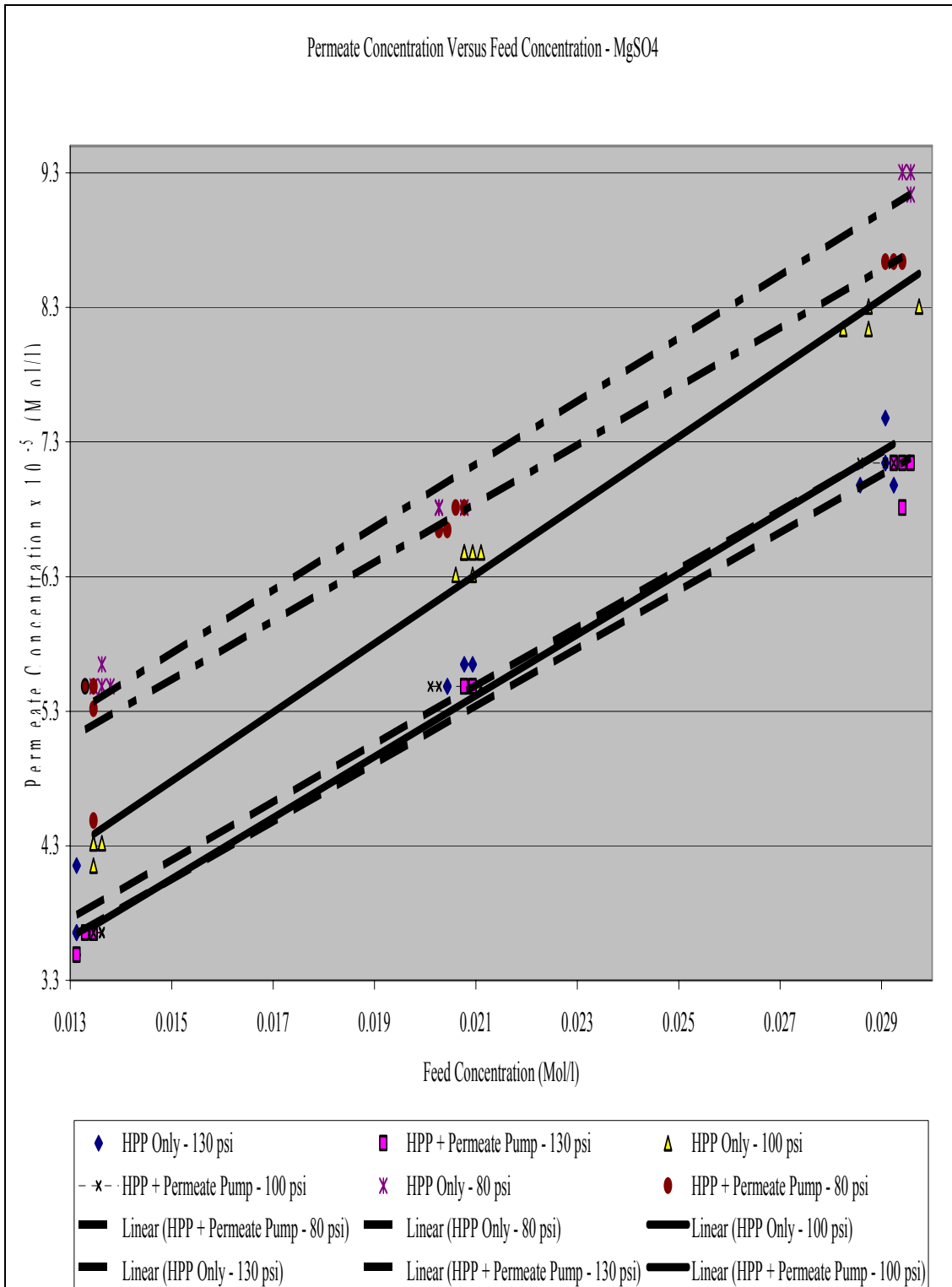


Figure 4-13. Permeate concentration versus feed concentration – MgSO<sub>4</sub>

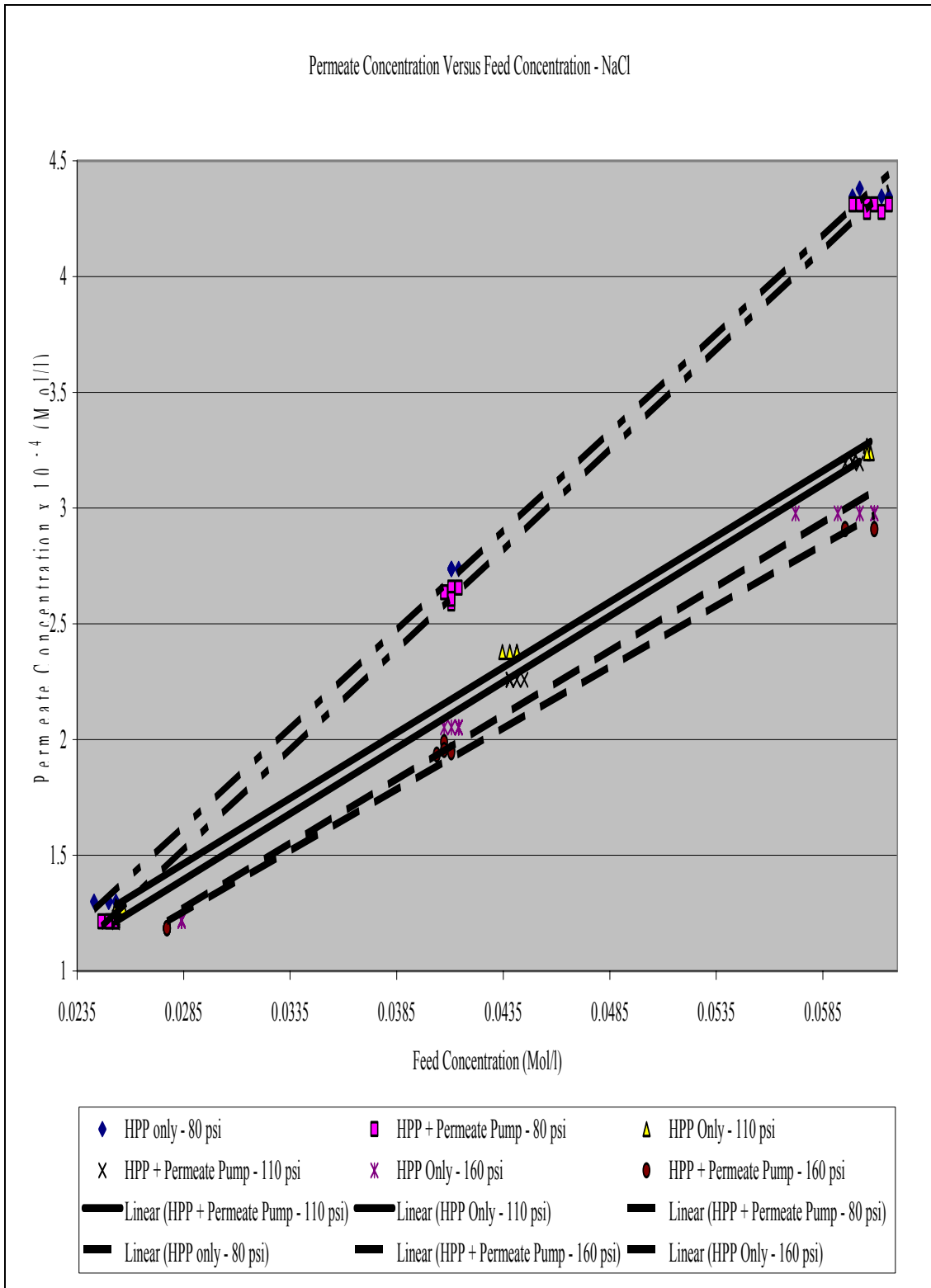


Figure 4-14. Permeate concentration versus Feed concentration – NaCl

#### 4.5 Effect of Permeate Suction on Concentrate Concentration

Concentrate concentration is generally increased due to permeate suction for all dilute solutions at different concentrations and pressures as shown in Figures (4-15, 4-16, and 4-17). The increase is due to the reduction in the membrane wall concentration as it will be explained later in item 4.6. Especially at the medium feed pressure range (100 to 110 psi), the rate of increase of the concentrate concentration due to suction in  $MgSO_4$  solutions was higher. This was due to the higher rejection of its two divalent ions  $Mg^{++}$ , and  $SO_4^{--}$ , as opposed to the lower rejection of the monovalent ion  $Cl^-$  that is available in the  $MgCl_2$  solutions, as was indicated in item 4.1 above.

Concentrate Concentration Versus Feed Concentration - MgCl<sub>2</sub>

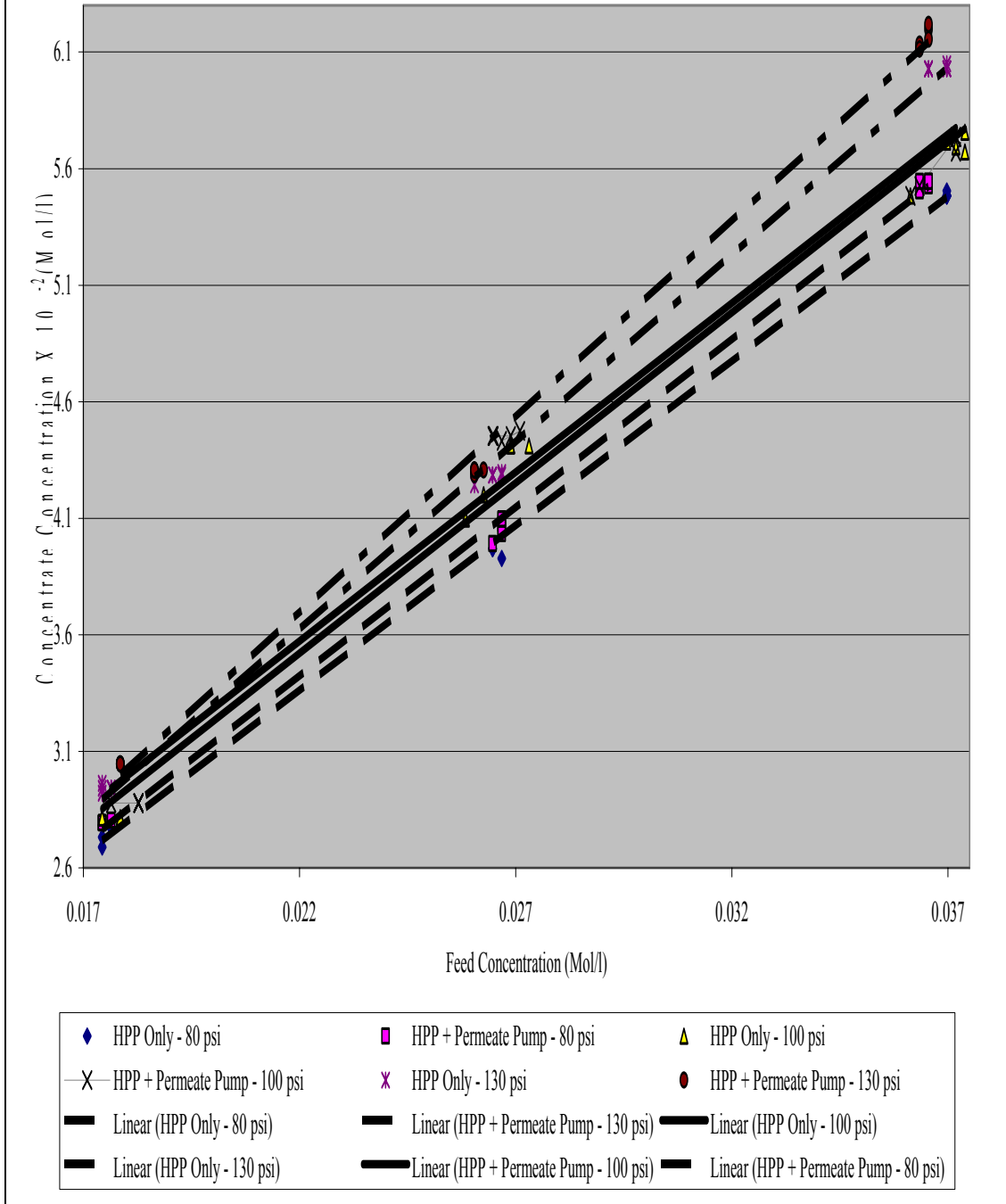


Figure 4-15. Concentrate concentration versus feed concentration - MgCl<sub>2</sub>

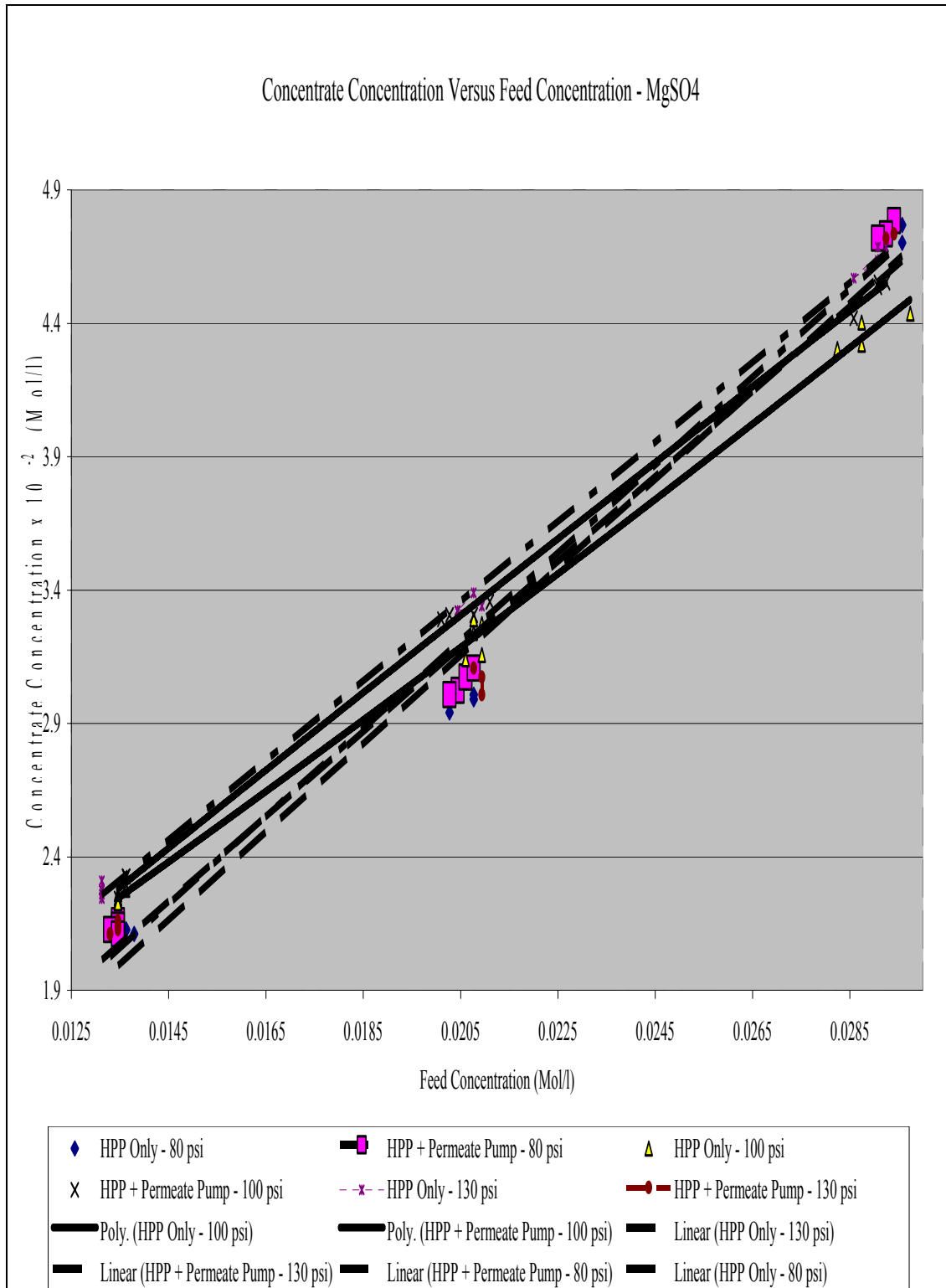


Figure 4-16. Concentrate concentration versus feed concentration - MgSO<sub>4</sub>

Concentrate Concentration Versus Feed Concentration -NaCl

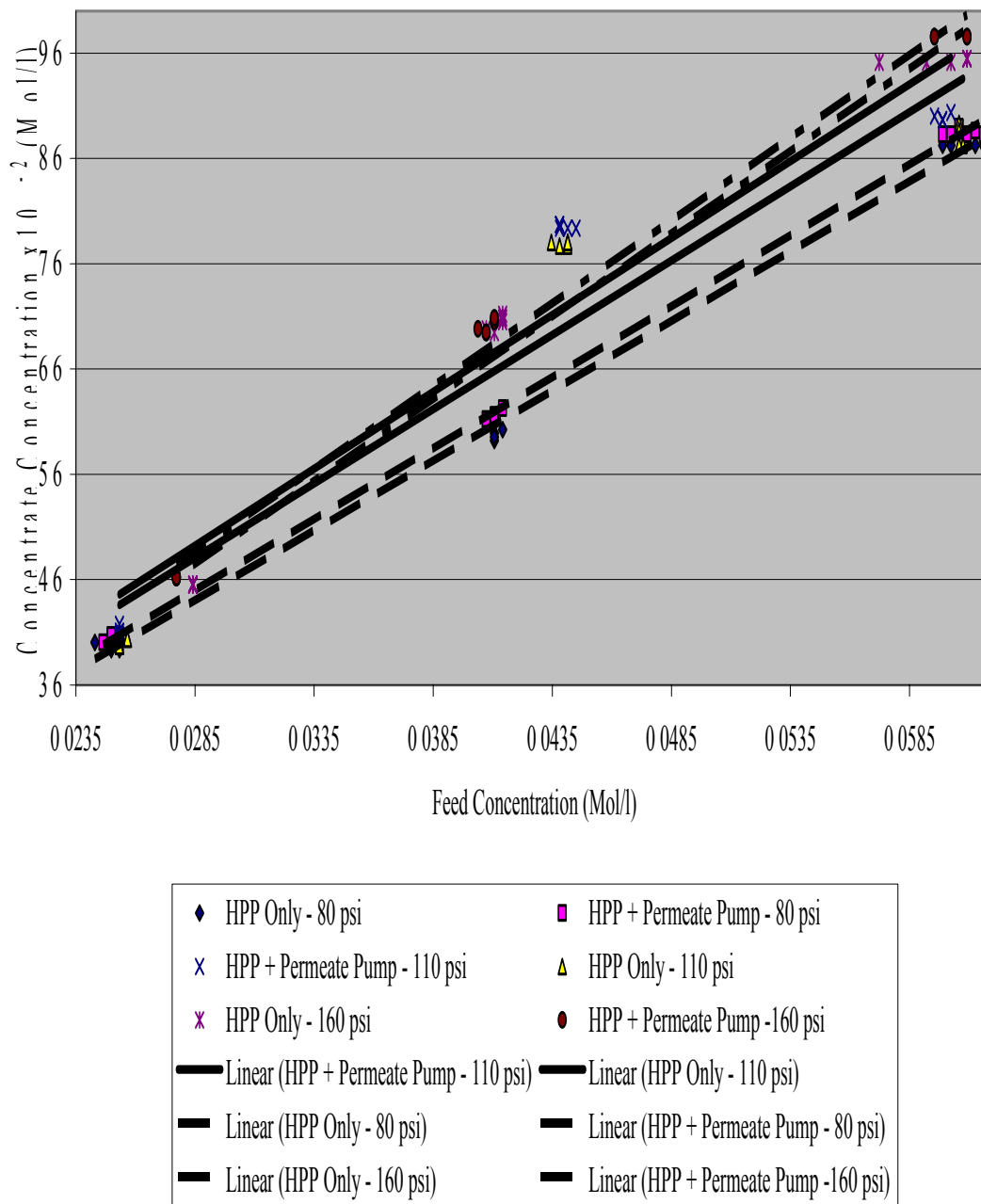


Figure 4-17. Concentrate concentration versus feed concentration - NaCl

#### 4.6 Effect of Permeate Suction on Membrane Wall Concentration

Membrane wall concentration can not be experimentally measured. Therefore it was calculated using the solution diffusion model, as it was discussed in Chapter 2.

Figures 4-18, 4-19, and 4-20 show that the calculated membrane wall concentration is lower with permeate suction if compared to the case of running the high pressure pump only at all pressures for all the tested solutions. A more detailed analysis of the above-mentioned figures can be illustrated if they are compared to the corresponding three figures of the concentrate concentration in item 4.5, namely Figures (4-15, 4-16, and 4-17). It is deduced from that comparison that the membrane wall concentration is a function of the effect of concentration polarization. The higher the feed pressure, the more pronounced the difference in concentration between no suction, and permeate suction. The difference between the ionic species radii of chloride element ion, and sulfate compound ions as it was discussed in item 4.1 and 4.4 above, has contributed to the distinction. For example, at the medium pressure range (100 to 110 psi), where the permeate suction had the greatest impact, the fact that the sulfate compound anion has a radius greater than that of the chloride element anion has helped the latter in its higher passage rate through the membrane in both  $NaCl$ , and  $MgCl_2$  solutions such that the membrane wall concentration in those cases is greater than the case of  $MgSO_4$  solutions.



Membrane Wall Concentration Versus Feed Concentration - MgCl<sub>2</sub>

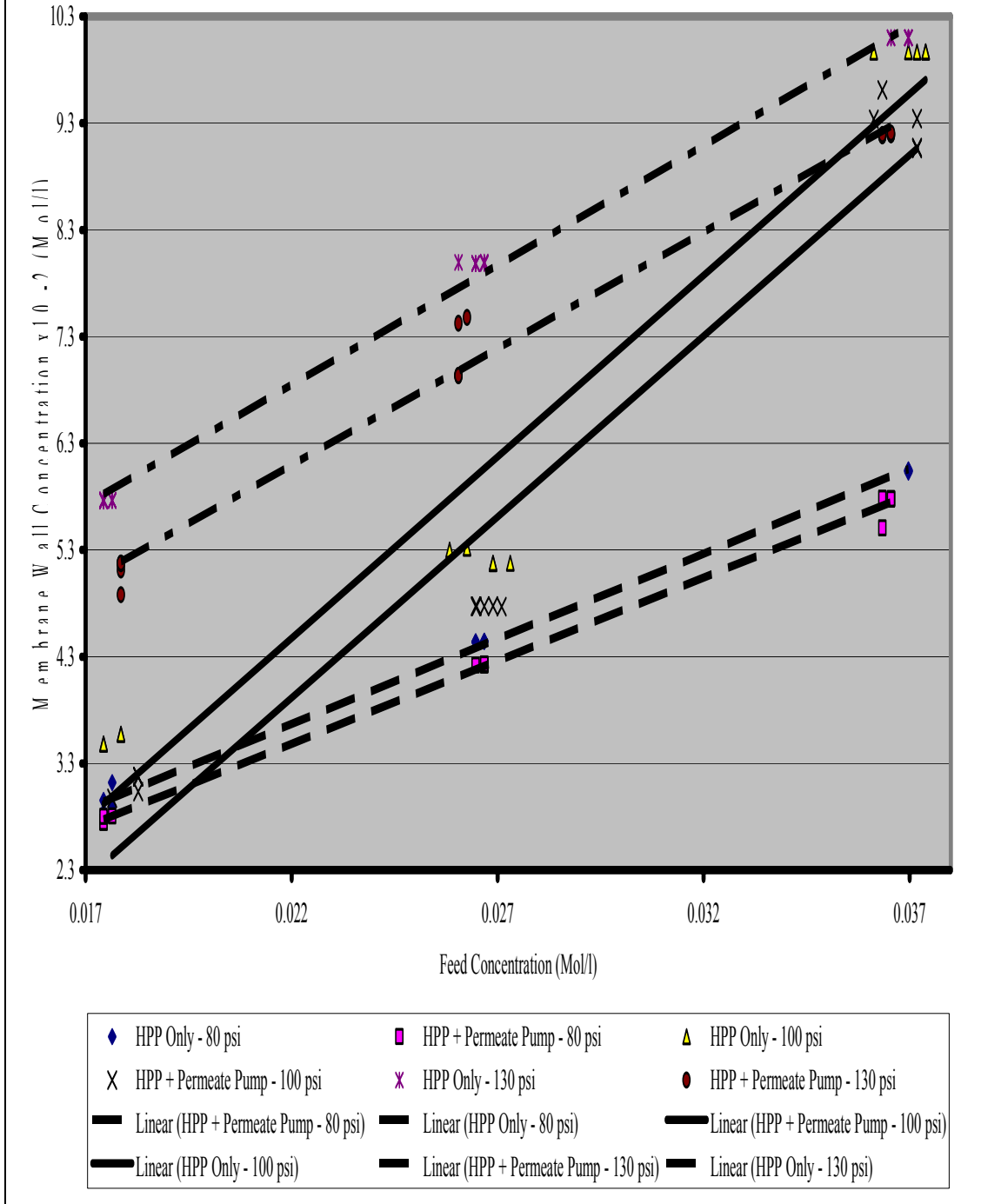


Figure 4-18. Membrane wall concentration versus feed concentration - MgCl<sub>2</sub>

Membrane Wall Concentration Versus Feed Concentration - MgSO<sub>4</sub>

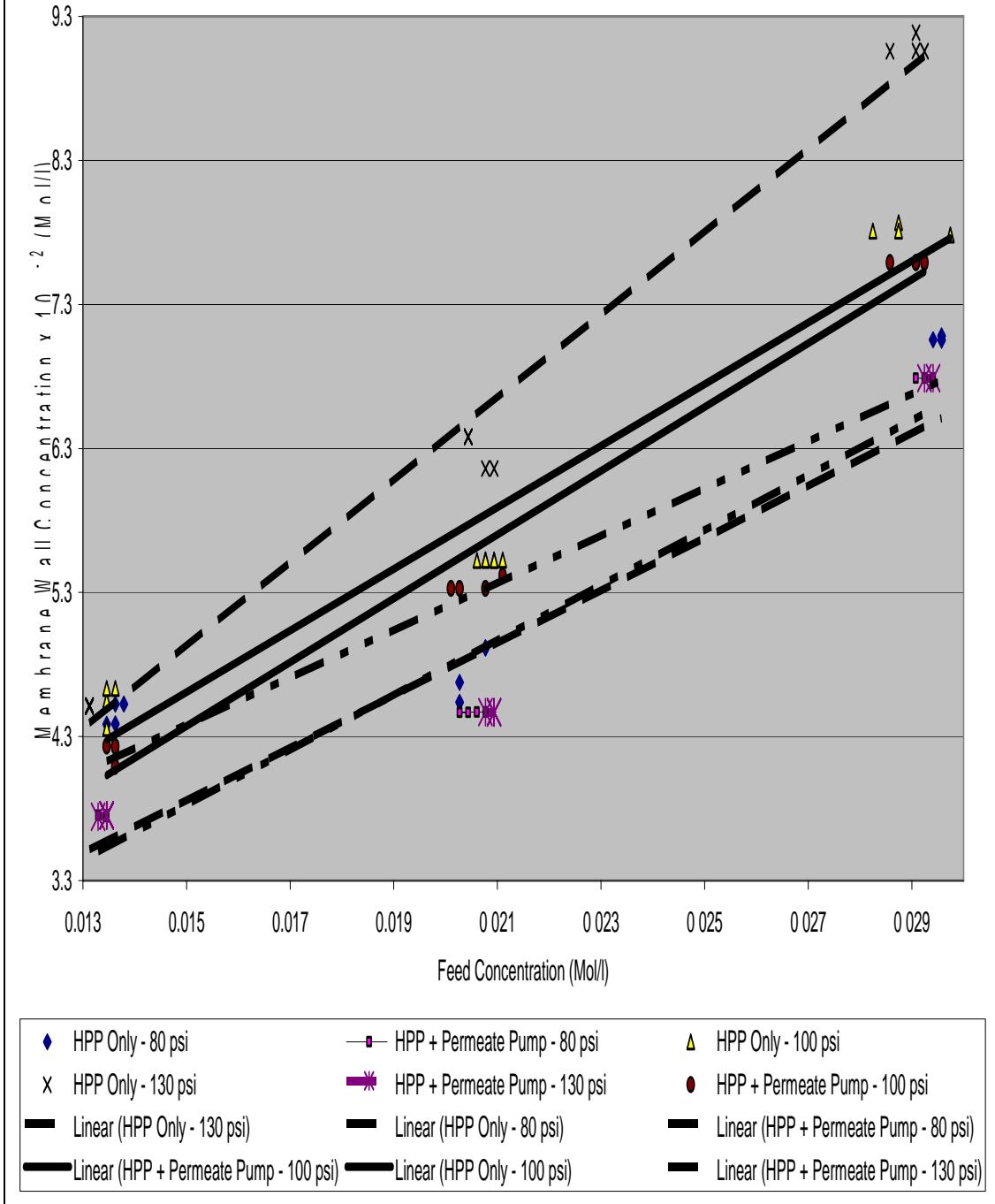


Figure 4-19. Membrane wall concentration versus feed concentration - MgSO<sub>4</sub>

Membrane Wall Concentration Versus Feed Concentration - NaCl

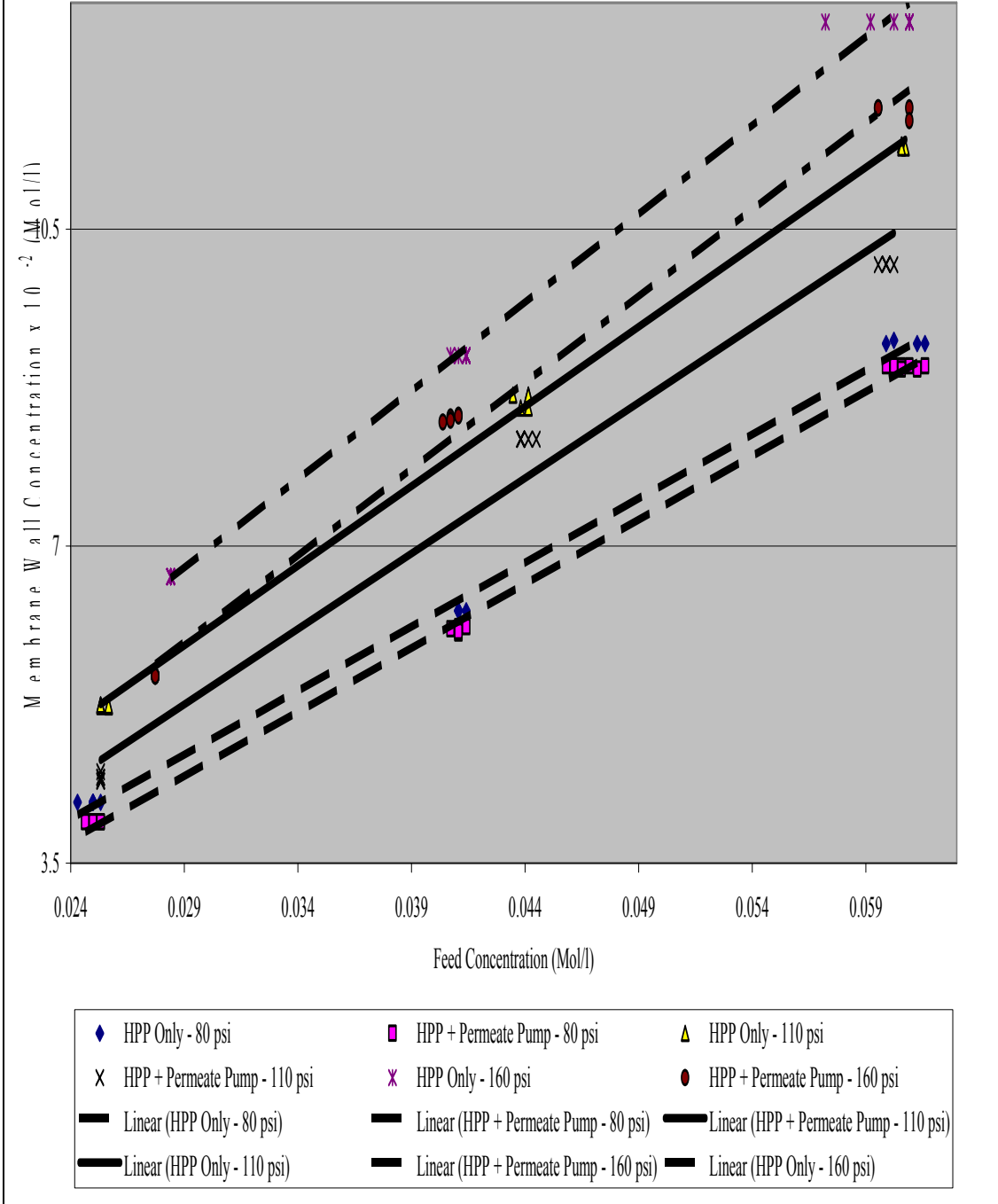
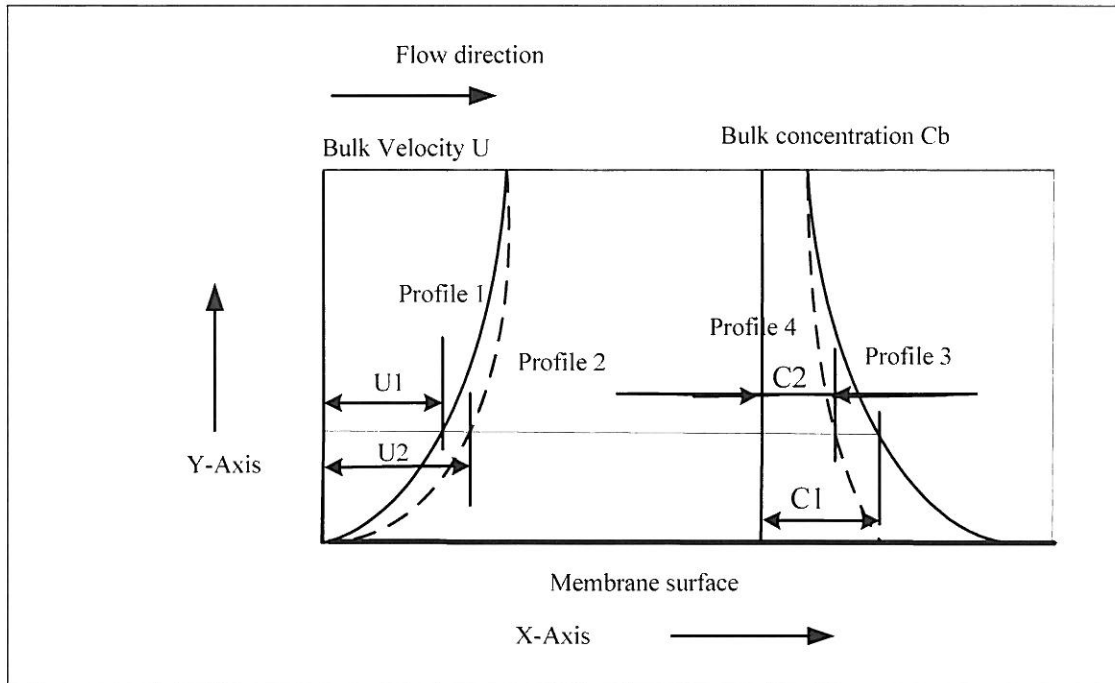


Figure 4-20. Membrane wall concentration versus feed concentration - NaCl



Profile 1: velocity gradient w/o permeate suction      profile 2: velocity gradient with permeate suction  
 Profile 3: concentration gradient w/o permeate suction      profile 4: concentration gradient with permeate suction

Figure 4-21. Fully developed Velocity profiles and concentration profiles in the boundary layer without and with permeate suction

In an attempt to explain the relationship between the change in the velocity profile and the concentration profile due to suction, refer to Figure 4-21 above. Adding positive pressure by the permeate suction to the feed pressure should increase the permeate flow, and consequently the average concentrate concentration of the bulk solution should increase, as it was expected. However, the permeate suction has decreased the concentration gradient in addition to the increase of permeate flow rate, as it was observed in the experiments. Since our principle concern is the dilute solution, it was mentioned previously in Chapter 2 that the concentration polarization layer is embedded in the viscous boundary layer, and the velocity in that layer is that close to the wall (Probstein, 1944). Referring to Figures 4-15, 4-16, and 4-17 in item 4.5 above, in conjunction with the sketch in Figure 4-21, it is suspected that permeate suction will

alter the velocity profile from profile number (1) to profile number (2) due to the de-stabilization of the boundary layer. In addition, let us take a cross section perpendicular to the membrane at steady state condition. Also, let us consider a random point at the boundary layer velocity profile, and its correspondent point at the concentration profile. Suction will increase velocity U1 to velocity U2, which will increase the local flow at that point. Since the corresponding point at the concentration profile without suction is C1, the concentration at the same point after applying suction will be decreased to C2 because the corresponding velocity and flow rates have increased. When applying the mass balance equation for the whole system at steady state conditions, the average concentrate concentration at the bulk solution at the case of applying suction will be increased, if compared to the average concentrate concentration of the bulk solution before suction. This is due to the increased flow near the membrane that will partially wash away the accumulated species on the membrane. This was the observation of the experiment for the concentrate concentration as indicated in Figures 4-15, 4-16, and 4-17 in item 4.5 above for all the solutions at all pressures.

#### 4.7 Effect of Permeate Suction on Peclet Number

Peclet number is defined as the dimensionless ratio of the rate of mass transported by convection to the membrane, to the rate of mass transported by diffusion back to the bulk solution. In other words, the diffusive membrane Peclet number which is expressed as per equation (2-31) in Chapter 2 is:

$$P_e = \frac{V_w h_d}{D_{1-2}}$$

where  $V_w$  is the permeate velocity which is equal to the permeate flux per one sheet of

membranes;  $D_{1-2}$  is the diffusivity coefficient of the ionized electrolyte; and  $h_d$  is the hydraulic diameter of the spiral wound membrane. The diffusive Peclet number is a measure of how permeate goes through the membrane. It is observed that for the dilute solutions the Schmidt number is very large, as a consequence of which the diffusion Peclet number is large. This is true even at moderate Reynolds number (Probstien,1994).

In the case of using the standard high pressure pump only, both the permeate concentration and the concentration polarization layer increase as the Peclet number increase (Probstein, 1994). However Figures 4-22, 4-23, and 4-24 show a remarkable result. They show that the diffusive Peclet number for the binary dilute solutions has increased with the permeate suction at all pressures, although the associated permeate concentration, and concentration polarization layer thicknesses have decreased as was discussed in item 4.1 and 4.3 above. This is a proof that the permeate suction has stabilized the flow conditions, and has enhanced the mass transfer coefficient.

From the above mentioned figures, at permeate suction, and at different feed operating conditions, the diffusive Peclet number can be expressed according to the equation :

$P_e = a_1x^2 + b_1x + c_1$  , with  $R^2 > 0.99$ , where  $x$  is the feed concentration in Mol/l, and  $a_1$  ,  $b_1$  , and  $c_1$  are coefficients dependent on feed pressure for every binary salt solution.

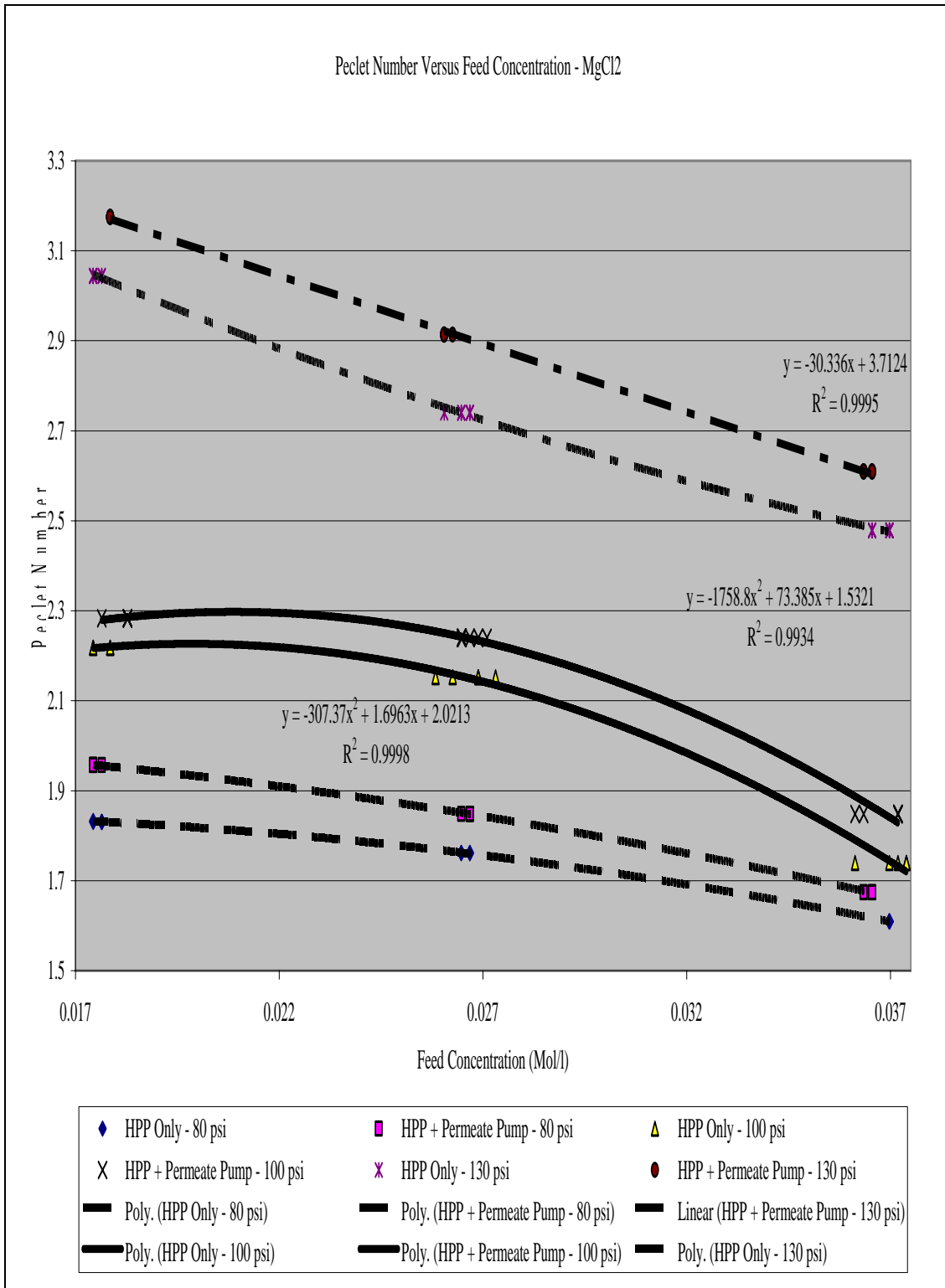


Figure 4-22. Diffusive Peclet number versus feed concentration - MgCl<sub>2</sub>

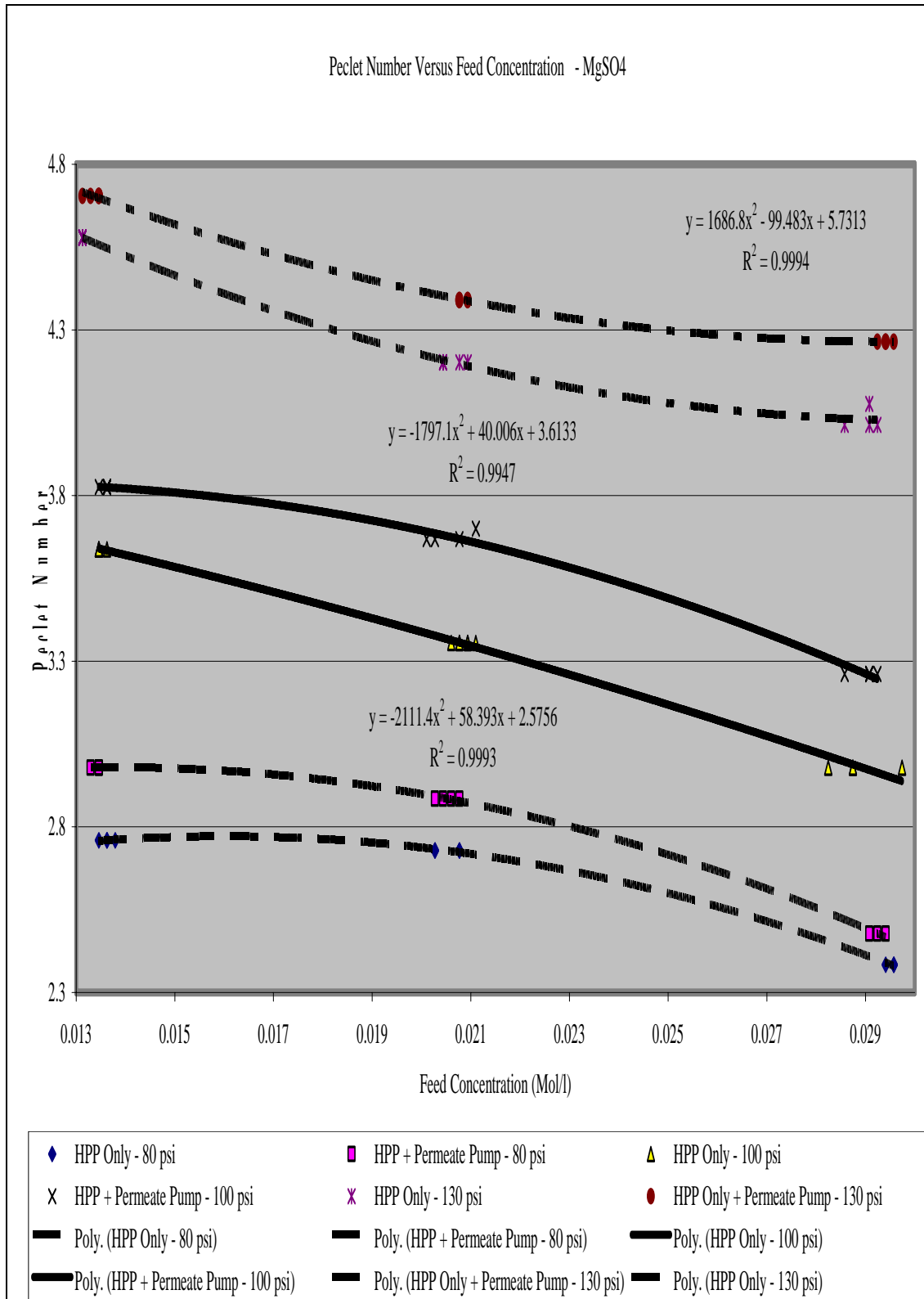


Figure 4-23. Diffusive Peclet number versus feed concentration - MgSO<sub>4</sub>



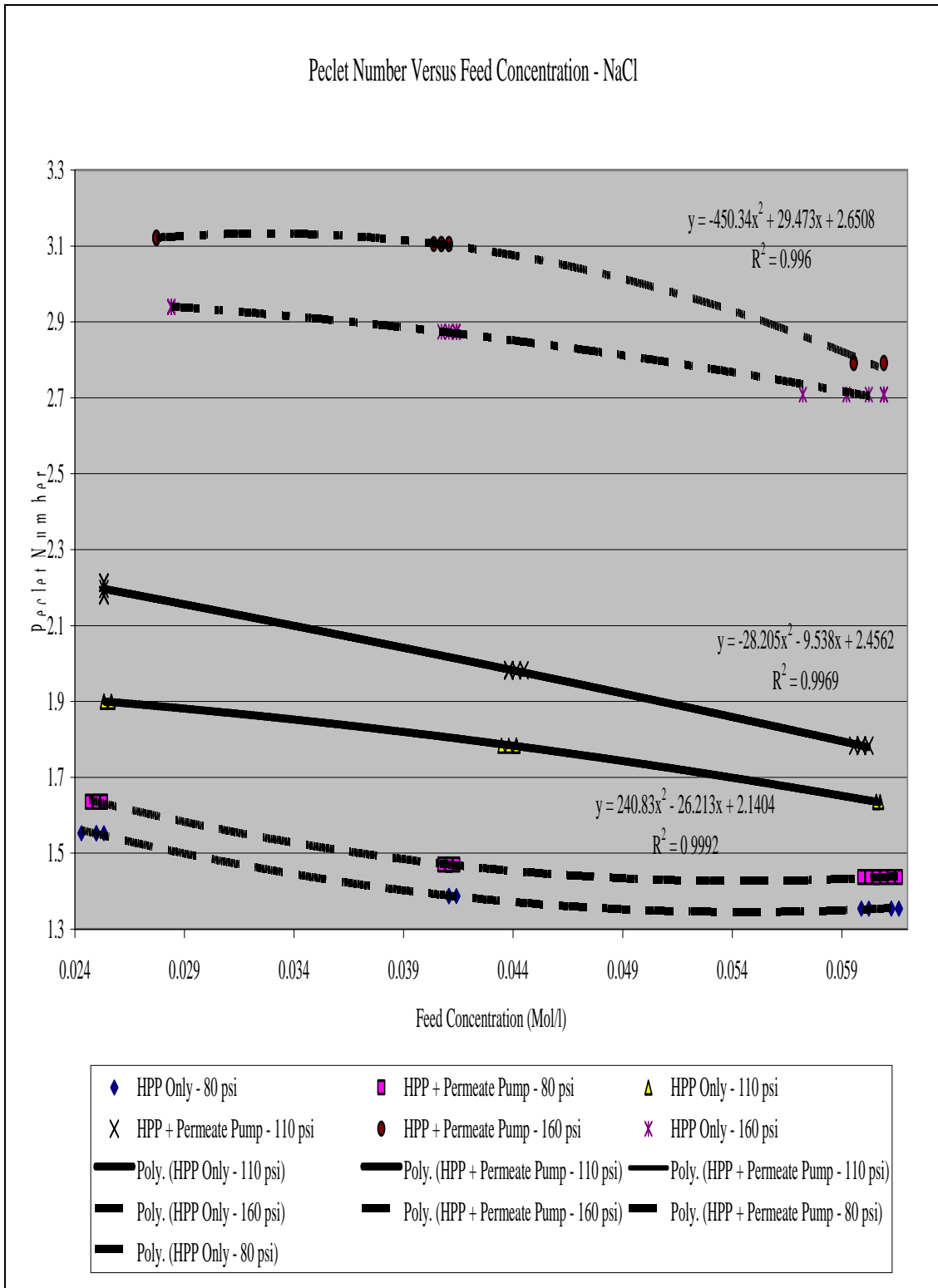


Figure 4-24. Diffusive Peclet number versus feed concentration – NaCl

## CHAPTER 5

### CONCLUSION AND RECOMMENDATIONS

This chapter consists of three parts. The first part concludes the results of the experiments. The second part emphasizes the importance of the findings on the design improvements for NF plants. The third part discusses the suggested and recommended future researches that can be carried out as a further step to this research.

#### 5.1 Conclusion

The goal of this research was to make use of the effect of the de-stabilization of the laminar flow that exists at the membrane surface due to the gradually increased permeate suction, in an attempt to reduce the concentration polarization layer in the module. Previous researches showed that the concentration polarization is almost always the reason behind membrane fouling. The technique of using permeate suction is not practically used in the NF or RO membrane industry so far, despite that it has been theoretically investigated at the laboratory scale by a few researchers.

- (1) This research showed that when using binary dilute solutions, the permeate suction reduced the concentration polarization at the feed side of the industry scale NF membrane surface that helped to increase mass transfer coefficient, and increased the product flux without subjecting the membrane to less favorable conditions.

- (2) The research also showed that permeate suction had the greatest impact at the medium range (100 to 110 psi) feed pressure, resulting in a reduction of concentration polarization layer thickness with an average between 14 to 20%.
- (3) The magnitude of the measured concentration polarization layer thickness in the experiments was very small in the order of  $3 \times 10^{-5}$  to  $8 \times 10^{-4}$  meters. To eliminate experimental errors, the analysis of the variances of the experiments (ANOVA) were tested in both experiment treatments (without suction, and with suction) to investigate the significance of the permeate suction. ANOVA Tables for the three tested binary dilute salt solutions showed that the permeate suction was significant, and applying the permeate suction was statistically different from the case of not applying suction.
- (4) This research showed that calculating the concentration polarization layer using the traditional way of using Sherwood number correlation would lead to erroneous results due to the changes in the solution properties because of suction, that are not considered in this relationship. In addition, it is even believed that the use of the correlation of Sherwood number in the literature for the traditional high pressure pump design only might be inadequate. This is shown by the different values of the coefficients that were deduced by different researchers in calculating the relationships in that correlation.
- (5) The use of Peclet number instead, which does not primarily depend on most of the changed physical properties of the solutions would eliminate the need to use the Sherwood number. The values used in calculating the diffusive Peclet number could be easily and appropriately calculated. Although the Peclet

number is a function of the solute diffusion coefficient, keeping the temperature constant through all the experiments has eliminated the change that could occur in the solute diffusivity back to the bulk solution. The velocity term in the Peclet number was easily calculated from the experimentally measurable permeate flux. The hydraulic diameter coefficient in Peclet number is dependent on the membrane structure, which was calculated from the geometrical dimensions of the tested membrane.

- (6) The diffusive Peclet number increased with the permeate suction at all the experimental testes. The Peclet number followed a pattern of  $P_e = a_1x^2 + b_1x + c_1$ , with  $R^2 > 0.99$ , where  $x$  is the feed concentration in Mol/l. The terms  $a_1$ ,  $b_1$ , and  $c_1$  are coefficients dependent on feed pressure for every binary salt solution. The results showed that the permeate flow increased at the same time, while the concentration polarization was reduced. This was opposite to the traditional case where permeate suction is not used. In the later case, the increase of the Peclet number increases the concentration polarization layer.
- (7) Although some researchers used the concentration polarization layer thickness, and boundary layer thickness interchangeably (e.g. Lisdonk, C., et al. 2001; Sablani S., et al, 2001) they are actually different. At the dilute solutions where Schmidt number is  $\gg 1$ , the concentration polarization layer is imbedded in the viscous boundary layer, and its velocity is that the one close to the wall. Schlichting (1979) estimated the boundary layer thickness at the porous wall suction as a function of Reynold's number. The calculations for this estimation

are based on an assumption of a constant viscosity along the membrane width, which may not be accurate, especially for highly concentrated solutions.

- (8) It is worthy to mention that the equation of transport in the membrane is complex for multi component solutions with more than one anion and one cation because more than one cation can be accompanied by one anion or vice versa, depending on the ion valence. It has been shown that the concentration polarization for individual salts changes substantially with the presence of other salts (Srinivasan and Tein, 1970). The solution-diffusion model is valid only for binary solution systems, and can not be used for a mixture of salts. To estimate the transport in the membrane for a multi component solution, one alternative is the use of the Nernst-Planck model, which is for a mixture of  $n$  ions  $(3n+2)$  equations are required (Ghiu and Carnahan, 2003).

## 5.2 Recommendations

- (1) The NF membrane makers traditionally use the standard testing pressure of 70 to 75 psi range. It is suggested that the membrane manufacturers might have to change their standard test conditions to 100 to 110 psi, since this research showed that the greatest impact on the NF membranes was achieved at the medium feed pressure which was 100 to 110 psi.
- (2) The applications of NF membrane in the water treatment industry are numerous, and based on the above-mentioned results using the permeate suction can help reduce the concentration polarization layer in NF modules, and increase mass transfer coefficient, that will elongate the useful membrane life.

- (3) One interesting recent application is using two staged NF-NF to desalinate seawater is very promising. In this case using the permeate suction at the end of both stages may be a way to reduce concentration polarization in this application for seawater desalination, which would lead to a prolonged life of the membrane, in addition to increasing the NF plant productivity.

### 5.3 Future Researches

- (1) It is thought that an economical study of adding the cost of the permeate suction pump to the existing traditional module design should be addressed in the upcoming researches, and the total water cost of a system should be evaluated based on that addition.
- (2) Another proposed future study is determining the minimum suction pressure required to reduce the concentration polarization layer, so that the plant modification from the current standard system design can be optimized.
- (3) It is also believed that extending the application of the permeate suction to the higher concentration of brackish water RO modules, or seawater RO plants can critically be investigated, despite the complexity of predicting the mass transfer model for highly concentrated mixed salt solutions.

## LIST OF REFERENCES

- Afonso, Maria et al, 2000, Transport Of  $MgSO_4$ ,  $MgCl_2$ , And  $Na_2SO_4$  Across an Amphoteric Nanofiltration Membrane, *Journal of Membrane Science*, 179-137-154.
- Al-Bastaki N., 2001, Use of Fluid Instabilities To Enhance Membrane Performance: A Review, *Desalination* 136 - 255-262.
- Amjad, Z., 1993, *Reverse Osmosis Membrane Technology*, Van Nostrand Reinhold, New York.
- Bartels, Craig, 2007, *Novel New Fouling Nanofiltration Membranes*, Hydranautics Membrane Manufacturer.
- Bhattacharyya et al, 1999, Separation Of Organic Pollutants By Reverse Osmosis and Nanofiltration Membranes: Mathematical Models and Experimental Verification, Department of Chemical and Materials Engineering, University of Kentucky, Lexington, Kentucky.
- Bhattacharyya, D, S.L. Back and R.I. Kermode, 1990, Prediction of Concentration Polarization and Flux Behavior in Reverse Osmosis by Numerical Analysis, *Membrane Science*, 48 - 231.
- Chiolle, A., G Gianotti, M. Gramondo and G Parrini, 1978, Mathematical Model of Reverse Osmosis in Parallel Wall Channels with Turbulence Promoting Nets, *Desalination*, 26 - 3-16.
- Cruver, J. E., 1978, IJS Department of Interior, Office of Saline Water Resource, Development Progress Report, NTIS: PB 223 181, No. 882, *Desalination*, 34 - 297-303.
- Cussler, E. L., 1984, *Diffusion Mass Transfer in Fluid Systems*, Press Syndicate of the University of Cambridge.
- Drioli, E. and F. Bellucci, 1978, Concentration Polarization and Solute-Membrane Interactions Affecting Pressure Driven Membrane Processes, *Desalination*, 26 - 17- 36.
- FilmTec membrane handbook, 2009, FilmTec Membrane Manufacturer.

Flemming, Hans Curt, 1993, Mechanistic Aspects of Reverse Osmosis Membrane Biofouling and Prevention in Reverse Osmosis Membrane Technology, edited by Zahid Amjad, Van Nostrand Reinhold, New York.

Flugzeugbau, DG, 1990, Performance Increase Possibilities of Gliders, Internet Wikipedia Encyclopedia,

Fritzmann, C., 2007, State-of-Art of Reverse Osmosis Desalination, Desalination 216-1-76.

Gekas and Hallsrom, 1987, Mass Transfer in the Membrane Concentration Polarization Layer under Turbulent Cross Flow,

Geraldes, V., V. Semiao, 2003, Hydrodynamics and Concentration Polarization in NF/RO Spiral Wound Modules with Ladder-Type Spacers, Desalination 157 - 395-402.

Ghiu, S. and R. Carnahan, 2003, Mass Transfer of Ionic Species in Direct and Reverse Osmosis Processes, Dissertation, University of South Florida.

Gill and Soltanieh, 1981, Review of Reverse Osmosis Membranes and Transport Models, 1981, Gordon and Breach Science Publisher, Inc, USA.

Gupta, Sharad K. et al, 2005, Modeling of Spiral- Wound Module and Estimation of Model Parameters using Numerical Techniques, Desalination 173 - 269-286.

Hassan, A., 2004, Development of a Novel NF-Seawater Desalination Process and Review of Application From Pilot Plant to Commercial Production Plant Stages, Beirut Conference.

Hydranautics Membrane Manufacturer, 2009.

Jamal, J., M.A. Khan, M. Kamil, 2004, Mathematical Modeling Of Reverse Osmosis Systems, Desalination 160 - 29-42.

Le Gouelle, Yann et al, 2006, A Novel Approach to Seawater Desalination using Dual- Staged Nanofiltration, American Water Works Association.

Lide, D.R., 1995, Handbook of Chemistry and Phsics,76<sup>th</sup> Edition, CRC Press, Inc.

Lisdonk, C. A. et al, 2001,The Influence of Concentration Polarization on the Risk of Scaling in Spiral Wound Membrane System, Kiua Research and Consultancy, Netherlands.



- Mahlab, D., N. Ben Yosef and G. Belfort, 1998, Concentration Polarization Profile for Dissolved Species in Unstirred Batch Hyperfiltration (Reverse Osmosis), *Desalination*, 119- 57
- Mohammadi, Toraj, 2005, Mathematical Modeling of Flux Decline in Ultrafiltration, *Desalination* 184-367-373.
- Montgomery, Douglas C., 2004, *Design and Analysis of Experiments*, Wiley Interscience Publication, John Wiley & Sons, Inc., New York.
- Mukiibi, Mo, 2008, *Reverse Osmosis Opportunities and Challenges*, Water Conditioning & Purification Magazine, USA.
- Probstein, Ronald F., 1994, *Physicochemical Hydrodynamics*, Wiley Interscience Publication, John Wiley & Sons, Inc., New York.
- Robinson, R. and Stokes, R, 1965, *Electrolyte Solutions*, Second Edition, London Butterworth.
- Rogers, *Laminar Flow Analysis*, 1992, Cambridge University Press.
- Sablani, S. S., M.F. A. Goosen, R. Al-Belushi, M. Wilf, 2001, Concentration Polarization in Ultrafiltration and RO: A Critical Review, *Desalination* 141, 269-289.
- Sablani, Shyam et al, Influence of Spacer Thickness on Permeate Flux in Spiral-Wound Seawater Reverse Osmosis Systems, *Desalination* 146 (2002) 225-230.
- Sangyoun, Lee, Jaeweon Cho, Menachem Elimelech, Influence of Colloidal Fouling and Feed Water Recovery on Salt Rejection of RO and NF Membranes, *Desalination* 160(2004) 1-12.
- Schaep, Johan, et al, 2001, Modeling the Retention of Ionic Components for Different Nanofiltration Membranes, *Separation and Purification Technology*, 22-23-169-179.
- Schlichting, *Boundary Layer Theory*, Mc Graw-Hill, Inc., 1979, pages 26, 379-385.
- Schock, G., and Miquel, A., 1987, Mass Transfer and Pressure Loss in Spiral Wound Modules, *Desalination* 64-339-352.
- Singh, R., *Hybrid Membrane Systems for Water Purification: Technology, Systems Design and Operation*, Elsevier Science Publishers, UK.
- Sirshendu, De, & Bhattacharya, P. K., 1999, Mass Transfer Coefficient with Suction Including Property Variations in Applications of Cross-Flow Ultrafiltration, *Separation Purification Technology*, 16-61-73.

Song L., 1998, A New Model For The Calculation of The Limiting Flux in Ultrafiltration, Journal of Membrane Science, 173-185.

Srinivasan, S. and Tien, C., 1970, A Simplified method for the Prediction of Concentration Polarization in Reverse Osmosis Operation for Multi Component Systems, Desalination, 7: 133-145.

Taylor, Water Quality and Treatment, edited by Letterman, 1999, Chapter 11, McGraw Hill inc.

Tepper, F. et al., 2006, Emerging Technology, Performance Testing of a New Electropositive Filter, Ultra Pure Water Periodical.

Vicevic Glenn, 2003, RO Pretreatment with Immersed Hollow Fiber Ultrafiltration, Zenon Environmental, International Water Conference.

Waal, M.J. van der, P.M. van der Veiden, J. Koning, C.A. Smolders and W.P.M. van Swaay, Use of Fluidized Beds as Turbulence Promoters in Tubular Membrane, Desalination 22 (1977) 465 -483.

Williams M., 2003, A Brief Review of Reverse Osmosis in Membrane Technology, Williams Engineering Services Company, Inc.

Williams M., 2003, A Review of Reverse Osmosis Theory, EET Corporation and Williams Engineering Services Company, Inc.

Yu Zhao, Yu, 2004, Modeling of Membrane Solute Mass Transfer in NF/RO Membrane Systems, Dissertation, University of Florida.

## **APPENDICES**

**APPENDIX A:**

Tables of Test Results for *NaCl* Solutions

Table A-1. Readings for distilled water before running NaCl solutions

DESCRIPTION	HPP Only								HPP + Permeate Pump								Average
	1	2	3	4	5	6	7	8	Average	1	2	3	4	5	6		
pre-filter inlet press (psi)	31	31	28	41	41	41	40	40.5	36.6875	30.5	30.5	29	42	42	40.5		
pre-filter outlet press (psi)	30	30	27	40	40	40	39	39.5	35.6875	29.5	29.5	28	41	41	39.5		
HPP Press (psi)	114	115	116	65	72	70	72	70	86.75	112	112	112	65	70	70		
Conc. Press (psi)	105	106	109	60	66	65	65	65	80.125	104	104	105	58	65	65		
(Suc) Perm. Press. (psi)	10.1	14.3	13.7	7.5	8.5	8.5	10	9.5	10.2625	3.6	3.6	3.5	1.5	2	2		
(Disch) Perm Press (psi)	0.5	0.5	0	0	0	0	0	0	0.125	0.7	0.7	0.5	0	0	0		
Feed TDS ( mg/l)	5.7	5.8	5.4	5.6	5.8	5.9	6.5	6.5	5.9	5.5	5.8	5.6	5.7	5.9	6.5		
Conc. TDS (mg/l)	7.7	7.7	7.3	6.6	6.9	7.1	7.7	7.7	7.3375	7.5	7.8	7.7	6.8	7.2	7.9		
Perm TDS (mg/l)	1.5	1.5	1.5	2	1.5	1.5	1.5	1.5	1.5625	1.5	1.5	1.5	1.5	1.5	1.5		
Perm Flow ( gpm)	0.71	0.71	0.71	0.43	0.46	0.46	0.44	0.46	0.5475	0.77	0.77	0.78	0.46	0.49	0.49		
Conc Flow (gpm)	1.7	1.7	1.7	1.7	1.6	1.6	1.6	1.6	1.65	1.7	1.7	1.7	1.7	1.6	1.6		
Feed Flow (gpm)	2.41	2.41	2.41	2.13	2.06	2.06	2.04	2.06	2.1975	2.47	2.47	2.48	2.16	2.09	2.09		
Recovery %	29.46	29.46	29.46	20.19	22.33	22.33	21.57	22.33	24.64	31.17	31.17	31.45	21.30	23.44	23.44		
HPP (RPM)	1000	1000	1000	1000	800	800	800	800	900	1000	1000	1000	1000	800	800		
Perm Pump (RPM)	0	0	0	0	0	0	0	0	0	500	500	500	500	200	200		
Temp	25	25	25	25	25	25	25	25	25	25	25	25	25	25	25		
Surface Area (ft2)	28	28	28	28	28	28	28	28	28	28	28	28	28	28	28		
Flux (gpm/ft2)	2.54E-02	2.54E-02	2.54E-02	1.54E-02	1.64E-02	1.64E-02	1.57E-02	1.64E-02	1.96E-02	2.75E-02	2.75E-02	2.79E-02	1.64E-02	1.75E-02	1.75E-02		
Delta P (psi)	103.9	100.7	102.3	57.5	63.5	61.5	62	60.5	76.4875	108.4	108.4	108.5	63.5	68	68		
A (g/ ft2- min-psi)	2.44E-04	2.52E-04	2.48E-04	2.67E-04	2.59E-04	2.67E-04	2.53E-04	2.72E-04	2.56E-04	2.54E-04	2.54E-04	2.57E-04	2.59E-04	2.57E-04	2.57E-04		
A (g/ ft2- min-psi) average				0.000258								2.56E-04					
A (m3/m2-s-atm)				2.57E-06								9.20E-03					
A (m3/m2-h-atm)				0.009257								2.53E-08					
A (m/s.Kpa)				2.55E-08													
NF - Distilled Water	pH = 6.2																
before NaCl solutions	Biocide = 0.3 mg/l																

Table A-2. Readings for NaCl solution at 730 mg/l and 80 psi feed pressure

Description	HPP Only						HPP + Permeate Pump						Average
	1	2	3	4	5	Average	1	2	3	4	5	Average	
Pre-filter inlet press (psi)	54	54	54	54	54	54	54	54	54	54	54	54	54
Pre-filter outlet press (psi)	53	53	53	53	53	53	53	53	53	53	53	53	53
HPP Press (psi)	80	80	80	80	80	80	80	80	80	80	80	80	80
Conc. Press (psi)	76	76	76	76	76	76	76	76	76	76	76	76	76
(Suc) Perm. Press. (psi)	4.5	4.5	4.5	4.5	4.5	4.5	4.5	4.5	4.5	4.5	4.5	4.5	4.5
(Disc) Perm Press (psi)	0	0	0	0	0	0	0	0	0	0	0	0	0
Feed TDS ( mg/l)	730	730	710	740	730	728	730	740	730	740	720	732	732
Feed TDS ( Mol/l)	0.02498	0.02498	0.02430	0.02533	0.02498	0.02491	0.02498	0.02533	0.02498	0.02533	0.02464	0.02505	0.02505
Conc. TDS (mg/l)	1170	1160	1170	1150	1150	1160	1190	1190	1190	1180	1170	1184	1184
Conc. TDS (Mol/l)	0.04004	0.03970	0.04004	0.03936	0.03936	0.03970	0.04073	0.04073	0.04073	0.04038	0.04004	0.04052	0.04052
Perm TDS (mg/l)	380	380	380	380	380	380	355	355	355	355	355	355.0	355.0
Perm TDS (Mol/l)	0.01300	0.01300	0.01300	0.01300	0.01300	0.01300	0.01215	0.01215	0.01215	0.01215	0.01215	0.01215	0.01215
Perm Flow ( gpm)	0.47	0.47	0.47	0.47	0.47	0.47	0.495	0.495	0.495	0.495	0.495	0.495	0.495
Perm Flow ( m3/s)	2.9653E-05	2.9653E-05	2.9653E-05	2.9653E-05	2.9653E-05	2.9653E-05	3.123E-05	3.123E-05	3.123E-05	3.123E-05	3.123E-05	3.123E-05	3.123E-05
Conc Flow (gpm)	1.1	1.1	1.1	1.1	1.1	1.1	1.1	1.1	1.1	1.1	1.1	1.1	1.1
Feed Flow (gpm)	1.57	1.57	1.57	1.57	1.57	1.57	1.595	1.595	1.595	1.595	1.595	1.595	1.595
HPP (RPM)	600	600	600	600	600	600	600	600	600	600	600	600	600
Perm Pump (RPM)	0	0	0	0	0	0	300	300	300	300	300	300	300
Temp C	25	25	25	25	25	25	25	25	25	25	25	25	25
Surface Area (ft2)	28	28	28	28	28	28	28	28	28	28	28	28	28
Flux (gpm/ft2)	0.01678571	0.0167857	0.0167857	0.0167857	0.01678571	0.0167857	0.0167857	0.0167857	0.0167857	0.0167857	0.0167857	0.0167857	0.0167857
Surface Area (m2)	2.6	2.6	2.6	2.6	2.6	2.6	2.6	2.6	2.6	2.6	2.6	2.6	2.6
Flux (m3/m2.s)	1.140E-05	1.140E-05	1.140E-05	1.140E-05	1.140E-05	1.140E-05	1.201E-05	1.201E-05	1.201E-05	1.201E-05	1.201E-05	1.201E-05	1.201E-05
Delta P (psi)	75.5	75.5	75.5	75.5	75.5	75.5	78.5	78.5	78.5	78.5	78.5	78.5	78.5
Delta P (atm)	5.1361	5.1361	5.1361	5.1361	5.1361	5.1361	5.3401	5.3401	5.3401	5.3401	5.3401	5.3401	5.3401
Pi Product (atm)	0.3180	0.3180	0.3180	0.3180	0.3180	0.3180	0.2971	0.2971	0.2971	0.2971	0.2971	0.2971	0.2971
Delta Pi (atm)	0.7022	0.7022	0.7022	0.7022	0.7022	0.7022	0.6704	0.6704	0.6704	0.6704	0.6704	0.6704	0.6704
Pi Feed ( atm)	1.0202	1.0202	1.0202	1.0202	1.0202	1.0202	0.9675	0.9675	0.9675	0.9675	0.9675	0.9675	0.9675
c mem (mg/l)	1218.4	1218.4	1218.4	1218.4	1218.4	1218.4	1155.5	1155.5	1155.5	1155.5	1155.5	1211.3	1211.3
Cmem (mol/l)	0.041698	0.041698	0.041698	0.041698	0.041698	0.041698	0.039545	0.039545	0.039545	0.039545	0.039545	0.0414535	0.0414535
A ( m3/m2-s-atm)	2.57E-06	2.57E-06	2.57E-06	2.57E-06	2.57E-06	2.57E-06	2.57E-06	2.57E-06	2.57E-06	2.57E-06	2.57E-06	2.57E-06	2.57E-06
C mem - Cp	0.0287	0.0287	0.0287	0.0287	0.0287	0.0287	0.0274	0.0274	0.0274	0.0274	0.0274	0.0273946	0.0273946
Cf - Cp	0.0120	0.0120	0.0113	0.0123	0.0120	0.0119	0.0128	0.0132	0.0128	0.0132	0.0125	0.0264613	0.0264613
ln (Cmem-Cp/Cf-Cp)	0.87359	0.87359	0.93243	0.84542	0.87359	0.87932	0.75831	0.73199	0.75831	0.73199	0.78534	0.03466	0.03466
Mass Transf Coef. (m/s)	1.306E-05	1.306E-05	1.223E-05	1.349E-05	1.306E-05	1.297E-05	1.584E-05	1.641E-05	1.584E-05	1.641E-05	1.529E-05	1.596E-05	1.596E-05
Diffus. Coef. ( m2/s)	1.61E-09	1.61E-09	1.61E-09	1.61E-09	1.61E-09	1.61E-09	1.61E-09	1.61E-09	1.61E-09	1.61E-09	1.61E-09	1.61E-09	1.61E-09
d F (m)	1.235E-04	1.235E-04	1.318E-04	1.195E-04	1.235E-04	1.243E-04	1.018E-04	9.824E-05	1.018E-04	9.824E-05	1.054E-04	1.011E-04	1.011E-04
h d (m)	8.78E-04	8.78E-04	8.78E-04	8.78E-04	8.78E-04	8.78E-04	8.78E-04	8.78E-04	8.78E-04	8.78E-04	8.78E-04	8.78E-04	8.78E-04
Vw = Flux/4 ( m/s)	2.85E-06	2.85E-06	2.85E-06	2.85E-06	2.85E-06	2.85E-06	3.00E-06	3.00E-06	3.00E-06	3.00E-06	3.00E-06	3.00E-06	3.00E-06
Pe	1.5524	1.5524	1.5524	1.5524	1.5524	1.5524	1.6350	1.6350	1.6350	1.6350	1.6350	1.6350	1.6350

pH = 5.9

Biocide = 0.2 mg/l

NF- NaCl

TDS = 730 mg/l

Table A-3. Readings for NaCl solution at 730 mg/l and 110 psi feed pressure

Description	HPP Only					HPP + Permeate Pump					Average	
	1	2	3	4	5	Average	1	2	3	4		5
Pre-filter inlet press (psi)	35	35	34	34	34	34.4	33	33	33	33	33	33
Pre-filter outlet press (psi)	34	34	33	33	33	33.4	32	32	32	32	32	32
HPP Press (psi)	109	109	109	109	109	109	105	105	105	105	105	105
Conc. Press (psi)	99	99	99	99	99	99	94	94	94	94	94	94
(Suc) Perm. Press. (psi)	15	15	15	15	15	15	0.5	0.5	0.5	0.5	0.5	0.5
(DiscH) Perm. Press (psi)	0	0	0	0	0	0	0	0	0	0	0	0
Feed TDS ( mg/l)	750	750	740	740	740	744	740	740	740	740	740	740
Feed TDS ( Mol/l)	0.02567	0.02567	0.02533	0.02533	0.02533	0.02546	0.02533	0.02533	0.02533	0.02533	0.02533	0.02533
Conc. TDS (mg/l)	1180	1180	1160	1160	1160	1168	1220	1200	1200	1190	1190	1200
Conc. TDS (Mol/l)	0.04038	0.04038	0.03970	0.03970	0.03970	0.03997	0.04175	0.04107	0.04107	0.04073	0.04073	0.04107
Perm TDS (mg/l)	369	372	374	370	374	371.8	357	359	360	356	354	357.2
Perm TDS (Mol/l)	0.012628	0.012731	0.012799	0.012663	0.012799	0.012724162	0.012218	0.012286	0.012320	0.012183	0.012115	0.0122245
Perm Flow ( gpm)	0.575	0.575	0.575	0.575	0.575	0.575	0.67	0.67	0.665	0.66	0.66	0.665
Perm Flow ( m3/s)	0.000036	0.000036	0.000036	0.000036	0.000036	3.62771E-05	0.000042	0.000042	0.000042	0.000042	0.000042	4.196E-05
Feed Flow (gpm)	1.5	1.51	1.51	1.51	1.51	1.508	1.5	1.5	1.5	1.5	1.5	1.5
Feed Flow (m3/s)	2.075	2.085	2.085	2.085	2.085	2.083	2.17	2.17	2.165	2.16	2.16	2.165
HPP (RPM)	900	900	900	900	900	900	900	900	900	900	900	900
Perm Pump (RPM)	0	0	0	0	0	0	455	450	448	448	448	451.2
Temp C	25	25	25	25	25	25	25	25	25	25	25	25
Surface Area (ft2)	28	28	28	28	28	28	28	28	28	28	28	28
Flux (gpm/ft2)	0.02053571	0.020535714	0.020535714	0.020535714	0.020535714	0.020535714	0.023928571	0.02392857	0.02375	0.023571429	0.023571429	0.02375
Surface Area (m2)	2.6	2.6	2.6	2.6	2.6	2.6	2.6	2.6	2.6	2.6	2.6	2.6
Flux (m3/m2.s)	1.3953E-05	1.39527E-05	1.39527E-05	1.39527E-05	1.39527E-05	1.39527E-05	1.6258E-05	1.6258E-05	1.6137E-05	1.60153E-05	1.60153E-05	1.614E-05
Delta P (psi)	94	94	94	94	94	94	104.5	104.5	104	103	103	103.8
Delta P (atm)	6.39456	6.39456	6.39456	6.39456	6.39456	6.39456	7.10884	7.10884	7.07483	7.00680	7.00680	7.06122
Pi Product (atm)	0.3090	0.3115	0.3131	0.3098	0.3131	0.3113	0.2989	0.3006	0.3014	0.2981	0.2964	0.2991
Delta Pi (atm)	0.9701	0.9701	0.9701	0.9701	0.9701	0.9701	0.7882	0.7882	0.8013	0.7805	0.7805	0.7877
Pi Feed (atm)	1.27908	1.28159	1.28327	1.27992	1.28327	1.281	1.08710	1.08878	1.10277	1.07856	1.07689	1.087
c mem (mg/l)	1527.6	1530.6	1532.6	1528.6	1532.6	1530.429758	1298.4	1300.4	1317.1	1288.2	1286.2	1298.0
Cmem (mol/l)	0.05228	0.05238	0.05245	0.05231	0.05245	0.05238	0.04443	0.04450	0.04507	0.04408	0.04402	0.04442
A (m3/m2.s-arm)	2.57E-06	2.57E-06	2.57E-06	2.57E-06	2.57E-06	2.5722E-06	2.57E-06	2.57E-06	2.57E-06	2.57E-06	2.57E-06	2.572E-06
C mem - Cp	0.0397	0.0397	0.0397	0.0397	0.0397	0.0397	0.0322	0.0322	0.0328	0.0319	0.0319	0.0322
Cf - Cp	0.0130	0.0129	0.0125	0.0127	0.0125	0.0127	0.0131	0.0130	0.0131	0.0131	0.0131	0.0131
In (Cmem-Cp/Cf-Cp)	1.1122	1.1201	1.1524	1.1415	1.1524	1.1356	0.8993	0.9045	0.9237	0.8869	0.8817	0.8992
Mass Transf Coef. (m/s)	1.255E-05	1.246E-05	1.211E-05	1.222E-05	1.211E-05	1.229E-05	1.808E-05	1.797E-05	1.747E-05	1.806E-05	1.817E-05	1.794E-05
Diffus. Coef. ( m2/s)	1.61E-09	1.61E-09	1.61E-09	1.61E-09	1.61E-09	1.61E-09	1.61E-09	1.61E-09	1.61E-09	1.61E-09	1.61E-09	1.61E-09
d F (m)	1.285E-04	1.294E-04	1.331E-04	1.319E-04	1.331E-04	1.312E-04	8.916E-05	8.968E-05	9.227E-05	8.926E-05	8.874E-05	8.983E-05
h d (m)	8.78E-04	8.78E-04	8.78E-04	8.78E-04	8.78E-04	8.78E-04	8.78E-04	8.78E-04	8.78E-04	8.78E-04	8.78E-04	8.78E-04
Vw = Flux/4 (m/s)	3.49E-06	3.49E-06	3.49E-06	3.49E-06	3.49E-06	3.49E-06	4.06E-06	4.06E-06	4.03E-06	4.00E-06	4.00E-06	4.03E-06
Pe	1.8992	1.8992	1.8992	1.8992	1.8992	1.8992	2.2130	2.2130	2.1965	2.1800	2.1800	2.1965

pH =5.9

Biocide = 0.2 mg/l

TDS = 750 mg/l

Table 4-A. Readings for NaCl solution at 830 mg/l and 160 psi feed pressure

Description	HPP Only					HPP + Permeate Pump					Average
	1	2	3	4	5	1	2	3	4	5	
Pre-filter inlet press (psi)	10.2	10.2	10.2	10.2	10.2	10	9.5	9.5	9.9	9.9	9.76
Pre-filter outlet press (psi)	9	9	9	9	9	8.5	8	8	8.5	8.5	8.3
HPP Press (psi)	160	160	160	160	160	150	150	150	150	150	150
Conc. Press (psi)	153	153	153	153	153	145	145	145	145	145	145
(Suc) Perm. Press. (psi)	17	17	17	17	17	3.2	3.2	3.2	3.2	3.2	3.2
(Disch) Perm Press (psi)	2	2	2	2	2	1	1	1	1	1	1
Feed TDS ( mg/l)	830	830	830	830	830	810	810	810	810	810	810
Feed TDS ( Mol/l)	0.02841	0.02841	0.02841	0.02841	0.02841	0.02772	0.02772	0.02772	0.02772	0.02772	0.0277207
Conc. TDS (mg/l)	1330	1330	1330	1330	1330	1350	1350	1350	1350	1350	1350
Conc. TDS (Mol/l)	0.04552	0.04552	0.04552	0.04552	0.04552	0.04620	0.04620	0.04620	0.04620	0.04620	0.0462012
Perm TDS (mg/l)	356	356	356	356	356	346	346	346	346	346	346
Perm TDS (Mol/l)	0.01218	0.01218	0.01218	0.01218	0.01218	0.01184	0.01184	0.01184	0.01184	0.01184	0.0118412
Perm Flow ( gpm)	0.89	0.89	0.89	0.89	0.89	0.945	0.945	0.945	0.945	0.945	0.945
Perm Flow ( m3/s)	0.000056	0.000056	0.000056	0.000056	0.000056	0.000060	0.000060	0.000060	0.000060	0.000060	0.000060
Conc Flow (gpm)	1.4	1.4	1.4	1.4	1.4	1.4	1.4	1.4	1.4	1.4	1.4
Feed Flow (gpm)	2.29	2.29	2.29	2.29	2.29	2.345	2.345	2.345	2.345	2.345	2.345
HPP (RPM)	1000	1000	1000	1000	1000	1000	1000	1000	1000	1000	1000
Perm Pump (RPM)	0	0	0	0	0	665	665	665	665	665	665
Temp C	25	25	25	25	25	25	25	25	25	25	25
Surface Area (ft2)	28	28	28	28	28	28	28	28	28	28	28
Flux (gpm/ft2)	3.18E-02	3.18E-02	3.18E-02	3.18E-02	3.18E-02	3.38E-02	3.38E-02	3.38E-02	3.38E-02	3.38E-02	0.03375
Surface Area (m2)	2.6	2.6	2.6	2.6	2.6	2.6	2.6	2.6	2.6	2.6	2.6
Flux (m3/m2.s)	2.160E-05	2.160E-05	2.160E-05	2.160E-05	2.160E-05	2.293E-05	2.293E-05	2.293E-05	2.293E-05	2.293E-05	2.293E-05
Delta P (psi)	143	143	143	143	143	146.8	146.8	146.8	146.8	146.8	146.8
Delta P (atm)	9.7279	9.7279	9.7279	9.7279	9.7279	9.9864	9.9864	9.9864	9.9864	9.9864	9.9863946
Pi Product (atm)	0.2981	0.2981	0.2981	0.2981	0.2981	0.2897	0.2897	0.2897	0.2897	0.2897	0.2897045
Delta Pi (atm)	1.33180	1.33180	1.33180	1.33180	1.33180	1.07144	1.07144	1.07144	1.07144	1.07144	1.0714432
Pi Feed ( atm)	1.62988	1.62988	1.62988	1.62988	1.62988	1.36115	1.36115	1.36115	1.36115	1.36115	1.3611477
c mem (mg/l)	1946.6	1946.6	1946.6	1946.6	1946.6	1625.6	1625.6	1625.6	1625.6	1625.6	1625.6462
Cmem (mol/l)	0.06662	0.06662	0.06662	0.06662	0.06662	0.05563	0.05563	0.05563	0.05563	0.05563	0.0556347
A (m3/m2-s-atm)	2.57E-06	2.57E-06	2.57E-06	2.57E-06	2.57E-06	2.5722E-06	2.5722E-06	2.5722E-06	2.5722E-06	2.5722E-06	2.572E-06
C mem - Cp	0.0544	0.0544	0.0544	0.0544	0.0544	0.0438	0.0438	0.0438	0.0438	0.0438	0.0437935
Cf - Cp	0.0162	0.0162	0.0162	0.0162	0.0162	0.0159	0.0159	0.0159	0.0159	0.0159	0.0158795
ln (Cmem-Cp)/Cf-Cp)	1.21066	1.21066	1.21066	1.21066	1.21066	1.01445	1.01445	1.01445	1.01445	1.01445	1.0144544
Mass Transf Coef. (m/s)	1.784E-05	1.784E-05	1.784E-05	1.784E-05	1.784E-05	2.260E-05	2.260E-05	2.260E-05	2.260E-05	2.260E-05	2.260E-05
Diffus. Coeff. ( m2/s)	1.612E-09	1.612E-09	1.612E-09	1.612E-09	1.612E-09	1.612E-09	1.612E-09	1.612E-09	1.612E-09	1.612E-09	1.612E-09
h d (m)	9.04E-05	9.04E-05	9.04E-05	9.04E-05	9.04E-05	7.13E-05	7.13E-05	7.13E-05	7.13E-05	7.13E-05	7.13E-05
d F (m)	8.78E-04	8.78E-04	8.78E-04	8.78E-04	8.78E-04	8.78E-04	8.78E-04	8.78E-04	8.78E-04	8.78E-04	8.78E-04
Vw = Flux/4 (m/s)	5.40E-06	5.40E-06	5.40E-06	5.40E-06	5.40E-06	5.73E-06	5.73E-06	5.73E-06	5.73E-06	5.73E-06	5.73E-06
Pe	2.9397	2.9397	2.9397	2.9397	2.9397	3.1214	3.1214	3.1214	3.1214	3.1214	3.1213666

NF- NaCl

pH = 5.9

TDS = 830 mg/l

Biocide = 0.2 mg/l



Table A-5. Readings for NaCl solution at 1,200 mg/l and 80 psi feed pressure

Description	HPP Only					HPP + Permeate Pump						Average
	2	3	4	5	Average	1	2	3	4	5	6	
Pre-filter inlet press (psi)	55	55	55	55	55	54	54	54	54	54	54	54
Pre-filter outlet press (psi)	54	54	54	54	54	53	53	53	53	53	53	53
HPP Press (psi)	80	80	80	80	80	75	75	75	75	75	75	75
Conc. Press (psi)	66	66	66	66	66	70	70	70	70	70	70	70
(Suc) Perm. Press (psi)	9	9	9	9	9	0.5	0.5	0.5	0.5	0.5	0.5	0.5
(Disch) Perm Press (psi)	0	0	0	0	0	1	1	0	0	0	0	0
Feed TDS (mg/l)	1200	1200	1210	1200	1202.5	1200	1200	1200	1200	1190	1210	1200.0
Feed TDS (Mol/l)	0.041067762	0.041067762	0.04140999	0.04106776	0.04115332	0.041067762	0.041067762	0.041067762	0.041067762	0.0407255	0.04141	0.041068
Conc. TDS (mg/l)	1730	1750	1760	1740	1745	1800	1800	1800	1800	1790	1820	1802
Conc. TDS (Mol/l)	0.059206023	0.059890486	0.06023272	0.05954825	0.05971937	0.061601643	0.061601643	0.061601643	0.061601643	0.0612594	0.0622861	0.061659
Perm TDS (mg/l)	800	800	800	800	800	770	776	756	762	770	776	768.33
Perm TDS (Mol/l)	0.027378508	0.027378508	0.02737851	0.02737851	0.02737851	0.026351814	0.02655715	0.02587269	0.026078029	0.0263518	0.0265572	0.026295
Perm Flow (gpm)	0.42	0.42	0.42	0.42	0.42	0.445	0.445	0.445	0.445	0.445	0.445	0.445
Perm Flow (m3/s)	2.64981E-05	2.64981E-05	2.64981E-05	2.64981E-05	2.64981E-05	2.80754E-05	2.80754E-05	2.80754E-05	2.80754E-05	2.808E-05	2.808E-05	2.81E-05
Conc Flow (gpm)	1.2	1.2	1.2	1.2	1.2	1.2	1.2	1.2	1.2	1.2	1.2	1.2
Feed Flow (gpm)	1.62	1.62	1.62	1.62	1.62	1.645	1.645	1.645	1.645	1.645	1.645	1.645
HPP (RPM)	600	600	600	600	600	600	600	600	600	600	600	600
Perm Pump (RPM)	0	0	0	0	0	200	200	200	200	200	200	200
Temp C	25	25	25	25	25	25	25	25	25	25	25	25
Surface Area (ft2)	28	28	28	28	28	28	28	28	28	28	28	28
Flux (gpm/ft2)	0.015	0.015	0.015	0.015	0.015	0.01589	0.01589	0.01589	0.01589	0.01589	0.01589	0.01589
Surface Area (m2)	2.6	2.6	2.6	2.6	2.6	2.6	2.6	2.6	2.6	2.6	2.6	2.6
Flux (m3/m2.s)	1.019E-05	1.019E-05	1.019E-05	1.019E-05	1.019E-05	1.080E-05	1.080E-05	1.080E-05	1.080E-05	1.080E-05	1.080E-05	1.080E-05
Delta P (psi)	71	71	71	71	71	74.5	74.5	74.5	74.5	74.5	74.5	74.5
Delta P (atm)	4.8299	4.8299	4.8299	4.8299	4.8299	5.0680	5.0680	5.0680	5.0680	5.0680	5.0680	5.0680
Pi Product (atm)	0.66984	0.66984	0.66984	0.66984	0.66984	0.64472	0.64472	0.63300	0.63802	0.64472	0.64974	0.64332
Delta Pi (atm)	8.68E-01	8.68E-01	8.68E-01	8.68E-01	8.6773135	8.45E-01	8.45E-01	8.45E-01	8.45E-01	8.45E-01	8.45E-01	8.44696
Pi Feed (atm)	1.54E+00	1.54E+00	1.54E+00	1.54E+00	1.53756845	1.49E+00	1.49E+00	1.48E+00	1.48E+00	1.49E+00	1.49E+00	1.488019
c mem (mg/l)	1836.3	1836.3	1836.3	1836.3	1836.3	1778.8	1784.8	1764.8	1770.8	1778.8	1784.8	1777.2
C mem (mg/l)	0.062846	0.062846	0.062846	0.062846	0.062846	0.060877	0.061083	0.060398	0.060604	0.060877	0.061083	0.060820
A (m3/m2-s-atm)	2.57E-06	2.57E-06	2.57E-06	2.57E-06	2.5722E-06	2.56E-06	2.56E-06	2.56E-06	2.56E-06	2.56E-06	2.56E-06	2.56E-06
C mem - Cp	0.0355	0.0355	0.0355	0.0355	0.03546712	0.0345	0.0345	0.0345	0.0345	0.0345	0.0345	0.034526
Cf - Cp	0.013689254	0.013689254	0.01403149	0.01368925	0.01377481	0.014715948	0.01451061	0.015195072	0.014989733	0.0143737	0.0148528	0.014773
ln (Cmem-Cp)/Cf-Cp)	0.951994797	0.951994797	0.92730218	0.9519948	0.94582164	0.852768578	0.86682033	0.820729225	0.834334877	0.8762991	0.8435093	0.849077
Mass Transf Coef. (m/s)	1.07055E-05	1.07055E-05	1.0991E-05	1.0705E-05	1.0777E-05	1.26625E-05	1.2457E-05	1.31569E-05	1.29423E-05	1.232E-05	1.28E-05	1.27E-05
Diffus. Coeff. ( m2/s)	1.612E-09	1.612E-09	1.612E-09	1.612E-09	1.612E-09	1.612E-09	1.612E-09	1.612E-09	1.612E-09	1.612E-09	1.612E-09	1.61E-09
d F (m)	1.5058E-04	1.5058E-04	1.4667E-04	1.5058E-04	1.4960E-04	1.2730E-04	1.2940E-04	1.2252E-04	1.2455E-04	1.3082E-04	1.259E-04	1.268E-04
h d (m)	8.78E-04	8.78E-04	8.78E-04	8.78E-04	8.78E-04	8.78E-04	8.78E-04	8.78E-04	8.78E-04	8.78E-04	8.78E-04	8.78E-04
Vw = Flux/4 (m/s)	2.55E-06	2.55E-06	2.55E-06	2.55E-06	2.55E-06	2.70E-06	2.70E-06	2.70E-06	2.70E-06	2.70E-06	2.70E-06	2.70E-06
Pc	1.3873	1.3873	1.3873	1.3873	1.3873	1.4698	1.4698	1.4698	1.4698	1.4698	1.4698	1.4698

pH = 5.9

Biocide = 0.3 mg/l

NF- NaCl

TDS = 1,200 mg/l

Table A-6. Readings for NaCl solution at 1,200 mg/l and 110 psi feed pressure

Description	HPP Only						HPP + Permeate Pump						Average
	1	2	3	4	5	Average	1	2	3	4	5	Average	
Pre-filter inlet press (psi)	30	30	30	30	30	30	49	49	49	49	49	49	49
Pre-filter outlet press (psi)	29	29	29	29	29	29	48	48	48	48	48	48	48
HPP Press (psi)	109	109	109	109	109	109	107	107	107	107	107	107	107
Conc. Press (psi)	95	95	95	95	95	95	103	103	103	103	103	103	103
(Suc) Perm. Press. (psi)	11.5	11.5	12	11.5	12	6	2.5	2.5	2.5	2.5	2.5	2.5	2.5
(Disch) Perm Press (psi)	0	0	0	0	0	0	0	0	0	0	0	0	0
Feed TDS ( mg/l)	1290	1290	1290	1290	1280	1288	1300	1290	1280	1280	1280	1286	1286
Feed TDS ( Mol/l)	0.04415	0.04415	0.04415	0.04415	0.04381	0.04408	0.04449	0.04415	0.04381	0.04381	0.04381	0.04401	0.04401
Conc. TDS (mg/l)	2280	2280	2270	2280	2270	2276	2320	2320	2320	2330	2330	2324	2324
Conc. TDS (Mol/l)	0.0780	0.0780	0.0777	0.0780	0.0777	0.0779	0.0794	0.0794	0.0794	0.0797	0.0797	0.0795	0.0795
Perm TDS (mg/l)	695	695	695	695	695	695	660	660	660	660	660	698	698
Perm TDS (Mol/l)	0.02379	0.02379	0.02379	0.02379	0.02379	0.02379	0.02259	0.02259	0.02259	0.02259	0.02259	0.02389	0.02389
Perm Flow ( gpm)	0.54	0.54	0.54	0.54	0.54	0.54	0.6	0.6	0.6	0.6	0.6	0.6	0.6
Perm Flow ( m3/s)	0.000034	0.000034	0.000034	0.000034	0.000034	0.000034	0.000038	0.000038	0.000038	0.000038	0.000038	0.000038	0.000038
Conc Flow (gpm)	1.1	1.1	1.1	1.1	1.1	1.1	1.1	1.1	1.1	1.1	1.1	1.1	1.1
Conc Flow (m3/s)	1.64	1.64	1.64	1.64	1.64	1.64	1.7	1.7	1.7	1.7	1.7	1.7	1.7
HPP (RPM)	800	800	800	800	800	800	800	800	800	800	800	800	800
Perm Pump (RPM)	0	0	0	0	0	0	390	390	390	390	390	390	390
Temp C	25	25	25	25	25	25	25	25	25	25	25	25	25
Surface Area (ft2)	1.93E-02	1.93E-02	1.93E-02	1.93E-02	1.93E-02	1.93E-02	2.14E-02	2.14E-02	2.14E-02	2.14E-02	2.14E-02	2.14E-02	2.14E-02
Flux (gpm/ft2)	2.6	2.6	2.6	2.6	2.6	2.6	2.6	2.6	2.6	2.6	2.6	2.6	2.6
Surface Area (m2)	1.310E-05	1.310E-05	1.310E-05	1.310E-05	1.310E-05	1.310E-05	1.456E-05	1.456E-05	1.456E-05	1.456E-05	1.456E-05	1.456E-05	1.456E-05
Flux (m3/m2.s)	97.5	97.5	97	97.5	97	97.3	104.5	104.5	104.5	104.5	104.5	104.5	104.5
Delta P (psi)	6.6327	6.6327	6.5986	6.6327	6.5986	6.6190	7.1088	7.1088	7.1088	7.1088	7.1088	7.1088	7.1088
Delta P (atm)	0.5819	0.5819	0.5819	0.5819	0.5819	0.5819	0.5526	0.5526	0.5526	0.5526	0.5526	0.5844	0.5844
Pi Product (atm)	1.53840	1.53840	1.50438	1.53840	1.50438	1.52479	1.44856	1.44856	1.44856	1.44856	1.44856	1.44856	1.44856
Delta Pi (atm)	2.12032	2.12032	2.08630	2.12032	2.08630	2.10671	2.00117	2.00117	2.00117	2.00117	2.00117	2.00117	2.00117
c mem (mg/l)	2532.3	2532.3	2491.7	2532.3	2491.7	2516.1	2390.0	2390.0	2390.0	2390.0	2390.0	2390	2390
Cmem (mol/l)	0.08666	0.08666	0.08527	0.08666	0.08527	0.08611	0.08179	0.08179	0.08179	0.08179	0.08179	0.08179	0.08179
A (m3/m2.s-atm)	2.57E-06	2.57E-06	2.57E-06	2.57E-06	2.57E-06	2.5722E-06	2.572E-06	2.57E-06	2.57E-06	2.57E-06	2.57E-06	2.5722E-06	2.5722E-06
C mem - Cp	0.0629	0.0629	0.0615	0.0629	0.0615	0.0623	0.0592	0.0592	0.0592	0.0592	0.0592	0.0592	0.0592
Cf - Cp	0.0204	0.0204	0.0204	0.0204	0.0200	0.0203	0.0219	0.0216	0.0212	0.0212	0.0212	0.0212	0.0212
ln (Cmem-Cp/Cf-Cp)	1.12751	1.12751	1.10515	1.12751	1.12210	1.12199	0.99443	1.01018	1.02618	1.02618	1.02618	1.01655	1.01655
Mass Transf Coef. (m/s)	1.1622E-05	1.1622E-05	1.186E-05	1.1622E-05	1.1678E-05	1.1679E-05	1.46E-05	1.44E-05	1.42E-05	1.42E-05	1.42E-05	1.4323E-05	1.4323E-05
Diffus. Coeff. ( m2/s)	1.612E-09	1.612E-09	1.612E-09	1.612E-09	1.612E-09	1.612E-09	1.612E-09	1.612E-09	1.612E-09	1.612E-09	1.612E-09	1.612E-09	1.612E-09
d F (m)	1.387E-04	1.387E-04	1.360E-04	1.387E-04	1.380E-04	1.380E-04	1.101E-04	1.118E-04	1.136E-04	1.136E-04	1.136E-04	1.126E-04	1.126E-04
h d (m)	8.78E-04	8.78E-04	8.78E-04	8.78E-04	8.78E-04	8.78E-04	8.78E-04	8.78E-04	8.78E-04	8.78E-04	8.78E-04	8.78E-04	8.78E-04
Vw = Fluxv4 ( m/s)	3.28E-06	3.28E-06	3.28E-06	3.28E-06	3.28E-06	3.28E-06	3.64E-06	3.64E-06	3.64E-06	3.64E-06	3.64E-06	3.64E-06	3.64E-06
Pe	1.7836	1.7836	1.7836	1.7836	1.7836	1.7836	1.9818	1.9818	1.9818	1.9818	1.9818	1.9818	1.9818

pH = 5.9

Biocide = 0.2 mg/l

TDS = 1,200 mg/l

Table A-7. Readings for NaCl solution at 1,200 mg/l and 160 psi feed pressure

Description	HPP Only						HPP + Permeate Pump						Average
	1	2	4	5	6	Average	1	2	3	4	5	Average	
Pre-filter inlet press (psi)	14	16	13	14	14	14.2	13	13	15	13	13	13.40	
Pre-filter outlet press (psi)	13	15	12	13	13	13.2	12	12	14	12	12	12.40	
HPP Press (psi)	159	159	159	159	159	159.0	154	154	154	154	154	154	
Conc. Press (psi)	147	148	148	147	149	147.8	144	144	144	144	144	144	
(Suc) Perm. Press. (psi)	13	13	13	13	13	13	0.5	0.5	0.5	0.3	0.3	0.42	
(Disch) Perm Press (psi)	2.5	2.5	2.5	2.5	2.5	2.5	3	3	3	3	3	3	
Feed TDS ( mg/l)	1210	1210	1200	1210	1190	1204.0	1180	1190	1190	1200	1200	1192.0	
Feed TDS ( Mol/l)	0.04141	0.04141	0.04107	0.04141	0.04073	0.04120	0.04038	0.04073	0.04073	0.04107	0.04107	0.04079	
Conc. TDS (mg/l)	2060	2070	2030	2080	2040	2056	2040	2030	2030	2060	2070	2046	
Conc. TDS (Mol/l)	0.07050	0.07084	0.06947	0.07118	0.06982	0.07036	0.06982	0.06947	0.06947	0.07050	0.07084	0.0700205	
Perm TDS (mg/l)	600	600	600	600	600	600	565	581	571	571	568	571.2	
Perm TDS (Mol/l)	0.02053	0.02053	0.02053	0.02053	0.02053	0.02053	0.01934	0.01988	0.01954	0.01954	0.01944	0.01955	
Perm Flow ( gpm)	0.87	0.87	0.87	0.87	0.87	0.87	0.94	0.94	0.94	0.94	0.94	0.94	
Perm Flow ( m3/s)	5.5E-05	5.5E-05	5.5E-05	5.5E-05	5.5E-05	5.5E-05	5.9E-05	5.9E-05	5.9E-05	5.9E-05	5.9E-05	5.9E-05	
Conc Flow (gpm)	1.7	1.7	1.7	1.7	1.7	1.7	1.7	1.7	1.7	1.7	1.7	1.7	
Feed Flow (gpm)	2.61	2.61	2.6	2.6	2.6	2.60	2.64	2.64	2.64	2.64	2.64	2.64	
HPP (RPM)	1200	1200	1200	1200	1200	1200	690	690	690	690	690	690	
Temp C	0	0	0	0	0	0	25	25	25	25	25	25	
Surface Area (ft2)	28	28	28	28	28	28	28	28	28	28	28	28	
Flux (gpm/ft2)	0.03107	0.03107	0.03107	0.03107	0.03107	0.03107	0.03357	0.03357	0.03357	0.03357	0.03357	0.03357	
Surface Area (m2)	2.6	2.6	2.6	2.6	2.6	2.6	2.6	2.6	2.6	2.6	2.6	2.6	
Flux (m3/m2.s)	2.11E-05	2.11E-05	2.11E-05	2.11E-05	2.11E-05	2.11E-05	2.28E-05	2.28E-05	2.28E-05	2.28E-05	2.28E-05	2.28E-05	
Delta P (psi)	146	146	146	146	146	146	153.5	153.5	153.5	153.7	153.7	153.58	
Delta P (atm)	9.932	9.932	9.932	9.932	9.932	9.932	10.442	10.442	10.442	10.456	10.456	10.448	
PI Product (atm)	0.502	0.502	0.502	0.502	0.502	0.502	0.473	0.486	0.478	0.478	0.476	0.478	
Delta Pi (atm)	1.725	1.725	1.725	1.725	1.725	1.725	1.57439	1.57439	1.57439	1.58800	1.58800	1.5798367	
PI Feed ( atm)	2.227	2.227	2.227	2.227	2.227	2.227	2.04747	2.06086	2.05249	2.06610	2.06358	2.0581004	
c mem (mg/l)	2659.7	2659.7	2659.7	2659.7	2659.7	2659.7	2445.3	2461.3	2451.3	2467.6	2464.6	2458.0	
Cmem (mol/l)	0.09102	0.09102	0.09102	0.09102	0.09102	0.09102	0.08369	0.08423	0.08389	0.08445	0.08435	0.0841215	
A (m3/m2.s-atm)	2.57E-06	2.57E-06	2.57E-06	2.57E-06	2.57E-06	2.57E-06	2.57E-06	2.57E-06	2.57E-06	2.57E-06	2.57E-06	2.572E-06	
C mem - Cp	0.0705	0.0705	0.0705	0.0705	0.0705	0.0705	0.0644	0.0644	0.0644	0.0649	0.0649	0.0645733	
Cf - Cp	0.0209	0.0209	0.0205	0.0209	0.0202	0.0207	0.0210	0.0208	0.0212	0.0215	0.0216	0.0212457	
In (Cmem-Cp/Cf-Cp)	1.2168	1.2168	1.2334	1.2168	1.2502	1.2268	1.118	1.127	1.111	1.104	1.099	1.112	
Mass Transf Coef. (m/s)	1.73E-05	1.73E-05	1.71E-05	1.73E-05	1.69E-05	1.72E-05	2.04E-05	2.02E-05	2.03E-05	2.07E-05	2.08E-05	2.05E-05	
Diffus. Coeff. ( m2/s)	1.61E-09	1.61E-09	1.61E-09	1.61E-09	1.61E-09	1.61E-09	1.61E-09	1.61E-09	1.61E-09	1.61E-09	1.61E-09	1.61E-09	
d F (m)	9.29E-05	9.29E-05	9.42E-05	9.3E-05	9.546E-05	9.3677E-05	7.898E-05	7.967E-05	7.852E-05	7.800E-05	7.766E-05	7.856E-05	
h d (m)	8.78E-04	8.78E-04	8.78E-04	8.78E-04	8.78E-04	8.78E-04	8.78E-04	8.78E-04	8.78E-04	8.78E-04	8.78E-04	8.78E-04	
Vw = Flux/4 (m/s)	5.28E-06	5.28E-06	5.28E-06	5.28E-06	5.28E-06	5.28E-06	5.70E-06	5.70E-06	5.70E-06	5.70E-06	5.70E-06	5.70E-06	
Pe	2.8736	2.8736	2.8736	2.8736	2.8736	2.8736	3.1049	3.1049	3.1049	3.1049	3.1049	3.1049	

pH = 5.6

Biocide = 0.3 mg/l

NF- NaCl

TDS = 1,200 mg/l

Table A-8. Readings for NaCl solution at 1,750 mg/l and 80 psi feed pressure

Description	HPP Only					HPP + Permeate Pump							Average
	1	2	3	4	Average	1	2	3	4	5	6	7	
Pre-filter inlet press (psi)	55	55	54	54	54.5	54	54	54	54	54	54	54	54
Pre-filter outlet press (psi)	54	54	53	53	53.5	53	53	53	53	53	53	53	53
HPP Press (psi)	80	80	80	80	80	78	78	78	78	78	78	78	78
Conc. Press (psi)	76	76	76	76	76	71	71	71	71	71	71	71	71
(Suc) Perm. Press. (psi)	5.5	5.5	5.5	5.5	5.5	0.8	0.8	0.8	0.8	0.8	0.8	0.8	0.8
(Disch) Perm Press (psi)	0	0	0	0	0	0	0	0	0	0	0	0	0
Feed TDS ( mg/l)	1750	1760	1790	1800	1775	1800	1790	1760	1780	1750	1770	1770	1774.2857
Feed TDS ( Mol/l)	0.059890	0.060233	0.061259	0.061602	0.060746	0.061602	0.061259	0.060233	0.060917	0.059890	0.060575	0.060575	0.060722
Conc. TDS (mg/l)	2550	2550	2550	2550	2550	2580	2590	2580	2580	2580	2600	2600	2587.1429
Conc. TDS (Mol/l)	0.087269	0.087269	0.087269	0.087269	0.087269	0.088296	0.088638	0.088296	0.088296	0.088296	0.088980	0.088980	0.088540
Perm TDS (mg/l)	1270	1280	1270	1270	1272.5	1260	1250	1260	1260	1260	1260	1250	1257.1429
Perm TDS (Mol/l)	0.043463	0.043806	0.043463	0.043463	0.043549	0.043121	0.042779	0.043121	0.043121	0.043121	0.043121	0.042779	0.043023
Perm Flow ( gpm)	0.4	0.4	0.4	0.4	0.4	0.435	0.435	0.435	0.435	0.435	0.435	0.435	0.435
Perm Flow ( m3/s)	0.000025	0.000025	0.000025	0.000025	0.000025	0.000027	0.000027	0.000027	0.000027	0.000027	0.000027	0.000027	0.000027
Conc Flow (gpm)	1.2	1.2	1.2	1.2	1.2	1.2	1.2	1.2	1.2	1.2	1.2	1.2	1.2
Feed Flow (gpm)	1.61	1.61	1.61	1.61	1.61	1.635	1.635	1.635	1.635	1.635	1.635	1.635	1.635
HPP (RPM)	600	600	600	600	600	600	600	600	600	600	600	600	600
Perm Pump (RPM)	0	0	0	0	0	200	200	200	200	200	200	200	200
Temp C	25	25	25	25	25	25	25	25	25	25	25	25	25
Surface Area (ft2)	28	28	28	28	28	28	28	28	28	28	28	28	28
Flux (gpm/ft2)	0.0143	0.0143	0.0143	0.0143	0.0143	1.55E-02	1.55E-02	1.55E-02	1.55E-02	1.55E-02	1.55E-02	1.55E-02	1.55E-02
Surface Area (m2)	2.6	2.6	2.6	2.6	2.6	2.6	2.6	2.6	2.6	2.6	2.6	2.6	2.6
Flux (m3/m2.s)	9.71E-06	9.71E-06	9.71E-06	9.71E-06	9.71E-06	1.06E-05	1.06E-05	1.06E-05	1.06E-05	1.06E-05	1.06E-05	1.06E-05	1.06E-05
Delta P (psi)	74.5	74.5	74.5	74.5	74.5	77.2	77.2	77.2	77.2	77.2	77.2	77.2	77.2
Delta P (atm)	5.068	5.068	5.068	5.068	5.068	5.252	5.252	5.252	5.252	5.252	5.252	5.252	5.252
Pi Product (atm)	1.063	1.072	1.063	1.063	1.065	1.055	1.047	1.055	1.055	1.055	1.055	1.047	1.053
Delta Pi (atm)	1.2913	1.2913	1.2913	1.2913	1.2945	1.1445	1.1445	1.1445	1.1445	1.1445	1.1445	1.1445	1.1480
Pi Feed ( atm)	2.35464	2.36301	2.35464	2.35464	2.35996	2.19947	2.19110	2.19947	2.19947	2.19947	2.19947	2.19110	2.20059
c mem (mg/l)	2812.2	2822.2	2812.2	2812.2	2818.6	2626.9	2616.9	2626.9	2626.9	2626.9	2626.9	2616.9	2628.2
Cmem (mol/l)	0.09624	0.09658	0.09624	0.09624	0.09646	0.08990	0.08956	0.08990	0.08990	0.08990	0.08990	0.08956	0.08995
A (m3/m2-s-atm)	2.57E-06	2.57E-06	2.57E-06	2.57E-06	2.57E-06	2.57E-06	2.57E-06	2.57E-06	2.57E-06	2.57E-06	2.57E-06	2.57E-06	2.57E-06
C mem - Cp	0.0528	0.0528	0.0528	0.0528	0.0529	0.0468	0.0468	0.0468	0.0468	0.0468	0.0468	0.0468	0.0469
Cf - Cp	0.0164	0.0164	0.0178	0.0181	0.0172	0.0185	0.0185	0.0171	0.0178	0.0168	0.0175	0.0178	0.0177
ln (Cmem-Cp/Cf-Cp)	1.1672	1.1672	1.0871	1.0681	1.1239	0.9287	0.9287	1.0057	0.9665	1.0259	0.9859	0.9665	0.9750
Mass Transf Coef. (m/s)	8.316E-06	8.316E-06	8.93E-06	9.088E-06	8.637E-06	1.14E-05	1.14E-05	1.05E-05	1.09E-05	1.03E-05	1.07E-05	1.09E-05	1.083E-05
Diffus. Coef. ( m2/s)	1.61E-09	1.61E-09	1.61E-09	1.61E-09	1.61E-09	1.61E-09	1.61E-09	1.61E-09	1.61E-09	1.61E-09	1.61E-09	1.61E-09	1.61E-09
d F (m)	1.938E-04	1.938E-04	1.81E-04	1.774E-04	1.866E-04	1.42E-04	1.42E-04	1.54E-04	1.48E-04	1.57E-04	1.51E-04	1.48E-04	1.489E-04
h d (m)	8.78E-04	8.78E-04	8.78E-04	8.78E-04	8.78E-04	8.78E-04	8.78E-04	8.78E-04	8.78E-04	8.78E-04	8.78E-04	8.78E-04	8.78E-04
Vw = Flux/4 (m/s)	2.43E-06	2.43E-06	2.43E-06	2.43E-06	2.43E-06	2.64E-06	2.64E-06	2.64E-06	2.64E-06	2.64E-06	2.64E-06	2.64E-06	2.64E-06
Pe	1.3212	1.3212	1.3212	1.3212	1.3212	1.4368	1.4368	1.4368	1.4368	1.4368	1.4368	1.4368	1.4368

NF - NaCl

TDS = 1,750 mg/l

Biocide = 0.3 Mg/l

Table A-9. Readings for NaCl solution at 1.750 mg/l and 1.10 psi feed pressure

Description	HPP Only					HPP + Permeate Pump					Average
	1	2	3	4	Average	1	2	3	4	Average	
Pre-filter inlet press (psi)	4	3.5	4	4	3.875	2	2	2	2	2	
Pre-filter outlet press (psi)	3	2.5	3	3	2.875	1	1	1	1	1	
HPP Press (psi)	109	109	109	109	109	105	105	105	105	105	
Conc. Press (psi)	97	97	97	97	97	94	95	95	95	94.75	
(Suc) Perm. Press. (psi)	11	11	11	11	11	2	2	2	2	2	
(Disch) Perm. Press (psi)	0	0	0	0	0	0	0	0	0	0	
Feed TDS ( mg/l)	1770	1770	1775	1770	1771.25	1750	1750	1760	1740	1750	
Feed TDS ( Mol/l)	0.060575	0.060575	0.060746	0.060575	0.060617728	0.059890	0.059890	0.060233	0.059548	0.059890486	
Conc. TDS (mg/l)	2610	2590	2550	2550	2575	2620	2620	2640	2630	2627.5	
Conc. TDS (Mol/l)	0.089322	0.088638	0.087269	0.087269	0.088124572	0.089665	0.089665	0.090349	0.090007	0.089921287	
Perm TDS (mg/l)	955	955	946	946	950.5	934	935	933	933	933.75	
Perm TDS (Mol/l)	0.0327	0.0327	0.0324	0.0324	0.03252909	0.0320	0.0320	0.0319	0.0319	0.031955852	
Perm Flow ( gpm)	0.000031	0.495	0.495	0.495	0.495	0.54	0.54	0.54	0.54	0.54	
Perm Flow ( m3/s)	0.000031	0.000031	0.000031	0.000031	3.12299E-05	0.000034	0.000034	0.000034	0.000034	3.4069E-05	
Conc Flow (gpm)	2.3	2.3	2.4	2.4	2.35	1.8	1.8	1.8	1.8	1.8	
Feed Flow (gpm)	2.80	2.80	2.90	2.90	2.845	2.34	2.34	2.34	2.34	2.34	
HPP (RPM)	1200	1200	1200	1200	1200	1200	1200	1200	1200	1200	
Perm Pump (RPM)	0	0	0	0	0	320	320	320	320	320	
Temp C	25	25	25	25	25	25	25	25	25	25	
Surface Area (ft2)	28	28	28	28	28	28	28	28	28	28	
Flux (gpm/ft2)	0.0177	0.0177	0.0177	0.0177	0.017678571	0.0193	0.0193	0.0193	0.0193	0.019285714	
Surface Area (m2)	2.6	2.6	2.6	2.6	2.6	2.6	2.6	2.6	2.6	2.6	
Flux (m3/m2.s)	1.20E-05	1.20E-05	1.20E-05	1.20E-05	1.20115E-05	1.31E-05	1.31E-05	1.31E-05	1.31E-05	1.31035E-05	
Delta P (psi)	98	98	98	98	98	103	103	103	103	103	
Delta P (atm)	6.667	6.667	6.667	6.667	6.666666667	7.007	7.007	7.007	7.007	7.006802721	
PI Product (atm)	0.800	0.800	0.792	0.792	0.795850202	0.782	0.783	0.781	0.781	0.781825488	
Delta PI (atm)	1.997	1.997	1.997	1.997	1.996930218	1.882	1.882	1.882	1.882	1.881861277	
PI Feed ( atm)	2.797	2.797	2.789	2.789	2.79278042	2.664	2.665	2.663	2.663	2.663686765	
c mem (mg/l)	3340.0	3340.0	3331.0	3331.0	3335.474167	3181.5	3182.5	3180.5	3180.5	3181.295002	
Cmem (mol/l)	0.114304	0.114304	0.113996	0.113996	0.114150	0.108882	0.108917	0.108848	0.108848	0.108874	
A (m3/m2.s-atm)	2.57E-06	2.57E-06	2.57E-06	2.57E-06	2.5722E-06	2.55680E-06	2.55680E-06	2.55680E-06	2.55680E-06	2.5568E-06	
C mem - Cp	0.0816	0.0816	0.0816	0.0816	0.081621292	0.0769	0.0769	0.0769	0.0769	0.076918036	
Cf - Cp	0.0279	0.0279	0.0284	0.0282	0.0280888638	0.0279	0.0279	0.0283	0.0276	0.027934634	
ln (Cmem-Cp/Cf-Cp)	1.073755458	1.07375546	1.05672342	1.062773042	1.066751844	1.013179434	1.014405676	0.99978909	1.02427012	1.012911082	
Mass Transf Coef. (m/s)	1.12E-05	1.12E-05	1.14E-05	1.13E-05	1.12604E-05	1.29E-05	1.29E-05	1.31E-05	1.28E-05	1.29374E-05	
Diffus. Coeff. ( m2/s)	1.61E-09	1.61E-09	1.61E-09	1.61E-09	1.612E-09	1.61E-09	1.61E-09	1.61E-09	1.61E-09	1.612E-09	
d F (m)	1.44E-04	1.44E-04	1.42E-04	1.43E-04	1.43E-04	1.25E-04	1.25E-04	1.23E-04	1.26E-04	1.25E-04	
h d (m)	8.78E-04	8.78E-04	8.78E-04	8.78E-04	8.78E-04	8.78E-04	8.78E-04	8.78E-04	8.78E-04	8.78E-04	
V w = Flux/4 (m/s)	3.00E-06	3.00E-06	3.00E-06	3.00E-06	3.00E-06	3.28E-06	3.28E-06	3.28E-06	3.28E-06	3.28E-06	
Pe	1.6350	1.6350	1.6350	1.6350	1.6350	1.7836	1.7836	1.7836	1.7836	1.7836	

pH 6.7

Biocide = 0.3 mg/l

NF - NaCl

TDS = 1,750 mg/l

Table A-10. Readings for NaCl solution at 1,750 mg/l and 160 psi feed pressure

Description	HPP Only					HPP + Permeate Pump				Average
	1	2	3	4	5	1	2	3	4	
Pre-filter inlet press (psi)	6.0	6.5	4.5	7.0	7.5					6.3
Pre-filter outlet press (psi)	5.0	5.5	3.5	6.0	6.5					5.3
HPP Press (psi)	160.0	160.0	160.0	160.0	160.0					160.0
Conc. Press (psi)	149.0	149.0	149.0	149.0	149.0					149.0
(Suc) Perm. Press. (psi)	11.0	11.0	11.0	11.0	11.0					11.0
(Disch) Perm Press (psi)	2.5	2.0	2.0	2.0	2.0					2.1
Feed TDS ( mg/l)	1730.0	1730.0	1730.0	1730.0	1730.0					1730.0
Feed TDS ( Mol/l)	0.0592	0.0592	0.0592	0.0592	0.0592					0.0592
Conc. TDS (mg/l)	2790	2790	2780	2780	2780					2784.0
Conc. TDS (Mol/l)	0.0955	0.0955	0.0951	0.0951	0.0951					0.0953
Perm TDS (mg/l)	870.0	870.0	870.0	870.0	870.0					870.0
Perm TDS (Mol/l)	0.0298	0.0298	0.0298	0.0298	0.0298					0.0298
Perm Flow ( gpm)	0.8200	0.8200	0.8200	0.8200	0.8200					0.82
Perm Flow ( m3/s)	0.00005173	0.00005173	0.00005173	0.00005173	0.00005173					0.00005173
Conc Flow (gpm)	2.05	2.05	2.05	2.05	2.05					2.05
Feed Flow (gpm)	2.87	2.87	2.87	2.87	2.87					2.87
HPP (RPM)	1380	1380	1380	1380	1380					1380.0
Perm Pump (RPM)	0	0	0	0	0					0.0
Temp C	25	25	25	25	25					25.0
Surface Area (ft2)	28	28	28	28	28					28.0
Flux (gpm/ft2)	0.0293	0.0293	0.0293	0.0293	0.0293					0.0292857
Surface Area (m2)	2.6	2.6	2.6	2.6	2.6					2.6
Flux (m3/m2.s)	1.99E-05	1.99E-05	1.99E-05	1.99E-05	1.99E-05					0.0000199
Delta P (psi)	149.0000	149.0000	149.0000	149.0000	149					149.0
Delta P (atm)	10.1361	10.1361	10.1361	10.1361	10.1361					10.136054
Pi Product (atm)	0.728448	0.728448	0.728448	0.728448	0.728448					0.72845
Delta Pi (atm)	2.4003	1.7300	1.7400	1.5400	1.5700					1.7961
Pi Feed ( atm)	3.1288	3.1288	3.1288	3.1288	3.1288					3.1288
c mem (mg/l)	3736.76	3736.76	3736.76	3736.76	3736.76					3736.8
Cmem (mol/l)	0.127884	0.127884	0.127884	0.127884	0.127884					0.127884
A (m3/m2-s-atm)	2.57220E-06	2.57220E-06	2.57220E-06	2.57220E-06	2.57220E-06					2.57220E-06
C mem - Cp	0.0981	0.0981	0.0981	0.0981	0.0981					0.0981
Cf - Cp	0.0294	0.0294	0.0294	0.0294	0.0294					0.0294
ln (Cmem-Cp/Cf-Cp)	1.204006048	1.204006048	1.204006048	1.204006048	1.204006048					1.2040
Mass Transf Coef (m/s)	1.65E-05	1.65E-05	1.65E-05	1.65E-05	1.65E-05					1.6526E-05
Diffus. Coef. ( m2/s)	1.612E-09	1.612E-09	1.612E-09	1.612E-09	1.612E-09					1.612E-09
d F (m)	9.75E-05	9.75E-05	9.75E-05	9.75E-05	9.75E-05					9.754E-05
h d (m)	8.78E-04	8.78E-04	8.78E-04	8.78E-04	8.78E-04					8.78E-04
Vw = Flux/4 (m/s)	4.97E-06	4.97E-06	4.97E-06	4.97E-06	4.97E-06					4.97E-06
Pe	2.7085	2.7085	2.7085	2.7085	2.7085					2.7

pH = 6.6

Biocide = 0.3 mg/l

NF-NaCl  
TDS = 1750 mg/l

**APPENDIX B:**

Tables of Test Results for  $MgSO_4$  Solutions

Table B-1. Readings for distilled water before running MgSO4 solutions experiments

DESCRIPTION	HPP Only						HPP + Permeate Pump					
	1	2	3	4	5	6	1	2	3	4	5	6
pre-filter inlet press (psi)	29	29	29	3.5	1	8	29	29	29	5	8	8
pre-filter outlet press (psi)	29	29	29	3	1	8	29	29	29	5	8	8
HPP Press (psi)	60	60	60	130	130	130	59	59	59	126	126	126
Conc. Press (psi)	54	54	54	120	120	124	52	54	54	119	119	120
(Suc) Perm. Press. (psi)	3.2	3	3.8	7.5	6.5	7	0.5	0.5	0.5	0.5	1	1
(Disch) Perm Press (psi)	0	0	0	0	0	1	0	0	0	1	1	1
Feed TDS ( mg/l)	6	6	6	7	8	7	7	8	7	7	8	8
Conc. TDS (mg/l)	11	8	9	11	12	12	8	8	8	12	12	12
Perm TDS (mg/l)	1	1	1	1	1	1	1	1	1	1	1	1
Perm Flow ( gpm)	0.42	0.42	0.42	0.9	0.89	0.91	0.44	0.44	0.44	0.92	0.91	0.91
Conc Flow (gpm)	1.4	1.4	1.4	1.8	1.8	1.6	1.4	1.4	1.4	1.6	1.6	1.6
Feed Flow (gpm)	1.82	1.82	1.82	2.7	2.69	2.51	1.84	1.84	1.84	2.52	2.92	2.92
HPP (RPM)	700	700	700	1200	1200	1100	700	700	700	1100	1100	1100
Perm Pump (RPM)	0	0	0	0	0	0	110	110	110	660	600	600
Temp	25	25	25	25	25	25	25	25	25	25	25	25
A (ft2)	28	28	28	28	28	28	28	28	28	28	28	28
Flux (gpm/ft2)	0.015	0.015	0.015	0.03214286	0.03179	0.0325	0.01571	0.01571	0.01571429	0.03286	0.0325	0.0325
Surface Area (m2)	2.6	2.6	2.6	2.6	2.6	2.6	2.6	2.6	2.6	2.6	2.6	2.6
Delta P (psi)	56.8	57	56.2	122.5	123.5	123	58.5	58.5	58.5	125.5	125	125
Delta P (atm)												
A (g/ ft2- min-psi)	0.00026	0.00026	0.00027	0.00026239	0.00026	0.00026423	0.00027	0.00027	0.00026862	0.00026	0.00026	0.00026
A (g/ ft2- min-psi)				0.00026302					0.00026461			
A (m3/m2-s-atm)				2.6244E-06					2.6402E-06			
A (m3/m2-h-atm)				0.00944771					0.00950478			
A (m/s.Kpa)				2.5984E-08					2.6141E-08			
A (g/ ft2- min-psi) average						0.000264						
A (m3/m2-s-atm) average						2.63E-06						

NF - Distilled Water pH = 6.2  
 before MgSO4 solutions Biocide= 0.2 ppm



Table B-2. Readings for MgSO4 solution at 800 mg/l and 80 psi feed pressure

Description	HPP Only					HPP + Permeate Pump					Average
	1	2	3	4	Average	1	2	3	4	Average	
Pre-filter inlet press (psi)	32	32	32	32	32	32	32	31	31	31	31.5
Pre-filter outlet press (psi)	31	31	31	31	31	31	31	30	30	30	30.5
HPP Press (psi)	80	80	80	80	80	78	78	78	78	78	78
Conc. Press (psi)	75	75	75	75	75	75	75	75	75	75	75
(Suc) Perm. Press. (psi)	4.5	4.5	4.5	4.5	4.5	0.5	0.5	0.5	0.5	0.5	0.5
(Disch) Perm Press (psi)	0	0	0	0	0	0	0	0	0	0	0
Feed TDS ( mg/l)	830	820	810	820	820	810	810	800	810	810	807.5
Feed TDS ( Mol/l)	0.0137908	0.0136247	0.0134585	0.0136247	0.0136247	0.0134585	0.0134585	0.0132923	0.0134585	0.0134170	
Conc. TDS (mg/l)	1270	1280	1270	1280	1275	1300	1290	1280	1270	1285	
Conc. TDS (Mol/l)	0.0211016	0.0212678	0.0211016	0.0212678	0.0211847	0.0216001	0.0214339	0.0212678	0.0211016	0.0213508	
Perm TDS (mg/l)	33	33	33	34	33.25	32	33	33	27	31.25	
Perm TDS (Mol/l)	0.000548	0.000548	0.000548	0.000565	0.000552	0.000532	0.000548	0.000548	0.000449	0.0005192	
Perm Flow ( gpm)	0.44	0.44	0.44	0.44	0.44	0.475	0.475	0.475	0.475	0.43	
Perm Flow ( m3/s)	0.000028	0.000028	0.000028	0.000028	2.77599E-05	0.000030	0.000030	0.000030	0.000030	0.000030	
Conc Flow (gpm)	1.3	1.3	1.3	1.3	1.3	1.3	1.3	1.3	1.3	1.3	
Feed Flow (gpm)	1.74	1.74	1.74	1.74	1.74	1.775	1.775	1.775	1.775	1.775	
HPP (RPM)	650	650	650	650	650	650	650	650	650	650	
Perm Pump (RPM)	0	0	0	0	0	115	115	115	115	115	
Temp C	25	25	25	25	25	25	25	25	25	25	
Surface Area (ft2)	28	28	28	28	28	28	28	28	28	28	
Flux (gpm/ft2)	0.01571429	0.01571429	0.01571429	0.01571429	0.015714286	0.0169643	0.01696429	0.0169643	0.01696429	0.016964286	
Surface Area (m2)	2.6	2.6	2.6	2.6	2.6	2.6	2.6	2.6	2.6	2.6	
Flux (m3/m2.s)	1.0677E-05	1.0677E-05	1.0677E-05	1.0677E-05	1.0677E-05	1.153E-05	1.1526E-05	1.153E-05	1.1526E-05	1.15262E-05	
Delta P (psi)	75.5	75.5	75.5	75.5	75.5	77.5	77.5	77.5	77.5	77.5	
Delta P (atm)	5.136054	5.136054	5.136054	5.136054	5.136054	5.272109	5.272109	5.272109	5.272109	5.272109	
Pi Product (atm)	0.013415	0.013415	0.013415	0.013821	0.013516455	0.013008	0.013415	0.013415	0.010976	0.012703435	
Delta Pi (atm)	1.06E+00	1.06E+00	1.06E+00	1.06E+00	1.06E+00	9.06E-01	9.06E-01	9.06E-01	9.06E-01	9.06E-01	
Pi Feed ( atm)	1.07432	1.07432	1.07432	1.07473	1.074423771	0.91914	0.91955	0.91955	0.91711	0.918833824	
c mem (mg/l)	2639.7	2639.7	2639.7	2640.7	2639.970285	2258.4	2259.4	2259.4	2253.4	2257.6697	
Cmem (mol/l)	0.043860	0.043860	0.043860	0.043877	0.043864	0.037525	0.037541	0.037541	0.037442	0.037512	
A (m3/m2-s-atm)	2.62E-06	2.62E-06	2.62E-06	2.62E-06	0.00000262	2.64E-06	2.64E-06	2.64E-06	2.64E-06	0.00000264	
C mem - Cp	0.043312	0.043312	0.043312	0.043312	0.043312	0.036993	0.036993	0.036993	0.036993	0.036993	
Cf - Cp	0.020553	0.020719	0.020553	0.020703	0.020632	0.021068	0.020886	0.020719	0.020653	0.020832	
ln (Cmem-Cp/Cf-Cp)	0.745404	0.737352	0.745404	0.738154	0.741579	0.741712	0.740482	0.741257	0.741150	0.741150	
Mass Transf Coef. (m/s)	0.000014	0.000014	0.000014	0.000014	0.000014	0.000016	0.000016	0.000016	0.000016	0.000016	
Diffus. Coef. ( m2/s)	8.49E-10	8.49E-10	8.49E-10	8.49E-10	8.49E-10	8.49E-10	8.49E-10	8.49E-10	8.49E-10	8.49E-10	
d F (m)	5.927E-05	5.863E-05	5.927E-05	5.870E-05	5.897E-05	5.463E-05	5.454E-05	5.460E-05	5.459E-05	5.459E-05	
h d (m)	8.78E-04	8.78E-04	8.78E-04	8.78E-04	8.78E-04	8.78E-04	8.78E-04	8.78E-04	8.78E-04	8.78E-04	
Vw = Flux/4 (m/s)	2.67E-06	2.67E-06	2.67E-06	2.67E-06	2.67E-06	2.88E-06	2.88E-06	2.88E-06	2.88E-06	2.88E-06	
Pe	2.7595	2.7595	2.7595	2.7595	2.7595	2.9790	2.9790	2.9790	2.9790	2.9790	

pH = 5.2

Biocide= 0.2 ppm

NF-MgSO4

TDS 820 mg/l

Table B-3. Readings for MgSO4 solution at 800 mg/l and 100 psi feed pressure

Description	HPP Only					HPP + Permeate Pump					Average
	1	2	3	4	Average	1	2	3	4	Average	
Pre-filter inlet press (psi)	20	20	19	17	19	18	17	18	18	17.75	
Pre-filter outlet press (psi)	19	19	18	16	18	17	16	17	17	16.75	
HPP Press (psi)	100	100	100	100	100	99	99	99	99	99	
Conc. Press (psi)	90	89	89	94	90.5	93	91	94	93	92.75	
(Suc) Perm. Press. (psi)	4.8	4.5	4.5	5.5	4.825	2	1.5	1.5	1.5	1.625	
(Disch) Perm Press (psi)	0	0	0	0	0	0	0	0	0	0	
Feed TDS ( mg/l)	810	810	820	810	812.5	820	810	820	820	817.5	
Feed TDS ( Mol/l)	0.013458503	0.013458503	0.013624657	0.013458503	0.013500004	0.013624657	0.013458503	0.013624657	0.013624657	0.0135831	
Conc. TDS (mg/l)	1360	1350	1370	1340	1355	1380	1350	1400	1400	1382.5	
Conc. TDS (Mol/l)	0.022596993	0.022430838	0.022763147	0.022264684	0.02251392	0.022929301	0.022430838	0.02326161	0.02326161	0.0229708	
Perm TDS (mg/l)	25	26	26	26	25.75	26	27	26	25	26	
Perm TDS (Mol/l)	0.000415	0.000432	0.000432	0.000432	0.00042785	0.000432	0.000449	0.000432	0.000415	0.000432	
Perm Flow ( gpm)	0.58	0.58	0.58	0.58	0.58	0.61	0.61	0.61	0.61	0.61	
Perm Flow ( m3/s)	0.000037	0.000037	0.000037	0.000037	3.6593E-05	0.000038	0.000038	0.000038	0.000038	3.849E-05	
Conc Flow (gpm)	1.5	1.55	1.6	1.6	1.5625	1.6	1.5	1.5	1.6	1.55	
Feed Flow (gpm)	2.08	2.13	2.18	2.18	2.1425	2.21	2.11	2.11	2.21	2.16	
HPP (RPM)	900	900	900	900	900	900	900	900	900	900	
Perm Pump (RPM)	0	0	0	0	0	420	410	410	410	412.5	
Temp C	25	25	25	25	25	25	25	25	25	25	
Surface Area (ft2)	28	28	28	28	28	28	28	28	28	28	
Flux (gpm/ft2)	0.020714286	0.020714286	0.020714286	0.020714286	0.02071429	0.021785714	0.021785714	0.021785714	0.021785714	0.0217857	
Surface Area (m2)	2.6	2.6	2.6	2.6	2.6	2.6	2.6	2.6	2.6	2.6	
Flux (m3/m2.s)	1.40741E-05	1.40741E-05	1.40741E-05	1.40741E-05	1.4074E-05	1.4802E-05	1.4802E-05	1.4802E-05	1.4802E-05	1.48E-05	
Delta P (psi)	95.2	95.5	95.5	94.5	95.175	97	97.5	97.5	97.5	97.375	
Delta P (atm)	6.476190476	6.496598639	6.496598639	6.428571429	6.4744898	6.598639456	6.632653061	6.632653061	6.632653061	6.6241497	
Pi Product (atm)	0.010163	0.010569	0.010569	0.010569	0.01046763	0.010569	0.010976	0.010569	0.010163	0.0105693	
Delta Pi (atm)	1.10E+00	1.12E+00	1.12E+00	1.06E+00	1.10270497	9.92E-01	1.03E+00	1.03E+00	1.03E+00	1.0173142	
Pi Feed ( atm)	1.11457	1.13538	1.13538	1.06736	1.11317261	1.00237	1.03679	1.03639	1.03598	1.0278834	
c mem (mg/l)	2738.6	2789.8	2789.8	2622.6	2735.18018	2462.9	2547.5	2546.5	2545.5	2525.6159	
Cmem (mol/l)	0.045503195	0.046352972	0.046352972	0.043575703	0.04544621	0.040922732	0.042327963	0.042311366	0.04229477	0.0419642	
A (m3/m2-s-atm)	2.62E-06	2.62E-06	2.62E-06	2.62E-06	0.00000262	2.64E-06	2.64E-06	2.64E-06	2.64E-06	2.64E-06	
C mem - Cp	0.045088	0.045921	0.045921	0.043144	0.045018	0.040491	0.041879	0.041879	0.041879	0.041532	
Cf - Cp	0.022182	0.021999	0.022331	0.021833	0.022086	0.022497	0.021982	0.022830	0.022846	0.022539	
ln (Cmem-Cp)/Cf-Cp)	0.709348485	0.735932299	0.720939514	0.681128406	0.71212347	0.587677781	0.644558752	0.606734905	0.606007829	0.6112292	
Mass Transf Coef. (m/s)	1.98408E-05	1.91241E-05	1.95219E-05	2.06629E-05	1.9764E-05	2.51873E-05	2.29646E-05	2.43962E-05	2.44255E-05	2.422E-05	
Diffus. Coeff. ( m2/s)	8.49E-10	8.49E-10	8.49E-10	8.49E-10	8.49E-10	8.49E-10	8.49E-10	8.49E-10	8.49E-10	8.49E-10	
d F (m)	4.27905E-05	4.43941E-05	4.34897E-05	4.10882E-05	4.2958E-05	3.37074E-05	3.69699E-05	3.48005E-05	3.47588E-05	3.506E-05	
h d (m)	8.78E-04	8.78E-04	8.78E-04	8.78E-04	8.78E-04	8.78E-04	8.78E-04	8.78E-04	8.78E-04	8.78E-04	
VW = Flux/4 (m/s)	3.52E-06	3.52E-06	3.52E-06	3.52E-06	3.52E-06	3.70E-06	3.70E-06	3.70E-06	3.70E-06	3.70E-06	
Pc	3.6375	3.6375	3.6375	3.6375	3.6375	3.8256	3.8256	3.8256	3.8256	3.8256	

pH = 5.2

Biocide= 0.2 ppm

NF-MgSO4

TDS 800 mg/l

Table B-4. Readings for MgSO4 solution at 800 mg/l and 130 psi feed pressure

Description	HPP Only						HPP + Permeate Pump						Average
	1	2	3	4	5	Average	1	2	3	4	5	6	
Pre-filler inlet press (psi)	8	8	8	7.5	7.5	7.8	7	5	6	6	6	6	6
Pre-filler outlet press (psi)	7	7	7	6.5	6.5	6.8	6	4	5	5	5	5	5
HPP Press (psi)	129	129	129	129	129	129	127	127	127	127	127	127	127
Conc. Press (psi)	124	124	124	124	124	124	123	123	123	123	123	123	123
(Suc) Perm. Press. (psi)	4.5	4.5	4.5	4.5	4.5	4.5	2	1.5	2	1.5	2	1.8	1.8
(Disch) Perm Press (psi)	0	0	0	0	0	0	0	0	0	0	0	0	0
Feed TDS ( mg/l)	790	790	790	790	790	790	810	810	810	800	790	804	804
Feed TDS ( Mol/l)	0.01313	0.01313	0.01313	0.01313	0.01313	0.01313	0.01346	0.01346	0.01346	0.01329	0.01313	0.01336	0.01336
Conc. TDS (mg/l)	1390	1360	1350	1370	1370	1368	1410	1390	1390	1400	1340	1386	1386
Conc. TDS (Mol/l)	0.02310	0.02260	0.02243	0.02276	0.02276	0.02273	0.02267	0.02272	0.02271	0.02270	0.02269	0.02270	0.02270
Perm TDS (mg/l)	22	25	22	21	22	22.4	22	22	22	22	21	21.8	21.8
Perm TDS (Mol/l)	0.000366	0.000415	0.000366	0.000349	0.000366	0.00037219	0.000366	0.000366	0.000366	0.000366	0.000349	0.0003622	0.0003622
Perm Flow ( gm)	0.73	0.73	0.73	0.73	0.73	0.73	0.75	0.75	0.75	0.75	0.75	0.75	0.75
Perm Flow ( m3/s)	0.000046	0.000046	0.000046	0.000046	0.000046	4.6056E-05	0.000047	0.000047	0.000047	0.000047	0.000047	4.732E-05	4.732E-05
Conc Flow (gpm)	1.7	1.7	1.7	1.7	1.7	1.7	1.75	1.75	1.75	1.75	1.75	1.75	1.75
Feed Flow (gpm)	2.43	2.43	2.43	2.43	2.43	2.43	2.5	2.5	2.5	2.5	2.5	2.5	2.5
HPP (RPM)	1100	1100	1100	1100	1100	1100	1100	1100	1100	1100	1100	1100	1100
Perm Pump (RPM)	0	0	0	0	0	0	527	525	527	527	525	526.2	526.2
Temp C	25	25	25	25	25	25	25	25	25	25	25	25	25
Surface Area (ft2)	28	28	28	28	28	28	28	28	28	28	28	28	28
Flux (gpm/ft2)	0.02607	0.02607	0.02607	0.02607	0.02607	0.02607	0.02679	0.02679	0.02679	0.02679	0.02679	0.02679	0.02679
Surface Area (m2)	2.6	2.6	2.6	2.6	2.6	2.6	2.6	2.6	2.6	2.6	2.6	2.6	2.6
Flux (m3/m2.s)	1.771E-05	1.771E-05	1.771E-05	1.771E-05	1.771E-05	1.771E-05	1.820E-05	1.820E-05	1.820E-05	1.820E-05	1.820E-05	1.820E-05	1.820E-05
Delta P (psi)	124.5	124.5	124.5	124.5	124.5	124.5	125	125.5	125	125.5	125	125.2	125.2
Delta P (atm)	8.4694	8.4694	8.4694	8.4694	8.4694	8.4694	8.5034	8.5374	8.5034	8.5374	8.5034	8.5170	8.5170
Pi Product (atm)	0.0089	0.0102	0.0089	0.0085	0.0089	0.0091	0.0089	0.0089	0.0089	0.0089	0.0085	0.0089	0.0089
Delta Pi (atm)	1.7083	1.7083	1.7083	1.7083	1.7083	1.7083	1.6098	1.6438	1.6098	1.6438	1.6098	1.6234	1.6234
Pi Feed ( atm)	1.7173	1.7185	1.7173	1.7169	1.7173	1.7175	1.6187	1.6527	1.6187	1.6527	1.6183	1.6322	1.6322
c mem (mg/l)	4219.6	4222.6	4219.6	4218.6	4219.6	4220.0	3977.3	4060.9	3977.3	4060.9	3976.3	4010.5	4010.5
C mem (mol/l)	0.07011	0.07016	0.07011	0.07009	0.07011	0.07012	0.06608	0.06747	0.06608	0.06747	0.06607	0.06664	0.06664
A (m3/m2.s-atm)	0.0000026	0.0000026	0.0000026	0.0000026	0.0000026	0.0000026	0.0000026	0.0000026	0.0000026	0.0000026	0.0000026	0.0000026	0.0000026
C mem - Cp	0.06974	0.06974	0.06974	0.06974	0.06974	0.06974	0.06572	0.06711	0.06572	0.06711	0.06572	0.06627	0.06627
Cf - Cp	0.01276	0.01271	0.01276	0.01278	0.01276	0.01275	0.01309	0.01309	0.01309	0.01293	0.01278	0.01300	0.01300
ln (Cmem-Cp/C-F-Cp)	1.6985	1.7024	1.6985	1.6972	1.6985	1.6990	1.6133	1.6342	1.6133	1.6470	1.6377	1.6291	1.6291
Mass Transf Coef. (m/s)	1.043E-05	1.0405E-05	1.0429E-05	1.0437E-05	1.043E-05	1.0426E-05	1.12807E-05	1.1136E-05	1.1281E-05	1.105E-05	1.1113E-05	1.117E-05	1.117E-05
Diffus. Coeff. ( m2/s)	8.49E-10	8.49E-10	8.49E-10	8.49E-10	8.49E-10	8.49E-10	8.49E-10	8.49E-10	8.49E-10	8.49E-10	8.49E-10	8.49E-10	8.49E-10
dF (m)	8.1405E-05	8.1592E-05	8.1405E-05	8.1343E-05	8.1405E-05	8.1430E-05	7.5262E-05	7.6237E-05	7.5262E-05	7.6833E-05	7.6400E-05	7.5999E-05	7.5999E-05
h d (m)	8.78E-04	8.78E-04	8.78E-04	8.78E-04	8.78E-04	8.78E-04	8.78E-04	8.78E-04	8.78E-04	8.78E-04	8.78E-04	8.78E-04	8.78E-04
Vw = Flux/4 (m/s)	4.43E-06	4.43E-06	4.43E-06	4.43E-06	4.43E-06	4.43E-06	4.55E-06	4.55E-06	4.55E-06	4.55E-06	4.55E-06	4.55E-06	4.55E-06
Pe	4.5782	4.5782	4.5782	4.5782	4.5782	4.5782	4.7036	4.7036	4.7036	4.7036	4.7036	4.7036	4.7036

pH = 5.9

Biocide = 0.2 ppm

NF-MgSO4

TDS 820 mg/l

Table B-5. Readings for MgSO4 solution at 1,250 mg/l and 80 psi feed pressure

Description	HPP Only					HPP + Permeate Pump					Average
	1	2	3	4	Average	1	2	3	4	Average	
Pre-filter inlet press (psi)	11	11	11	11	11	10	10	10	10	10	10
Pre-filter outlet press (psi)	12	12	12	12	12	11	11	11	11	11	11
HPP Press (psi)	80	80	80	80	80	79	79	79	79	79	79
Conc. Press (psi)	69	69	69	69	69	69	69	68	68	68.5	68.5
(Suc) Perm. Press. (psi)	4	4	4	3.5	3.875	1	1	1	1	1	1
(Disch) Perm Press (psi)	0	0	0	0	0	0	0	0	0	0	0
Feed TDS ( mg/l)	1250	1250	1220	1220	1235	1230	1220	1240	1250	1235	1235
Feed TDS ( Mol/l)	0.02077	0.02077	0.02027	0.02027	0.02052	0.02044	0.02027	0.02060	0.02077	0.02052	0.02052
Conc. TDS (mg/l)	1800	1810	1800	1770	1795	1820	1810	1850	1870	1837.5	1837.5
Conc. TDS (Mol/l)	0.02991	0.03007	0.02991	0.02941	0.02982	0.03024	0.03007	0.03074	0.03107	0.03053	0.03053
Perm TDS (mg/l)	41	41	41	41	41	40	40	41	41	40.5	40.5
Perm TDS (Mol/l)	0.000681	0.000681	0.000681	0.000681	0.00068123	0.000665	0.000665	0.000681	0.000681	0.00067293	0.00067293
Perm Flow ( gpm)	0.435	0.435	0.435	0.435	0.435	0.46	0.46	0.46	0.46	0.46	0.46
Perm Flow ( m3/s)	0.000027	0.000027	0.000027	0.000027	2.7444E-05	0.000029	0.000029	0.000029	0.000029	2.9022E-05	2.9022E-05
Conc Flow (gpm)	1.9	1.9	1.9	1.9	1.9	1.9	1.9	1.9	1.9	1.9	1.9
Feed Flow (gpm)	2.335	2.335	2.335	2.335	2.335	2.36	2.36	2.36	2.36	2.36	2.36
HPP (RPM)	1000	1000	1000	1000	1000	1000	1000	1000	1000	1000	1000
Perm Pump (RPM)	0	0	0	0	0	120	120	120	120	120	120
Temp C	25	25	25	25	25	25	25	25	25	25	25
Surface Area (ft2)	28	28	28	28	28	28	28	28	28	28	28
Flux (gpm/ft2)	0.015536	0.015536	0.015536	0.015536	0.015536	0.016429	0.016429	0.016429	0.016429	0.016429	0.016429
Surface Area (m2)	2.6	2.6	2.6	2.6	2.6	2.6	2.6	2.6	2.6	2.6	2.6
Flux (m3/m2-s)	1.0556E-05	1.0556E-05	1.0556E-05	1.0556E-05	1.0556E-05	1.1162E-05	1.1162E-05	1.1162E-05	1.1162E-05	1.1162E-05	1.1162E-05
Delta P (psi)	76	76	76	76.5	76.125	78	78	78	78	78	78
Delta P (atm)	5.1700680	5.1700680	5.1700680	5.2040816	5.1785714	5.3061224	5.3061224	5.3061224	5.3061224	5.3061224	5.3061224
Pi Product (atm)	0.016667	0.016667	0.016667	0.016667	0.01666691	0.016260	0.016260	0.016667	0.016667	0.0166667	0.0166667
Delta Pi (atm)	1.14E+00	1.14E+00	1.14E+00	1.18E+00	1.14973281	1.08E+00	1.08E+00	1.08E+00	1.08E+00	1.08E+00	1.078017
Pi Feed (atm)	1.15790	1.15790	1.15790	1.19191	1.16639972	1.09428	1.09428	1.09468	1.09468	1.09448065	1.09448065
c mem (mg/l)	2845.1	2845.1	2845.1	2928.6	2865.9647	2688.8	2688.8	2689.8	2689.8	2689.25211	2689.25211
Cmem (mol/l)	0.047272	0.047272	0.047272	0.048661	0.047619	0.044675	0.044675	0.044691	0.044691	0.044683	0.044683
A (m3/m2-s-atm)	2.62E-06	2.62E-06	2.62E-06	2.62E-06	2.62E-06	2.64E-06	2.64E-06	2.64E-06	2.64E-06	2.64E-06	2.64E-06
C mem - Cp	0.046591	0.046591	0.046591	0.047979	0.046938	0.044010	0.044010	0.044010	0.044010	0.044010	0.044010
Cf - Cp	0.020088	0.020088	0.019590	0.019590	0.019839	0.019772	0.019606	0.019922	0.020088	0.020088	0.020088
ln (Cmem-Cp/Cf-Cp)	0.841279	0.841279	0.866406	0.895775	0.861187	0.800136	0.808574	0.792601	0.784295	0.837970	0.837970
Mass Transf Coef. (m/s)	1.2547E-05	1.2547E-05	1.2183E-05	1.1784E-05	1.2257E-05	1.395E-05	1.3805E-05	1.4083E-05	1.4232E-05	1.4018E-05	1.4018E-05
Diffus. Coeff. (m2/s)	8.49E-10	8.49E-10	8.49E-10	8.49E-10	8.49E-10	8.49E-10	8.49E-10	8.49E-10	8.49E-10	8.49E-10	8.49E-10
d F (m)	6.7665E-05	6.7665E-05	6.9686E-05	7.2049E-05	6.9266E-05	6.0859E-05	6.15E-05	6.0285E-05	5.96537E-05	6.0575E-05	6.0575E-05
h d (m)	8.78E-04	8.78E-04	8.78E-04	8.78E-04	8.78E-04	8.78E-04	8.78E-04	8.78E-04	8.78E-04	8.78E-04	8.78E-04
Vw = Flux/4 (m/s)	2.64E-06	2.64E-06	2.64E-06	2.64E-06	2.64E-06	2.79E-06	2.79E-06	2.79E-06	2.79E-06	2.79E-06	2.79E-06
Pe	2.7281	2.7281	2.7281	2.7281	2.7281	2.8849	2.8849	2.8849	2.8849	2.8849	2.8849

pH = 6.8

Biocide= 0.2 mg/l

NF-MgSO4

TDS 1250 mg/l

Table B-6. Readings for MgSO4 solution at 1,250 mg/l and 100 psi feed pressure.

Description	HPP Only							HPP - Permeate Pump							Average
	1	2	3	4	5	6	Average	1	2	3	4	Average			
Pre-filler inlet press (psi)	14	15	16	15	15	15	15	15	14	14	14	13	14		
Pre-filler outlet press (psi)	13	14	15	14	14	14	14	14	13	13	13	12	13		
HPP Press (psi)	100	100	100	100	100	109	101.5	99	99	99	101	99.5	99.5		
Conc. Press (psi)	96	96	96	96	96	97	96.16666667	90	92	92	95	92.25	92.25		
(Sue) Perm. Press. (psi)	7.5	7.5	7.5	7.5	7.5	16.5	9	1	1	1	2	1.25	1.25		
(Disch) Perm Press (psi)	0	0	0	0	0	0	0	0	0	0	0	0	0		
Feed TDS ( mg/l)	1260	1240	1260	1270	1250	1250	1255	1250	1220	1210	1270	1237.5	1237.5		
Feed TDS ( Mol/l)	0.020935449	0.02060314	0.020935449	0.021101603	0.020769295	0.020769295	0.020852372	0.020769295	0.02070832	0.02010468	0.0211016	0.02085616	0.02085616		
Conc. TDS (mg/l)	1900	1890	1970	1975	1980	1950	1944.166667	1990	1990	1980	2020	1995	1995		
Conc. TDS (Mol/l)	0.031569328	0.031403174	0.032732408	0.032815486	0.032898563	0.0324001	0.0322303176	0.0330364717	0.0330364717	0.03289856	0.03356318	0.03314779	0.03314779		
Perm. TDS (mg/l)	39	38	38	39	39	39	38.66666667	38	38	37	37	37.5	37.5		
Perm. TDS (Mol/l)	0.000648	0.000631	0.000631	0.000648	0.000648	0.000648	0.000642464	0.000631	0.000631	0.000615	0.000615	0.00062308	0.00062308		
Perm Flow ( gpm)	0.535	0.535	0.535	0.535	0.535	0.535	0.535	0.585	0.585	0.585	0.59	0.58625	0.58625		
Perm Flow ( m3/s)	0.000034	0.000034	0.000034	0.000034	0.000034	0.000034	3.37535E-05	0.000037	0.000037	0.000037	0.000037	3.6987E-05	3.6987E-05		
Conc Flow (gpm)	1.7	1.7	1.7	1.7	1.7	1.7	1.7	1.7	1.7	1.7	1.75	1.7125	1.7125		
Feed Flow (gpm)	2.235	2.235	2.235	2.235	2.235	2.235	2.235	2.285	2.285	2.285	2.34	2.29875	2.29875		
HPP (RPM)	960	960	960	960	960	960	960	960	960	960	960	960	960		
Temp C	0	0	0	0	0	0	0	300	300	300	300	300	300		
Surface Area (ft2)	28	28	28	28	28	28	28	28	28	28	28	28	28		
Flux (gpm/ft2)	0.019107	0.019107	0.019107	0.019107	0.019107	0.019107	0.019107	0.020893	0.020893	0.020893	0.021071	0.020938	0.020938		
Surface Area (m2)	2.6	2.6	2.6	2.6	2.6	2.6	2.6	2.6	2.6	2.6	2.6	2.6	2.6		
Flux (m3/m2.s)	1.29821E-05	1.29821E-05	1.29821E-05	1.29821E-05	1.29821E-05	1.29821E-05	1.29821E-05	1.41954E-05	1.41954E-05	1.41954E-05	1.4317E-05	1.42204E-05	1.42204E-05		
Delta P (psi)	92.5	92.5	92.5	92.5	92.5	92.5	92.5	98	98	98	99	98.25	98.25		
Delta P (atm)	6.2925	6.2925	6.2925	6.2925	6.2925	6.2925	6.2925	6.666667	6.666667	6.666667	6.734694	6.683673	6.683673		
Pi Product (atm)	0.0159	0.0154	0.0154	0.0159	0.0159	0.0159	0.0157	0.015447	0.015447	0.015041	0.015041	0.015244	0.015244		
Delta Pi (atm)	1.3375	1.3375	1.3375	1.3375	1.3375	1.3375	1.3375	1.289620	1.289620	1.289620	1.311689	1.295137	1.295137		
Pi Feed ( atm)	1.3534	1.3530	1.3530	1.3534	1.3534	1.3534	1.3532	1.305067	1.305067	1.304660	1.326730	1.310381	1.310381		
c mem (mg/l)	3325.352	3324.353	3324.353	3325.352	3325.352	3325.352	3325.019	3206.684	3206.684	3205.685	3259.913	3219.742	3219.742		
Cmem (mol/l)	0.055	0.055	0.055	0.055	0.055	0.055	0.055	0.05328	0.05328	0.05326	0.05416	0.05350	0.05350		
A (m3/m2.s-atm)	2.62E-06	2.62E-06	2.62E-06	2.62E-06	2.62E-06	2.62E-06	0.00000262	2.64E-06	2.64E-06	2.64E-06	2.64E-06	0.00000264	0.00000264		
C mem - Cp	0.054604	0.054604	0.054604	0.054604	0.054604	0.054604	0.054604	0.052649	0.052649	0.052649	0.053550	0.052874	0.052874		
Cf - Cp	0.02029	0.01997	0.02030	0.02045	0.02012	0.02012	0.02021	0.02014	0.01964	0.01949	0.02049	0.02352	0.02352		
ln (C mem-Cp/Cf-Cp)	0.99011	1.00579	0.98929	0.98195	0.99833	0.99833	0.99394	0.96104	0.98611	0.99375	0.96084	0.48592	0.48592		
Mass Transf Coef. (m/s)	0.000013	0.000013	0.000013	0.000013	0.000013	0.000013	0.000013	0.000015	0.000015	0.000014	0.000015	0.000015	0.000015		
Diffus. Coeff. ( m2/s)	8.49E-10	8.49E-10	8.49E-10	8.49E-10	8.49E-10	8.49E-10	8.49E-10	8.49E-10	8.49E-10	8.49E-10	8.49E-10	8.49E-10	8.49E-10		
d F (m)	6.4751E-05	6.5776E-05	6.4697E-05	6.4217E-05	6.5289E-05	6.5289E-05	6.5001E-05	5.7478E-05	5.8977E-05	5.9434E-05	5.6979E-05	5.8217E-05	5.8217E-05		
h d (m)	8.78E-04	8.78E-04	8.78E-04	8.78E-04	8.78E-04	8.78E-04	8.78E-04	8.78E-04	8.78E-04	8.78E-04	8.78E-04	8.78E-04	8.78E-04		
Vw = Flux/4 (m/s)	3.25E-06	3.25E-06	3.25E-06	3.25E-06	3.25E-06	3.25E-06	3.25E-06	3.55E-06	3.55E-06	3.55E-06	3.58E-06	3.56E-06	3.56E-06		
Pe	3.3552	3.3552	3.3552	3.3552	3.3552	3.3552	3.3552	3.6688	3.6688	3.6688	3.7002	3.6767	3.6767		

pH= 6.8

Biocide = 0.2 ppm

TDS 1250 mg/l

Table B-7. Readings for MgSO4 solution at 1,250 mg/l and 130 psi feed pressure

Description	HIPP Only					HIPP + Permeate Pump					Average	
	1	2	3	4	5	1	2	3	4	5		
Pre-filter inlet press (psi)	5	5	5	5	5	4	4	4	4	4	4	4
Pre-filter outlet press (psi)	6	6	6	6	6	5	5	5	5	5	5	5
HIPP Press (psi)	129	129	129	129	129	128	128	128	128	128	128	128
Conc. Press (psi)	125	125	125	125	125	124	124	124	124	124	124	124
(Suc) Perm. Press. (psi)	6.8	7	7	6.8	6.9	2.5	2.2	2.2	2.2	2.2	2.2	2.275
(Disch) Perm Press (psi)	0	0	0	0	0	0	0	0	0	0	0	0
Feed TDS ( mg/l)	1250	1230	1230	1260	1242.5	1260	1260	1250	1250	1250	1250	1255
Feed TDS ( Mol/l)	0.020769	0.020437	0.020437	0.020935	0.020645	0.020935	0.020935	0.020769	0.020769	0.020769	0.020769	0.020852
Conc. TDS (mg/l)	2040	2000	2000	2010	2012.5	2090	2100	2080	2080	2080	2080	2087.5
Conc. TDS (Mol/l)	0.0333895	0.033231	0.033231	0.033397	0.033439	0.034726	0.034892	0.034560	0.034560	0.034560	0.034560	0.034685
Perm TDS (mg/l)	34	33	33	34	33.5	33	33	33	33	33	33	33
Perm TDS (Mol/l)	0.000565	0.000548	0.000548	0.000565	0.000566	0.000548	0.000548	0.000548	0.000548	0.000548	0.000548	0.0005483
Perm Flow ( gpm)	0.67	0.67	0.67	0.67	0.67	0.7	0.7	0.7	0.7	0.7	0.7	0.7
Perm Flow ( m3/s)	0.000042	0.000042	0.000042	0.000042	4.2271E-05	0.000044	0.000044	0.000044	0.000044	0.000044	0.000044	4.4163E-05
Conc Flow (gpm)	1.8	1.8	1.8	1.8	1.8	1.8	1.8	1.8	1.8	1.8	1.8	1.8
Conc Flow (m3/s)	2.47	2.47	2.47	2.47	2.47	2.5	2.5	2.5	2.5	2.5	2.5	2.5
HPP (RPM)	1100	1100	1100	1100	1100	1100	1100	1100	1100	1100	1100	1100
Perm Pump (RPM)	0	0	0	0	0	485	485	485	485	485	485	485
Temp C	28	28	28	28	28	28	28	28	28	28	28	28
Surface Area (ft2)	0.02393	0.02393	0.02393	0.02393	0.02393	0.02500	0.02500	0.02500	0.02500	0.02500	0.02500	0.02500
Flux (gpm/ft2)	1.6258E-05	1.6258E-05	1.6258E-05	1.6258E-05	1.6258E-05	1.699E-05	1.6986E-05	1.6986E-05	1.6986E-05	1.6986E-05	1.6986E-05	1.6986E-05
Surface Area (m2)	122.2	122	122	122.2	122.2	125.5	125.8	125.8	125.8	125.8	125.8	125.725
Flux (m3/m2.s)	8.31293	8.29932	8.29932	8.31293	8.30612	8.53741	8.55782	8.55782	8.55782	8.55782	8.55782	8.55272
Delta P (psi)	0.01382	0.01341	0.01341	0.01382	0.01362	0.01341	0.01341	0.01341	0.01341	0.01341	0.01341	0.01341
Pi Product (atm)	2.11E+00	2.09E+00	2.09E+00	2.11E+00	2.10078481	2.10E+00	2.12E+00	2.12E+00	2.12E+00	2.12E+00	2.12E+00	2.11864758
Delta Pi (atm)	2.12141	2.10740	2.10740	2.12141	2.11440289	2.11676	2.13716	2.13716	2.13716	2.13716	2.13716	2.1320624
Pi Feed ( atm)	5212.5	5178.1	5178.1	5212.5	5195.30651	5201.1	5251.2	5251.2	5251.2	5251.2	5251.2	5238.69775
c mem (mg/l)	0.086608	0.086036	0.086036	0.086608	0.086322	0.086418	0.087252	0.087252	0.087252	0.087252	0.087252	0.087043
C mem (mol/l)	2.62E-06	2.62E-06	2.62E-06	2.62E-06	0.00000262	2.64E-06	2.64E-06	2.64E-06	2.64E-06	2.64E-06	2.64E-06	0.00000264
A (m3/m2.s-atm)	0.086043	0.085488	0.085488	0.086043	0.085766	0.085870	0.086703	0.086703	0.086703	0.086703	0.086703	0.086495
C mem - Cp	0.020204	0.019889	0.019889	0.020371	0.020088	0.020387	0.020387	0.020387	0.020387	0.020387	0.020387	0.020304
ln (C mem-Cp)/(C-Cp)	1.448953	1.458225	1.458225	1.440763	1.451493	1.437931	1.47587	1.455770	1.455770	1.455770	1.455770	1.449265
Mass Transf Coef. (m/s)	0.000011	0.000011	0.000011	0.000011	0.000011	0.000012	0.000012	0.000012	0.000012	0.000012	0.000012	0.000012
Diffus. Coef. ( m2/s)	8.49E-10	8.49E-10	8.49E-10	8.49E-10	8.49E-10	8.49E-10	8.49E-10	8.49E-10	8.49E-10	8.49E-10	8.49E-10	8.49E-10
d F (m)	7.5665E-05	7.61492E-05	7.6149E-05	7.5237E-05	7.5798E-05	7.187E-05	7.2354E-05	7.2763E-05	7.2763E-05	7.2763E-05	7.2763E-05	7.2438E-05
h d (m)	8.78E-04	8.78E-04	8.78E-04	8.78E-04	8.78E-04	8.78E-04	8.78E-04	8.78E-04	8.78E-04	8.78E-04	8.78E-04	8.78E-04
Vw = Flux/4 (m/s)	4.06E-06	4.06E-06	4.06E-06	4.06E-06	4.06E-06	4.25E-06	4.25E-06	4.25E-06	4.25E-06	4.25E-06	4.25E-06	4.25E-06
Pe	4.2019	4.2019	4.2019	4.2019	4.2019	4.3900	4.3900	4.3900	4.3900	4.3900	4.3900	4.3900

pH 6.8

Biocide= 0.2 ppm

TDS 1250 mg/l

Table B-8. Readings for MgSO4 solution at 1.750 mg/l and 80 psi feed pressure

Description	HPP Only			HPP + Permeate Pump			Average
	1	2	3	1	2	3	
Pre-filter inlet press (psi)	28.5	28.5	28.5	28.5	27	28	27.66667
Pre-filter outlet press (psi)	27.5	27.5	27.5	27.5	26	27	26.66667
HPP Press (psi)	80	80	80	78	78	78	78
Conc. Press (psi)	75	75	75	75	75	75	75
(Suc) Perm. Press. (psi)	3.2	3.1	3.2	3.16667	0.5	0.5	0.5
(Disch) Perm Press (psi)	0	0	0	0	0	0	0
Feed TDS ( mg/l)	1770	1780	1780	1776.67	1760	1750	1760
Feed TDS ( Mol/l)	0.02941	0.02958	0.02958	0.02952	0.02941	0.02908	0.02924
Conc. TDS (mg/l)	2870	2830	2870	2856.6667	2880	2840	2856.6667
Conc. TDS (Mol/l)	0.0477	0.0470	0.0477	0.0475	0.0479	0.0472	0.0475
Perm TDS (mg/l)	56	56	55	55.6667	52	52	52
Perm TDS (Mol/l)	0.000930	0.000930	0.000914	0.0009249	0.000864	0.000864	0.00086400
Perm Flow ( gpm)	0.38	0.38	0.38	0.38	0.395	0.395	0.395
Perm Flow ( m3/s)	0.000024	0.000024	0.000024	2.397451E-05	0.000025	0.000025	2.492081E-05
Conc Flow (gpm)	1.4	1.4	1.4	1.4	1.4	1.4	1.4
Feed Flow (gpm)	1.78	1.78	1.78	1.78	1.795	1.795	1.795
HPP (RPM)	700	700	700	700	700	700	700
Perm Pump (RPM)	0	0	0	0	130	130	130
Temp C	25	25	25	25	25	25	25
Surface Area (ft2)	28	28	28	28	28	28	28
Flux (gpm/ft2)	0.013571	0.013571	0.013571	0.013571	0.014107	0.014107	0.014107
Surface Area (m2)	2.6	2.6	2.6	2.6	2.6	2.6	2.6
Flux (m3/m2-s)	9.221E-06	9.221E-06	9.221E-06	9.221E-06	9.585E-06	9.585E-06	9.585E-06
Delta P (psi)	76.8	76.9	76.8	76.83333333	77.5	77.5	77.5
Delta P (atm)	5.224490	5.231293	5.224490	5.226757	5.272109	5.272109	5.272109
Pi Product (atm)	0.022765	0.022765	0.022358	0.022629	0.021139	0.021139	0.021139
Delta Pi (atm)	1.71E-00	1.71E+00	1.71E+00	1.707312142	1.64E+00	1.64E+00	1.641453076
Pi Feed ( atm)	1.72781	1.73461	1.72740	1.72994	1.66259	1.66259	1.6626
c mem (mg/l)	4245.4	4262.1	4244.4	4250.6444	4085.2	4085.2	4085.1594
C mem (mol/l)	0.070539	0.070817	0.070523	0.070626	0.067877	0.067877	0.067877
A (m3/m2-s-atm)	2.62E-06	2.62E-06	2.62E-06	0.00000262	2.64E-06	2.64E-06	0.00000264
C mem - Cp	0.069609	0.069887	0.069609	0.069701	0.067013	0.067013	0.067013
Cf - Cp	0.02848	0.02865	0.02866	0.02860	0.028545	0.028213	0.028379
ln (C mem-Cp)/(Cf-Cp)	0.89373	0.89189	0.88733	0.89098	0.8533892	0.8592270	0.8592270
Mass Transf Coef. (m/s)	1.03174E-05	1.03386E-05	1.03918E-05	1.034921E-05	1.12316E-05	1.10796E-05	1.11553E-05
Diffus. Coef. ( m2/s)	8.49E-10	8.49E-10	8.49E-10	8.49E-10	8.49E-10	8.49E-10	8.49E-10
d F (m)	8.2288E-05	8.2119E-05	8.1699E-05	8.2033E-05	7.5990E-05	7.6627E-05	7.6107E-05
ln d (m)	8.78E-04	8.78E-04	8.78E-04	8.78E-04	8.78E-04	8.78E-04	8.78E-04
VW = Flux/4 (m/s)	2.31E-06	2.31E-06	2.31E-06	2.31E-06	2.40E-06	2.40E-06	2.40E-06
Pc	2.3832	2.3832	2.3832	2.3832	2.4772	2.4772	2.4772

pH = 7.4

TDS 1750 mg/l Blockle= 0.2 ppm

Table B-9. Readings for MgSO4 solution at 1.750 mg/l and 100 psi feed pressure

Description	HPP Only					HPP + Permeate Pump				
	1	2	3	4	Average	1	2	3	4	Average
Pre-filter inlet press (psi)	19	19	18	18	18.5	15	18	18	18	17.25
Pre-filter outlet press (psi)	18	18	17	17	17.5	14	17	17	17	16.25
HPP Press (psi)	100	100	100	100	100	99	99	99	99	99
C conc. Press (psi)	98	98	98	98	98	95	95	95	95	95
(Suc) Perm. Press. (psi)	7.6	7.3	7.5	7.5	7.475	1.7	1.7	1.7	1.7	1.7
(Disch) Perm Press (psi)	0	0	0	0	0	0	0	0	0	0
Feed TDS ( mg/l)	1790	1730	1700	1730	1737.5	1720	1760	1750	1750	1745
Feed TDS ( Mol/l)	0.029742	0.028745	0.028246	0.028745	0.028869	0.028579	0.029243	0.029077	0.029077	0.028994
C conc. TDS (mg/l)	2670	2650	2590	2600	2627.5	2660	2740	2730	2740	2717.5
C conc. TDS (Mol/l)	0.044363	0.044031	0.043034	0.043200	0.043657	0.044197	0.045526	0.045360	0.045526	0.045152
Perm TDS (mg/l)	50	50	49	49	49.5	49	49	49	49	49
Perm TDS (Mol/l)	0.000831	0.000831	0.000814	0.000814	0.000822464	0.000814	0.000814	0.000814	0.000814	0.000814156
Perm Flow ( gpm)	0.475	0.475	0.475	0.475	0.475	0.52	0.52	0.52	0.52	0.52
Perm Flow ( m3/s)	0.000030	0.000030	0.000030	0.000030	2.99681E-05	0.000033	0.000033	0.000033	0.000033	3.28072E-05
C conc Flow (gpm)	1.65	1.65	1.65	1.65	1.65	1.65	1.7	1.7	1.7	1.6875
Feed Flow (gpm)	2.125	2.125	2.125	2.125	2.125	2.17	2.22	2.22	2.22	2.2075
HPP (RPM)	900	900	900	900	900	900	900	900	900	900
Perm Pump (RPM)	0	0	0	0	0	200	200	200	200	200
Temp C	25	25	25	25	25	25	25	25	25	25
Surface Area (ft2)	28	28	28	28	28	28	28	28	28	28
Flux (gpm/ft2)	0.016964	0.016964	0.016964	0.016964	0.016964	0.018571	0.018571	0.018571	0.018571	0.018571
Surface Area (m2)	2.6	2.6	2.6	2.6	2.6	2.6	2.6	2.6	2.6	2.6
Flux (m3/m2.s)	1.15262E-05	1.15262E-05	1.15262E-05	1.15262E-05	1.15262E-05	1.26181E-05	1.26181E-05	1.26181E-05	1.26181E-05	1.26181E-05
Delta P (psi)	92.4	92.7	92.5	92.5	92.525	97.3	97.3	97.3	97.3	97.3
Delta P (atm)	6.285714	6.306122	6.292517	6.292517	6.294218	6.619048	6.619048	6.619048	6.619048	6.619048
Pi Product (atm)	0.020325	0.020325	0.019919	0.019919	0.020122	0.019919	0.019919	0.019919	0.019919	0.019919
Delta Pi (atm)	1.89E+00	1.91E+00	1.89E+00	1.89E+00	1.894911153	1.84E+00	1.84E+00	1.84E+00	1.84E+00	1.85937
Pi Feed ( atm)	1.90673	1.92714	1.91313	1.91313	1.915033394	1.85937	1.85937	1.85937	1.85937	1.859369
c mem (mg/l)	4685.0	4735.2	4700.8	4700.8	4705.435035	4568.7	4568.7	4568.7	4568.7	4568.662207
C mem (mol/l)	0.0778440	0.0786772	0.0781051	0.0781051	0.0781829	0.0759103	0.0759103	0.0759103	0.0759103	0.0759103
A (m3/m2-s-atm)	2.62E-06	2.62E-06	2.62E-06	2.62E-06	0.00000262	2.64E-06	2.64E-06	2.64E-06	2.64E-06	0.00000264
C mem - Cp	0.077013	0.077846	0.077291	0.077291	0.077360	0.075096	0.075096	0.075096	0.075096	0.075096
C f - Cp	0.028911	0.027914	0.027432	0.027931	0.028047	0.027764	0.028429	0.028263	0.028263	0.028180
ln (C mem-Cp/C-Cp)	0.97976	1.02561	1.03586	1.01786	1.01460	0.99502	0.97136	0.97722	0.97722	0.98016
Mass Transf Coef. (m/s)	1.17643E-05	1.12383E-05	1.11271E-05	1.1324E-05	1.13603E-05	1.26814E-05	1.29902E-05	1.2912E-05	1.2912E-05	1.28735E-05
Diffus. Coef. ( m2/s)	8.49E-10	8.49E-10	8.49E-10	8.49E-10	8.49E-10	8.49E-10	8.49E-10	8.49E-10	8.49E-10	8.49E-10
d F (m)	7.21675E-05	7.55449E-05	7.63001E-05	7.49736E-05	7.47337E-05	6.69487E-05	6.5357E-05	6.5751E-05	6.5751E-05	6.59495E-05
h d (m)	8.78E-04	8.78E-04	8.78E-04	8.78E-04	8.78E-04	8.78E-04	8.78E-04	8.78E-04	8.78E-04	8.78E-04
Vw = Flux/4 (m/s)	2.88E-06	2.88E-06	2.88E-06	2.88E-06	2.88E-06	3.15E-06	3.15E-06	3.15E-06	3.15E-06	3.15E-06
Pc	2.9790	2.9790	2.9790	2.9790	2.9790	3.2612	3.2612	3.2612	3.2612	3.2612
NF-MgSO4	pH=6.9									
TDS l/750 mg/l	Biocide= 0.2 ppm									



Table B-10. Readings for MgSO4 solution at 1,700 mg/l and 130 psi feed pressure

Description	HIPP Only					HIPP - Permeate Pump					Average
	1	2	3	4	5	1	2	3	4	5	
Pre-filter inlet press (psi)	4	4	5.5	4	4	4.5	5	4.5	4.5	4.5	4.625
Pre-filter outlet press (psi)	3	3	4.5	4	4	3.5	4	3.5	3.5	3.5	3.625
HIPP Press (psi)	124	124	124	126	124	124	124	124	124	124	124
Conc. Press (psi)	115	119	119	121	118.5	119	120	120	120	119.75	
(Suc) Perm. Press. (psi)	4.5	4.5	4.5	4.7	4.55	1.8	1.8	1.8	1.8	1.8	
(DiscH) Perm Press (psi)	0	0	0	0	0	0	0	0	0	0	
Feed TDS ( mg/l)	1760	1720	1750	1750	1745	1770	1760	1770	1780	1770	
Feed TDS ( Mol/l)	0.02924317	0.02857855	0.02907701	0.02907703	0.028993935	0.029409321	0.029243167	0.02940932	0.02957548	0.029409321	
Conc. TDS (mg/l)	2820	2750	2790	2820	2795	2900	2890	2910	2940	2910	
Conc. TDS (Mol/l)	0.04685553	0.04569245	0.04635707	0.046855529	0.046440143	0.048184764	0.048018609	0.04835092	0.04884938	0.048350918	
Perm TDS (mg/l)	42	42	43	45	43	41	43	43	43	42.5	
Perm TDS (Mol/l)	0.000698	0.000698	0.000714	0.000748	0.000714464	0.000681	0.000714	0.000714	0.000714	0.000706156	
Perm Flow ( gpm)	0.64	0.64	0.64	0.65	0.6425	0.68	0.68	0.68	0.68	0.68	
Perm Flow ( m3/s)	0.000040	0.000040	0.000040	0.000041	4.05338E-05	0.000043	0.000043	0.000043	0.000043	4.29017E-05	
Conc Flow (gpm)	1.9	1.9	1.9	1.9	1.9	1.9	1.9	1.9	1.9	1.9	
Feed Flow (gpm)	2.54	2.54	2.54	2.55	2.5425	2.58	2.58	2.58	2.58	2.58	
HIPP (RPM)	1100	1100	1100	1100	1100	1100	1100	1100	1100	1100	
Perm Pump (RPM)	0	0	0	0	0	450	450	450	450	450	
Temp C	25	25	25	25	25	25	25	25	25	25	
Surface Area (ft2)	28	28	28	28	28	28	28	28	28	28	
Flux (gpm/ft2)	0.02285714	0.02285714	0.02285714	0.023214286	0.022946429	0.024285714	0.024285714	0.02428571	0.02428571	0.024285714	
Surface Area (m2)	2.6	2.6	2.6	2.6	2.6	2.6	2.6	2.6	2.6	2.6	
Flux (m3/m2.s)	1.553E-05	1.553E-05	1.553E-05	1.57727E-05	1.559007E-05	1.650006E-05	1.650006E-05	1.6501E-05	1.6501E-05	1.650006E-05	
Delta P (psi)	119.5	119.5	119.5	121.3	119.95	122.2	122.2	122.2	122.2	122.2	
Delta P (atm)	8.1292517	8.1292517	8.1292517	8.25170068	8.159863946	8.31292517	8.31292517	8.31292517	8.31292517	8.31292517	
Pi Product (atm)	0.017073	0.017073	0.017480	0.018293	0.017479927	0.016667	0.017480	0.017480	0.017480	0.017276672	
Delta Pi (atm)	2.20E+00	2.20E+00	2.20E+00	2.23E+00	2.209223002	2.06E+00	2.06E+00	2.06E+00	2.06E+00	2.06268233	
Pi Feed ( atm)	2.21884	2.21884	2.21924	2.24989	2.226702929	2.07935	2.08016	2.08016	2.08016	2.079959002	
c mem (mg/l)	5451.9	5451.9	5452.9	5528.2	5471.239303	5109.2	5111.2	5111.2	5111.2	5110.7	
C mem (mol/l)	0.09058595	0.09058595	0.09060255	0.091853655	0.090907025	0.084891186	0.084924379	0.08492438	0.08492438	0.08491608	
A (m3/m2-s-atm)	2.62E-06	2.62E-06	2.62E-06	2.62E-06	0.00000262	2.64E-06	2.64E-06	2.64E-06	2.64E-06	0.00000264	
C mem - Cp	0.089888	0.089888	0.089888	0.091106	0.090193	0.084210	0.084210	0.084210	0.084210	0.084210	
Cf - Cp	0.028545	0.027881	0.028363	0.028329	0.028279	0.028728	0.028529	0.028695	0.028861	0.028703	
ln (C mem - Cp / (C - Cp))	1.14707263	1.17063085	1.15349579	1.168125988	1.159831314	1.075437792	1.082401958	1.07659474	1.07082105	1.076305378	
Mass Transf C coef. (m/s)	1.3539E-05	1.3266E-05	1.3463E-05	1.35025E-05	1.34428E-05	1.53432E-05	1.52445E-05	1.5327E-05	1.5409E-05	1.53308E-05	
Diffus. Ccoeff. ( m2/s)	8.49E-10	8.49E-10	8.49E-10	8.49E-10	8.49E-10	8.49E-10	8.49E-10	8.49E-10	8.49E-10	8.49E-10	
d F (m)	6.2709E-05	6.3996E-05	6.306E-05	6.2877E-05	6.31604E-05	5.5334E-05	5.56923E-05	5.5394E-05	5.5096E-05	5.53787E-05	
h d (mm)	8.78E-04	8.78E-04	8.78E-04	8.78E-04	8.78E-04	8.78E-04	8.78E-04	8.78E-04	8.78E-04	8.78E-04	
Vw = Flux/4 (m/s)	3.88E-06	3.88E-06	3.88E-06	3.94E-06	3.90E-06	4.13E-06	4.13E-06	4.13E-06	4.13E-06	4.13E-06	
Pc	4.0137	4.0137	4.0137	4.0765	4.0294	4.2646	4.2646	4.2646	4.2646	4.2646	

pH=7.1

Biocide = 0.2 ppm

NF-MgSO4

TDS 1750 mg/l

**APPENDIX C:**

Tables of Test Results for  $MgCl_2$  Solutions

Table C-1. Readings for distilled water before running MgCl2 experiments

Description	HPP Only					HPP + Permeate Pump				
	1	2	3	4	5	1	2	3	4	5
pre-filter inlet press (psi)	21	21.5	22	22	22	20.5	21	22	22	21
pre-filter outlet press (psi)	20	20	20.5	21	21	19.5	20	21	21	20
HPP Press (psi)	80	80	80	80	80	79	80	80	80	80
Conc. Press (psi)	75	75	75	75	75	75	75	75	75	75
(Suc) Perm. Press. (psi)	3.2	3.2	3.2	3	3	1	1	1.2	1.2	1.2
(Disch) Perm Press (psi)	0	0	0	0	0	0	0	0	0	0
Feed TDS ( mg/l)	16	16	17	17	17	17	17	18	18	18
Conc. TDS (mg/l)	20	21	21	22	22	22	22	23	24	23
Perm TDS (mg/l)	2	2	2	2	2	2	2	2	2	2
Perm Flow ( gpm)	0.5	0.5	0.5	0.505	0.505	0.515	0.515	0.515	0.515	0.515
Conc Flow (gpm)	1.45	1.45	1.45	1.45	1.45	1.45	1.45	1.45	1.45	1.45
HPP (RPM)	800	800	800	800	800	800	800	800	800	800
Perm Pump (RPM)	0	0	0	0	0	360	360	360	360	360
Temp	24	24	24	26	24	26	25	25	25	24
Surface Area (ft2)	28	28	28	28	28	28	28	28	28	28
Flux (gpm/ft2)	0.01786	0.01786	0.01785714	0.018036	0.018036	0.018393	0.018393	0.01839286	0.01839	0.01839286
Delta P (psi)	76.8	76.8	76.8	77	77	78	79	78.8	78.8	78.8
A (g/ ft2- min-psi)	0.00023	0.00023	0.00023251	0.000234	0.000234	0.000236	0.000233	0.00023341	0.00023	0.00023341
A (g/ ft2- min-psi) average			0.0002332					0.00023377		
A (m3/m2-s-atm)			2.3268E-06					2.3325E-06		

NF - MgCl2 pH = 7.5  
 Distilled water before MgCl Biocide = 0.2 ppm

Table C-2. Readings for MgCl<sub>2</sub> solution at 800 mg/l and 800 psi feed pressure

Description	HPP Only						HPP + Permeate Pump						Average
	1	2	3	4	5	Average	1	2	3	4	5	Average	
Pre-filter inlet press (psi)	21.5	22	22	22	22.5	22	22	22	22	22	22	22	22
Pre-filter outlet press (psi)	20.5	21	21	21	21.5	21	21	21	21	21	21	21	21
HPP Press (psi)	80	80	80	80	81	80.2	79	79	79	79	79	79	79
Conc. Press (psi)	76	76	76	76	76	76	76	75	75	75	75	75	75.2
(Sue) Perm. Press. (psi)	5.5	6	5.8	5.8	6	5.82	1.2	1.2	1.2	1.2	1.2	1.2	1.2
(Disch) Perm Press (psi)	0	0	0	0	0	0	0	0	0	0	0	0	0
Feed TDS ( mg/l)	830	830	840	840	840	836	830	830	840	830	830	830	832
Feed TDS ( Mcl/l)	0.017435	0.017435	0.017645	0.017645	0.017645	0.017561	0.017435	0.017435	0.017645	0.017435	0.017435	0.017435	0.017477
Conc. TDS (mg/l)	1280	1300	1320	1320	1320	1308	1330	1330	1330	1330	1330	1330	1331
Conc. TDS (Mcl/l)	0.026888	0.027308	0.027728	0.027728	0.027728	0.027476	0.027938	0.027938	0.028043	0.027938	0.027938	0.027938	0.027959
Perm TDS (mg/l)	98	102	102	101	101	100.8	93	92	94	93	93	93	93
Perm TDS (Mcl/l)	0.002059	0.002143	0.002143	0.002122	0.002122	0.002117	0.001954	0.001933	0.001975	0.001954	0.001954	0.001954	0.001954
Perm Flow ( gpm)	0.4215	0.421	0.421	0.421	0.421	0.4211	0.45	0.45	0.45	0.45	0.45	0.45	0.45
Perm Flow ( m3/s)	0.000027	0.000027	0.000027	0.000027	0.000027	0.000027	0.000028	0.000028	0.000028	0.000028	0.000028	0.000028	0.000028
Conc Flow (gpm)	1.55	1.55	1.55	1.55	1.55	1.55	1.55	1.55	1.55	1.55	1.55	1.55	1.55
Feed Flow (gpm)	1.9715	1.971	1.971	1.971	1.971	1.9711	2	2	2	2	2	2	2
HPP (RPM)	800	800	800	800	800	800	800	800	800	800	800	800	800
Perm Pump (RPM)	0	0	0	0	0	0	210	210	210	210	210	210	210
Temp C	25	25	25	25	25	25	25	25	25	25	25	25	25
Surface Area (ft2)	28	28	28	28	28	28	28	28	28	28	28	28	28
Flux (gpm/ft2)	0.015054	0.015036	0.015036	0.015036	0.015036	0.015039	0.016071	0.016071	0.016071	0.016071	0.016071	0.016071	0.016071
Surface Area (m2)	2.6	2.6	2.6	2.6	2.6	2.6	2.6	2.6	2.6	2.6	2.6	2.6	2.6
Flux (m3/m2.s)	1.022E-05	1.022E-05	1.022E-05	1.022E-05	1.022E-05	1.022E-05	1.092E-05	1.092E-05	1.092E-05	1.092E-05	1.092E-05	1.092E-05	1.092E-05
Delta P (psi)	74.5	74	74.2	74.2	75	74.38	77.8	77.8	77.8	77.8	77.8	77.8	77.8
Delta P (atm)	5.06803	5.03401	5.04762	5.04762	5.10204	5.05986	5.29252	5.29252	5.29252	5.29252	5.29252	5.29252	5.29252
Pi Product (atm)	0.050365	0.052421	0.052421	0.051907	0.051907	0.051804	0.047796	0.047796	0.048310	0.047796	0.047796	0.047796	0.047795807
Delta Pi (atm)	6.72E-01	6.44E-01	6.57E-01	6.57E-01	7.12E-01	6.68E-01	6.11E-01	6.11E-01	6.11E-01	6.11E-01	6.11E-01	6.11E-01	6.11E-01
Pi Feed I (atm)	0.72267	0.69593	0.70953	0.70902	0.76344	0.72012	0.65886	0.65834	0.65937	0.65886	0.65886	0.65886	0.658857256
c mem (mg/l)	1406.2	1354.1	1380.6	1379.6	1485.5	1401.2	1282.0	1281.0	1283.0	1282.0	1282.0	1282.0	1281.989539
C mem (mol/l)	0.029537908	0.028444811	0.0290009	0.028979905	0.031204307	0.029433569	0.026929725	0.026929725	0.026950731	0.026929725	0.026929725	0.026929725	0.026929725
A (m3/m2-s-atm)	2.33E-06	2.33E-06	2.33E-06	2.33E-06	2.33E-06	2.33E-06	2.33E-06	2.33E-06	2.33E-06	2.33E-06	2.33E-06	2.33E-06	2.33E-06
C mem - Cp	0.027479	0.026302	0.026858	0.026858	0.029083	0.027316	0.024976	0.024976	0.024976	0.024976	0.024976	0.024976	0.024976
CF - Cp	0.015377	0.015293	0.015503	0.015524	0.015524	0.015444	0.015482	0.015503	0.015482	0.015482	0.015482	0.015482	0.015524
ln (C mem-Cp/C-Cp)	0.5805903	0.5422885	0.5495681	0.5482140	0.6377827	0.5702731	0.4782712	0.4769153	0.4661335	0.4782712	0.4782712	0.4782712	0.4755612
Mass Transf Coef. (m/s)	0.0000176	0.0000188	0.0000186	0.0000186	0.0000163	0.0000179	0.0000228	0.0000228	0.0000234	0.0000228	0.0000228	0.0000228	0.0000230
Diffus. Coef. (m2/s)	1.2243E-09	1.2243E-09	1.2243E-09	1.2243E-09	1.2243E-09	1.2243E-09	1.2243E-09	1.2243E-09	1.2243E-09	1.2243E-09	1.2243E-09	1.2243E-09	1.2243E-09
d F (m)	6.94973E-05	6.49897E-05	6.5861E-05	6.56998E-05	7.52356E-05	6.83272E-05	5.36238E-05	5.34718E-05	5.22629E-05	5.36238E-05	5.36238E-05	5.36238E-05	5.33212E-05
h d (m)	8.78E-04	8.78E-04	8.78E-04	8.78E-04	8.78E-04	8.78E-04	8.78E-04	8.78E-04	8.78E-04	8.78E-04	8.78E-04	8.78E-04	8.78E-04
Vw - Flux/4 (m/s)	2.56E-06	2.55E-06	2.55E-06	2.55E-06	2.55E-06	2.55E-06	2.73E-06	2.73E-06	2.73E-06	2.73E-06	2.73E-06	2.73E-06	2.73E-06
Pc	1.8331	1.8309	1.8309	1.8309	1.8309	1.8314	1.9571	1.9571	1.9571	1.9571	1.9571	1.9571	1.9571
NF- MgCl2	pH = 6.5												
Feed - 840 mg/l	Biocide 0.2 mg/l												

Table C-3. Readings for MgCl2 solution at 800 mg/l and 100 psi feed pressure

Description	HPP Only					HPP - Permeate Pump					Average
	1	2	3	4	Average	1	2	3	4	Average	
Pre-filter inlet press (psi)	12	12	12	12	12	12.5	12	12	12	12	12.125
Pre-filter outlet press (psi)	11	11	11	11	11	11	11	11	11	11	11
HPP Press (psi)	100	100	100	100	100	92	92	92	92	92	92
Conc. Press (psi)	92	92	92	92	92	90	90	90	90	90	90
(Suc) Perm. Press. (psi)	10.5	10.5	10.5	10.5	10.5	1.7	1.2	1.1	1.2	1.3	1.3
(Disch) Perm Press (psi)	0	0	0	0	0	0	0	0	0	0	0
Feed TDS ( mg/l)	830	850	830	850	840	840	870	870	870	862.5	862.5
Feed TDS ( Mol/l)	0.01743514	0.017855	0.017435	0.01785527	0.017645205	0.0176452	0.01827539	0.018275	0.0182754	0.018117845	0.018117845
Conc. TDS (mg/l)	1340	1340	1340	1340	1340	1370	1370	1370	1370	1370	1370
Conc. TDS (Mol/l)	0.0281483	0.028148	0.028148	0.0281483	0.028148304	0.0287785	0.02877849	0.028778	0.0287785	0.02877849	0.02877849
Perm TDS (mg/l)	93	98	93	98	95.5	93	93	93	93	93	93
Perm TDS (Mol/l)	0.00195358	0.002059	0.001954	0.00205861	0.002006092	0.0019536	0.00195358	0.001954	0.0019536	0.001953576	0.001953576
Perm Flow ( gpm)	0.51	0.51	0.51	0.51	0.51	0.525	0.525	0.525	0.525	0.525	0.525
Perm Flow ( m3/s)	0.000032	0.000032	0.000032	0.000032	0.000032	0.000033	0.000033	0.000033	0.000033	0.000033	0.000033
Conc Flow (gpm)	1.7	1.7	1.7	1.7	1.7	1.7	1.7	1.7	1.7	1.7	1.7
Feed Flow (gpm)	2.21	2.21	2.21	2.21	2.21	2.225	2.225	2.225	2.225	2.225	2.225
HPP (RPM)	940	940	940	940	940	940	940	940	940	940	940
Perm Pump (RPM)	0	0	0	0	0	250	250	250	250	250	250
Temp C	25	25	25	25	25	25	25	25	25	25	25
Surface Area (ft2)	28	28	28	28	28	28	28	28	28	28	28
Flux (gpm/ft2)	0.01821429	0.018214	0.018214	0.01821429	0.018214286	0.01875	0.01875	0.01875	0.01875	0.01875	0.01875
Surface Area (m2)	2.6	2.6	2.6	2.6	2.6	2.6	2.6	2.6	2.6	2.6	2.6
Flux (m3/m2.s)	1.23755E-05	1.24E-05	1.24E-05	1.23755E-05	1.23755E-05	1.274E-05	1.2739E-05	1.27E-05	1.274E-05	1.27395E-05	1.27395E-05
Delta P (psi)	89.5	89.5	89.5	89.5	89.5	90.3	90.8	90.9	90.8	90.7	90.7
Delta P (atm)	6.08843337	6.088435	6.088435	6.08843537	6.088435374	6.1428571	6.17687075	6.183673	6.1768707	6.170068027	6.170068027
Pi Product (atm)	0.047796	0.050365	0.047796	0.050365	0.049080641	0.047796	0.047796	0.047796	0.047796	0.047796	0.047796
Delta Pi (atm)	7.70E-01	7.70E-01	7.70E-01	7.70E-01	7.70E-01	6.81E-01	7.15E-01	7.22E-01	7.15E-01	7.08369876	7.08369876
Pi Feed ( atm)	0.81756	0.82013	0.81756	0.82013	0.818846244	0.72895	0.76297	0.76977	0.76297	0.756165683	0.756165683
c mem (mg/l)	1590.8	1595.8	1590.8	1595.8	1593.292491	1418.4	1484.6	1497.8	1484.6	1471.330076	1471.330076
C mem (mol/l)	0.0334165	0.033522	0.033417	0.03352153	0.033469016	0.0297948	0.0311851	0.031463	0.0311851	0.030907049	0.030907049
A (m3/m2-s-atm)	2.33E-06	2.33E-06	2.33E-06	2.33E-06	2.3268E-06	2.33E-06	2.33E-06	2.33E-06	2.33E-06	2.33251E-06	2.33251E-06
C mem - Cp	0.031463	0.031463	0.031463	0.031463	0.031462924	0.027841	0.029232	0.029510	0.029232	0.028953473	0.028953473
Cf - Cp	0.015482	0.015797	0.015482	0.015797	0.015639114	0.015692	0.016322	0.016322	0.016322	0.016164268	0.016164268
ln (C mem-Cp/Cf-Cp)	0.70915974	0.689011	0.70916	0.68901131	0.699085522	0.5733921	0.58274513	0.592212	0.5827451	0.582773644	0.582773644
Mass Transf Coef. (m/s)	1.7451E-05	1.8E-05	1.75E-05	1.7961E-05	1.7776E-05	2.222E-05	2.1861E-05	2.15E-05	2.186E-05	2.18629E-05	2.18629E-05
Diffus. Coef. ( m2/s)	1.22E-09	1.22E-09	1.22E-09	1.22E-09	1.2243E-09	1.22E-09	1.22E-09	1.22E-09	1.22E-09	1.2243E-09	1.2243E-09
d F (m)	7.0157E-05	6.82E-05	7.02E-05	6.8164E-05	6.91602E-05	5.51E-05	5.6004E-05	5.69E-05	5.6E-05	5.60063E-05	5.60063E-05
h d (m)	8.78E-04	8.78E-04	8.78E-04	8.78E-04	8.78E-04	8.78E-04	8.78E-04	8.78E-04	8.78E-04	8.78E-04	8.78E-04
Vw = Flux/4 (m/s)	3.09E-06	3.09E-06	3.09E-06	3.09E-06	3.09E-06	3.18E-06	3.18E-06	3.18E-06	3.18E-06	3.18E-06	3.18E-06
Pe	2.2180	2.2180	2.2180	2.2180	2.2180	2.2832	2.2832	2.2832	2.2832	2.2832	2.2832

pH = 6.5

Biocide = 0.2 ppm

Feed = 800 ppm

Table C-4. Readings for MgCl2 solution at 800 mg/l and 130 psi feed pressure

Description	HPP Only											HPP + Permeate Pump										
	1	2	3	4	5	Average	1	2	3	4	5	Average	1	2	3	4	5	Average				
Pre-filter inlet press (psi)	7.5	7.5	6	6	6	6.6	7.5	7.5	8	8	8	7.9	7.5	7.5	8	8	8	7.9				
Pre-filter outlet press (psi)	6.2	6.2	5	5	5	5.48	6.2	6.2	6.2	6.2	6.2	6.2	6.2	6.2	6.2	6.2	6.2	6.2				
HPP Press (psi)	132	132	132	132	132	132	132	132	130	130	130	130	130	130	130	130	130	130				
Conc. Press (psi)	125	125	125	125	125	125	122	122	122	122	122	122	122	122	122	122	122	122				
(Sue) Perm. Press. (psi)	5	5	5	5	5	5	1.8	1	0.8	0.8	0.8	1.04	0.8	0.8	0.8	0.8	0.8	0.8				
(Disch) Perm Press (psi)	0	0	0	0	0	0	0	0	0	0	0	0	0	0	0	0	0	0				
Feed TDS ( mg/l)	830	830	830	840	840	834	850	850	850	850	850	850	850	850	850	850	850	850				
Feed TDS ( Mol/l)	0.01744	0.01744	0.01744	0.01765	0.01765	0.01752	0.01786	0.01786	0.01786	0.01786	0.01786	0.01786	0.01786	0.01786	0.01786	0.01786	0.01786	0.01786				
Conc. TDS (mg/l)	1410	1390	1400	1400	1400	1400	1450	1450	1450	1450	1450	1450	1450	1450	1450	1450	1450	1450				
Conc. TDS (Mol/l)	0.02962	0.02920	0.02941	0.02941	0.02941	0.02941	0.03046	0.03046	0.03046	0.03046	0.03046	0.03046	0.03046	0.03046	0.03046	0.03046	0.03046	0.03046				
Perm TDS (mg/l)	85	87	89	87	87	87	82	85	86	87	88	85.6	87	88	86	87	88	85.6				
Perm TDS (Mol/l)	0.001786	0.001828	0.001870	0.001828	0.001828	0.001828	0.001723	0.001786	0.001807	0.001828	0.001849	0.001798	0.001828	0.001828	0.001807	0.001828	0.001849	0.001798				
Perm Flow ( gpm)	0.7	0.7	0.7	0.7	0.7	0.7	0.73	0.73	0.73	0.73	0.73	0.73	0.73	0.73	0.73	0.73	0.73	0.73				
Perm Flow ( m3/s)	0.000044	0.000044	0.000044	0.000044	0.000044	0.000044	0.000046	0.000046	0.000046	0.000046	0.000046	0.000046	0.000046	0.000046	0.000046	0.000046	0.000046	0.000046				
Conc Flow (gpm)	1.7	1.7	1.7	1.7	1.7	1.7	1.7	1.7	1.7	1.7	1.7	1.7	1.7	1.7	1.7	1.7	1.7	1.7				
Feed Flow (gpm)	2.4	2.4	2.4	2.4	2.4	2.4	2.43	2.43	2.43	2.43	2.43	2.43	2.43	2.43	2.43	2.43	2.43	2.43				
HPP (RPM)	1090	1090	1090	1090	1090	1090	1090	1090	1090	1090	1090	1090	1090	1090	1090	1090	1090	1090				
Perm Pump (RPM)	0	0	0	0	0	0	500	515	515	515	515	515	515	515	515	515	515	515				
Temp C	28	28	28	28	28	28	28	28	28	28	28	28	28	28	28	28	28	28				
Surface Area (ft2)	0.025	0.025	0.025	0.025	0.025	0.025	0.025	0.025	0.025	0.025	0.025	0.025	0.025	0.025	0.025	0.025	0.025	0.025				
Flux (gpm/ft2)	1.6986E-05	1.6986E-05	1.6986E-05	1.6986E-05	1.6986E-05	1.6986E-05	0.026071429	0.026071429	0.026071429	0.026071429	0.026071429	0.026071429	0.026071429	0.026071429	0.026071429	0.026071429	0.026071429	0.026071429				
Surface Area (m2)	2.6	2.6	2.6	2.6	2.6	2.6	2.6	2.6	2.6	2.6	2.6	2.6	2.6	2.6	2.6	2.6	2.6	2.6				
Flux (m3/m2.s)	1.6986E-05	1.6986E-05	1.6986E-05	1.6986E-05	1.6986E-05	1.6986E-05	1.77139E-05	1.77139E-05	1.77139E-05	1.77139E-05	1.77139E-05	1.77139E-05	1.77139E-05	1.77139E-05	1.77139E-05	1.77139E-05	1.77139E-05	1.77139E-05				
Delta P (psi)	127	127	127	127	127	127	128.2	129	129.2	129.2	129.2	128.96	129.2	129.2	129.2	129.2	129.2	128.96				
Delta P (atm)	8.63946	8.63946	8.63946	8.63946	8.63946	8.63946	8.72109	8.77551	8.78912	8.78912	8.78912	8.77279	8.78912	8.78912	8.78912	8.78912	8.77279	8.77279				
Pi Product (atm)	0.06960	0.07124	0.07287	0.07124	0.07124	0.07124	0.06714	0.06960	0.07042	0.07124	0.07205	0.07009	0.07124	0.07205	0.07042	0.07124	0.07205	0.07009				
Delta Pi (atm)	1.34E+00	1.34E+00	1.34E+00	1.34E+00	1.34E+00	1.34E+00	1.13E+00	1.18E+00	1.19E+00	1.19E+00	1.19E+00	1.178427877	1.19E+00	1.19E+00	1.19E+00	1.19E+00	1.19E+00	1.178427877				
Pi Feed ( atm)	1.40892	1.41056	1.41219	1.41056	1.41056	1.41056	1.19387	1.25075	1.26517	1.26599	1.26681	1.248517318	1.26517	1.26599	1.26517	1.26599	1.26681	1.248517318				
Cmem (mg/l)	2741.4	2744.6	2747.8	2744.6	2744.6	2744.6	2323.0	2433.7	2461.7	2463.3	2464.9	2429.336744	2463.3	2464.9	2461.7	2463.3	2464.9	2429.336744				
Cmem (atm)	0.057587	0.057654	0.057721	0.057654	0.057654	0.057654	0.048797	0.051122	0.051712	0.051745	0.051779	0.051031	0.051745	0.051779	0.051712	0.051745	0.051779	0.051031				
A ( m3/m2-s-atm)	2.33E-06	2.33E-06	2.33E-06	2.33E-06	2.33E-06	2.33E-06	2.33E-06	2.33E-06	2.33E-06	2.33E-06	2.33E-06	2.33251E-06	2.33E-06	2.33E-06	2.33E-06	2.33E-06	2.33E-06	2.33251E-06				
C mem - Cp	0.055802	0.055827	0.055852	0.055827	0.055827	0.055827	0.047075	0.049337	0.049905	0.049918	0.049930	0.049233	0.049918	0.049930	0.049905	0.049918	0.049930	0.049233				
Cf - Cp	0.015650	0.015608	0.015566	0.015818	0.015818	0.015818	0.016133	0.016070	0.016049	0.016028	0.016007	0.016057	0.016028	0.016007	0.016049	0.016028	0.016007	0.016057				
ln (Cmem-Cp/Cf-Cp)	1.27136	1.27449	1.27764	1.26112	1.26112	1.26915	1.07089	1.12173	1.13450	1.13606	1.13762	1.12016	1.13606	1.13762	1.13450	1.13606	1.13762	1.12016				
Mass Transf Coef. (m/s)	1.3360E-05	1.3328E-05	1.3295E-05	1.3469E-05	1.3469E-05	1.3384E-05	1.6541E-05	1.5792E-05	1.5661E-05	1.5592E-05	1.5571E-05	1.5822E-05	1.5592E-05	1.5571E-05	1.5661E-05	1.5592E-05	1.5571E-05	1.5822E-05				
Diffus. Coeff. ( m2/s)	1.22E-09	1.22E-09	1.22E-09	1.22E-09	1.22E-09	1.2243E-09	1.22E-09	1.22E-09	1.22E-09	1.22E-09	1.22E-09	1.2243E-09	1.22E-09	1.22E-09	1.22E-09	1.22E-09	1.22E-09	1.2243E-09				
d F (m)	9.1636E-05	9.18619E-05	9.2088E-05	9.0898E-05	9.08983E-05	9.14766E-05	7.40146E-05	7.529E-05	7.84109E-05	7.85187E-05	7.863E-05	7.74199E-05	7.85187E-05	7.863E-05	7.84109E-05	7.85187E-05	7.863E-05	7.74199E-05				
h d (m)	8.78E-04	8.78E-04	8.78E-04	8.78E-04	8.78E-04	8.78E-04	8.78E-04	8.78E-04	8.78E-04	8.78E-04	8.78E-04	8.78E-04	8.78E-04	8.78E-04	8.78E-04	8.78E-04	8.78E-04	8.78E-04				
Vw = Flux/A (m/s)	4.25E-06	4.25E-06	4.25E-06	4.25E-06	4.25E-06	4.25E-06	4.43E-06	4.43E-06	4.43E-06	4.43E-06	4.43E-06	4.43E-06	4.43E-06	4.43E-06	4.43E-06	4.43E-06	4.43E-06	4.43E-06				
Pe	3.0443	3.0443	3.0443	3.0443	3.0443	3.0443	3.1748	3.1748	3.1748	3.1748	3.1748	3.1748	3.1748	3.1748	3.1748	3.1748	3.1748	3.1748				

pH = 6.7

Biocide 0.2 mg/l

TDS = 800 mg/l

Table C-5. Readings for MgCl2 solution at 1,250 mg/l and 80 psi feed pressure

Description	HPP Only						HPP + Permeate Pump						Average
	1	2	3	4	Average		1	2	3	4	5	6	
Pre-filter inlet press (psi)	21.5	21.5	21	21	21.25		21	21	21.5	21	21.5	21.5	21.25
Pre-filter outlet press (psi)	20.5	20.5	20	20	20.25		20	20	20.5	20	20.5	20.5	20.25
HPP Press (psi)	80	80	80	80	80		80	80	80	80	80	80	80
Conc. Press (psi)	76	75	76	76	75.75		75	75	75	75	75	75	75
(Suc) Perm. Press. (psi)	3	3	3	3	3		0.8	0.8	0.8	0.8	0.8	0.8	0.8
(Disch) Perm Press (psi)	0	0	0	0	0		0	0	0	0	0	0	0
Feed TDS ( mg/l)	1260	1270	1260	1270	1265		1270	1270	1270	1270	1270	1260	1268.333333
Feed TDS ( Mol/l)	0.02646781	0.02667787	0.026467808	0.02667787	0.026572839		0.02667787	0.02667787	0.02667787	0.02667787	0.02667787	0.026467808	0.02664286
Conc. TDS (mg/l)	1890	1930	1890	1870	1895		1940	1930	1950	1920	1950	1900	1931.666667
Conc. TDS (Mol/l)	0.03970171	0.04054196	0.039701712	0.03928159	0.039806743		0.040752022	0.04054196	0.040962084	0.040331898	0.04096208	0.039911774	0.04057697
Perm TDS (mg/l)	139	141	139	143	140.5		134	128	132	128	133	128	130.5
Perm TDS (Mol/l)	0.00291986	0.00296187	0.002919861	0.00300389	0.002951371		0.00281483	0.002688793	0.002772818	0.002688793	0.00279382	0.002688793	0.002741309
Perm Flow ( gpm)	0.405	0.405	0.405	0.405	0.405		0.425	0.425	0.425	0.425	0.425	0.425	0.425
Perm Flow ( m3/s)	0.000026	0.000026	0.000026	0.000026	0.000026		0.000027	0.000027	0.000027	0.000027	0.000027	0.000027	0.000027
Conc Flow (gpm)	1.6	1.6	1.6	1.6	1.6		1.6	1.6	1.6	1.6	1.6	1.6	1.6
Feed Flow (gpm)	2.005	2.005	2.005	2.005	2.005		2.025	2.025	2.025	2.025	2.025	2.025	2.025
HPP (RPM)	800	800	800	800	800		800	800	800	800	800	800	800
Perm Pump (RPM)	0	0	0	0	0		110	110	110	110	110	110	110
Temp C	25	25	25	25	25		25	25	25	25	25	25	25
Surface Area (ft2)	28	28	28	28	28		28	28	28	28	28	28	28
Flux (gpm/ft2)	0.01446429	0.01446429	0.014464286	0.01446429	0.014464286		0.015178571	0.01517857	0.015178571	0.015178571	0.01517857	0.015178571	0.015178571
Surface Area (m2)	2.6	2.6	2.6	2.6	2.6		2.6	2.6	2.6	2.6	2.6	2.6	2.6
Flux (m3/m2.s)	9.8276E-06	9.8276E-06	9.82759E-06	9.8276E-06	9.82759E-06		1.03129E-05	1.0313E-05	1.03129E-05	1.03129E-05	1.0313E-05	1.03129E-05	1.03129E-05
Delta P (psi)	77	77	77	77	77		79.2	79.2	79.2	79.2	79.2	79.2	79.2
Delta P (atm)	5.23809524	5.23809524	5.238095238	5.23809524	5.238095238		5.387755102	5.3877551	5.387755102	5.387755102	5.3877551	5.387755102	5.387755102
Pi Product (atm)	0.071437	0.072465	0.071437	0.073492	0.072207644		0.068867	0.065783	0.067839	0.065783	0.068353	0.065783	0.06706831
Delta Pi (atm)	1.01E+00	1.01E+00	1.01E+00	1.01E+00	1.014445714		9.66E-01	9.66E-01	9.66E-01	9.66E-01	9.66E-01	9.66E-01	9.66E-01
Pi Feed ( atm)	1.08588	1.08691	1.08588	1.08794	1.086653358		1.03525	1.03216	1.03422	1.03216	1.03473	1.03216	1.033448719
c mem (mg/l)	2112.9	2114.9	2112.9	2116.9	2114.385514		2014.4	2008.4	2012.4	2008.4	2013.4	2008.4	2010.86113
Cmem (mol/l)	0.0438369	0.0444257	0.04383689	0.04446771	0.044415198		0.042314066	0.04218803	0.042272054	0.042188029	0.04229306	0.042188029	0.042240545
A (m3/m2-s-atm)	2.3268E-06	2.3268E-06	2.3268E-06	2.3268E-06	2.3268E-06		2.3325E-06	2.3325E-06	2.3325E-06	2.3325E-06	2.3325E-06	2.3325E-06	2.3325E-06
C mem - Cp	0.041464	0.041464	0.041464	0.041464	0.041463828		0.039499	0.039499	0.039499	0.039499	0.039499	0.039499	0.039499
Cf - Cp	0.023548	0.023716	0.023548	0.023674	0.023621468		0.023863	0.023989	0.023905	0.023989	0.023884	0.023779	0.039499
ln (Cmem-Cp/Cf-Cp)	0.5657828	0.55867166	0.565782798	0.56044471	0.56267049		0.503950529	0.49868274	0.502191513	0.498682738	0.50307063	0.507477869	0.50234267
Mass Transf Coef. (m/s)	1.737E-05	1.7591E-05	1.73699E-05	1.7535E-05	1.74665E-05		2.04641E-05	2.068E-05	2.05358E-05	2.06803E-05	2.05E-05	2.03219E-05	2.05304E-05
Diffus. Coef. ( m2/s)	1.22E-09	1.22E-09	1.22E-09	1.22E-09	1.2243E-09		1.22E-09	1.22E-09	1.22E-09	1.22E-09	1.22E-09	1.22E-09	1.2243E-09
d F (m)	7.0484E-05	6.9598E-05	7.0484E-05	6.9819E-05	7.00963E-05		5.98267E-05	5.9201E-05	5.96179E-05	5.92013E-05	5.9722E-05	6.02454E-05	5.96358E-05
h d (m)	8.78E-04	8.78E-04	8.78E-04	8.78E-04	8.78E-04		8.78E-04	8.78E-04	8.78E-04	8.78E-04	8.78E-04	8.78E-04	8.78E-04
Vw = Flux/A (m/s)	2.46E-06	2.46E-06	2.46E-06	2.46E-06	2.46E-06		2.58E-06	2.58E-06	2.58E-06	2.58E-06	2.58E-06	2.58E-06	2.58E-06
Pe	1.7613	1.7613	1.7613	1.7613	1.7613		1.8483	1.8483	1.8483	1.8483	1.8483	1.8483	1.8483

pH = 6.7

NF - MgCl2

Biocide 0.2 mg/l

Table C-6. Readings for MgCl2 solution at 1,250 mg/l and 100 psi feed pressure

Description	HPP Only					HPP + Permeate Pump					Average
	1	2	3	4	5	1	2	3	4	5	
Pre-filler inlet press (psi)	21.5	21.5	21.5	21.5	21.5	20.5	22	22	22	22	21.7
Pre-filler outlet press (psi)	20.5	20.5	20.5	20.5	20.5	19	21	21	21	21	20.6
HPP Press (psi)	100	100	100	100	100	96	96	96	96	96	96
Conc. Press (psi)	95	95	95	95	95	90	90	90	90	90	90
(Suc) Perm. Press. (psi)	6.5	6.5	6.5	6.5	6.5	1	1	1	1	1	1
(Disch) Perm Press (psi)	0	0	0	0	0	0	0	0	0	0	0
Feed TDS ( mg/l)	1230	1250	1280	1300	1280	1270	1290	1280	1260	1261	1272.2
Feed TDS ( Mol/l)	0.025837622	0.0262577	0.0268879	0.0273081	0.0268879	0.0266779	0.027098	0.0268879	0.0264678	0.026488814	0.026724084
Conc. TDS (mg/l)	1950	2000	2100	2100	2100	2110	2130	2120	2120	2120	2120
Conc. TDS (Mol/l)	0.040962084	0.0420124	0.044113	0.044113	0.044113	0.0443231	0.0447432	0.0445331	0.0445331	0.044533137	0.044533137
Perm TDS (mg/l)	125	133	131	133	133	122	120	123	121	121	121.4
Perm TDS (Mol/l)	0.002625775	0.0027938	0.0027518	0.0027938	0.0027938	0.0025628	0.0025207	0.0025838	0.0025417	0.00254175	0.002550152
Perm Flow ( gpm)	0.495	0.495	0.495	0.495	0.495	0.515	0.515	0.515	0.515	0.515	0.515
Perm Flow ( m3/s)	0.000031	0.000031	0.000031	0.000031	0.000031	0.000032	0.000032	0.000032	0.000032	0.000032	0.000032
Conc Flow (gpm)	1.45	1.45	1.45	1.45	1.45	1.45	1.45	1.45	1.45	1.45	1.45
Conc Flow (gpm)	1.945	1.945	1.945	1.945	1.945	1.965	1.965	1.965	1.965	1.965	1.965
HPP (RPM)	900	900	900	900	900	900	900	900	900	900	900
Perm Pump (RPM)	0	0	0	0	0	0	0	0	0	0	0
Temp C	25	25	25	25	25	25	25	25	25	25	25
Surface Area (ft2)	28	28	28	28	28	28	28	28	28	28	28
Flux (gpm/ft2)	0.017678571	0.0176786	0.0176786	0.0176786	0.0176786	0.0183929	0.0183929	0.0183929	0.0183929	0.018392857	0.018392857
Surface Area (m2)	2.6	2.6	2.6	2.6	2.6	2.6	2.6	2.6	2.6	2.6	2.6
Flux (m3/m2.s)	1.201E-05	1.201E-05	1.201E-05	1.201E-05	1.201E-05	1.250E-05	1.250E-05	1.250E-05	1.250E-05	1.250E-05	1.250E-05
Delta P (psi)	93.5	93.5	93.5	93.5	93.5	95	95	95	95	95	95
Delta P (atm)	6.360544218	6.3605442	6.3605442	6.3605442	6.3605442	6.462585	6.462585	6.462585	6.462585	6.462585034	6.462585034
Pi Product (atm)	0.064242	0.068353	0.067325	0.068353	0.068353	0.062700	0.061672	0.063214	0.062186	0.062186	0.062391516
Delta Pi (atm)	1.20E+00	1.20E+00	1.20E+00	1.20E+00	1.20E+00	1.10E+00	1.10E+00	1.10E+00	1.10E+00	1.10E+00	1.104919229
Pi Feed ( atm)	1.26255	1.26666	1.26563	1.26666	1.26666	1.16762	1.16659	1.16813	1.16711	1.16711	1.167310745
c mem (mg/l)	2456.6	2464.6	2462.6	2464.6	2464.6	2271.9	2269.9	2272.9	2270.9	2270.9	2271.326832
Cmem (mol/l)	0.05160459	0.0517726	0.0517306	0.0517726	0.0517726	0.0477245	0.0476825	0.0477455	0.0477035	0.047703536	0.047711938
A (m3/m2-s-atm)	2.33E-06	2.33E-06	2.33E-06	2.33E-06	2.33E-06	2.33E-06	2.33E-06	2.33E-06	2.33E-06	2.33E-06	2.33251E-06
C mem - Cp	0.048979	0.048979	0.048979	0.048979	0.048979	0.048979	0.048979	0.048979	0.048979	0.048979	0.045161786
Cf - Cp	0.023212	0.023464	0.024136	0.024514	0.024094	0.024115	0.024577	0.024304	0.023926	0.023947	0.024174
In (Cmem-Cp/Cf-Cp)	0.746725057	0.7359239	0.7076784	0.692134	0.7094206	0.6274125	0.6084301	0.6196034	0.6352831	0.634405548	0.625026922
Mass Transf Coef. (m/s)	1.60856E-05	1.632E-05	1.697E-05	1.735E-05	1.693E-05	1.992E-05	2.054E-05	2.017E-05	1.967E-05	1.96985E-05	1.99992E-05
Diffus. Coef. ( m2/s)	1.22E-09	1.22E-09	1.22E-09	1.22E-09	1.22E-09	1.22E-09	1.22E-09	1.22E-09	1.22E-09	1.22E-09	1.2243E-09
d F (m)	7.61117E-05	7.501E-05	7.213E-05	7.053E-05	7.231E-05	6.147E-05	5.961E-05	6.07E-05	6.224E-05	6.21521E-05	6.12333E-05
h d (m)	8.78E-04	8.78E-04	8.78E-04	8.78E-04	8.78E-04	8.78E-04	8.78E-04	8.78E-04	8.78E-04	8.78E-04	8.78E-04
Vw = Flux/A (m/s)	3.00E-06	3.00E-06	3.00E-06	3.00E-06	3.00E-06	3.12E-06	3.12E-06	3.12E-06	3.12E-06	3.12E-06	3.12E-06
Pe	2.1528	2.1528	2.1528	2.1528	2.1528	2.2397	2.2397	2.2397	2.2397	2.2397	2.2397

pH = 6.7

Biocide = 0.2 mg/l

NF- MgCl2

TDS = 1260 mg/l



Table C-7. Readings for MgCl2 solution at 1,250 mg/l and 130 psi feed pressure

Description	HPP Only						HPP + Permteate Pump						Average
	1	2	3	4	5	Average	1	2	3	4	5	Average	
Pre-filter inlet press (psi)	7.5	7.5	6	6	6	6.6	7.5	8	8	8	8	7.9	
Pre-filter outlet press (psi)	6.2	6.2	5	5	5	5.48	6.2	6.2	6.2	6.2	6.2	6.2	
HPP Press (psi)	132	132	132	132	132	132	130	130	130	130	130	130	
Conc. Press (psi)	125	125	125	125	125	125	122	122	122	122	122	122	
(Suc) Perm. Press. (psi)	5	5	5	5	5	5	1.8	1	0.8	0.8	0.8	1.04	
(Disch) Perm Press (psi)	0	0	0	0	0	0	0	0	0	0	0	0	
Feed TDS ( mg/l)	830	830	830	840	840	834	850	850	850	850	850	850	
Feed TDS ( Mol/l)	0.01744	0.01744	0.01744	0.01765	0.01765	0.01752	0.01786	0.01786	0.01786	0.01786	0.01786	0.01786	
Conc. TDS (mg/l)	1410	1390	1400	1400	1400	1400	1450	1450	1450	1450	1450	1450	
Conc. TDS (Mol/l)	0.029619	0.029199	0.029409	0.029409	0.029409	0.029409	0.030459	0.030459	0.030459	0.030459	0.030459	0.030459	
Perm TDS (mg/l)	85	87	89	87	87	87	82	85	86	87	88	85.6	
Perm TDS (Mol/l)	0.00179	0.00183	0.00187	0.00183	0.00183	0.00183	0.00172	0.00179	0.00181	0.00183	0.00185	0.00180	
Perm Flow ( gpm)	0.7	0.7	0.7	0.7	0.7	0.7	0.73	0.73	0.73	0.73	0.73	0.73	
Perm Flow ( m3/s)	0.000044	0.000044	0.000044	0.000044	0.000044	0.000044	0.000046	0.000046	0.000046	0.000046	0.000046	0.000046	
Conc Flow (gpm)	1.7	1.7	1.7	1.7	1.7	1.7	1.7	1.7	1.7	1.7	1.7	1.7	
Feed Flow (gpm)	2.4	2.4	2.4	2.4	2.4	2.4	2.43	2.43	2.43	2.43	2.43	2.43	
HPP (RPM)	1000	1000	1000	1000	1000	1000	1000	1000	1000	1000	1000	1000	
Perm Pump (RPM)	0	0	0	0	0	0	500	515	515	515	515	512	
Temp C	25	25	25	25	25	25	25	25	25	25	25	25	
Surface Area (ft2)	28	28	28	28	28	28	28	28	28	28	28	28	
Flux (gpm/ft2)	0.025	0.025	0.025	0.025	0.025	0.025	0.026071	0.026071	0.026071	0.026071	0.026071	0.026071	
Surface Area (m2)	2.6	2.6	2.6	2.6	2.6	2.6	2.6	2.6	2.6	2.6	2.6	2.6	
Flux (m3/m2.s)	1.6986E-05	1.6986E-05	1.6986E-05	1.6986E-05	1.6986E-05	1.6986E-05	1.77139E-05	1.7714E-05	1.77139E-05	1.77139E-05	1.77139E-05	1.77139E-05	
Delta P (psi)	127	127	127	127	127	127	128.2	129	129.2	129.2	129.2	128.96	
Delta P (atm)	8.639456	8.639456	8.639456	8.639456	8.639456	8.639456	8.721088	8.775510	8.789116	8.789116	8.789116	8.772789	
PI Product (atm)	0.069598	0.071236	0.072873	0.071236	0.071236	0.071235763	0.067142	0.069598	0.070417	0.071236	0.072055	0.07008944	
Delta PI (atm)	1.34E+00	1.34E+00	1.34E+00	1.34E+00	1.34E+00	1.339320802	1.13E+00	1.18E+00	1.19E+00	1.19E+00	1.19E+00	1.178427877	
PI Feed ( atm)	1.40892	1.41056	1.41219	1.41056	1.41056	1.410556565	1.19387	1.25075	1.26517	1.26599	1.26681	1.248517318	
c mem (mg/l)	2741.4	2744.6	2747.8	2744.6	2744.6	2744.629045	2323.0	2433.7	2461.7	2463.3	2464.9	2429.336744	
Cmem (mol/l)	0.057587	0.057654	0.057721	0.057654	0.057654	0.057654	0.048797	0.051122	0.051712	0.051745	0.051779	0.051031	
A ( m3/m2.s-atm)	2.33E-06	2.33E-06	2.33E-06	2.33E-06	2.33E-06	2.3268E-06	2.33E-06	2.33E-06	2.33E-06	2.33E-06	2.33E-06	2.33251E-06	
C mem - Cp	0.055802	0.055827	0.055852	0.055827	0.055827	0.05583	0.047075	0.049337	0.049905	0.049918	0.049930	0.049233	
Cf - Cp	0.015650	0.015608	0.015566	0.015818	0.015818	0.01569	0.016133	0.016070	0.016049	0.016028	0.016007	0.016057	
ln (Cmem-Cp/Cf-Cp)	1.27136	1.27449	1.27764	1.26112	1.26915	1.26915	1.07089	1.12173	1.13450	1.13606	1.13762	1.12016	
Mass Transf Coef. (m/s)	1.336E-05	1.329E-05	1.329E-05	1.347E-05	1.347E-05	1.338E-05	1.654E-05	1.579E-05	1.561E-05	1.559E-05	1.557E-05	1.582E-05	
Diffus. Coef. ( m2/s)	1.224E-09	1.224E-09	1.224E-09	1.224E-09	1.224E-09	1.224E-09	1.224E-09	1.224E-09	1.224E-09	1.224E-09	1.224E-09	1.224E-09	
d F (m)	9.16E-05	9.19E-05	9.21E-05	9.09E-05	9.09E-05	9.15E-05	7.40E-05	7.75E-05	7.84E-05	7.85E-05	7.86E-05	7.74E-05	
h d (m)	8.78E-04	8.78E-04	8.78E-04	8.78E-04	8.78E-04	8.78E-04	8.78E-04	8.78E-04	8.78E-04	8.78E-04	8.78E-04	8.78E-04	
Vw = Flux/4 (m/s)	4.25E-06	4.25E-06	4.25E-06	4.25E-06	4.25E-06	4.25E-06	4.43E-06	4.43E-06	4.43E-06	4.43E-06	4.43E-06	4.43E-06	
Pe	3.0443	3.0443	3.0443	3.0443	3.0443	3.0443	3.1748	3.1748	3.1748	3.1748	3.1748	3.1748	

pH = 6.7

Biocide = 0.2 mg/l

Table C-8. Readings for MgCl2 solution at 1,750 mg/l and 80 psi feed pressure

Description	HPP Only					HPP + Permeate Pump					Average	
	1	2	3	4	5	Average	1	2	3	4		5
Pre-filter inlet press (psi)	21.5	22	22	22	21.5	21.8	21.5	21.5	21	21.5	21.5	21.4
Pre-filter outlet press (psi)	20.5	21	21	21	20.5	20.8	20.5	20.5	19.5	20.5	19.5	19.9
HPP Press (psi)	80	80	80	80	80	80	79	79	79	79	79	79
Conc. Press (psi)	75	75	75	75	75	75	75	75	75	75	75	75
(Suc) Perm. Press. (psi)	2.8	2.8	2.8	2.8	2.8	2.8	1.5	0.5	0.5	0.5	0.5	0.7
(Disch) Perm Press (psi)	0	0	0	0	0	0	0	0	0	0	0	0
Feed TDS ( mg/l)	1760	1760	1760	1760	1760	1760	1720	1730	1740	1730	1730	1730
Feed TDS ( Mol/l)	0.036971	0.036971	0.036971	0.036971	0.036971	0.036971	0.036131	0.036341	0.036551	0.036341	0.036341	0.036341
Conc. TDS (mg/l)	2610	2610	2620	2610	2610	2612	2620	2630	2640	2640	2640	2634
Conc. TDS (Mol/l)	0.054826	0.054826	0.055036	0.054826	0.054826	0.054868	0.055036	0.055246	0.055456	0.055456	0.055456	0.055330
Perm TDS (mg/l)	160	166	166	166	170	165.6	157	154	156	151	153	154.2
Perm TDS (Mol/l)	0.0033610	0.0034870	0.0034870	0.0034870	0.0035711	0.0034786	0.0032980	0.0032350	0.0032770	0.0031719	0.0032139	0.0032392
Perm Flow ( gpm)	0.37	0.37	0.37	0.37	0.37	0.385	0.385	0.385	0.385	0.385	0.385	0.385
Perm Flow ( m3/s)	0.000023	0.000023	0.000023	0.000023	0.000023	2.3344E-05	0.000024	0.000024	0.000024	0.000024	0.000024	2.429E-05
Conc Flow (gpm)	1.6	1.6	1.6	1.6	1.6	1.6	1.6	1.6	1.6	1.6	1.6	1.6
Feed Flow (gpm)	1.97	1.97	1.97	1.97	1.97	1.97	1.985	1.985	1.985	1.985	1.985	1.985
HPP (RPM)	800	800	800	800	800	800	800	800	800	800	800	800
Perm Pump (RPM)	0	0	0	0	0	0	90	80	80	80	80	82
Temp C	25	25	25	25	25	25	25	25	25	25	25	25
Surface Area (ft2)	28	28	28	28	28	28	28	28	28	28	28	28
Flux (gpm/ft2)	0.0132143	0.0132143	0.0132143	0.0132143	0.0132143	0.0132143	0.01375	0.01375	0.01375	0.01375	0.01375	0.01375
Surface Area (m2)	2.6	2.6	2.6	2.6	2.6	2.6	2.6	2.6	2.6	2.6	2.6	2.6
Flux (m3/m2.s)	8.9783E-06	8.9783E-06	8.9783E-06	8.9783E-06	8.9783E-06	8.9783E-06	9.3423E-06	9.3423E-06	9.3423E-06	9.3423E-06	9.3423E-06	9.3423E-06
Delta P (psi)	77.2	77.2	77.2	77.2	77.2	77.2	77.5	78.5	78.5	78.5	78.5	78.3
Delta P (atm)	5.251701	5.251701	5.251701	5.251701	5.251701	5.251701	5.272109	5.340136	5.340136	5.340136	5.340136	5.326531
Pi Product (atm)	0.082229	0.085313	0.085313	0.085313	0.087369	0.08510737	0.080688	0.079146	0.080174	0.077604	0.078632	0.07924853
Delta Pi (atm)	1.39E+00	1.39E+00	1.39E+00	1.39E+00	1.39E+00	1.39305791	1.27E+00	1.33E+00	1.33E+00	1.33E+00	1.33E+00	1.3212853
Pi Feed ( atm)	1.47529	1.47837	1.47837	1.47837	1.48043	1.47816528	1.34755	1.41404	1.41506	1.41249	1.41352	1.40053383
c mem (mg/l)	2870.6	2876.6	2876.6	2876.6	2880.6	2876.18	2622.0	2751.4	2753.4	2748.4	2750.4	2725.13
Cmem (mol/l)	0.060300	0.060426	0.060426	0.060426	0.060510	0.060418	0.055079	0.057796	0.057838	0.057733	0.057775	0.057245
A (m3/m2-s-attm)	2.33E-06	2.33E-06	2.33E-06	2.33E-06	2.33E-06	2.3268E-06	2.33E-06	2.33E-06	2.33E-06	2.33E-06	2.33E-06	2.3325E-06
C mem - Cp	0.056939	0.056939	0.056939	0.056939	0.056939	0.056939	0.051781	0.054561	0.054561	0.054561	0.054561	0.0540054
In (Cmem-Cp/Cf-Cp)	0.033610	0.033484	0.033484	0.033484	0.033400	0.033492	0.032833	0.033106	0.033274	0.033169	0.033127	0.03310156
Mass Transf Coef. (m/s)	0.527159	0.530916	0.530916	0.530916	0.533429	0.530665	0.455599	0.499621	0.494558	0.497719	0.498987	0.489297
Diffus. Coef. ( m2/s)	0.000017	0.000017	0.000017	0.000017	0.000017	0.000017	0.000021	0.000019	0.000019	0.000019	0.000019	0.000019
d F (m)	1.22E-09	1.22E-09	1.22E-09	1.22E-09	1.22E-09	1.22E-09	1.22E-09	1.22E-09	1.22E-09	1.22E-09	1.22E-09	1.2243E-09
h d (m)	7.188E-05	7.240E-05	7.240E-05	7.240E-05	7.274E-05	7.236E-05	5.971E-05	6.548E-05	6.481E-05	6.523E-05	6.539E-05	6.412E-05
h d (m)	8.78E-04	8.78E-04	8.78E-04	8.78E-04	8.78E-04	8.78E-04	8.78E-04	8.78E-04	8.78E-04	8.78E-04	8.78E-04	8.78E-04
Vw = Flux/A (m/s)	2.24E-06	2.24E-06	2.24E-06	2.24E-06	2.24E-06	2.24E-06	2.34E-06	2.34E-06	2.34E-06	2.34E-06	2.34E-06	2.34E-06
Pe	1.6091	1.6091	1.6091	1.6091	1.6091	1.6091	1.6744	1.6744	1.6744	1.6744	1.6744	1.6744

pH = 6.7

NF - MgCl2

TDS = 1750 mg/l

Table C-9. Readings for MgCl2 solution at 1,750 mg/l and 100 psi feed pressure

Description	HPP Only					HPP + Permeme Pump					Average	
	1	2	3	4	5	Average	1	2	3	4		5
Pre-filter inlet press (psi)	15.5	15	14.5	14.5	15	14.9	15	14.5	14.5	15	15	14.8
Pre-filter outlet press (psi)	14.5	13.5	13	13	13.5	13.5	14.5	13	13	13.5	13.5	13.5
HPP Press (psi)	100	100	100	100	100	100	98	99	98	97	97	97.8
Conc. Press (psi)	95	94	93	94	93	93.8	91	92	91	91	91	91.2
(Suc) Perm. Press. (psi)	3.7	3	3	3	3	3.14	0.5	0.5	0.5	0.5	0.5	0.5
(Disch) Perm Press (psi)	0	0	0	0	0	0	0	0	0	0	0	0
Feed TDS ( mg/l)	1720	1730	1780	1770	1760	1752	1720	1730	1770	1770	1770	1752
Feed TDS ( Mol/l)	0.03613	0.03634	0.03739	0.03718	0.03697	0.03680	0.03613	0.03634	0.03718	0.03718	0.03718	0.03680
Conc. TDS (mg/l)	2610	2700	2740	2710	2720	2696	2610	2630	2730	2730	2700	2680
Conc. TDS (Mol/l)	0.05483	0.05672	0.05756	0.05693	0.05714	0.05663	0.05483	0.05525	0.05735	0.05735	0.05672	0.05630
Perm TDS (mg/l)	155	155	156	154	156	155.2	142	141	145	148	144	144
Perm TDS (Mol/l)	0.00326	0.00326	0.00328	0.00323	0.00328	0.00326	0.00298	0.00296	0.00305	0.00311	0.00302	0.00302
Perm Flow ( gpm)	0.4	0.4	0.4	0.4	0.4	0.4	0.425	0.425	0.425	0.425	0.425	0.425
Perm Flow ( m3/s)	0.000025	0.000025	0.000025	0.000025	0.000025	2.524E-05	0.000027	0.000027	0.000027	0.000027	0.000027	2.681E-05
Conc Flow (gpm)	1.7	1.7	1.7	1.7	1.7	1.7	1.7	1.7	1.7	1.7	1.7	1.7
Feed Flow (gpm)	2.1	2.1	2.1	2.1	2.1	2.1	2.125	2.125	2.125	2.125	2.125	2.125
HPP (RPM)	900	900	900	900	900	900	900	900	900	900	900	900
Perm Pump (RPM)	0	0	0	0	0	0	180	180	180	180	180	180
Temp C	25	25	25	25	25	25	25	25	25	25	25	25
Surface Area (ft2)	28	28	28	28	28	28	28	28	28	28	28	28
Flux (gpm/ft2)	0.0142857	0.0142857	0.0142857	0.014286	0.0142857	0.0142857	0.0151786	0.0151786	0.0151786	0.0151786	0.0151786	0.0151786
Surface Area (m2)	2.6	2.6	2.6	2.6	2.6	2.6	2.6	2.6	2.6	2.6	2.6	2.6
Flux (m3/m2.s)	9.706E-06	9.706E-06	9.7063E-06	9.71E-06	9.70626E-06	9.70626E-06	1.031E-05	1.031E-05	1.031E-05	1.031E-05	1.031E-05	1.031E-05
Delta P (psi)	96.3	97	97	97	97	96.86	97.5	98.5	97.5	96.5	96.5	97.3
Delta P (atm)	6.5510204	6.5986395	6.59863946	6.598639	6.598639456	6.589115646	6.6326531	6.7006803	6.6326531	6.5646259	6.5646259	6.6190476
Pi Product (atm)	0.07966	0.07966	0.08017	0.07915	0.08017	0.07976	0.07298	0.07246	0.07452	0.07606	0.07401	0.07401
Delta Pi (atm)	2.3795	2.4271	2.4271	2.4271	2.4271	2.4176	2.2113	2.2793	2.2113	2.1433	2.1433	2.1977
Pi Feed (atm)	2.4592	2.5068	2.5073	2.5063	2.5073	2.4974	2.2843	2.3518	2.2858	2.2193	2.2173	2.2717
c mem (mg/l)	4785.0059	4877.6619	4878.6619	4876.6619	4878.6619	4859.3307	4444.6554	4576.0212	4447.6554	4318.2896	4318.2896	4420.1822
Cmem (mol/l)	0.1005	0.1025	0.1025	0.1024	0.1025	0.1021	0.0934	0.0961	0.0934	0.0907	0.0906	0.0929
A (m3/m2-s-atm)	0.0000	0.0000	0.0000	0.0000	0.0000	0.0000	0.0000	0.0000	0.0000	0.0000	0.0000	0.0000
Cf - Cp	0.0973	0.0992	0.0992	0.0992	0.0992	0.0988	0.0904	0.0932	0.0904	0.0876	0.0876	0.0898
In (Cmem-Cp/Cf-Cp)	0.0516	0.0535	0.0543	0.0537	0.0539	0.0534	0.0518	0.0523	0.0543	0.0542	0.0537	0.0533
Mass Transf Coef. (m/s)	0.6344	0.6182	0.6030	0.6139	0.6108	0.6161	0.5558	0.5777	0.5095	0.4794	0.4895	0.5224
Diffus. Coef. ( m2/s)	1.22E-09	1.22E-09	1.22E-09	1.22E-09	1.22E-09	1.2243E-09	1.22E-09	1.22E-09	1.22E-09	1.22E-09	1.22E-09	1.224E-09
d F (m)	8.002E-05	7.798E-05	7.6064E-05	7.74E-05	7.70438E-05	7.77103E-05	6.598E-05	6.858E-05	6.049E-05	5.691E-05	5.812E-05	6.202E-05
h d (m)	8.78E-04	8.78E-04	8.78E-04	8.78E-04	8.78E-04	8.78E-04	8.78E-04	8.78E-04	8.78E-04	8.78E-04	8.78E-04	8.78E-04
Vw = Flux/4 (m/s)	2.43E-06	2.43E-06	2.43E-06	2.43E-06	2.43E-06	2.43E-06	2.58E-06	2.58E-06	2.58E-06	2.58E-06	2.58E-06	2.58E-06
Pe	1.7396	1.7396	1.7396	1.7396	1.7396	1.7396	1.8483	1.8483	1.8483	1.8483	1.8483	1.8483

pH = 6.7

Biocide = 0.2 mg/l

TDS = 1750 mg/l

Table C-10. Readings for MgCl2 solution at 1.750 mg/l and 1.30 psi feed pressure

Description	HPP Only						HPP + Permeate Pump						Average
	1	2	3	4	5	Average	1	2	3	4	5	6	
Pre-filter inlet press (psi)	16.5	16.5	16	16	16	16.2	16	16	15.5	16	16	16	15.92
Pre-filter outlet press (psi)	15.3	15.2	14.8	14.8	14.8	14.98	14.9	14.9	14.2	15	15	14.5	14.75
HPP Press (psi)	130	130	130	130	130	130	125	125	125	125	125	125	125.00
Conc. Press (psi)	123	123	123	122	122	122.6	119	118	119	118	117	117	118.00
(Suc) Perm. Press. (psi)	8	8	8	8	8	8	1.8	1.8	1.8	1.8	1.8	1.8	1.80
(Disch) Perm Press (psi)	0	0	0	0	0	0	0	0	0	0	0	0	0.00
Feed TDS ( mg/l)	0.036971	0.03697091	0.03697091	0.0365508	0.0365508	0.0368029	0.0363407	0.0365508	0.0363407	0.0365508	0.03655078	0.036341	0.04
Conc. TDS ( Mol/l)	2880	2870	2870	2870	2870	2872	2910	2950	2920	2960	2930	2910	2930.00
Conc. TDS (mg/l)	0.060498	0.06028778	0.06028778	0.0602878	0.0602878	0.0603298	0.061128	0.0619683	0.0613381	0.0621783	0.06154816	0.061128	0.06
Perm TDS (mg/l)	142	142	142	142	142	142	131	134	132	135	138	135	134.17
Perm TDS (Mol/l)	0.002983	0.00298288	0.00298288	0.0029829	0.0029829	0.0029829	0.0027518	0.0028148	0.0027728	0.0028358	0.00289886	0.002836	0.0028183
Perm Flow ( gpm)	0.57	0.57	0.57	0.57	0.57	0.57	0.6	0.6	0.6	0.6	0.6	0.6	0.6
Perm Flow ( m3/s)	0.000036	0.000036	0.000036	0.000036	0.000036	0.000036	0.000038	0.000038	0.000038	0.000038	0.000038	0.000038	0.000038
Conc Flow (gpm)	1.6	1.6	1.6	1.6	1.6	1.6	1.6	1.6	1.6	1.6	1.6	1.6	1.6
Feed Flow (gpm)	2.17	2.17	2.17	2.17	2.17	2.17	2.2	2.2	2.2	2.2	2.2	2.2	2.2
HPP (RPM)	900	900	900	900	900	900	400	400	400	400	400	400	900
Perm Pump (RPM)	0	0	0	0	0	0	25	25	25	25	25	25	25
Temp C	25	25	25	25	25	25	28	28	28	28	28	28	28
Surface Area (ft2)	28	28	28	28	28	28	28	28	28	28	28	28	28
Flux (gpm/ft2)	0.020357	0.02035714	0.02035714	0.0203571	0.0203571	0.0203571	0.0214286	0.0214286	0.0214286	0.0214286	0.02142857	0.021429	0.0214286
Surface Area (m2)	2.6	2.6	2.6	2.6	2.6	2.6	2.6	2.6	2.6	2.6	2.6	2.6	2.6
Flux (m3/m2.s)	1.38E-05	1.3831E-05	1.3831E-05	1.383E-05	1.383E-05	1.383E-05	1.456E-05	1.456E-05	1.456E-05	1.456E-05	1.4559E-05	1.46E-05	1.456E-05
Delta P (psi)	122	122	122	122	122	122	123.2	123.2	123.2	123.2	123.2	123.2	123.2
Delta P (atm)	8.29932	8.29931973	8.29931973	8.2993197	8.2993197	8.2993197	8.3810	8.3810	8.3810	8.3810	8.3810	8.3810	8.3810
Pi Product (atm)	0.116270	0.116270	0.116270	0.116270	0.116270	0.1162699	0.1073	0.1097	0.1081	0.1105	0.1130	0.1105	0.1099
Delta Pi (atm)	2.35E+00	2.35E+00	2.35E+00	2.35E+00	2.35E+00	2.3549241	2.14E+00	2.14E+00	2.14E+00	2.14E+00	2.14E+00	2.14E+00	2.1390116
Pi Feed ( atm)	2.47119	2.47119	2.47119	2.47119	2.47119	2.471194	2.246	2.249	2.247	2.250	2.252	2.250	2.249
c mem (mg/l)	4808.4	4808.4	4808.4	4808.4	4808.4	4808.3933	4370.8	4375.5	4372.3	4377.1	4381.9	4377.1	4375.7956
Cmem (mol/l)	0.101006	0.10100606	0.10100606	0.1010061	0.1010061	0.1010061	0.0918128	0.0919132	0.0918463	0.0919467	0.09204711	0.091947	0.0919188
A (m3/m2.s-aim)	2.33E-06	2.33E-06	2.33E-06	2.33E-06	2.33E-06	2.327E-06	2.33E-06	2.33E-06	2.33E-06	2.33E-06	2.33E-06	2.33E-06	2.33E-06
C mem - Cp	0.098023	0.098023	0.098023	0.098023	0.098023	0.0980232	0.089061	0.089098	0.089073	0.089111	0.089148	0.089111	0.0891005
Cf - Cp	0.033988	0.033988	0.033988	0.033568	0.033568	0.03382	0.033589	0.033736	0.033568	0.033715	0.033652	0.033505	0.0336274
ln (Cmem-Cp/Cf-Cp)	1.059196	1.05919564	1.05919564	1.0716336	1.0716336	1.0641708	0.975126	0.971126	0.9711775	0.9758915	0.97423049	0.97819	0.974426
Mass Transf Coef. (m/s)	1.31E-05	1.3058E-05	1.3058E-05	1.291E-05	1.291E-05	1.3E-05	1.493E-05	1.499E-05	1.492E-05	1.498E-05	1.4945E-05	1.49E-05	1.494E-05
Diffus. Coef. ( m2/s)	1.22E-09	1.22E-09	1.22E-09	1.22E-09	1.22E-09	1.224E-09	1.22E-09	1.22E-09	1.22E-09	1.22E-09	1.22E-09	1.22E-09	1.224E-09
d F (m)	9.38E-05	9.3756E-05	9.3756E-05	9.486E-05	9.486E-05	9.42E-05	8.2E-05	8.167E-05	8.206E-05	8.173E-05	8.1923E-05	8.23E-05	8.194E-05
h d (m)	8.78E-04	8.78E-04	8.78E-04	8.78E-04	8.78E-04	8.78E-04	8.78E-04	8.78E-04	8.78E-04	8.78E-04	8.78E-04	8.78E-04	8.78E-04
V/w = Flux/4 (m/s)	3.46E-06	3.46E-06	3.46E-06	3.46E-06	3.46E-06	3.46E-06	3.64E-06	3.64E-06	3.64E-06	3.64E-06	3.64E-06	3.64E-06	3.64E-06
Pe	2.4789	2.4789	2.4789	2.4789	2.4789	2.4789	2.6094	2.6094	2.6094	2.6094	2.6094	2.6094	2.6094

pH = 6.7

Biocide = 0.2 mg/l

TDS = 1750 ppm

## **ABOUT THE AUTHOR**

Awad A. El-Shamy is currently a senior design engineer at Crane Environmental Company, Florida, USA. His duties include working closely with engineering design and technical proposals for water treatment systems. He has extensive experience working in several technical positions for over 20 years, with American and Saudi companies, in the field of design, operation, and maintenance of seawater and brackish water desalination plants.

He submitted two papers at the International Desalination Association (IDA) conferences, and published a number of technical articles in the specialized engineering magazines in the United States and Egypt.

He received his B.Sc. degree in Mechanical Engineering, and M. Sc. in Operations Research from Cairo University, Egypt.

His research interests are in the field of pressure-driven membranes.